THE UNIVERSITY
of EDINBURGH

Defining mechanisms of neurodegeneration associated with protein misfolding diseases

Fiona Mary Lane

Doctor of Philosophy

The University of Edinburgh

2015

Declaration

Unless otherwise acknowledged, the work in this thesis is entirely my own. No part has been submitted for another degree at the University of Edinburgh or any other institute.

Fiona Lane

August 2015

Abstract

Protein misfolding diseases (PMDs) are a broad group of disorders including Alzheimer's, Parkinson's and prion diseases. They are characterised by the presence of aggregated, misfolded host proteins which are thought to cause cell death.

Prion diseases are associated with misfolded prion protein (PrP^{Sc}), which has a tendency to form fibrillar aggregates. By contrast, Alzheimer's disease (AD) is associated with misfolded amyloid beta (Aβ), which aggregates to form characteristic Aβ plaques. A feature which is common across PMDs is that small assemblies (oligomers) of the misfolded proteins are thought to be the important neurotoxic species, and it has been proposed that there may be a shared mechanism leading to cell death across PMDs caused by oligomers.

In this study, the toxicity of different misfolded forms of recombinant PrP (recPrP) and recombinant Aβ (recAβ) and the mechanisms leading to cell death were investigated using a primary cell culture model. In addition, the importance of the disulphide bond in recPrP in relation to oligomer formation was explored using size exclusion chromatography and mass spectrometry, the toxicity of the different resulting oligomer populations were also investigated.

Both recPrP oligomers and fibrils were shown to cause toxicity to mouse primary cortical neurons. Interestingly, oligomers were shown to cause apoptotic cell death, while the fibrils did not, suggesting the activation of different pathways. By contrast, recAβ fibrils were shown to be non-toxic to cortical neurons, Aβ oligomers, however, were shown to cause toxicity. Similar to recPrP, my data showed that it is likely that recAβ 1-42 oligomers also cause apoptosis. However, by contrast this seemed to be caused by excitotoxicity, which was not found to be the case for recPrP. Additionally, I have shown that the presence or absence of the disulphide

bond in PrP has a profound effect on the size of oligomers which form. RecPrP lacking a disulphide bond leads to the formation of larger oligomers which are highly toxic to primary neurons.

Findings from this study suggest that structural properties such as the disulphide bond in PrP can affect the size and toxicity of oligomers, furthermore, whilst oligomers have been shown to be important in both AD and prion diseases, they may not trigger the same pathways leading to cell death.

Lay summary

Diseases such as Alzheimer's (AD) are prevalent in the modern world and put a large economic and social burden on society. There are currently no effective treatments for diseases such as AD, therefore, research into understanding these diseases is imperative for developing therapies.

AD falls into a group of disorders known as protein misfolding diseases (PMDs). As well as AD, this group of diseases includes Parkinson's disease, Amyotrophic lateral sclerosis and prion diseases. All of these disorders are caused by proteins found in the body, which ordinarily carry out a variety of functions. However, for reasons largely unknown these proteins can misfold into an abnormal structure, which not only stops them from carrying out their normal functions but can also be toxic. These toxic proteins have a tendency to clump together and form large structures known as plaques, which are commonly seen in the brains of individuals affected by these diseases. Additionally, they can form much smaller assemblies often referred to as oligomers. Therefore, while the PMDs mentioned previously are caused by different proteins, once the proteins have misfolded they can behave in a similar manner. This has led to the theory that there may be a common toxic structure formed by misfolded proteins, which may cause toxicity and death to cells in the brain by activating common pathways.

In this study I have investigated which misfolded structures are the most toxic, and how they cause toxicity. To do this, I have produced proteins known to be involved in AD and prion diseases and refolded them into different conformations to try and mimic those seen in disease. I have then tested the toxicity of these proteins using neuronal cells; a type of cell found in the brain. Additionally I have investigated how the misfolded proteins cause toxicity, in the hope that if we can understand

which pathways are activated by these proteins then blocking them may lead to successful treatments.

I found that the small assemblies formed from either the Alzheimer's protein or the prion protein were toxic to neurons. However, it seemed that they may not be activating the same pathways. This may mean that therapies developed for one PMD may not be effective in treating other PMDs. Furthermore, I found that large aggregates of the misfolded proteins were not comparatively toxic. Large aggregates of the prion protein were found to be extremely toxic to neurons; however, large aggregates of the Alzheimer's protein were not shown to cause any toxicity. This may suggest the end stage of the misfolding process, which is thought to be the large insoluble aggregates, may play different roles in different diseases. In prion diseases the large aggregates may contribute to toxicity and cell death, while in AD formation of the large aggregates may be a protective mechanism to sequester the smaller more toxic protein assemblies.

The data from this study would suggest that while there are many similarities between PMDs, it is also likely that there are some important differences which may impact on the development of common therapies.

Acknowledgments

Firstly, I would like to thank Dr Andrew Gill for giving me the opportunity to undertake this project, for always being patient and for supporting me throughout. I would like to thank Prof. Giles Hardingham for his guidance and technical support with all of the primary cell experiments. I would also like to thank Prof. Jean Manson for her valued comments which were much appreciated.

I would like to thank my friends and family for their support over the last 4 years. I would particularly like to thank Sonya Agarwal for her continued encouragement in the lab, for our day to day chats and generally making work brighter. I would like to thank the girls upstairs for lots of fun tea breaks, particularly Marie and Eliza. I would also like to thank my sister, Melanie, and my parents for believing in me throughout my project and for always being supportive.

Lastly, I would like to thank my fiancé Robert, you inspired me to do a PhD and have shown me love and encouragement throughout. I dedicate this thesis to you.

Table of contents

List of tables and figures

Abbreviations

A list of abbreviations used in this work:

AD	Alzheimer's disease
AFM	Atomic force microscopy
Ala	Alanine
ANS	8-anilino-1-naphthalenesulfonic acid
apoE	Apolipoprotein E
APP	Amyloid precursor protein
Aβ 1-40	Amyloid beta species from amino acids 1-40
Aβ 1-42	Amyloid beta species from amino acids 1-42
Aβ	Amyloid beta
BiP	Binding immunoglobulin protein
Bis-ANS	4,4′-dianilino- 1,1′-binaphthyl-5,5′-disulfonate
BSE	Bovine spongiform encephalopathy
CD	Circular dichroism

CHOP C/EBP homologous protein

CJD Creutzfeldt-Jakob disease

CV Column volume

Disulphide-reduced RecPrP recombinant PrP without a disulphide bond

DLS Dynamic light scattering

DMSO Dimethyl sulfoxide

DTT Dithiothreitol

E.coli Escherichia coli

EC Extinction coefficient

EDTA Ethylenediaminetetraacetic acid

EIF2α Eukaryotic initiation factor 2 α subunit

EM Electron microscopy

ER Endoplasmic reticulum

ERAD Endoplasmic reticulum - associated degradation pathway

FAD Familial Alzheimer's disease

FFI	Fatal familial insomnia
FTD	Fronto-temporal dementia with Parkinsonism
FTIR	Fourier transform infrared spectroscopy
g	Gram
GdnHCl	Guanidine hydrochloride
GPI	Glycosylphosphatidylinositol
GSS	Gerstmann- Straussler- Scheinker disease
HFIP	Hexafluoroisopropanol
hGH	Human growth hormone
iCJD	Iatrogenic CJD
IMAC	Immobilised metal ion affinity chromatography
IPTG	Isopropyl β-D-1-thiogalactopyranoside
kDa	Kilo Dalton
LB	Luria broth
LC-MS	Liquid chromatography mass spectrometry

LMW	Low molecular weight species
LOAD	Late onset Alzheimer's disease
LS	Light scattering
MAPT	Microtubule associated protein tau gene
mg	Milligram
ml	Millilitre
mM	Millimolar
MW	Molecular mass
NaCl	Sodium chloride
NF	Non-fibrillar
NFT	Neurofibrillary tangles of the protein tau
nm	Nanometre
nM	Nanomolar
NMDA	N-methyl-D-aspartate
NMR	Nuclear magnetic resonance

OSCs	Organotypic slice cultures
Oxidised recPrP	Recombinant PrP with an intact disulphide bond
PBS	Phosphate buffered saline
PK	Proteinase K
PMDs	Protein misfolding diseases
PRNP	Human PrP gene
Prnp	Mammalian PrP gene
PrP	Prion protein
PrP^{C}	Cellular form of the prion protein
PrP^{Sc}	Disease associated form of the prion protein
PSEN1	Presenilin 1
PSEN2	Presenilin 2
QLS	Quasi-elastic light scattering
RAW	Murine monocyte-macrophage cell line
recAβ	Recombinant Aβ

recPrP	Recombinant PrP
RP	Reverse phase
sAPPα	Soluble secreted form of APP
SAXS	Small-angle X-ray scattering
sCJD	Sporadic CJD
SDS-PAGE	Sodium dodecyl sulphate-polyacrylamide gel electrophoresis
SE	Standard error
SEC	Size exclusion chromatography
SLS	Static light scattering
SNPs	Single nucleotide polymorphisms
TB	Terrific broth
TBS-T	Tris buffered saline with tween 20
TEM	Transmission electron microscopy
TEV	Tobacco etch virus protease
TFA	Trifluoroacetic acid

ThT	Thioflavin T
TIC	Total ion count
TSEs	Transmissible spongiform encephalopathies
UPR	Unfolded protein response
Val	Valine
vCJD	Variant CJD
μg	Microgram
μM	Micromolar

Chapter 1:

Introduction

1.1 Protein misfolding diseases (PMDs)

1.1.1 What are protein misfolding diseases and why study them?

Protein misfolding diseases (PMDs) are a broad group of disorders that are characterised by the misfolding of native host proteins. Once misfolded these proteins are prone to accumulation and aggregation, leading to the cellular toxicity seen in these diseases. Well characterised PMDs include Alzheimer's (AD), Parkinson's, Huntington's and prion disease. The impact of PMDs on society today is huge, with an estimated 25 million people suffering from AD (Mancuso and Gaetani, 2014) worldwide and between 7-10 million with Parkinson's disease (Bhimani, 2014). The prevalence of both these diseases is set to more than double by 2030 and this is not accounting for the large number of other PMDs. This is a massive problem facing both the western and developing world, since it will cause both an economic burden to society and an emotional burden for family and friends of those affected. Therefore, it is imperative to better understand the disease mechanisms of PMDs in the hope that effective treatments may be developed.

The misfolded proteins associated with PMDs, for example the prion protein (PrP) in prion diseases, and amyloid-β (Aβ) in AD, are prone to aggregation leading to the formation of large insoluble fibrillar aggregates (Bucciantini et al., 2002, Caughey and Lansbury, 2003, Knowles et al., 2014, Braak et al., 2003). For many years it was thought that these aggregates caused the neurodegeneration seen in these diseases, however, in more recent years it has been suggested that it is intermediates during the aggregation process which cause neuronal toxicity (Kuo et al., 1996, Lue et al., 1999, Naslund et al., 2000, McLean et al., 1999, Mucke et al., 2000a, Walsh et al., 2002, Quist et al., 2005, Kristiansen et al., 2007, Simoneau et al., 2007, Volles et al., 2001). Small soluble assemblies composed of the misfolded protein, often termed oligomers, which have a high β-sheet content have repeatedly been found to be neurotoxic in many PMDs (Kuo et al., 1996, Lue et al., 1999,

McLean et al., 1999, Mucke et al., 2000a, Walsh et al., 2002, Quist et al., 2005, Kristiansen et al., 2007, Simoneau et al., 2007, Volles et al., 2001, Winner et al., 2011, Caughey and Lansbury, 2003, Zhang et al., 2010, Kayed et al., 2003, Bucciantini et al., 2002). Evidence for this has come from many types of studies, including those which have used human tissue, animal models or *in vitro* cell systems. Studies which have used human tissue have correlated the presence of soluble Aβ oligomers with disease and found the concentration of soluble Aβ to be significantly higher in AD patients' brains than in age matched controls (McLean et al., 1999, Lue et al., 1999, Kuo et al., 1996). Studies using animal models have allowed the toxicity of oligomers and fibrils to be tested directly, rather than looking at correlations between concentration of oligomers and severity of disease in humans. These studies have shown that Aβ oligomers are highly toxic *in vivo*, which supports the findings from human studies (Mucke et al., 2000b, Walsh et al., 2002, Winner et al., 2011). Additionally, many studies have shown oligomers to be cytotoxic using *in vitro* systems. These studies have directly tested the toxicity of different conformations of misfolded proteins, including Aβ, PrP and α-synuclein (Kristiansen et al., 2007, Volles et al., 2001, Zhang et al., 2010, Kayed et al., 2003, Bucciantini et al., 2002). The combined evidence from a wide array of studies, which suggest that oligomers are the important toxic species in PMDs, is very compelling. Furthermore, this has led to the hypothesis that oligomeric forms of misfolded proteins may induce similar mechanisms of toxicity across PMDs (Glabe, 2006, Kayed et al., 2003, Haass and Selkoe, 2007, Quist et al., 2005).

1.1.2 Transmissible spongiform encephalopathy (prion disease)

Prion diseases are a group of fatal neurodegenerative disorders, which affect a variety of mammals. They are also known as the transmissible spongiform encephalopathies (TSEs) (Collinge, 2001). Well characterised TSEs include bovine spongiform encephalopathy (BSE) in cattle (Hope et al., 1988), scrapie in sheep and goats (Greig, 1950, Parry, 1962, Brotherston et al., 1968) and chronic wasting disease

in deer and elk (Williams and Young, 1980, Williams and Miller, 2002). In addition, kuru, Creutzfeldt-Jakob disease (CJD), Gerstmann-Straussler-Scheinker (GSS) disease and fatal familial insomnia (FFI) affect humans (Collins et al., 2001, Goldgaber et al., 1989). At post-mortem, prion-infected brains of humans and other mammals have spongiform degeneration in addition to astrocytic gliosis (Prusiner, 1998b). According to the protein-only hypothesis, prion disease is caused by misfolding of the normal cellular prion protein (PrP^{C}) to a conformationally different species referred to as PrP^{Sc}. This form is prone to aggregation and is likely to represent the cause of neuronal toxicity and cell death seen in prion diseases (Prusiner et al., 1998, Prusiner, 1998a, Prusiner, 1998b, Wang et al., 2010). This will be discussed further in section 1.2.1.

1.1.2.1 Animal prion diseases

The most well studied animal prion disease is scrapie, which affects sheep and goats. Scrapie has been endemic in the UK sheep flock for over 200 years (Greig, 1950); symptoms include pruritus and progressive ataxia (Greig, 1950). However, it wasn't until the 1960's that it was recognised as a prion disease when similarities were drawn between scrapie and kuru, a human prion disease (discussed in section 1.1.3.3). The first inoculation of scrapie into a mouse model was in 1961, when infected brain from a scrapie infected sheep was inoculated into a mouse and found to cause neurodegeneration (Chandler, 1961). Histological analysis of the mouse showed vacuolation, resembling that seen in sheep with scrapie(Chandler, 1961). This showed that the agent causing scrapie was transmissible to other species.

In the 1980's a new form of prion disease emerged, which affected approximately 170,000 cattle (Pattison, 1998). This prion disease, referred to as BSE, was traced back to the consumption of contaminated food stuffs, which contained meat and bone meal (MBM) (Pattison, 1998). The banning of MBM in animal feed in 1988, led to a rapid decline in the number of cases (Pattison, 1998). The outbreak of BSE also led to

the emergence of a new human prion disease, variant CJD, which will be discussed further in section 1.1.2.3. Symptoms of cattle affected with BSE include nervousness, heightened reactivity and difficulty moving (Pattison, 1998). Vacuolation and astrocytosis is seen in the brains of cattle affected with BSE(Bradley, 1991).

Another important animal prion disease is chronic wasting disease (CWD), which affects deer, elk and moose (Baeten et al., 2007, Williams et al., 2002). CWD is the only known prion disease to affect free-ranging animals, it has been endemic in Northern America for over 20 years but the prevalence has increased over the last decade (Williams et al., 2002). CWD is thought to be transmitted between deer and elk in the environment through saliva, faeces and other bodily fluids (Mathiason et al., 2006, Safar et al., 2008). It is not yet known whether CWD poses a threat to humans, but evidence so far suggests that the risk to humans is low (Race et al., 2014, Kong et al., 2005).

Genetic variations within the *Prnp* gene can increase susceptibility or resistance to prion disease. This has been extensively investigated in sheep and it has been shown that polymorphisms found at codons 136, 154 and 171 are important in dictating susceptibility to scrapie(Elsen et al., 1999, Baylis et al., 2004). Sheep which are homozygous for alanine at codon 136 and are homozygous for arginine at codon 154 and 171 (known as ARR genotype) show resistance to scrapie, alternatively, those who are homozygous for valine at codon 136, homozygous for arginine at codon 154 and homozygous for glutamine at 171 (VRQ) are highly susceptible to scrapie (Elsen et al., 1999, Baylis et al., 2004). Understanding which genotypes are more resistant to scrapie means that sheep can be selectively bred for resistance.

Back in the early 2000s a new type of scrapie was discovered, which was termed atypical scrapie (Saunders et al., 2006). Atypical scrapie cases tested positive in a standard immunoassay but they were negative when analysed for immunohistochemistry(Saunders et al., 2006). It is now possible to confirm atypical

cases by immunohistochemistry and it seems that it is a novel strain of the disease (Saunders et al., 2006). The polymorphisms within the *Prnp* gene which confer susceptibility to classical scrapie vary for atypical scrapie. For atypical scrapie a homozygous or heterozygous combination of ARR, ARQ or AHQ seems to confer susceptibility, however, the most susceptible genotype is conferred by phenylalanine (F) at position 141 ($AF_{141}RQ$)(Saunders et al., 2006, Gesine et al., 2007).

1.1.2.2 Familial human prion diseases

The prion protein in humans is encoded by the *PRNP* gene; familial or genetic forms of human prion disease are caused by mutations in this gene. These include familial CJD, GSS disease and FFI (Collins et al., 2001, Goldgaber et al., 1989). They are associated with approximately 37 point mutations in the *PRNP* gene (Rossetti et al., 2011) and are inherited in an autosomal-dominant manner. The mutations all result in the production of misfolded PrP, which accumulates in the brain. Common symptoms include rapidly progressive dementia (Ironside et al., 2005), ataxia (Collinge, 2001) and a short clinical phase (Ironside et al., 2005, Collinge, 2001). However, symptoms vary widely depending on the causative mutation(Collinge, 2001, Gambetti et al., 2003).

Whilst prion diseases are associated with a short clinical phase, relative to other PMDs, the incubation period or pre-clinical phase is long, often lasting for decades (Imran and Mahmood, 2011). A polymorphism found at codon 129 in the *PRNP* gene, in which an individual can have a methionine or a valine residue, can alter the phenotype of many prion diseases. For example, a person with the D178N mutation will have FFI if this is combined with a methionine residue at codon 129, and those who are homozygous for methionine generally have more severe symptoms (Imran and Mahmood, 2011). However, if a person has the D178N mutation and they are homozygous for valine at the 129 codon then they present with a familial CJD phenotype (Imran and Mahmood, 2011). The presentation of prion disease causing

mutations vary geographically (Kovács et al., 2005). More common mutations such as the E200K mutation are found in most countries, however, others are only found in specific communities (Kovács et al., 2005). Genetic forms of prion disease account for only 10-15 %(Mastrianni, 2010, Prusiner and Hsiao, 1994) of cases the remaining 85-90% are sporadic or acquired forms of the disease, with the majority being sporadic(Mastrianni, 2010).

1.1.2.3 Sporadic and acquired forms of human prion disease

Sporadic forms of prion disease are the most common with sporadic CJD (sCJD) being most prevalent (Imran and Mahmood, 2011). However, with that said, sCJD is still very rare, with 1-2 in a million cases per year(Imran and Mahmood, 2011, Mead et al., 2003). Sporadic prion diseases, like genetic prion diseases, are associated with the production of PrP^{Sc} in the brain (Prusiner and Hsiao, 1994). The cause of sporadic prion disease is still unknown, with a spontaneous event leading to the production of pathogenic PrP^{Sc} (Prusiner and Hsiao, 1994).

Acquired forms of human prion disease include variant CJD (vCJD), iatrogenic CJD (iCJD) and Kuru. The BSE crisis in the 1980s was linked to the emergence of a new human prion disease, vCJD, first described in the mid-1990s (Will, 2003). It was traced to the consumption of beef products contaminated with BSE (Will, 2003). At the height of the crisis many thousands of people were thought potentially to be infected (Will, 2003). To date, only 177 cases in the UK actually presented with the disease (Diack et al., 2014). Susceptibility to vCJD is also affected by the 129 codon, with almost all cases of vCJD having the 129MM genotype (Diack et al., 2014).

In addition to vCJD, prion infection has also been passed on through the use of contaminated surgical equipment (Belay et al., 2013), blood transfusion (McCutcheon et al., 2011, Llewelyn et al., 2004, Peden et al., 2004, Head et al., 2009), dura matter grafts (Brown et al., 2000, Thadani et al., 1988) and contaminated

human growth hormone (hGH) (Will, 2003, Brown et al., 2000, de Villemeur et al., 1994). However only vCJD and Kuru are systemic infections, caused by oral consumption and prion infection throughout the lymph system, and therefore present a risk for passing on the infection by blood transfusion. The sporadic event which causes sCJD occurs in the brain and the misfolded protein is therefore not present throughout the body, meaning it could not be transmitted by blood. vCJD and sCJD could both potentially be transmissible through surgical procedures if the surgical equipment came into contact with infected tissue (the brain in sCJD)(Will, 2003, Head et al., 2009, de Villemeur et al., 1994). It is possible to transmit prions by surgical equipment, since prions are resistant to normal surgical sterilisation procedures (Belay et al., 2013). In the case of hGH, before the advent of recombinant hGH, it was derived from the pituitary gland of cadavers (de Villemeur et al., 1994). One cadaver could provide the hormone for many recipients; it is thought that one or more of the cadavers used must have had a prion infection, which resulted in over 100 people acquiring iCJD (Will, 2003, de Villemeur et al., 1994).

Kuru was a prion disease discovered in the 1950s in the Fore tribe of Papua New Guinea (Mead et al., 2003, Collinge et al., 2006). This population of people were isolated from the wider population and still practiced cannibalistic rituals, which were thought to be the cause of the widespread prion infection present in the tribe (Mead et al., 2003). It was thought that at some point in the past a member of the tribe had developed a prion infection, which was passed on through the cannibalistic rituals (Mead et al., 2003). The individuals which consumed the infected brain then developed prion disease often decades later and the process would have then been repeated, with their remains consumed by members of the tribe (Collinge et al., 2006). Those with the 129MM genotype were found to have shorter incubation periods than those who were heterozygous (Mead et al., 2003, Collinge et al., 2006). This is a characteristic example of how prion disease can be passed by an oral/ digestive route.

1.1.3 Alzheimer's disease

AD is a fatal neurodegenerative disorder of humans. Clinical symptoms tend to include progressive memory loss, confusion and changes in mood and personality (Selkoe, 2001). Pathologically, AD is characterised by atrophy of certain areas of the brain, particularly the cortex and hippocampus (Braak and Braak, 1991, Thal et al., 2002). Within these regions extracellular senile plaques are found, which are comprised of aggregates of Aβ. Aβ is a small peptide formed from the processing of the amyloid precursor protein (APP, see section 1.2.2). Additionally, neurofibrillary tangles (NFT) made up of hyperphosphorylated tau (Braak and Braak, 1991, Thal et al., 2002, Selkoe, 2001) are found intracellularly. For many years it was thought that Aβ plaques were causing the cellular toxicity and cell death seen in AD. However, it was noted that plaque density did not correlate with cognitive impairment, and so was perhaps not the sole cause of neuronal loss (Selkoe, 2001, Hardy and Selkoe, 2002). During the process of plaque deposition Aβ likely exists as smaller assemblies, or oligomers, which are thought to be important in causing toxicity. Aβ is formed by processing of the APP, which is cleaved by either α- or β-secretase. If it is cleaved by β-secretase then cleavage by the γ-secretase complex will follow, giving rise to Aβ peptides. The γ-secretase complex includes presenilin proteins; mutations in presenilin genes can cause genetic forms of AD (Borchelt et al., 1996, Price et al., 1998, Shepherd et al., 2009) (see section 1.1.3.1), the γ-secretase complex can cleave the APP at multiple sites, giving rise to Aβ peptides of varying length (for further details of Aβ formation and APP processing see section 1.2.2.1). The most common forms of Aβ tend to terminate at either Val40 or Ala42 giving rise to two main forms known as Aβ 1-40 and Aβ 1-42. The latter fragment has been shown to be more neurotoxic and prone to aggregation, however, the presence of both Aβ 1-40 and Aβ 1-42 in a soluble form correlates more closely with the degree of cognitive decline than the number of senile plaques (Hardy and Selkoe, 2002, Naslund et al., 2000). The Aβ cascade hypothesis, which speculates that misfolded Aβ is the cause of AD, is the most extensively studied theory behind what causes

the neuronal loss seen in AD (Hardy and Higgins, 1992). Other theories include the importance of tau in causing toxicity in AD (Mandelkow and Mandelkow, 1998), since NFT deposits correlate better with the severity of AD symptoms than Aβ plaques (Treusch et al., 2009). However, it is thought that Aβ deposition precedes NFT formation (Hardy and Selkoe, 2002).

1.1.3.1 Familial forms of Alzheimer's disease

Approximately 5 % of AD cases are caused by autosomal dominant mutations (Price et al., 1998). These mutations tend to occur in either the APP gene, in presenilin 1 (PSEN1) or presenilin 2 (PSEN2) (Price et al., 1998). Mutations in the PSEN genes are the most common cause of familial AD (Kumar-Singh et al., 2006) (FAD), with mutations in PSEN1 accounting for 18-50% of FAD (Rogaeva et al., 2001, Cruts and Van Broeckhoven, 1998). Mutations in the APP gene are thought to affect the cleavage of APP and increase the production of Aβ (Price et al., 1998, Shepherd et al., 2009, Tamaoka et al., 1994) (see Aβ processing in section 1.2.2.1). The presenilin genes encode subunits of the γ-secretase protein complex, which cleaves APP. Mutations in these genes lead to increased production of Aβ 1-42 (Borchelt et al., 1996, Price et al., 1998, Shepherd et al., 2009). FAD tends to be early onset (before the age of 60) and often clinical signs occur when an individual is in their 40's or 50's (Price et al., 1998, Shepherd et al., 2009). Once clinical symptoms develop they are similar to those of late onset AD (Price et al., 1998). The pathology of FAD is similar to that of late-onset AD, but in FAD there is a higher concentration of plaques and soluble Aβ made up of Aβ 1-42 (Shepherd et al., 2009, Tamaoka et al., 1994, Kumar-Singh et al., 2006).

1.1.3.2 Late onset Alzheimer's disease

Late onset AD (LOAD) is the most common cause of dementia worldwide, accounting for 60-80% of cases (Barnes and Yaffe, 2011). Like FAD, LOAD is

associated with Aβ plaques and NFT. LOAD differs from FAD in several ways, clinical onset occurs in people over the age of 65 and the incidence increases with increasing age (Naj et al., 2014, Fratiglioni et al., 1999). LOAD is a genetically complex disease and while there are polymorphisms that convey an increased or decreased risk of LOAD, the disease does not follow a Mendelian pattern of inheritance. The biggest genetic risk factor for LOAD is the apolipoprotein E (apoE) ε4 allele, which is found on chromosome 19 and has been shown to increase the chances of developing LOAD (Corder et al., 1993). Those with no ε4 allele have a 20 % risk of developing LOAD, one ε4 allele increases that risk to 47 % and with two ε4 alleles the risk goes up to 90 % (Corder et al., 1993). This means that those who are homozygous for the ε4 allele have an 8-fold increased risk of developing LOAD by the time they are 80 (Corder et al., 1993). The presence of the ε4 allele also decreases the age of onset in LOAD, with the average age decreasing to 68 with two copies as opposed to 84 with no ε4 allele (Corder et al., 1993).

In recent years, with the advent of genome wide association studies, which allow millions of single nucleotide polymorphisms (SNPs) to be screened and compared between healthy individuals and those with LOAD, polymorphisms in many genes have been uncovered which are associated with the disease. These include: BIN1, PICALM and clusterin (Hu et al., 2011, Wijsman et al., 2011, Harold et al., 2009, Carrasquillo et al., 2010). At the present time it is difficult to predict whether an individual will develop LOAD before the onset of clinical symptoms. However, in the future it is possible that a panel of polymorphisms that increase the risk of developing LOAD will be able to highlight at risk individuals.

In addition to genetic risk factors, there are also various environmental factors which have been shown to increase the chances of an individual developing LOAD. These include smoking, obesity and lack of physical activity (Scarmeas et al., 2009, Barnes and Yaffe, 2011, Luchsinger et al., 2012). Those who made healthy life style choices, such as a Mediterranean-style diet, had a decreased risk of LOAD

(Scarmeas et al., 2009, Devanand et al., 2013). When this was combined with regular physical activity the risk of LOAD decreased further (Scarmeas et al., 2009, Devanand et al., 2013). Additionally, it has been shown that individuals with higher intelligence have a decreased risk of LOAD (Devanand et al., 2013).

1.1.4 Commonalities between PMDs

In the past, diseases such as AD, Parkinson's, Huntington's and prion disease were all thought to be distinct neurodegenerative conditions. However, once it was established that they all were caused by misfolded proteins, similarities between them became more apparent. The important toxic species in these diseases is thought to be soluble oligomeric forms of misfolded protein, which may cause toxicity by a variety of mechanisms (Kuo et al., 1996, Lue et al., 1999, Naslund et al., 2000, McLean et al., 1999, Mucke et al., 2000a, Walsh et al., 2002, Quist et al., 2005, Kristiansen et al., 2007, Simoneau et al., 2007, Volles et al., 2001). It is possible that pathways activated by oligomeric forms of these misfolded proteins may be the common link between PMDs (Glabe, 2006, Kayed et al., 2003, Haass and Selkoe, 2007, Quist et al., 2005).

The transmissible nature of prion disease has set it apart from other PMDs, however, these difference may be less defined than first thought. There have been studies which show injection of Aβ into the brains of rhesus monkeys (Ridley et al., 2006) or transgenic mice (Kane et al., 2000, Walker et al., 2002) causes Aβ plaque deposition, showing that injection of Aβ may accelerate the process of Aβ accumulation (Aizenstein et al., 2008). Prion disease is likely to be the only PMD that is truly transmissible through an oral route or in the environment, but the disease progression and spread within an organism may be "prion like" in other PMDs (Guo and Lee, 2014, Luk et al., 2009, Danzer et al., 2009, Clavaguera et al., 2009, Masuda-Suzukake et al., 2013). Seeds of misfolded proteins have been shown to recruit normal protein and, through a templating process, convert the normal

protein to a misfolded form (Guo and Lee, 2014). In transgenic AD mice, injected Aβ can be seen to spread between axonally connected regions in a "prion like" manner (Jucker and Walker, 2011). Additionally, in non-transgenic mice after intrastriatal inoculation of synthetic α synuclein fibrils, cell to cell transmission was seen accompanied by Parkinson's-like pathology in interconnected brain areas including Lewy body deposition, loss of substantia nigra neurons and impaired motor coordination (Luk et al., 2012). Tau has also been shown to spread by similar mechanisms, with injection of tau fibrils into wild type tau expressing mice resulting in fibrillar deposition and spread to other brain regions (Clavaguera et al., 2009). All these studies demonstrate that misfolded proteins likely propagate themselves by a similar process and spread throughout the brain by related mechanisms.

1.2. Proteins associated with PMDs

1.2.1 The prion protein

1.2.1.1 PrP^C structure and function

PrP^C is a ubiquitously expressed, membrane- bound glycoprotein (Millhauser, 2007). It is located on the outside of the cellular membrane where it is attached by a glycosylphosphatidylinositol (GPI) anchor *via* its C-terminus (Millhauser, 2007). The C-terminal region in PrP^C has a globular structure consisting mainly of α- helices with just one two stranded β-sheet and a disulphide bond (Millhauser, 2007) (figure 1.1). The N-terminal region, conversely, is largely unstructured in solution but has an octarepeat domain, which consists of tandem repeats of the sequence PHGGGWGQ. Most mammals have four or five repeats of this sequence (Millhauser, 2007).

The exact function of PrP^C is still to be determined. It was thought that by knocking out PrP^C, clues to its function may be uncovered. However, $PrP^{0/0}$ null mice have no overt phenotype, although disturbances in circadian rhythms (Tobler et al., 1996, Tobler et al., 1997) have been noted along with a potential role in modulating neuronal excitability (Maglio et al., 2006, Maglio et al., 2004, Mallucci et al., 2002, Curtis et al., 2003), additionally, PrP^C has been shown to be important in maintaining the integrity of peripheral myelin sheaths (Bremer et al., 2010). The subtle phenotypes associated with $PrP^{0/0}$ null mice suggest that PrP^C may have various roles possibly associated with neuroprotection. Furthermore, other studies have shown PrP^C to be involved with cellular signalling or apoptosis (Westergard et al., 2007, Roucou and LeBlanc, 2005, Petrakis and Sklaviadis, 2006, Caetano et al., 2008). The octarepeat domain in PrP^C is highly conserved between species, therefore, probably has an important functional role; it has been shown to bind copper ions and there is some evidence to suggest it plays a neuroprotective role(Millhauser, 2007, Aronoff-Spencer et al., 2000).

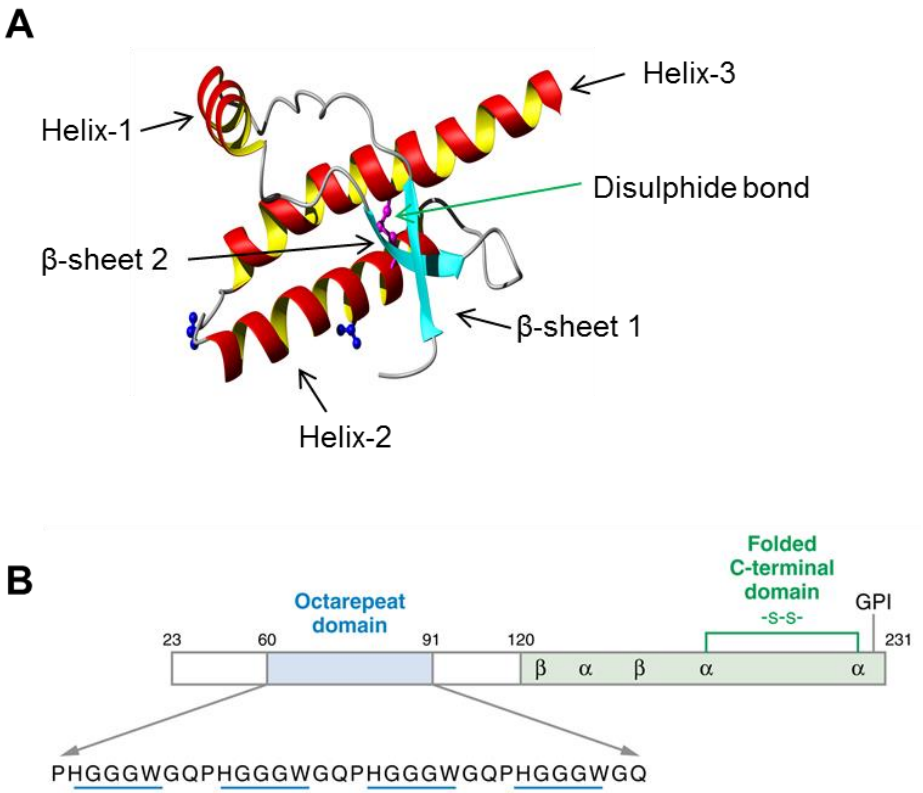

Figure 1.1 Schematic diagrams of PrP^C

A) Ribbon diagram of human PrP, residues 120-230, courtesy of AC Gill. The disulphide bond is shown in purple and is highlighted by the green arrow. The blue residues show Asn180 and Asn196 where glycans would be attached. B) Schematic of the domains found in PrP^C, from Millhauser *el al (Millhauser, 2007).*

1.2.1.2 Processing of PrP^C in the cell

Since PrP^C is located on the cell surface, it is expressed as part of the secretory pathway. As such, PrP^C is translated on ribosomes attached to the endoplasmic reticulum (ER). The ER has a high concentration of chaperone proteins to assist in folding proteins into their correct tertiary structure (Kleizen and Braakman, 2004). This includes oxidising components to support disulphide bond formation (Kleizen

and Braakman, 2004), which is an important component of PrP^C (the importance of the disulphide bond will be discussed in chapter 5). Other post-translational modifications to PrP^C are also made, such as cleavage of the N-terminal signal peptide (Harris, 2003), attachment of the GPI anchor and addition of core N-linked glycans to residues 180 and 196 in the murine amino acid sequence (Wiseman et al., 2005). *In vivo*, the site of glycan occupancy is variable; the protein can be un-, mono- or di- glycosylated. The glycosylation is thought to be important for stability of the protein but as yet it has not been proven to play a causative role in conversion of PrP^C to PrP^{Sc}, or in propagation of PrP^{Sc} (Wiseman et al., 2005, Tuzi et al., 2008). Following on from the modifications made in the ER, the protein is transported to the Golgi apparatus where the N-linked glycans are modified to contain sialic acid(Harris, 2003). PrP^C relocates to the cell membrane once it leaves the Golgi and then cycles continuously between the plasma membrane and endocytic compartments (Harris, 2003), this may be an important mechanism during conversion of PrP^C to PrP^{Sc}.

1.2.1.3 Conversion of PrP^C to PrP^{Sc}

The disease-associated form of PrP, namely PrP^{Sc}, is produced when PrP^C undergoes a conformational change, leading to a tertiary structure where the mainly α-helical conformation of PrP^C, is replaced by a structure consisting principally of β-sheets (Pan et al., 1993). PrP^C is soluble in mild detergents and is completely digested by proteinase K, however, PrP^{Sc} is only partially digested, with the main site of cleavage being around residue 90 leaving the C-terminal region intact (Hayashi et al., 2005, Kocisko et al., 1995). This protease resistant region is very difficult to degrade, methods used for destroying nucleic acids fail to have any effect on PrP^{Sc} concentration and infectivity (Alper et al., 1967, Giles et al., 2008, Peretz et al., 2006). Interestingly, the presence of PrP^C is needed to propagate prion disease since $PrP^{0/0}$ null mice are resistant to prion infection (Bueler et al., 1993, Weissmann, 2004). By

mechanisms largely unknown PrP^{Sc} seems to "replicate" by converting PrP^{C} into the misfolded conformation and so without PrP^{C} the disease cannot occur.

So far misfolded recombinant PrP (recPrP) alone has not been sufficient to cause disease in wild type animals. However, recombinant prions which were first refolded into amyloid or β-sheet rich structures have caused disease in transgenic mice overexpressing PrP (Legname et al., 2004, Colby et al., 2009). When recPrP is combined either with brain homogenate (Makarava et al., 2010) or with components such as RNA and lipids it has the ability to cause prion infection in wild type animals (Wang et al., 2010, Deleault et al., 2012). It is not yet understood how these cofactors allow the prion protein to cause disease, it has been proposed that they may stabilise the PrP^{Sc} conformation (Deleault et al., 2012).

The site of conversion for PrP^{C} to PrP^{Sc} is yet to be determined. Small quantities of abnormal PrP have been found to accumulate within the cell, so it is possible that PrP conversion may take place intracellularly (Ma et al., 2002). Potentially this could take place in the ER (Beranger et al., 2002) and the retention of misfolded PrP^{Sc} by the ER may play a role in the disease process (Beranger et al., 2002, Torres et al., 2010), or the misfolding may take place after PrP has exited the ER. However, most aggregates of PrP^{Sc} *in vivo* tend to be extracellular (Jeffrey et al., 2000) and since PrP^{C} is membrane bound it is likely that PrP^{Sc} conversion takes place at the cell surface. Lipid rafts are thought to be potentially important sites for conversion (Goold et al., 2011, Wadia et al., 2008), along with endocytic vesicles (Dimcheff et al., 2003, Wadia et al., 2008). It is also possible that the endosomes, which endocytic vesicles fuse with, may be another possible site for conversion (Shyng et al., 1994, Lakhan et al., 2009).

The exact mechanisms which lead to the formation of small assemblies of PrP^{Sc} (oligomers) and larger insoluble aggregates with a fibrillar structure are unknown, but it is believed that a nucleation process must take place to form a small "seed"

(Harper and Lansbury, 1997), which may be two or more PrP^{Sc} molecules. This nucleation and formation of a seed is known as the primary nucleation event (Knowles et al., 2014, Knowles et al., 2009). The protein aggregate can then increase in size by the ends of existing filaments recruiting soluble protein molecules, this results in a templated linear growth phase (Knowles et al., 2014, Knowles et al., 2009). The aggregates can then multiply by a secondary nucleation event, such as fragmentation, when a fibril fragments the broken filaments can then begin to recruit soluble molecules by the same process as in the primary nucleation event (Knowles et al., 2014, Knowles et al., 2009). This process can lead to many fibrillar deposits in PMDs. It has been shown that the size of the most infectious PrP assembly is made up of 14-28 PrP molecules (Silveira et al., 2005). It is likely that such infectious particles are a product of secondary nucleation events.

1.2.1.4 Strains of prion disease

There are multiple strains of prion disease, which can exhibit different incubation periods, symptoms and pathology within the same species (Gambetti et al., 2011). These differences were noted when prion infected brain homogenates were injected into transgenic mice and strain properties were stable with repeated passage (Gambetti et al., 2011). The incubation period of a strain can be affected by the conformation of the prion particle and genetic components in the mouse (Collinge and Clarke, 2007). In addition to the incubation period which can be indicative of a specific strain, the pathological changes seen in the brain can also be very specific for different strains (Bruce, 2003). For example, the extent of vacuolation in certain brain areas is indicative of strain, along with the amount and type of PrP deposition (fibrillar, diffuse fibrils or very little deposition) (Bruce, 2003).

Strains such as BSE and scrapie can be characterised though proteolytic digestion of isolated PrP^{Sc}, showing different fragment patterns suggesting differences in protein conformation. In addition to this, the glycoform ratios; the ratio of un- mono- or di-

glycosylated protein, vary between strains but remain stable through passage. Therefore, glycoform ratios can also be used for "strain typing"(Collinge and Clarke, 2007).

The occurrence of "strains" would normally be associated with viruses or bacteria, in which strain differences would be encoded in nucleic acid sequences. Prions are unusual since it is thought that the differences between strains are due to different conformations of PrP^{Sc} (Toyama et al., 2007, Tanaka et al., 2006, Collinge and Clarke, 2007). It is thought that a PrP^{Sc} molecule with a particular conformation interacts with a PrP^{C} molecule and acts as a template to propagate that conformation or "strain"(Collinge and Clarke, 2007). This propagation can be affected when TSEs attempt to cross the species barrier, with much longer incubation times, this is thought to be because of differences in PrP sequence and structure which affects the conversion of PrP^{C} to PrP^{Sc} (Aguzzi et al., 2007, Collinge and Clarke, 2007).

If different strains of prion disease can be caused by differences in PrP^{Sc} structure this could also be applicable to other PMDs, since other misfolded proteins could also have different conformational forms (Aguzzi et al., 2007, Guo et al., 2013, Bousset et al., 2013). α synuclein, which is associated with Parkinson's disease, has been shown to exhibit different strains with different structural conformations and different propagation properties *in vitro* (Bousset et al., 2013, Guo et al., 2013). It is hypothesised that this ability to propagate different "strains" may account for differences between α- synucleinopathies (Bousset et al., 2013). However, further studies are needed to study this *in vivo* and in patient tissue to show whether different strains really do account for the heterogeneity seen in synucleinopathies. Additionally, it is thought that strains of Aβ may also exist which have different structural conformations (Aguzzi et al., 2007, Meyer-Luehmann et al., 2006).

1.2.2 Amyloid β (Aβ)

1.2.2.1 Formation and processing of Aβ

The amyloid precursor protein (APP) is translated at the ER, following post-translational modifications, a small proportion is then transported to the cell membrane while the majority localises to the Golgi (Thinakaran and Koo, 2008). The APP is thought to be involved in neurite growth (Tyan et al., 2012), along with other potential roles in metal ion binding and cell adhesion (Thinakaran and Koo, 2008). When APP is localised to the cell membrane it is initially cleaved by α-secretase (ADAM10) or β-secretase (BACE1) and then further cleaved by the γ-secretase complex (Kaden et al., 2012) (figure 1.2). Cleavage by both β- and γ-secretases leads to the production of Aβ peptides, which are associated with AD (Kaden et al., 2012). Interestingly, cleavage of APP by α-secretase creates a soluble secreted form of APP (sAPPα) which is thought to have neuroprotective properties (Kaden et al., 2012, Furukawa et al., 1996, Mattson, 1997). Some mutations in APP that cause familial AD result in increased β-secretase cleavage and reduced cleavage by α-secretase(Furukawa et al., 1996). The down regulation of sAPPα is thought to contribute to neurodegeneration in AD, since lower levels of sAPPα mean the neurons are more vulnerable to toxicity (Mattson, 1997, Furukawa et al., 1996). Additionally, sAPPα is thought to act as a growth factor for many cell types and promote neuritogenesis, therefore, the loss or down regulation of this protein could contribute to disease (Gralle and Ferreira, 2007).

Aβ peptides are formed when the APP is cleaved by β-secretase and again by the γ-secretase complex (figure 1.2C). At low levels they are thought to be involved in synaptic homeostasis, potentially acting as regulators of a negative feedback loop for synaptic transmission (Kamenetz et al., 2003). However, when levels of Aβ increase this ability to depress synaptic transmission is detrimental (Kamenetz et al.,

2003). This is thought to be important in early pathological signs of AD (Kamenetz et al., 2003).

As shown in figure 1.2, once the APP has been cleaved by β-secretase, the γ-secretase complex can cleave at multiple sites, producing Aβ peptides which range in length from 38 to 43 amino acids (Thinakaran and Koo, 2008). Approximately 90% of Aβ produced is the Aβ 1-40 form, with less than 10 % being the longer Aβ 1-42 species (Thinakaran and Koo, 2008). Mutations in the APP gene can lead to an increased prevalence in cleavage at the 42 residue leading to increased production of Aβ 1-42 (Thinakaran and Koo, 2008).

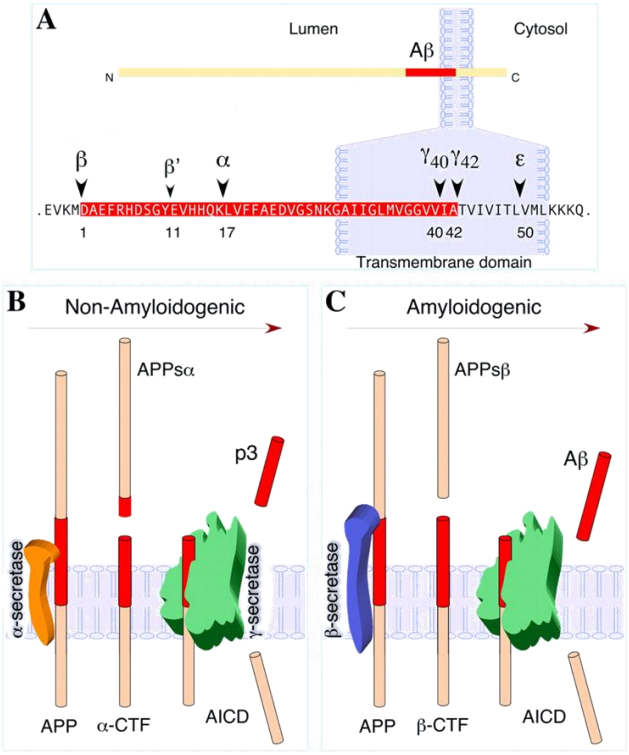

Figure 1.2 Processing of APP

Schematic diagram to show the proteolytic processing of APP, from Thinakaran and Koo(Thinakaran and Koo, 2008). A) Shows the major cleavage sites of the APP. B-secretase normally cleaves at residue 1 but can also cleave at residue 11. When β-secretase cleaves the APP, this is followed by cleavage with γ-secretase giving rise to Aβ peptides. APP can also be cleaved by α-secretase, giving rise to sAPPα. α-secretase cleaves the protein between residues 16 and 17, which prevents the formation of Aβ peptides. B) Shows cleavage by α- and γ-secretase, giving rise to non-amyloidogenic peptides. C) Shows cleavage of APP by β- and γ-secretase, giving rise to Aβ. AICD: Amyloid precursor protein intracellular domain and CTF: C-terminal fragment.

1.2.2.2 Aβ in disease

As mentioned in section 1.2.2.1, there are two main forms of Aβ formed in the brain; Aβ 1-40 and Aβ 1-42. The shorter species, Aβ 1-40 is most abundant whilst Aβ 1-42

is more prone to aggregation (Thinakaran and Koo, 2008). The ratio of these two isoforms is thought to be important in AD, with higher concentrations of Aβ 1-42 being associated with toxicity and disease (Hansson et al., 2007). In early AD, cerebral spinal fluid levels of Aβ 1-42 are reduced while Aβ 1-40 is increased which is thought to be due to Aβ 1-42 aggregating in the brain (Hansson et al., 2007, van Oijen et al., 2006). Aβ has a tendency to self-aggregate and form fibrillar plaques which are hallmark features of AD. Soluble assemblies of Aβ referred to as oligomers or protofibrils also form, possibly through different pathways or on the way to becoming fibrils. Soluble oligomers have been found at much higher concentrations in AD brains, sometimes up to 70-fold higher, than in those who are unaffected (Gong et al., 2003). The concentration of soluble oligomers correlates better with cognitive decline than the density of Aβ plaques (Lue et al., 1999, Zhang et al., 2011, Tomic et al., 2009) and they have been shown both *in vivo* and *in vitro* to be highly toxic (Kuo et al., 1996, Naslund et al., 2000, McLean et al., 1999, Mucke et al., 2000a, Manzoni et al., 2011, Haass and Selkoe, 2007, El-Agnaf et al., 2000, Cleary et al., 2005, Texido et al., 2011). Aβ oligomers are, therefore, thought to be important in causing cell death and neurodegeneration.

1.2.2.3 Tau and its relationship to Aβ

Another pathological feature of AD is intracellular neurofibrillary tangles (NFT), which are aggregates of the protein tau. Tau is a microtubule associated protein, which functionally stabilises microtubules (Mandelkow and Mandelkow, 1998). Tau is normally phosphorylated, but under disease conditions such as in AD tau becomes hyperphosphorylated (Mandelkow and Mandelkow, 1998) and detaches from the microtubules, which causes instability and altered cellular processes (Medina and Avila, 2014). Aggregated deposits of tau are not specific to AD, they fall into a group of diseases often referred to as the tauopathies (Medeiros et al., 2011, Medina and Avila, 2014). These include Pick's disease, progressive supranuclear palsy and corticobasal degeneration. Additionally, mutations in the

microtubule associated protein tau gene, *MAPT,* have been found to cause fronto-temporal dementia with Parkinsonism (FTD) (Medeiros et al., 2011, Medina and Avila, 2014). This demonstrates that dysfunction of tau can cause neurodegeneration. In AD it is likely that tau pathology may also be important in causing cell death and degeneration. Several studies have shown than Aβ pathology precedes tau deposition and that Aβ may cause tau hyperphosphorylation (Medeiros et al., 2011, Oddo et al., 2006, Oddo et al., 2004, Lewis et al., 2001, Oddo et al., 2007). On the other hand, tau does not seem to affect Aβ production; when tau is down-regulated it has no effect on levels of Aβ (Medeiros et al., 2011, Oddo et al., 2007).

1.3 Toxic species in PMDs and potential mechanisms leading to cell death

1.3.1 *In vivo* studies

In order to understand the disease mechanisms underlying PMDs it is essential to identify the toxic protein species and understand how and why a conformationally different protein structure can cause neuronal toxicity and cell death. There is much conflicting evidence in the literature, but recent studies appear to support the idea that a prefibrillar, oligomeric protein species is potentially the most toxic of the various protein assemblies (Simoneau et al., 2007, Zhang et al., 2010, Caughey and Lansbury, 2003, Kayed et al., 2003, Kuo et al., 1996, Lue et al., 1999, Naslund et al., 2000, McLean et al., 1999, Mucke et al., 2000a, Walsh et al., 2002, Quist et al., 2005, Kristiansen et al., 2007, Volles et al., 2001, Bucciantini et al., 2002).

Animal studies using transgenic APP over expressing mice have shown the earliest behavioural changes precede detectable fibrillar protein aggregation (Moechars et al., 1999, Hsia et al., 1999), and the presence of prefibrillar oligomers causes synaptic loss and precedes a behavioural phenotype (Caughey and Lansbury, 2003, Mucke et

al., 2000a). This supports the hypothesis that it is a prefibrillar protein species that causes the initial toxicity in AD.

In vivo studies of prion disease have been useful for understanding the different stages of neurodegeneration, since the starting point of the disease is defined by when the animals are inoculated with PrP^{Sc}. By examining animals at a pre-clinical phase, it is possible to uncover early changes in the disease process. Studies that have involved such experiments have shown that early stages of pathology include synaptic dysfunction and dendrite loss and these pathological changes seem to occur prior to neuronal cell death (Fuhrmann et al., 2007, Cunningham et al., 2003). Although fibril accumulation seems to occur around the same time as these pathological changes (Cunningham et al., 2003), it is still not clear whether the fibrils are causing the toxicity or if soluble oligomeric forms of PrP cause the damage prior to aggregation.

Genetic disorders can act as useful *in vivo* models for investigating certain aspects of the disease process. People with Down's syndrome have three copies of chromosome 21 meaning that they have three copies of the APP gene, which is the precursor for Aβ. This results in large quantities of Aβ being produced and generally an AD phenotype is seen by the time most individuals are in their fourth or fifth decade (Caughey and Lansbury, 2003, Lemere et al., 1996). The analysis of Down's syndrome patients' brains has highlighted that, in adults, there are dense Aβ plaques and NFT. Prior to this in the brains of children with Down's syndrome, accumulation of non-fibrillar Aβ can be seen which precedes plaque formation and AD phenotype (Lemere et al., 1996, Caughey and Lansbury, 2003).

Previous studies have suggested that it is only a subpopulation of fibrillar deposits with a β-sheet structure, which stain with dyes such as thioflavin-S, which are toxic to neurons (Caughey and Lansbury, 2003, Urbanc et al., 2002). Therefore, the β-sheet content of either fibrils or prefibrillar oligomers is an important factor in dictating

toxicity. *In vivo* studies show evidence for oligomers being important in the disease process of PMDs, however, since the pathology of the brain can only be analysed at set time points, it is difficult to show a definite cause and effect between misfolded protein species and neuronal toxicity. Therefore, *in vitro* studies can be used to look more closely at the mechanisms underlying neuronal loss.

1.3.2 *In vitro* studies

To date, *in vitro* studies have employed the use of a variety of cell lines as well as primary cell culture models (Novitskaya et al., 2006, Torres et al., 2010, Zhang et al., 2010, Ma et al., 2002). PrP oligomers have consistently been shown to be neurotoxic to a variety of cells (Novitskaya et al., 2006, Simoneau et al., 2007, Caughey and Lansbury, 2003), although, some variation has been seen. This variability may be due to differences in cell membrane composition of different cell types (Zhang et al., 2010), or differences in oligomer size or structure. When cells are incubated, *in vitro*, with fibrillar aggregates and assayed for toxicity the results have been variable (Novitskaya et al., 2006, Novitskaya et al., 2007, Quist et al., 2005, Simoneau et al., 2007, Kristiansen et al., 2007, Dahlgren et al., 2002, Ahmed et al., 2010). Some studies have suggested that the formation of fibrils may be protective since they sequester small soluble forms of misfolded protein (Haass and Selkoe, 2007, Treusch et al., 2009), or fibrils may just be the end point in the protein misfolding pathway (Caughey and Lansbury, 2003, Silveira et al., 2005, Soto, 2003, Ross and Poirier, 2004, Dobson, 2003). Other studies, however, have shown fibrils to be just as toxic as oligomers (Novitskaya et al., 2006, Novitskaya et al., 2007); these discrepancies may be due to differences in the structure of the fibrillar aggregates. Generally, protein preparations are often not extensively characterised prior to incubation with cells *in vitro*, therefore, differences in protein conformation may account for these inconsistencies. Presently, it is still not clear which protein species primarily causes neuronal cell death in PMDs.

The mechanisms associated with how misfolded proteins cause toxicity are also not well defined. Several studies have shown misfolded proteins to cause apoptotic cell death (Novitskaya et al., 2006, Simoneau et al., 2007, Youssef et al., 2008, Yang et al., 2009), while others have shown excitotoxicity to be important (Molinuevo et al., 2005, Esposito et al., 2013, Di et al., 2010, Dong et al., 2009, Tabrizi et al., 1999, Chiarlone et al., 2014, Muller et al., 1993, Sassoon et al., 2004, Thellung et al., 2013). Additionally, ER stress (Lindholm et al., 2006, Yoshida, 2007) and autophagy (Levine and Kroemer, 2008, Martinez-Vicente and Cuervo, 2007, Wong and Cuervo, 2010, Heiseke et al., 2010) have also been shown to be potential pathways leading to cell death after activation by misfolded proteins. Membrane disruption by oligomers, which affects the calcium levels within the cell triggering the apoptotic pathway (Simoneau et al., 2007, Zhang et al., 2010) has also been highlighted as a possible mechanism. It is thought that oligomers may insert into the phospholipid membrane, which causes a disruption in membrane potential (Kayed et al., 2004). This may provide another link between PMDs, since in some the misfolded protein accumulates inside the cell, while in others they accumulate in the extracellular space. Therefore, if it is the membrane which is affected this could be a plausible mechanism of toxicity for both intra and extracellular misfolded proteins.

Most *in vitro* studies of prion toxicity have been performed with recPrP or short fragments of recPrP, but studies have also been carried out using the yeast prion protein Ure2. Protofibrils of Ure2 were found to be toxic to neuronal cells in a dose dependent fashion (Zhang et al., 2010), whilst fibrils were also found to be toxic but to a lesser extent. Changes in conductivity and calcium levels leading to apoptosis were observed, which correlate with findings from mammalian recPrP studies (Zhang et al., 2010).

Many studies have also been undertaken using fragments of PrP, in particular the fragment corresponding with human residues 106-126. This fragment has been shown to fibrillise very quickly, particularly under slightly acidic conditions, and

has a β- sheet rich structure (Selvaggini et al., 1993). Additionally, it shows some resistance to proteinase K digestion as has been shown for PrP^{Sc} (Selvaggini et al., 1993). The size of the fibrils which it forms are thought to consist of approximately 6000 PrP molecules (Selvaggini et al., 1993). However, even in this fibrillar conformation PrP 106-126 has repeatedly been shown to be toxic to cells *in vitro* (O'Donovan et al., 2001, Jobling et al., 1999, Brown et al., 1996, Forloni et al., 1993). This may suggest that a fibrillar form of PrP can be toxic, and that perhaps toxicity is dependent on the structure or conformation of the fibrils.

The importance of PrP^{C} seems to be poorly defined in these *in vitro* studies; some show that the absence of PrP^{C} seems to attenuate the toxicity of oligomers and fibrils (Novitskaya et al., 2006), whilst other studies show that the toxicity of oligomers or fibrils seems to be unaffected by PrP^{C} expression (Simoneau et al., 2007). This adds another layer of complexity to the mechanisms which underlie neuronal toxicity in prion disease.

Most studies which have investigated the toxicity of Aβ *in vitro* have generally shown Aβ fibrils to be less toxic than oligomers (Dahlgren et al., 2002, Ahmed et al., 2010, Lesné et al., 2008). However, it has been proposed that fibrillar plaques may act as a reservoir of smaller oligomeric forms of Aβ, which can form a halo around the fibrillar plaque (Koffie et al., 2009). By contrast, Aβ oligomers have repeatedly been shown to be toxic (Manzoni et al., 2011, El-Agnaf et al., 2000). Various pathways have been shown to be activated by Aβ oligomers both *in vitro* and *in vivo*, including apoptosis (Youssef et al., 2008, Yang et al., 2009, Shimohama, 2000), excitotoxicity (Dong et al., 2009, Li et al., 2009, Alberdi et al., 2010, Li et al., 2011, Rammes et al., 2011, Rönicke et al., 2011), autophagy (Mizushima et al., 2008, Martinez-Vicente and Cuervo, 2007) and ER stress (Lindholm et al., 2006, Yoshida, 2007). All may be important under different conditions or for oligomers with different structures. Clinical trials are underway targeting some of these pathways; it remains to be seen whether any will reverse or slow disease progression.

1.4 Main objectives

To date, there is still uncertainty surrounding whether oligomers formed from different misfolded proteins cause cell death by similar mechanisms. Additionally, it is still unclear whether fibrils are inert and non-toxic or if they also play a role in causing disease. It has been hypothesised that oligomers composed of different disease associated misfolded proteins are toxic to neuronal cells and activate common intracellular pathways to cause cell death. In this thesis, I have tried to address these questions:

- Can recPrP and recAβ be produced in sufficient yield to allow them to be refolded into different disease associated structures and characterised?

I have produced recPrP and recAβ and refolded them into disease associated conformations, including fibrils and oligomers. I have characterised these misfolded species in order to clearly define links between structure and toxicity.

- Which misfolded species are most toxic? And is the toxic species the same for different proteins?

I have investigated the toxicity of the disease associated isoforms of recPrP and recAβ using murine primary cortical cells. This allowed me to establish the important toxic species associated with these diseases and compare their relative toxicities. This has brought new insights into how these misfolded isoforms may be involved in disease pathogenesis in two PMDs. As part of these investigations, I have explored how the disulphide bond in recPrP may be important in misfolding and associated toxicity. I found that the presence or absence of the disulphide bond was critically important in determining the size of oligomers which form and their associated toxicity.

- What pathways are activated by misfolded proteins? Do oligomers of recPrP and recAβ activate the same mechanisms?

Lastly, once I had established which of the misfolded proteins species were toxic I investigated the mechanisms and pathways that are activated by these misfolded proteins and lead to cell death. This work highlighted the complexity of these diseases and suggests that oligomers formed from different misfolded proteins may not cause cell death by activating the same pathways. Furthermore, fibrils may not be the same in all PMDs and may in some cases be involved in causing cellular toxicity and death.

Chapter 2:

Materials and Methods

2.1 General protein analysis

2.1.1 Denaturing SDS-PAGE

All SDS-PAGE analysis was carried out using the Novex NuPAGE SDS-PAGE gel system (Invitrogen). Protein samples were denatured with NuPAGE LDS sample buffer (4X) at a 3:1 ratio, the samples were heated at 100 °C for 10 minutes. The samples were centrifuged at 16100 g for 1 minute prior to loading to remove condensation. Samples were loaded onto a pre-cast NuPAGE Bis-Tris gel (Invitrogen), along with SeeBlue Plus2 pre-stained protein standard (Invitrogen). Proteins were resolved by electrophoresis at 180 V for 1 hour or until the lowest protein marker had reached the bottom of the gel. Gels were then analysed by coomassie, silver staining or western blotting.

2.1.2 Coomassie staining

To coomassie stain an SDS-PAGE gel, the gel was incubated with approximately 20 ml of InstantBlue (expedeon). Protein bands were left to develop for 2-24 hours. The gel was washed with MilliQ H_2O before being imaged with a flatbed scanner.

2.1.3 Silver staining

The gel was fixed for 1-24 hours (fixative: 30 % (v/v) ethanol, 10 % (v/v) acetic acid in MilliQ H_2O). Following fixation the gel was sensitised for 1 hour (sensitising solution (in a 100 ml final volume): 30 % ethanol, 0.2 % (w/v) sodium thiosulphate, 0.83 mM sodium acetate & 0.5 ml of 25% glutaraldehyde solution). The gel underwent 4 X 15 minute washes with MilliQ H_2O and was stained with silver nitrate for 1 hour (silver nitrate solution: (final volume 100 ml) 15 μM silver nitrate made up in MilliQ H_2O with 100 μl of 37 % formaldehyde solution). This was followed by two 1 minute washes with MilliQ H_2O, the gel was developed (developing solution: (final volume 100 ml) 0.24 mM sodium carbonate & 40 μl

formaldehyde) until the bands could be clearly seen. Once the bands were resolved the reaction was stopped with the stopping solution (50 μM EDTA). The gel was left in stopping solution for 1-24 hours and then washed in MilliQ H_2O before being imaged using a flatbed scanner.

2.1.4 Western blotting

Following SDS-PAGE the gel was transferred onto an Immobilon-P PVDF membrane using a semi dry transfer system (Invitrogen). Briefly, eight pieces of filter paper were cut to approximately 9 cm x 8 cm and soaked in transfer buffer (0.1 M tris, 0.19 M glycine, 5 % methanol (v/v)); a piece of PVDF membrane was cut to the same size and soaked in 100 % methanol. The semi-dry transfer stack was set up with four pieces of filter paper on the anode plate, the methanol soaked membrane was rinsed in transfer buffer and placed on top of the filter paper using tweezers. The SDS-PAGE gel was rinsed in transfer buffer and stacked on top of the membrane, the remaining four pieces of soaked filter paper were placed on top of the gel. A roller was used to push out any bubbles. The top cathode plate was placed on top of the stack and the screws fastened. The gel was transferred at 180 mA for 1 hour for 1 gel, or at 280 mA for 1 hour for 2 gels. The membrane was transferred to blocking solution: 5 % Marvel (w/v) made up in 1X TBS-T (0.01M tris, 0.14 M NaCl, 0.05 % tween (v/v)), for 1 hour or overnight. Once the membrane had been blocked, the blocking solution was replaced with the primary antibody which was diluted in 1 % Marvel (w/v) in TBS-T. The membrane was incubated with the primary antibody either for 1 hour at room temperature with agitation or overnight at 4 °C. The membrane was subjected to 3 X 15 minute washes in TBS-T with gentle agitation. The secondary antibody was applied, this was also diluted into 1 % Marvel (w/v) in TBS-T. The membrane was incubated with the secondary antibody for 1 hour at room temperature. The membrane was again subjected to 3 X 15 minute washes in TBS-T. Once the final wash was removed, the membrane was incubated with ECL western blotting detection reagent (GE Healthcare) for 2

minutes. The membrane was dried and exposed to Amersham Hyperfilm ECL for varying lengths of time. The film was developed using a Curix 60 processor (AGFA).

2.1.5 Native- PAGE

To analyse proteins in their native form, I used the Novex NativePAGE system (Invitrogen). Protein samples were mixed 1:3 with NativePAGE sample buffer (4X, Invitrogen) and not heated. Samples were loaded onto NativePAGE Novex 4-16% Bis-Tris protein gels, along with the NativeMark unstained protein standard. NativePAGE anode and cathode buffers were made according to manufacturer's guidelines (Invitrogen). Proteins were resolved by electrophoresis at 150 V for 105 minutes. Gels were fixed for 1-2 hours in fixative (40 % ethanol (v/v), 10 % (v/v) acetic acid), this was removed and replaced with more fixative for 8-16 hours, finally this was removed and fresh fixative was applied for a further 2 hours. The gel was silver stained either with the protocol outlined in section 2.1.3, or using SilverQuest silver staining kit (Invitrogen).

2.1.6 Determining protein concentration by spectroscopy

Protein concentration was determined by spectroscopy at 280 nm using a NanoDrop spectrophotometer. Before analysing the concentration of a protein, a reading was taken of the protein buffer which acted as the blank. Approximately 2 μl of the protein sample was loaded onto the NanoDrop and an absorbance reading at 280 nm was acquired. The molecular mass (MW) of the protein was then divided by the extinction coefficient (EC) and multiplied by the 280 nm absorbance reading to give the concentration of the protein in mg/ml. To obtain the molar concentration, the 280 nm absorbance reading was divided by the EC. The EC was calculated as shown in Gill and von Hippel(Gill and von Hippel, 1989). The MW and EC used for PrP was

MW: 23113 and EC: 61000. For Aβ 1-40, MW: 4329.8 and EC: 1490 and for Aβ 1-42, MW: 4514.1 and EC: 1490. For TEV MW: 28600, EC: 32290.

2.2 Expression of recombinant proteins

2.2.1 Expression of recombinant PrP

Full length recombinant murine PrP (recPrP) encompassing residues 23-230 was expressed in Rosetta *Escherichia coli (*Novagen). The Rosetta *E.coli* carrying the plasmid containing the mouse *prnp* gene were grown on selective plates containing ampicillin (100 μg/ ml) and chloramphenicol (50 μg/ ml) and left to grow overnight at 37 °C. A single colony was picked from the plate and grown in a 10 ml Luria broth (LB, Sigma) overnight culture containing ampicillin (100 μg/ ml) and chloramphenicol (50 μg/ ml). Approximately 3 ml of the overnight culture was added to 400 ml of terrific broth (TB, Sigma) containing ampicillin (100 μg/ ml) and chloramphenicol (50 μg/ ml) the culture was grown to an optical density with absorbance at 600 nm of 0.6- 1. Protein expression was induced using 1 mM Isopropyl β-D-1-thiogalactopyranoside (IPTG) and left for 16 hours. The cultures were transferred to 250 ml sorvall flasks the next day and centrifuged at 10 K rpm for 10 minutes (SLA-1500 rotor), the supernatant was disposed of and the pellets were frozen at -20° C for a minimum of 4 hours before lysis.

2.2.2 Expression of recombinant Aβ 1-40 and Aβ 1-42 fusion proteins

Plasmids for human recombinant Aβ 1-40 or Aβ 1-42 (recAβ 1-40 or recAβ 1-42) fusion proteins were obtained from Prof. Glockshuber's group(Finder et al., 2010). The fusion proteins consisted of a soluble polypeptide with 19 repeats of the amino acids NANP followed by the TEV recognition sequence ENLYFQ and then either the Aβ 1-40 or Aβ 1-42 sequence (a schematic of the fusion protein is shown in figure 3.8). The plasmids contained a T7 promoter and ampicillin resistance cassette.

The plasmids were transformed into BL21 (DE3) bacteria and selected for using ampicillin containing plates. A single colony containing either the recAβ 1-40 fusion protein plasmid or the recAβ 1-42 fusion protein plasmid were selected and grown in 10 ml LB overnight cultures containing ampicillin (100 μg/ ml). Approximately 3 ml of the overnight cultures was added to 400 ml TB cultures containing ampicillin (100 μg/ ml). The cultures were grown to an optical density (absorbance 600 nm) of 0.6- 1. Protein expression was induced using 1 mM IPTG and left for 16 hours. The cultures were transferred to 250 ml sorvall flasks the next day and centrifuged at 10 K rpm for 10 minutes (SLA-1500 rotor). The supernatant was disposed of and the pellets were frozen at -20° C for a minimum of 4 hours before purification.

2.2.3 Expression of recombinant tobacco etch virus (TEV) protease

Bacteria containing a plasmid encoding TEV protease and pLysS, (which decreases background expression of target genes) were available in the Gill group. Using a miniprep kit according to the manufacturer's protocol (Qiagen), I extracted the plasmids and transformed them into ArcticExpress competent cells (Agilent technologies) following the manufacturer's protocol. The transformed cells were grown on selective plates containing kanamycin (30 μg/ml), to select for the TEV plasmid. The cells were left to grow at 37 °C for 16 hours. Single colonies were selected and grown in 10 ml LB overnight cultures containing kanamycin (30 μg/ ml), gentamycin (20 μg/ ml, to select specifically for the arctic express bacteria) and chloramphenicol at (50 μg/ ml, to select for pLysS), the cultures were left to grow at 37 °C for 16 hours. Approximately 3 ml of the overnight culture was added to 250 ml of LB containing no antibiotics. The culture was grown to an optical density (absorbance 600 nm) of 0.6-1 at 30 °C at 225 rpm. The temperature was then reduced to 12 °C and left for 30 minutes to allow the bacteria to acclimatise. Protein expression was induced using 1 mM IPTG and left for 24 hours. The bacteria underwent centrifugation at 8 K rpm for 10 minutes (SLA-1500 rotor), the supernatant was then discarded and the cell pellet was suspended in TEV lysis

buffer (50 mM HEPES pH 7.5, 1 M NaCl, 10 % glycerol (v/v), 10 mM imidazole) 3 ml per gram of cells and snap frozen. The lysed bacteria were stored at -20 °C.

2.3 Bacterial cell lysis

2.3.1 RecPrP bacterial cell lysis

The cell pellets were re-suspended in lysis buffer (50 mM Tris, 1 mM EDTA, 100 mM NaCl pH 8), 9 ml per gram of cell pellet. Lysozyme was added to a final concentration of 0.2 mg/ml, this was left at 4 °C for 1 hour with stirring. Sodium deoxycholate was added to a final concentration of 1 mg/ml, this was left to stir at room temperature for 1 hour. DNAse was added to a final concentration of 4 μg/ml with $MgCl_2$ to a final concentration of 40 mM, this was left to stir at room temperature for a further 40 minutes. The inclusion bodies were pelleted by centrifugation at 12 K rpm for 15 minutes at 4 °C (SLA-1500 rotor). The inclusion body pellets were frozen at -20 °C for up to six months.

2.3.2 recAβ 1-40 and recAβ 1-42 fusion protein bacterial cell lysis

The frozen bacterial pellets were re-solubilised in 6 M guanidine hydrochloride (GdnHCl) pH 8.0 (10 ml per gram of cells) and mixed using a 10 ml pipette and stirred for 90 minutes at 4 °C. Cell debris was removed by centrifugation at 15 K rpm for 30 minutes at 4 °C (SLA-1500 rotor). The supernatant was collected and used for purification.

2.3.3 TEV bacterial cell lysis

See expression of TEV, section 2.2.3. Following storage at -20 °C the bacteria in lysis buffer were sonicated on ice for 10 minutes using a sonication water bath. The lysed bacteria underwent centrifugation at 15 K rpm for 30 minutes at 4 °C to pellet the

bacterial cell debris (SLA-1500 rotor). The TEV protease was produced as a soluble protein; the supernatant was collected and taken for purification.

2.4 Protein purifications

2.4.1 Purification of α-helical recPrP

2.4.1.1 Immobilised metal ion affinity chromatography (IMAC) for α-helical recPrP

The inclusion body pellets (refer to section 2.3.1) were first purified by means of nickel immobilised metal ion affinity chromatography (IMAC), which purifies PrP by binding of the histidine residues found on the N- terminal of the protein to nickel ions on the column. Any other proteins present were washed through leaving the PrP to be eluted. Buffer A (0.1 M sodium phosphate, 0.01 M tris, 8 M urea pH 8 & 210 μl β- mercaptoethanol) and buffer B (100 ml of buffer A pH 4.5 & 70 μl β-mercaptoethanol) were made up, the inclusion body pellets were re-suspended in buffer A; 5 ml of buffer per gram of cell pellet. They were left to re-suspend for 1 hour or more and then centrifuged at 15 K rpm for 20 minutes (SLA-1500 rotor). The supernatant was loaded onto a column made with nickel-NTA superflow resin (Qiagen), which had been equilibrated in buffer A. The column was washed with buffer A and the protein was eluted by a step gradient of 100 % buffer B, recPrP was detected as a single UV peak (absorbance 280 nm) which was collected. The eluted protein was analysed by SDS-PAGE to confirm the presence of recPrP. The recPrP containing fraction was diluted 1:1 with ion exchange buffer A (8 M urea, 0.05 M HEPES pH 8), this was left at 4 °C overnight.

2.4.1.2 Ion exchange chromatography for α-helical recPrP

The recPrP was purified further by means of ion exchange chromatography, which separated the recPrP from any other proteins by charge. PrP carries a positive

charge at neutral pH, therefore, a cation resin was used. Buffer A (8 M urea, 0.05 M HEPES pH 8) and buffer B (8 M urea, 0.05 M HEPES, 1.5 M NaCl, pH 8,) were made. The recPrP fraction from the IMAC step (section 2.4.1.1) was loaded onto a column made with SP sepharose fast flow cation resin (GE Healthcare), which had been equilibrated in buffer A. The column was washed with buffer A until the UV trace (absorbance 280 nm) reached baseline. The recPrP was eluted with a 0-50 % gradient of buffer B over 20 minutes. The eluting recPrP gave an absorbance peak at 280 nm, which was collected as one fraction. The eluted protein was analysed by SDS-PAGE to confirm the presence of recPrP and to assess the purity. The concentration of the recPrP was calculated using a spectrophotometer (see section 2.1.6). The recPrP was diluted to 0.1 mg/ml using buffers A + B. Following purification the protein was oxidised to form the disulphide bond at 4 °C for 16 hours with a five times molar excess of copper chloride.

2.4.1.3 Dialysis of α-helical recPrP

The oxidised and purified recPrP was dialysed to remove the 8 M urea present in the purification buffers. Approximately 5 litres of 50 mM sodium acetate and 10 mM EDTA (to chelate the copper ions) pH 5.5 was made, the recPrP was transferred to dialysis tubing with a molecular weight cut off of 12 kDa (Sigma). The PrP was dialysed for 4 hours at room temperature or overnight at 4 °C. Following this, the recPrP was dialysed for a further 4 hours at room temperature or overnight at 4 °C in 50 mM sodium acetate pH 5.5. Dialysis continued with buffer changes until the concentration of urea was calculated to be less than 100 nM, which was therefore dependent on the volume of recPrP (but usually would be 4-5 buffer changes). After dialysis the recPrP was removed from the dialysis tubing and concentrated.

2.4.1.4 Concentrating the purified protein

The recPrP was concentrated using an Amicon concentration cell with an Amicon filter with a molecular weight cut off of 10 kDa. The Amicon concentration cell uses nitrogen gas to create a vacuum and force the solution through the filter, leaving the recPrP which is larger than 10 kDa. The concentration of the sample was tested periodically until the concentration reached approximately 1 mg/ml. The concentrated recPrP was divided into 500 µl aliquots and stored at -80 °C.

2.4.2 Purification of recPrP for the production of oligomers and fibrils

The following method described in section 2.4.2 was modified from Makarava and Baskakov 2008 (Makarava and Baskakov, 2008).

2.4.2.1 IMAC for recPrP oligomers and fibrils

The inclusion body pellets were solubilised in IMAC buffer A (8 M Urea, 0.1 M Na_2HPO_4, 10 mM tris-HCl, 10 mM reduced glutathione, pH 8) with stirring for 1 hour at room temperature, the cell debris was pelleted by centrifugation at 15 K rpm for 30 minutes (SLA-1500 rotor). The supernatant was mixed with nickel-NTA agarose resin (Qiagen) and left to bind at room temperature on a rotator for 1 hour 30 minutes. The resin was then transferred to a 5 ml polyethylene column (Qiagen); the resin was washed with 4 column volumes of IMAC buffer A. The protein was then eluted with IMAC buffer B (IMAC buffer A adjusted to pH 4.5); 5 ml fractions were collected to which 50 µl of 0.5 M EGTA were added. SDS-PAGE gel analysis showed which fractions contained the eluted recPrP.

2.4.2.2 Desalting of recPrP for oligomers and fibrils

The recPrP was separated from the reduced glutathione present in the IMAC buffers by desalting. The fractions with the highest concentration of recPrP were pooled, up

to a maximum volume of 13 ml, this was loaded onto a HiPrep 26/10 desalting column (GE healthcare) equilibrated in desalting buffer (6 M Urea, 0.1 M tris-HCl, pH 7.5). The eluting recPrP gave an absorbance peak at 280 nm, which was collected as one fraction. The concentration of the recPrP containing fraction was determined using a spectrophotometer (see section 2.1.6).

2.4.2.3 Oxidation (disulphide-bond formation) of recPrP for oligomers and fibrils

The recPrP was diluted to 0.3 mg/ml in desalting buffer, EGTA was added to a final concentration of 5 mM and oxidised glutathione to a final concentration of 0.075 mM. The protein was left stirring overnight at 4 °C to oxidise (forming the disulphide bond) and refold. RecPrP with an intact disulphide bond will be referred to as oxidised PrP and recPrP without a disulphide bond will be referred to as disulphide-reduced PrP.

2.4.2.4 Reverse phase chromatography of recPrP for oligomers and fibrils

The recPrP was further purified by reverse phase (RP) chromatography, using a Dionex HPLC and Grace VYDAC® 214TP C4 reversed phase column. The oxidised recPrP sample was diluted 1:3 in RP buffer A (0.1 % trifluoroacetic acid (TFA) in H_2O) and then filtered. It was loaded onto the C4 column, which had been equilibrated in RP buffer A, in batches of approximately 6 mg of protein. The recPrP was eluted from the column by a gradient of buffer B (0.1 % TFA in acetonitrile) 0-15 % buffer B in 5 minutes, 15-35 % in 30 minutes, 35-50 % in 10 minutes and then up to 100 % B in 5 minutes, before returning to 0 % B. All fractions were analysed by SDS-PAGE to confirm which fractions contained recPrP and to assess the purity.

2.4.2.5 Analysis of intact proteins by online LC-MS

All mass spectrometry analyses were performed by dedicated staff in the Roslin Institute Proteomics and Metabolomics Facility. Samples for analysis were diluted to approximately 1 pmole/μl in HPLC A buffer (0.1 % (v/v) trifluoroacetic acid in water) except where their concentration could not be determined when they were used neat. 5 μl of the resulting sample was injected, by means of an Ultimate 3000 autosampler (Dionex, Thermo) onto a Vydac MS C4 reversed phase HPLC column. Buffer was pumped through the column at 10 μl/min by means of an Ultimate 3000 Pump (Dionex, Thermo) and retained components were eluted by means of a multistep gradient from 100% HPLC buffer A to 100% HPLC Buffer B (0.1 % (v/v) TFA in acetonitrile) as follows: 0 mins, 0% B; 3 mins, 20% B; 25 mins, 60% B; 26 mins, 100% B. These conditions produced rapid separation of proteinaceous species from salts/buffers and from each other.

The output from the HPLC column was routed to the electrospray source of an Amazon ETD ion trap mass spectrometer (Bruker) operated in positive ion mode. This instrument acquired full scan mass spectra from m/z 500-2000 (trap target 200,000; maximum accumulation time 200 ms, 5 averages per spectrum) and was operated in ultrascan mode (32,500 m/z per sec). All total ion count (TIC) chromatograms in this thesis were prepared without smoothing. Mass spectra were smoothed and deconvoluted to give accurate measures of mass and to confirm the presence or absence of modifications such as glutathione adducts.

2.4.2.6 RecPrP disulphide-bond reduction

Oxidised lyophilised recPrP was solubilised in ion exchange buffer A (8 M urea, 50.3 mM HEPES, pH 8, with DTT to a final concentration of 1 mM), this was left to reduce overnight on a roller at room temperature. The disulphide-reduced recPrP was then purified by RP; see purification of oxidised recPrP. The only modification

was that the eluting gradient was 0-20% buffer B in 5 minutes, 20-40% buffer B in 30 minutes and 40-50% B in 5 minutes. The eluted protein was analysed by SDS-PAGE for purity and mass spectrometry to confirm the disulphide-reduced state. Disulphide-reduced recPrP fractions were lyophilised and stored at -20 °C.

2.4.3 Purification of recAβ 1-40 and recAβ 1-42 fusion proteins

The following protocol was adapted from Finder *et al*.(Finder et al., 2010).

2.4.3.1 IMAC for recAβ 1-40 and recAβ 1-42

For either recAβ 1-40 or recAβ 1-42, the supernatant which was collected following centrifugation (see section 2.2.2) was loaded onto a column containing nickel-NTA superflow resin (Qiagen). The column had been previously equilibrated with 6 M GdnHCl pH 8.0. Following loading of the sample the column was washed with 20 ml of 6 M GdnHCl pH 8.0, followed by washing with 6 M GdnHCl pH 6.0 for 4 column volumes (CV). The fusion proteins were eluted with 3 CVs of 6 M GdnHCl pH 2.0 and stored at 4 °C overnight prior to RP chromatography. Fractions were confirmed to contain recAβ 1-40 or recAβ 1-42 by SDS-PAGE.

2.4.3.2 RP chromatography for recAβ 1-40 and recAβ 1-42

RecAβ 1-40 and recAβ 1-42 were purified further by reverse phase chromatography, using a Dionex HPLC and Grace VYDAC® 214TP C4 reversed phase column. RecAβ 1-40 or recAβ 1-42 IMAC fractions were diluted 1:3 in RP buffer A (0.1 % TFA in H_2O) and filtered using a 0.22 μM filter. The sample was loaded onto the C4 column which had been equilibrated in RP buffer A, in batches of approximately 6 mg of protein. RecAβ 1-40 or recAβ 1-42 was eluted from the column by a gradient of buffer B (0.1 % TFA in Acetonitrile) 0-10 % buffer B in 5 minutes, 10-50 % in 30 minutes, 50-100 % in 5 minutes, before returning to 0 % B. All fractions were analysed by SDS-PAGE to check which fractions contained the correct protein and

to assess the purity of the sample. Fractions containing recAβ fusion protein were lyophilised and stored at -20 °C.

2.4.4 Purification of recTEV protease

2.4.4.1 IMAC for recTEV produced as a soluble protein

The supernatant which was collected following centrifugation (see section 2.2.3) was loaded onto a column containing nickel-NTA superflow resin (Qiagen). The column had been previously equilibrated with load buffer (50 mM HEPES pH 7.5, 800 mM NaCl, 10 % (v/v) glycerol, 10 mM imidazole). Following loading of the sample the column was washed with 2 CVs of the load buffer and washed with 3 CVs of the wash buffer (load buffer with 50 mM NaCl). The recTEV protease was eluted with a step gradient to 100 % elution buffer (wash buffer with 400 mM imidazole pH 7.4). The peak at absorbance 280 nm was collected in one fraction and diluted 8 fold with the wash buffer. This was then stored at 4 °C overnight prior to cation exchange chromatography. Fractions were confirmed to contain recTEV by SDS-PAGE.

2.4.4.2 Cation exchange for recTEV protease

RecTEV containing fractions from IMAC were loaded onto an ion exchange column containing SP sepharose fast flow cation exchange resin (GE Healthcare). The column had first been equilibrated in the load buffer (50 mM HEPES pH 7.5, 50 mM NaCl, 10 % (v/v) glycerol, 10 mM imidazole). Following the sample being loaded, the column was washed with 3 CVs of the load buffer. The recTEV was eluted with a 0-100 % gradient over 25 minutes with the elution buffer (50 mM HEPES, pH 7.5, 800 mM NaCl, 10 % (v/v) glycerol, 10 mM imidazole). The UV peak at 280 nm was collected and analysed by SDS-PAGE. The recTEV containing fraction was concentrated and applied to a desalting column (see section 2.3.4.3).

2.4.4.3 Desalting buffer exchange for recTEV protease

Prior to buffer exchange using a desalting column (to exchange the imidazole containing purification buffer to a suitable storage buffer) the recTEV was first concentrated using a Vivaspin concentration column (GE healthcare). The protein was applied to the Vivaspin column which had a filter cut off of 10 kDa, and spun in a centrifuge until the volume was 1-2 ml. The concentrated protein was applied to a HiPrep 26/10 desalting column (GE healthcare), which was equilibrated in storage buffer (50 mM HEPES pH 7.5, 300 mM NaCl, 10% (v/v) glycerol). A peak at 280 nm showed the eluting recTEV protease, which was collected. The recTEV fraction was analysed by SDS-PAGE and the concentration was determined using a spectrophotometer (see section 2.1.6). The recTEV was split into aliquots which were snap frozen and stored at -20 °C until needed for cleavage reactions.

2.4.5 Cleavage of recAβ 1-40 and recAβ 1-42 fusion proteins and subsequent purification

2.4.5.1 Cleavage of fusion proteins

Cleavage of the recAβ 1-40 and recAβ 1-42 fusion proteins was achieved by solubilising either the lyophilised recAβ 1-40 or recAβ 1-42 fusion protein with TEV cleavage buffer (10 mM tris-HCl, 0.5 mM EDTA, 1 mM DTT, pH 8) so that the concentration was approximately 1 mg/ml. RecTEV was added to the solution (with the ratio of 1:20 TEV: fusion protein), this was mixed before being incubated at 30 °C for recAβ 1-40 for 16 hours or 4 °C for recAβ 1-42 for 16 hours (recAβ 1-42 aggregated at 30 °C). Cleavage was confirmed by SDS-PAGE as indicated by the presence of a low molecular weight band (4.5 kDa), which was the cleaved recAβ.

2.4.5.2 Purification by RP chromatography of recAβ 1-40 and recAβ 1-42 following TEV cleavage

Once cleaved, recAβ is prone to aggregation. To disaggregate the solution the cleaved recAβ was diluted 1:3 with 70 % formic acid. The sample was diluted 1:3 with RP buffer A (0.1 % TFA in H_2O) and filtered using a 0.22 μM filter. The recAβ sample was loaded onto a Zorbax SB300 C8 column (Agilent), which was heated at 80 °C on a heat block with a 2.5 ml coil preceding it to increase heat exchange. To separate recAβ 1-40, the column was equilibrated in 30 % RP buffer B (0.1 % TFA in acetonitrile) and 70 % buffer A, the recAβ 1-40 sample was loaded and would elute straight away. To separate recAβ 1-42, the column was equilibrated in 32 % RP buffer B and 68 % buffer A, the recAβ 1-42 sample was loaded and would elute straight away. The absorbance for both recAβ 1-40 and recAβ 1-42 was set to 214 nm since both absorb poorly at 280 nm, all separate absorbance peaks were collected. The purity of the fractions was analysed by SDS-PAGE. The recAβ 1-40 and recAβ 1-42 containing fractions were lyophilised and stored at -20 °C.

2.4.5.3 RecAβ monomerisation

Purified recAβ has a tendency to aggregate, therefore following purification it was important to monomerise the protein so that the starting material for oligomerisation and fibrillisation assays was defined. Pure lyophilised recAβ was solubilised in hexafluoroisopropanol (HFIP), 50 μl was added to each tube of cleaved Aβ and the tubes were pooled. Aβ was left in the HFIP for 30 minutes at room temperature. The HFIP was removed using a vacuum concentrator (speedvac). The dried recAβ monomer was stored at -20 °C.

2.5 Protein characterisation

2.5.1 Circular dichroism (CD) spectroscopy

The secondary structure of recPrP was analysed by CD spectroscopy (Jasco J-710, spectropolarimeter). Generally the concentration of the sample was 1 mg/ml so a cell with a path length of 0.1 mm was appropriate. Scans between 260 and 190 nm were acquired, with 20 scans taken for each sample. The following parameters were used: step resolution: 0.1 nm, speed: 100 nm/min, bandwidth 2.0 nm and sensitivity: 20 mdeg. A buffer control sample was also analysed and subtracted from the recPrP spectrum.

2.5.2 Dynamic light scattering (DLS)

DLS measures the hydrodynamic radii of proteins present in a sample. Larger proteins cause the light to scatter more than smaller proteins, and a protein assembly or oligomer would scatter the light more than a monomer. Samples were analysed by DLS to determine whether the proteins were in a monomeric form or assembled into oligomers or fibrils. Approximately 70 µl of sample was loaded onto a 384 well plate and applied to a Zetasizer auto plate sampler (Malvern Instruments ltd.) at 25 °C with a 830-nm laser. The hydrodynamic radii for proteins within each sample were determined by performing three independent runs of three measurements (13 × 10 second readings of each sample, with 120 second equilibration time). The mean diameter was then calculated within each run from the 3 replicates, and then an overall average was determined from 3 independent runs.

2.5.3 Congo red staining

To stain fibrils for amyloid, Congo red staining was used. Approximately 20 µL of fibrils (at approximately 1 mg/ml) underwent centrifugation at 16100 g at 4°C for 2

hours to pellet all fibrillar protein. The supernatant was discarded and 50 µl of alkaline NaCl solution (0.02 mM NaCl made up in 80 % (v/v) ethanol with 100 µL 1 % (w/v) NaOH) was added to the pellet, this was incubated at room temp for 20 minutes. The fibrils were again pelleted by centrifugation at 16100 g at 4°C for 15 minutes. The supernatant was again discarded and 50 µl of alkaline Congo red solution (2.9 µM Congo red, made up in 0.2 mM NaCl in 80 % (v/v) ethanol + 100 µL 1 % (w/v) sodium hydroxide) was added to the pellet. The pellet was mixed gently using a pipette and incubated for 20 minutes at room temperature. The fibrils were again pelleted by centrifugation at 16100 g at 4°C for 15 minutes. The supernatant was discarded and 50 µl of 20 % (v/v) ethanol was added to the pellet and mixed gently with a pipette. The fibrils were once again pelleted by centrifugation at 16100 g at 4°C for 15 minutes and the supernatant was discarded, 50 µl of 20 % (v/v) ethanol was added to wash the pellet. The ethanol was removed by pipette and the pellet was allowed to air dry. The pellet was reconstituted in phosphate buffered saline (137 mM NaCl, 3 mM KCl, 8 mM Na_2HPO_4, 1.5 mM KH_2PO_4, pH 7.5) and applied to a coverslip where it was allowed to air dry. The slides were mounted and analysed using a Nikon E800 x/y stage with cross polarisers. Amyloid was visualised under polarised light as yellow/ green birefringence.

2.5.4 Transmission electron microscopy (TEM)

All TEM sample preparation and analyses were performed by dedicated staff at king's buildings, University of Edinburgh. A droplet of the fibril suspension (fibrils were in 50 mM sodium acetate pH 5.5) was allowed to settle on a Formvar/Carbon 200 mesh Copper grid for 10 minutes. Excess liquid was removed by touching the grid edge with filter paper. A drop of 1% uranyl acetate was applied for 30 seconds then removed by touching the grid edge with filter paper. The grids were air dried and were viewed in a Philips CM120 Transmission electron microscope. Representative images were taken on a Gatan Orius CCD camera.

2.6 Oligomerisation assays

2.6.1 RecPrP oligomerisation

The following method was adapted from Rezaei *et al.* (Rezaei et al., 2005)

Lyophilised recPrP was solubilised in 20 mM sodium citrate pH 3.4 to 1 mg/ml, this was heated for 2.5 hours at 45 °C on a heat block. A TSKgelG4000SWxl gel filtration column (300 mm × 7.8 mm; TOSOH Bioscience) was equilibrated in 20 mM sodium citrate pH 3.4 and was used to analyse the oligomers. After 2.5 hours at 45 °C, approximately 15 μl of the oligomer sample was injected onto the column; 1 ml fractions were collected for SDS-PAGE gel analysis to confirm that the peaks at absorbance 280 nm were recPrP. When investigating the percentage of disulphide-reduced recPrP needed to form the larger oligomer species, the oxidised and disulphide-reduced recPrP were both solubilised in 20 mM sodium citrate pH 3.4 to 1 mg/ml, the disulphide-reduced recPrP was mixed with the oxidised recPrP to the desired percentage and then heated at 45 °C.

2.6.2 Aβ oligomerisation

The following method was adapted from Stine *et al*.(Stine et al., 2003)

Monomerised recAβ was solubilised in dimethyl sulfoxide (DMSO) and the concentration was analysed using a spectrophotometer (see section 2.1.6). The desired concentration was above 3000 μM. The monomer in DMSO was diluted into ice cold DMEM/F-12 cell culture media with no phenol red (Invitrogen), to a final concentration of 100 μM. This was mixed gently with a pipette and incubated at 4 °C for 24 hours. The resulting oligomers were analysed by DLS (see section 2.5.2).

2.7 Fibrillisation assays

2.7.1 RecPrP fibrillisation assay

The following protocol was modified from Breydo *et al.* (Breydo et al., 2008).

Lyophilised recPrP was solubilised in 6 M GdnHCl to a final concentration of 3-5 mg/ml. Fibrillisation reactions were carried out in black bottom 96 well plates. The final reaction mixture for each well consisted of PrP (55.56 μl of 3-5 mg/ml stock), MES buffer (16.6 μl of 0.5 M pH 6), thiourea (3.3 μl of 0.5 M pH 6) and thioflavin T (1.67 μl of 1 mM). Each well also contained 3 Teflon spheres. A no PrP control was also set up, which contained all buffers but no PrP. This acted as a background control which was subtracted from the PrP fibrillisation reactions. The 96 well plate was shaken continuously for 24 hours at 37 °C using a microplate reader, fluorescence readings were taken at 5 minute intervals to follow fibril formation. The fibrils were removed from the plate and dialysed into 50 mM sodium acetate and were stored at 4 °C. A non-fibrillar control was not shaken and instead left at room temperature for 24 hours to be used in characterisation experiments.

The fibrils were analysed by heating with a detergent to determine whether amyloid fibrils had formed or whether the protein had assembled into unstructured aggregates. Approximately 500-1500 ng of fibrils were mixed with triton X-100 and 1 M tris in 3 tubes, tube 3 was heated to 80 °C for 15 minutes. Proteinase K (1: 100 ratio of PK to PrP) was then added to tubes 2 and 3, they were both incubated at 37 °C for 1 hour. The reaction was stopped with pefabloc and 8 μl of loading buffer (125 mM TRIZMA base, 4.5 M urea, 20 % glycerol, 1.25 M β-mercaptoethanol, 4 % SDS and 0.02 % (w/v) bromophenol blue) was added to each tube. The samples were analysed by SDS-PAGE and the gel was silver stained. The fibrils which had been heated to 80 °C and digested with PK showed a 16 kDa band, which is

characteristic of amyloid fibrils(Breydo et al., 2008). The non-fibrillar control underwent the same characterisation and was compared with the fibrils.

2.7.2 Aβ fibrillisation assay

Monomerised recAβ was solubilised in 10 mM sodium hydroxide and the concentration was analysed using a spectrophotometer (see section 2.1.6). The desired concentration was as close to 1000 μM as possible. The solubilised recAβ was diluted into 50 mM HEPES pH 7.4 to a final concentration of 100 μM and thioflavin T was added to a final concentration of 20 μM. Once the recAβ had been diluted with HEPES, it was loaded onto a 96 well, black bottom plate. A no Aβ control was also set up, which contained only buffer and thioflavin T. The 96 well plate was incubated at 37 °C using a microplate reader for 24 hours. Fluorescence readings were taken at 1 minute intervals to follow fibril formation. Before each reading the plate was gently agitated for 10 seconds to ensure the sample was homogenous. The fibrils were removed from the plate and stored at 4 °C.

2.8 Primary cell culture experiments

2.8.1 Culturing of primary cortical cells

Cortical mouse neurons were cultured by members of the Hardingham lab and supplied to me after 9 days *in vitro* for toxicity experiments.

Cortical neurons from E17 mice were cultured using the methods described in Papadia et al 2008 (Papadia et al., 2008). Briefly, 24 well tissue culture plates were incubated for at least two hours at 37 °C in poly-D-lysine and Laminin (Sigma). Embryos were anaesthetised with an intraperitoneal injection of sodium pentobarbital (Merial Animal Health) and decapitated. Brains were removed, cortices dissected and placed in dissociation medium (81.8 mM Na_2SO_4, 30 mM

K_2SO_4, 5.84 mM $MgCl_2$, 252 μM $CaCl_2$, 1 mM HEPES, 0. 1% Phenol Red, 20 mM glucose, and 1 mM Kyurenic acid). Once the required number of cortices had been isolated they were placed in a tube, excess liquid was removed and they were incubated for 20 minutes at 37 °C in dissociation medium containing 10 units/ml of papain (Worthington Biochemical Corporation). The media was then removed and this digestion step was repeated. The cortices were then washed twice in dissociation media and twice in growth medium (NeuroBasal-A Medium, 2 % B-27 Supplement, 1 mM glutamine and anti-bacterial/anti-mycotic, (Invitrogen)). Following washing, the cortices were dissociated using a 2 ml disposable plastic pipette in 10 ml of warm growth medium. This cell suspension was then diluted using Opti-MEM (Invitrogen) containing 20 mM glucose, to a concentration of one cortical hemisphere per 14 ml of cell suspension. This solution was then plated into the pre-coated tissue culture plates, with 500 μl of cell suspension per well of the 24-well plate. The plates were then incubated at 37 °C with 5 % CO_2 for 2.5 hours, the cell suspension was then removed and replaced with 1 ml of growth medium. After 4 days *in vitro*, 1 ml of growth media supplemented with 9.6 μM cytosine β-D-arabinofuranoside hydrochloride (AraC, Sigma) was added to the cells to prevent proliferation of glial cells.

This cell model has been previously characterised and is shown in Gouix *et al*. 2009 (Gouix et al., 2009). It was shown that when AraC is used to inhibit glial proliferation, the cultures are enriched for neurons and contain less than 5 % glia (Gouix et al., 2009, Deighton et al., 2014). This was shown clearly in both studies by immunocytochemistry using both glial and neuronal markers.

2.8.2 Toxicity experiments

At day 9 post culturing, the cells were incubated with basal medium for 2 hours before being dosed with the recPrP or recAβ samples, which had been diluted into basal medium. The cells were incubated with either the recPrP of recAβ samples in

a 37 °C incubator for 24 hours, before being fixed in 4 % paraformaldehyde for 20 minutes. The cells were then washed with PBS and then incubated with PBS containing 0.05 % NP40 for 5 minutes to permeabilise the cells, this was then washed off with PBS. The cells were stained with DAPI mounting medium (VECTASHIELD®) and a coverslip was placed over the cells in each well. The cells were visualised using a Leica AF6000 LX imaging system with a DFC350 FX digital camera; 3-4 images were taken of each well using a 10 X 0.3 dry lens with a DAPI filter. For each image more than 500 cells were analysed. The images were analysed using IMAGE J, the pictures were converted into 8 bit files and the threshold of the fluorescence was adjusted until most nuclei could be seen without over exposing other nuclei, this was then converted into a black and white image (figure 2.1) A plug- in macro then numbered all nuclei and recorded the size of each (figure 2.1). They were then counted using the macro; cell viability was quantified by the number of non-apoptotic nuclei as a percentage of the total number of cells, which was determined by the size of the nuclei; with dead cells having small and shrunken nuclei compared to live cells. For each experiment the average size of a live cell nucleus was determined and the average size of a dead cell nucleus, this was then used to calculate the total number of live and dead cells. Cells were also dosed with the corresponding buffer controls: recPrP oligomers (20 mM sodium citrate pH 3.4), recPrP monomer or fibrils (50 mM sodium acetate pH 5.5), recAβ monomer (DMSO), recAβ oligomers (DMSO + DMEM/F12 media) or recAβ fibrils (sodium hydroxide and HEPES pH 7.4), to control for any background cell death caused by the buffer. The cell viability data was normalised to the buffer controls.

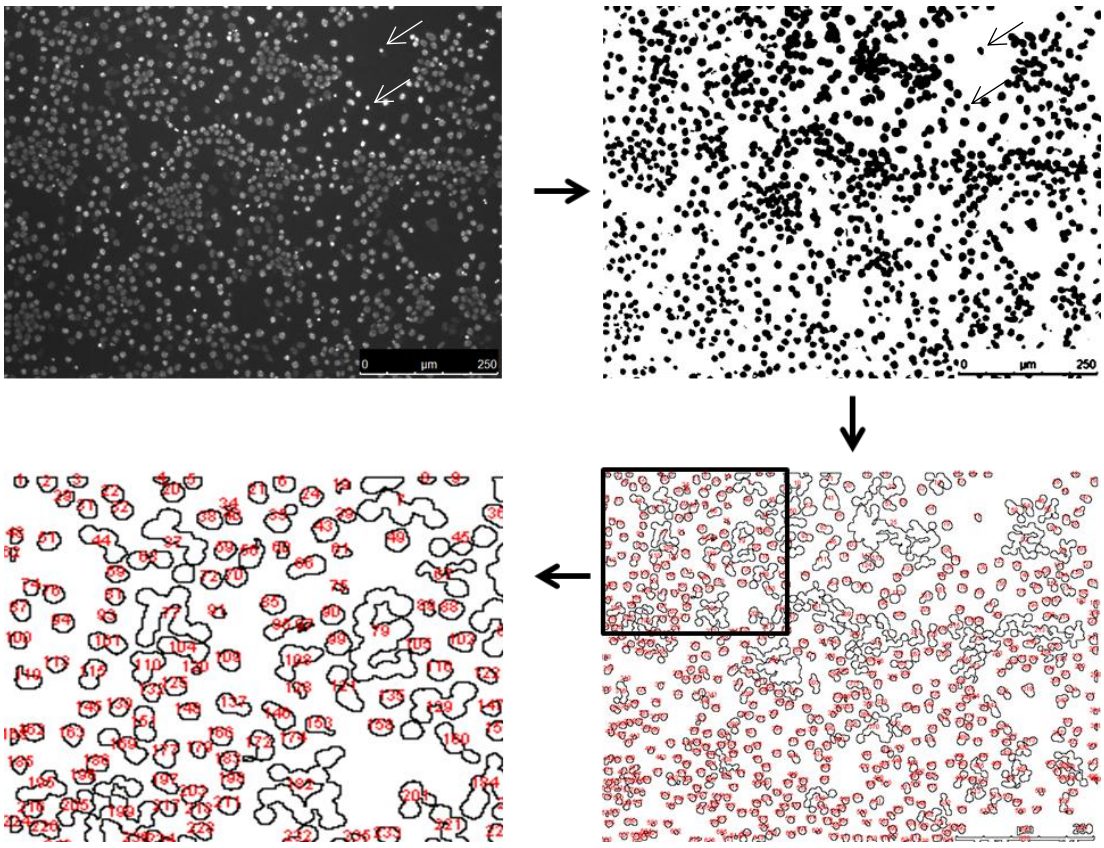

Figure 2.1 Cell viability image analysis

Top left, DAPI image of untreated murine cortical cells. The DAPI image was converted into a black and white image in image J, (top right). A plug-in macro converted this into an image in which all nuclei were numbered and measured for their size (bottom right). A magnified section of the numbered image is shown in the bottom left. A list of the numbered nuclei with their size was produced, allowing cell viability to be calculated. The arrows in the top two images show shrunken nuclei indicative of dead cells.

2.8.3 Caspase inhibitor experiments

To investigate whether cells were dying by apoptosis, the caspase inhibitor Q-VD – Oph was used (Merck). The cells at 9 days post culturing were first incubated with basal medium for 2 hours, this was removed and replaced with basal medium containing 50 μM Q-VD–Oph. The cells were incubated with the Q-VD–Oph for 1

hour, recPrP or recAβ was added and the cells were incubated in a 37 °C incubator for 24 hours, before being fixed and stained as shown for the toxicity experiments. Cells were also incubated with recPrP or recAβ alone so that the toxicity could be compared. Staurosporine (200 nM) was used as a positive control for apoptosis and was added to the cells in the same way as the recPrP or recAβ after the 1 hour incubation with Q-VD–Oph (50 μM). Cells were also treated with staurosporine alone so that toxicity could be compared between those treated with Q-VD–Oph and staurosporine or staurosporine alone.

2.8.4 NMDA receptor antagonist experiments

To investigate whether cells were dying by excitotoxicity, the NMDA receptor antagonist MK 801 (Tocris) was used. The cells at 9 days post culturing were first incubated with basal medium for 2 hours, this was removed and replaced with basal medium containing 10 μM MK 801. The cells were incubated with MK 801 for 1 hour, before recPrP or recAβ was added and the cells were incubated in a 37 °C incubator for 24 hours. The cells were fixed and stained as shown for the toxicity experiments. Cells were also incubated with recPrP or recAβ alone so that the toxicity could be compared. NMDA (50 μM) was used as a positive control for excitotoxicity and was added to the cells in the same way as the recPrP or recAβ after the 1 hour incubation with MK 801. Cells were also treated with NMDA alone so that toxicity could be compared between those treated with NMDA and MK 801 or NMDA alone.

2.8.5 Cell viability data analysis

For cell viability assays a minimum of 6 images were analysed for each condition (3-4 pictures per well with 2 wells for each), the treated cells were normalized to the buffer control and expressed as a percentage. A minimum of 3 repeats were carried out for each toxicity experiment. To test for significant differences in cell viability

between cells treated with different protein conformations, I first tested for normality using the Shapiro-Wilk test. This allowed me to ensure that the data was normally distributed within each group. I used the Shapiro-Wilk test because it is appropriate for small sample sizes. This analysis showed that the data was normally distributed which meant that a parametric statistical test such as an ANOVA was appropriate. I next used a one- way ANOVA with Bonferroni post hock correction, this corrected for the number of different pairwise comparisons making it less likely that there would be a significant difference found between two of the groups by chance. These analyses were done in SPSS version 21. To analyse whether there had been a significant recovery in cell viability in cells treated with the caspase inhibitor or NMDA receptor antagonist, a paired 2 tailed t-test was carried out to compare cells treated with protein alone (recPrP or recAβ, oligomers or fibrils) and cells treated with the protein and the inhibitor.

2.8.6 Western blotting for caspases and ER stress markers

Western blotting was used to probe for the presence or up-regulation of ER stress markers in cells treated with recPrP isoforms. Western blotting was also used to detect activated caspase 3 in recPrP treated cells, to test for cells undergoing apoptosis. The cells were lysed following incubation with the recPrP isoforms. The cell culture media was removed and replaced with 25 μl of RIPA lysis buffer (150 mM sodium chloride, 50 mM tris, 1 % (v/v) triton X-100, 0.5 % (w/v) sodium deoxycholate, 0.1 % (w/v) sodium dodecyl sulphate (SDS), containing 1X complete protease inhibitor cocktail (roche)) per well. The cells were left to lyse on ice for 45 minutes. The wells of the plate were scraped with a pipette tip and the lysates were transferred to 1.5 ml tubes. The lysates were sonicated in a sonicating water bath on ice for 10 minutes to ensure complete lysis. The cell debris was pelleted by centrifugation at 16100 g for 10 minutes at 4 °C. The lysate was removed being careful not to disturb the cell pellet. The lysate was either used straight away for western blotting, or frozen on dry ice and stored at -80 °C until use. The antibodies

used were: cleaved caspase-3 (Cell Signaling) used at 1:1000 dilution, BiP (Cell Signaling) used at 1:1000 dilution, caspase 12 (Cell Signaling) used at 1:1000 dilution, β-actin (Cell Signaling) used at 1:3000 dilution, CHOP (Cell Signaling) used at 1:800 dilution, phospho-eIF2α (Cell Signaling) used at 1:1000 dilution, EIF2α (Cell Signaling) used at 1:1000 dilution and anti-rabbit IgG (AG154) secondary antibody was used for all western blots (sigma) at a dilution of 1: 2500. When western blotting for ER stress markers or caspases the western blotting protocol shown in section 2.1.4 was followed except that for CHOP, phospho-eIF2α and EIF2α where the following modifications were made: 5% BSA was used for the primary antibody solution, 3 X 5 minute TBS-T washes were carried out first to wash off the blocking buffer and for all other wash steps 3 X 5 minute TBS-T washes were carried out.

Chapter 3:

Production and characterisation of disease associated isoforms of recPrP and recAβ

3.1 Introduction

Protein misfolding diseases (PMDs) are a group of related conditions commonly associated with large insoluble aggregates or fibrils of disease associated proteins in the brain (Bucciantini et al., 2002, Caughey and Lansbury, 2003, Knowles et al., 2014, Braak et al., 2003). These insoluble protein deposits are seen as the hallmark features of many of these diseases, such as the amyloid beta (Aβ) plaque in Alzheimer's (Alzheimer, 1907, Alzheimer, 1911, Braak and Braak, 1991) or Lewy bodies in Parkinson's disease(Braak et al., 2003). Although large fibrillar aggregates are associated with these diseases, it is widely debated whether these fibrillar deposits are themselves toxic to surrounding cells, simply the end point of the aggregation process(Soto, 2003, Ross and Poirier, 2004, Dobson, 2003), or perhaps a protective mechanism by the cells (Haass and Selkoe, 2007, Treusch et al., 2009). By contrast, small soluble assemblies of disease associated proteins, which are often termed oligomers, are generally accepted to be important in the pathogenesis of PMDs (Kuo et al., 1996, Lue et al., 1999, Naslund et al., 2000, McLean et al., 1999, Mucke et al., 2000a, Walsh et al., 2002, Quist et al., 2005, Kristiansen et al., 2007, Simoneau et al., 2007, Volles et al., 2001). This has led to the hypothesis that there could be a shared mechanism leading to cell death instigated by oligomers (Glabe, 2006, Kayed et al., 2003, Haass and Selkoe, 2007, Quist et al., 2005).

As I stated in chapter 1, my main aims were to produce and characterise disease associated isoforms, namely oligomers and fibrils, of recPrP and recAβ, and to assess the toxicity and related mechanisms caused by these misfolded proteins. In order to investigate relationships between conformation and toxicity, it is crucially important to characterise the misfolded proteins prior to any toxicity experiments. In this chapter, I will discuss the production of recPrP and recAβ, the assays used to refold these proteins into both oligomers and fibrils and the subsequent characterisation of these misfolded proteins.

Several studies have previously produced disease associated misfolded proteins *in vitro*, (Table 3.1). Clearly, the methods of producing oligomers and fibrils vary widely, as do the characterisation methods employed. This may explain why there is some variation seen in the literature regarding toxicity of oligomers and fibrils. This will be discussed further in chapter 4.

The disease associated proteins I chose to work with were PrP, which is associated with prion diseases, and Aβ, which is thought to play a fundamental role in Alzheimer's disease pathology. I chose PrP because it has been extensively used as a model for PMDs *in vitro*, and there are well developed methods for expressing and purifying PrP (Makarava and Baskakov, 2008), and producing oligomers and fibrils (Baskakov and Bocharova, 2005, Breydo et al., 2008, Rezaei et al., 2005). My project focused on PrP toxicity in the first instance, but in order to investigate whether misfolded proteins associated with different PMDs activate the same toxicity pathways, I needed to select another relevant protein to compare with PrP. I chose Aβ because there had been several papers published (Lee et al., 2005, Garai et al., 2009, Finder et al., 2010, Macao et al., 2008), which had developed methods for producing recombinant Aβ. Additionally, the toxicity of misfolded isoforms of PrP and Aβ had not previously been compared. Therefore, by studying both PrP and Aβ I could elucidate any similarities or differences in toxicity and mechanisms leading to cell death. In addition to producing recPrP oligomers and fibrils, it was important to produce a protein to act as a negative control for the toxicity experiments. I produced recPrP with an α-helical structure similar to that of normal cellular prion protein (PrP^{C}), which is not toxic *in vivo* (Westergard et al., 2007).

Paper	Protein	Oligomer/ pre-fibrillar methods	Fibril Methods	Characterisation methods
Carrotta (Carrotta et al., 2006)	Aβ	0.01 M Tris-HCl, pH 7.2, at 37 °C	0.1 M sodium citrate, pH 3, at 37 °C	ThT fluorescence staining, SLS, QLS
Ferrao-Gonzales (Ferrão-Gonzales et al., 2005)	Aβ	50 mM sodium phosphate, 100 mM sodium chloride, pH 7.4, 37 °C + ANS derivatives	50 mM sodium phosphate, 100 mM sodium chloride, pH 7.4, 37 °C + ANS derivatives	LS, SEC, NMR, CD
Finder (Finder et al., 2010)	Aβ	N/A	10 mM H_3PO_4, pH 7.4, 100 mM NaCl, 37 °C with stirring	CD, ThT fluorescence, EM,
Stine (Stine et al., 2003)	Aβ	Diluting into Ham's F12 media at 4 °C for 24 hours	Diluting into 10 mM HCl at 37 °C for 24 hours	CD, AFM, western blot, solubility tests
Novitskaya (Novitskaya et al., 2006)	PrP	Partially denaturing conditions (1 M GdmCl, 3 M urea) at 37 °C	Partially denaturing conditions (1 M GdmCl, 3 M urea) with shaking at 37 °C	CD, FTIR, SEC, ThT fluorescence, EM, epifluorescence microscopy
Rezaei (Rezaei et al., 2005)	PrP	20 mM sodium citrate, pH 3.4 at range of temps	N/A	CD, FTIR, SEC, epitope mapping, SAXS,
Simoneau (Simoneau et al., 2007)	PrP	Heating to 72 °C or tandem linked PrP	Aging oligomers at 4°C for 1 month	FTIR, PK resistance, SEC, ThT fluorescence
Torrent (Torrent et al., 2004)	PrP	20 mM Tris-HCl buffer at pH 8.5, 40 °C, transient pressure at 600 MPa	20 mM Tris-HCl buffer at pH 8.5, 40 °C, overnight pressure of 600 MPa	ANS + ThT fluorescence, LS, FTIR, congo red staining, PK resistance, EM.

Table 3.1 Published methods used for producing and characterising oligomers and fibrils

Methods used for producing Aβ and PrP oligomers and fibrils. Abbreviations: Thioflavin T (ThT), Static light scattering (SLS), Quasi-elastic light scattering (QLS), Light scattering (LS), Size exclusion chromatography (SEC), Nuclear magnetic resonance (NMR), Circular dichroism (CD), Electron microscopy (EM), Atomic force microscopy (AFM), Fourier transform infrared spectroscopy (FTIR), Small-angle X-ray scattering (SAXS), 8-anilino-1-naphthalenesulfonic acid (ANS).

Many studies which have investigated Aβ *in vitro* used synthetic Aβ (Ferrão-Gonzales et al., 2005, Paul and Axelsen, 2005, Stine et al., 2003, Lorenzo and

Yankner, 1994, Texido et al., 2011). However, it has been shown that synthetic Aβ is generally less pure and behaves less like Aβ *in vivo* than recAβ (Finder et al., 2010), for example synthetic Aβ fibrillises more slowly (Finder et al., 2010). I therefore decided to use recAβ. In addition, by using recAβ I had greater control over the production and resulting purity of the protein. RecAβ is difficult to express and purify on its own, since it is small and aggregation prone, there are however several published methods for producing recAβ (Lee et al., 2005, Garai et al., 2009, Finder et al., 2010, Macao et al., 2008). Commonly a fusion protein system was used where the Aβ peptide is linked to a soluble polypeptide, usually with a modification such as a HIS-tag to assist in purification. The fusion proteins are then expressed in *E.coli* and purified. The pure fusion proteins are then cleaved at the cleavage site separating the Aβ peptide from the rest of the fusion protein, the protein is then further purified to obtain recAβ alone. I decided to use the fusion protein method published in Finder *et al.* (Finder et al., 2010), since they showed the highest yield of recAβ and the protease needed to cleave the fusion proteins was the tobacco etch virus (TEV) protease, which I could also produce recombinantly. I obtained plasmids from Prof. Glockshuber's group for recAβ 1-40 and recAβ 1-42 fusion proteins. I followed the methods shown in their paper (Finder et al., 2010), but found that a lot of optimisation was needed to obtain pure recAβ at the end of the protocol as outlined in this chapter.

I wanted to produce oligomers and fibrils for both the recAβ 1-40 peptide and the slightly longer and more aggregation prone recAβ 1-42, since it has been shown that both Aβ 1-40 and Aβ 1-42 are important in the disease pathogenesis of Alzheimer's disease (van Oijen et al., 2006, Hartmann et al., 1997, Allan Butterfield, 2002, Dolev et al., 2013, Itkin et al., 2011).

RecPrP is much less aggregation prone than recAβ and is, therefore, easier to purify and does not require the use of fusion proteins or specific ligands. Most published methods express recPrP in *E.coli* as insoluble inclusion bodies, which are solubilised

using a denaturing buffer such as 8 M urea (Rezaei et al., 2000, Hornemann et al., 1997) or 8 M guanidine(Burns et al., 2003). Most methods then use purification techniques such as affinity chromatography and reverse phase chromatography. There are some variations between methods, which include different bacterial lysis techniques. Some employed the use of a French pressure cell (Hornemann et al., 1997), while others use enzymatic cell disruption (Rezaei et al., 2000). In addition, there are some variations in refolding PrP following purification. Once PrP has been purified, the disulphide bond must be reformed to allow normal folding of the protein. Some methods involve refolding on the column (Rezaei et al., 2000), while others refold after elution (Hornemann et al., 1997, Kirby et al., 2010). To produce α-helical PrP, which acted as a negative control in the toxicity experiments, I used the lysis and purification methods published in Kirby *et al*. (Kirby et al., 2010). This involved using lysozyme to lyse the bacterial cells, 8 M urea to solubilise the inclusion bodies, purification by means of affinity chromatography, and refolding of the protein after purification under oxidising conditions. However, to produce protein for production of oligomers and fibrils, I used the methods published in Makarava *et al.* (Makarava and Baskakov, 2008). The need for different purification procedures will be discussed in more detail later in this chapter.

I used a range of methods to robustly and reliably characterise the oligomers and fibrils for both recAβ and recPrP. The size of the oligomers were analysed by size exclusion chromatography (SEC) and dynamic light scattering (DLS), in addition, their resistance to PK digestion was investigated. The fibrils were characterised by thioflavin T (ThT) fluorescence, Congo red staining for amyloid and resistance to PK digestion. The recPrP proteins also underwent some additional analysis, the secondary structure of the oligomers was investigated by circular dichroism (CD) and the recPrP fibrils were analysed by electron microscopy.

3.2 Production and characterisation of α-helical recPrP

As previously outlined, I initially sought to produce recPrP with a structure similar to that of PrP^C, which is not toxic *in vivo*, to act as a negative control in subsequent toxicity experiments. I expressed murine recPrP 23-230 in *E.coli* and purified using a multistep purification procedure (for full details, see materials and methods section 2.4.1). Following purification, the recPrP was refolded under oxidising conditions. The purified protein was characterised using SDS-PAGE (figure 3.1A). The analysis revealed the protein to show a high level of purity and is the correct molecular weight. The secondary structure of the protein was investigated using CD. A typical CD spectrum for a protein with an α-helical secondary structure, such as PrP^C, would show a double minima at 208 and 222 nm. Figure 3.1B shows the CD spectrum for the purified PrP protein, the spectrum is typical of an α-helical protein. The secondary structure of the purified protein is therefore similar to PrP^C and so was stored at -80 °C and used in all cellular toxicity experiments.

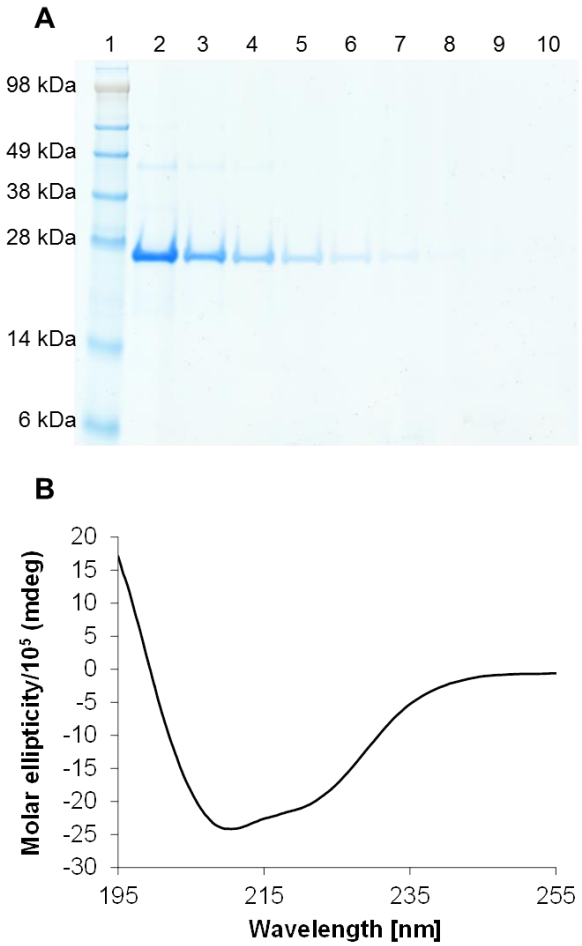

Figure 3.1 Characterisation of α-helical recPrP

A) A typical SDS-PAGE gel with coomassie staining, showing serial dilution of mouse recPrP 23-230. B) A typical circular dichroism spectrum of mouse recPrP.

3.3 Production and characterisation of recPrP disease associated isoforms

In PMDs, oligomers and fibrils have both been highlighted as potential toxic species, causing the cell death seen in these disorders (Bucciantini et al., 2002, Caughey and Lansbury, 2003, Knowles et al., 2014, Braak et al., 2003, Kuo et al., 1996, Naslund et al., 2000, McLean et al., 1999, Mucke et al., 2000a, Walsh et al., 2002, Quist et al., 2005, Kristiansen et al., 2007, Simoneau et al., 2007, Volles et al., 2001). Therefore, I wanted to produce both oligomers and fibrils and investigate their ability to cause toxicity.

The recPrP oligomerisation and fibrillisation protocols required different buffers, since recPrP fibrils form under partially denaturing conditions, while oligomers form under mildly acidic conditions. The purified recPrP was therefore needed in a lyophilised form, to allow solubilisation under either fibrillising or oligomerising conditions at specific concentrations. Therefore, this required a different purification procedure to that used to produce α-helical recPrP, with the final stage being reverse phase high performance liquid chromatography (HPLC), in which the protein is eluted in acetonitrile. Acetonitrile is a volatile solvent, which readily evaporates, meaning that under centrifugal vacuum the recPrP could be lyophilised (for full details see materials and methods section 2.4.2.4). A representative reverse phase (RP) chromatogram and SDS-PAGE analysis of the purification fractions is shown in supplementary figure 1 A+B.

RecPrP oligomers were formed at pH 3.4 with heating at 45 °C, as published in Rezaei *et al*. (Rezaei et al., 2005) (for full details see materials and methods section 2.6.1). The oligomers were analysed using SEC, as shown in figure 3.2A. Two main oligomer populations were formed under these conditions: larger oligomers thought to consist of approximately 36 PrP molecules, and smaller oligomers thought to consist of approximately 12 PrP molecules. The approximate size of the

oligomers which form when using this method was shown in Rezaei *et al*. (Rezaei et al., 2005). The larger oligomers which elute between 6-8 ml are labelled P1 in figure 3.2A, the smaller oligomers elute between 8.5 -10 ml are labelled P2. The recPrP which remained as a monomer elutes between 11-12 ml and is labelled as P3 in figure 3.2A. In order to confirm that the absorbance peaks shown in figure 3.2A were protein, fractions were collected at 1 ml intervals and analysed using SDS-PAGE and silver staining (figure 3.2B). Protein bands, which are the correct molecular weight to be recPrP, are shown in lanes corresponding with elution fractions from 7-8 ml (P1), 9-10 ml (P2) and 11-12 ml (P3), showing that the peaks in figure 3.2A are recPrP. Figure 3.2C shows a SEC at the start of the oligomerisation assay. The P1 peak shown in figure 3.2A is absent, and P2 is much smaller, with the majority of the protein being monomeric at the start of the assay (P3). This P3 peak is of much lower intensity once the oligomers have formed, as shown in figure 3.2A, since the monomer is converted to oligomers.

When the oligomers form, the ratio of the larger to smaller oligomer species can vary. One variable which impacts this ratio is the proportion of oxidised recPrP (with the disulphide bond) compared to recPrP lacking the disulphide bond. I have found that oligomerising oxidised recPrP with an intact disulphide bond leads to the production of the smaller oligomer (12 mer) species. By contrast, oligomerising recPrP lacking the disulphide bond leads to the production of the larger oligomer (36-mer) species. Interestingly, it was found that even small quantities of recPrP lacking the disulphide bond drives the formation of the larger oligomer species. This will be discussed in detail in chapter 5.

To investigate the secondary structure of the oligomers, I used CD as shown in figure 3.3. The structure is very different to that of the α-helical recPrP shown in figure 3.1B. The oligomer spectrum shows a single minimum at 215 nm, indicative of a β-sheet rich structure.

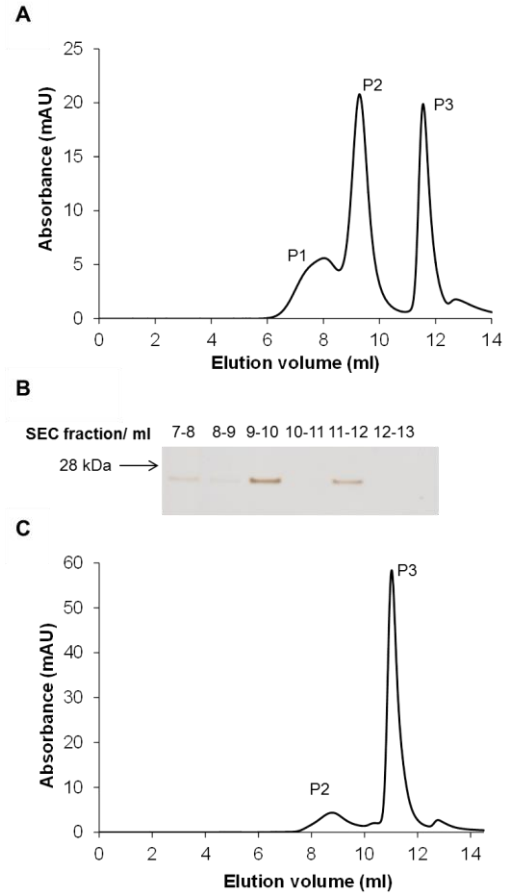

Figure 3.2 Characterisation of recPrP oligomers

A) SEC showing recPrP oligomers. P1 corresponds to a larger oligomer species thought to comprise approximately 36 PrP molecules. P2 corresponds to a smaller oligomer species, thought to comprise approximately 12 PrP molecules and P3 corresponds to monomeric PrP. B) SDS-PAGE gel stained with silver nitrate, showing 1 ml fractions collected from the chromatogram shown in A; the band at 7-8 ml corresponds with P1, a band at 9-10 ml with P2 and a band at 11-12 ml with P3. All bands show the correct molecular weight for recPrP. C) SEC chromatogram at time point 0 minutes of the oligomerisation assay. P2 corresponds to the smaller oligomer species which is beginning to form and P3 corresponds to monomeric PrP.

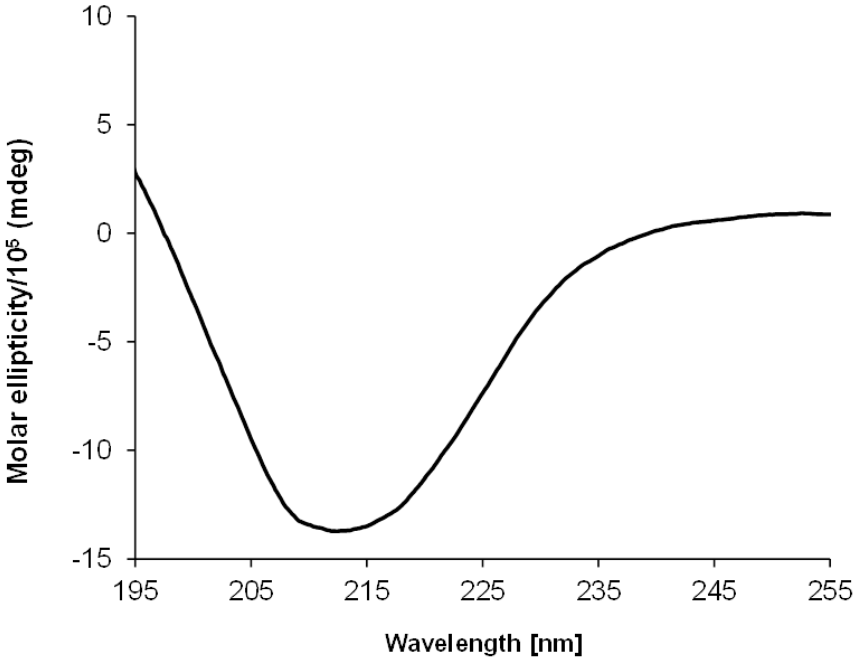

Figure 3.3 The secondary structure of recPrP oligomers

Circular dichroism spectrum of recPrP oligomers, showing a single minimum at 215 nm which is suggestive of a β-sheet rich structure.

As mentioned previously, I wanted to assess the toxicity of oligomeric species of PrP since they are thought to play an important role in disease pathogenesis in prion diseases. The oligomerisation assay used in the Gill lab had previously been optimised to investigate the rate and mechanisms of oligomerisation. The protein was therefore heated on a HPLC auto-sampler and at 15 minute intervals a sample was injected onto the SEC column. However, I needed to adapt the assay to produce larger volumes of oligomers in order to test these for toxicity. I did this by heating larger volumes of recPrP on a heat block at 45 °C, instead of the auto-sampler, and after 2.5 hours the oligomers were then analysed using SEC. Once the assay had been optimised, it was then important to investigate the stability of the oligomers under different storage conditions. The oligomers were kept at both 4 °C and -20 °C for increasing lengths of time. At regular intervals the oligomers were tested using SEC, to assess whether the sample contained the same proportion of oligomers as it

did when first made. Figure 3.4 shows the SEC results for oligomers stored at 4 °C for 24 hours (B) and 4 days (D), and oligomers stored at -20 °C for 24 hours (A), 4 days (C) and 4 months (E). The SEC chromatograms for the oligomers when first formed are shown in black, those stored at -20 °C are shown in green and those stored at 4 °C are shown in blue. Oligomers stored at 4 °C or -20 °C for 24 hours were both shown to be stable (figure 3.4 A + B), with the green and blue chromatograms overlaying the black chromatogram. At 4 days post oligomerisation, the oligomers stored at 4 °C shown by the blue chromatogram in figure 3.4D, shows a drop in the oligomer peak in comparison to the original chromatogram shown in black (indicated by the arrow). The drop in the oligomer peak for the green chromatogram in figure 3.4C in comparison to the original black chromatogram is much less, suggesting that the oligomers are more stable at -20 °C. A new batch of oligomers was made and stored at -20 °C for 4 months (figure 3.4E), the oligomers were shown to be stable with the green chromatogram overlaying the black chromatogram, with no drop in the oligomer peak. Once the stability of the oligomers had been established, oligomers for all cell experiments were stored at -20 °C until used.

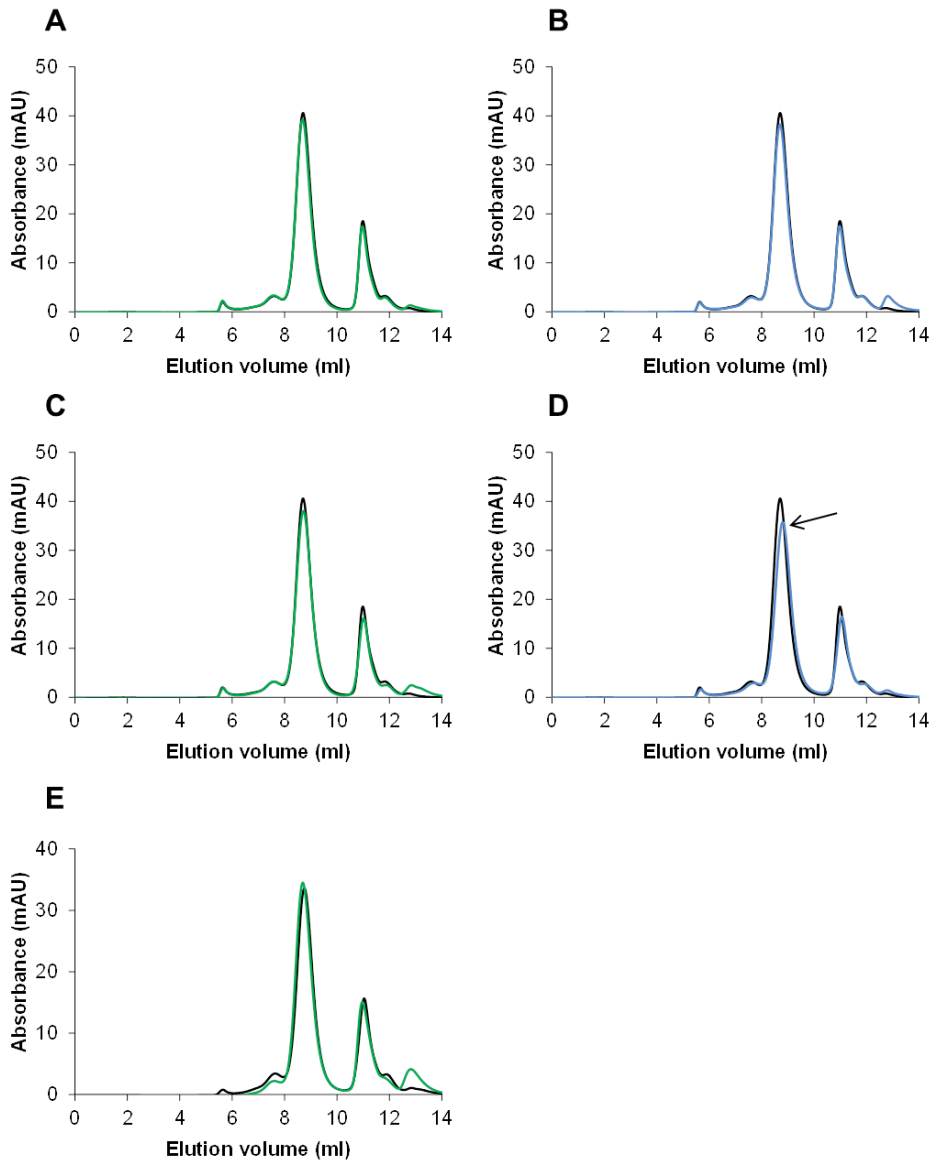

Figure 3.4 Storage conditions for recPrP oligomers.

SECs showing different storage conditions for recPrP oligomers. A + C) Show fresh oligomers (black) and those stored at -20 °C (green) for 24 hours or 4 days respectively. B + D) Show fresh oligomers (black) and those stored at 4 °C (blue) for 24 hours or 4 days respectively. The black arrow in D indicates the drop in absorbance for the oligomers stored under these conditions. E) Shows a different batch of fresh oligomers compared to A-D (black) and those stored at -20 °C for 4 months (green).

In addition to the oligomers, I also wanted to produce fibrils with an amyloid structure to mimic the fibrillar deposits found in individuals infected with prion disease. Fibrils were formed under partially denaturing conditions (2 M guanidine) with vigorous shaking at 37 °C in a 96 well plate in a fluorescence plate reader (full details can be found in materials and methods, section 2.7.1). The fibrillisation assay had to be optimised to produce fibrils for toxicity experiments. Similar to the oligomerisation assay, the fibrillisation assay had been used previously to investigate fibril formation and fibrillisation kinetics (Breydo et al., 2008) not form fibrils for subsequent experiments. The concentration of the fibrils at the end of the assay was usually ~0.1 mg/ml, which was too low to dose the cells at the required concentration range while still keeping the volume of fibrils added to the cells low. This was important since if large volumes were added, the fibril buffer began to show toxicity. I therefore adjusted the reaction so that the recPrP starting concentration prior to addition of the fibrillisation buffer was ~4 mg/ml instead of 3 mg/ml. Additionally, I omitted the 6 M guanidine from the fibrillisation buffer and instead increased the volume of recPrP (solubilised in 6 M guanidine) in each fibrillisation reaction to 53.6 µl from 26.8 µl. The result of this optimisation was fibrils which were ~1 mg/ml, which was concentrated enough for the cell experiments.

Fibril formation was monitored over 24 hours using the dye ThT, which fluoresces when bound to amyloid. Fluorescence readings were taken at 5 minute intervals. A representative fibrillisation assay is shown in figure 3.5A. ThT data were averaged for 4 fibrillisation reactions and any background fluorescence, shown by a no PrP control, was subtracted. The data was then expressed as a percentage, and standard deviation error bars are shown indicating the variation between the fibrillisation reactions. The first 75 minutes of the assay shows low fluorescence: this is known as "the lag time", which is generally thought to be the time it takes for monomeric recPrP to begin to nucleate and then aggregate into fibrils (Breydo et al., 2008, Bocharova et al., 2005). The increase in fluorescence seen between approximately

100 and 200 minutes indicates the fibrils forming, and the plateau seen after this is thought to indicate that all the monomeric recPrP has been incorporated into the fibrils. Once formed, the fibrils were dialysed into sodium acetate pH 5.5 and stored at 4 °C. For fibril toxicity experiments, I decided to make fibrils without ThT in case the ThT bound to the fibrils affected their toxicity. I therefore set up fibrillisation reactions without ThT, but under the same conditions and on the same plate as fibrils being monitored for ThT fluorescence. It was these ThT-free fibrils that were used in the cellular toxicity experiments.

Next, I investigated whether the fibrils had an amyloid structure or were just comprised of aggregated protein. PrP^{Sc} found in diseased tissues is known to be PK resistant (Parchi et al., 2000, Collinge et al., 1996); PK resistance is therefore a relevant characterisation method to investigate whether fibrils formed *in vitro* share properties with PrP^{Sc}. Additionally, it has been shown that fibrils have an insoluble PK resistant core of between 10-12 kDa (Breydo et al., 2008). When fibrils are heated to 80 °C with a mild detergent (known as maturation), this core expands to 16 kDa, which can be seen as a 16 kDa band after PK treatment by means of SDS-PAGE. This 16 kDa band is therefore thought to be indicative of amyloid fibrils (Breydo et al., 2008), and so I used this method to analyse the fibrils I had formed. The fibrils were digested with PK alone or following maturation, this was compared to the non-fibrillar (NF) control (recPrP which had been under the same buffer conditions as the fibrils, but not shaken for 24 hours). All samples were analysed using SDS-PAGE with silver staining as shown in figure 3.5B. The NF control was completely digested by PK in lanes 2 and 3. By contrast, the fibrils treated with PK in lane 5 show 10 and 12 kDa bands, indicative of PK resistance. In lane 6, where the fibrils have undergone maturation and PK treatment, there is also a 16 kDa band (highlighted by the arrow). As mentioned previously, this band is thought to be characteristic of amyloid fibrils (Breydo et al., 2008). It is thought that during maturation, the insoluble core of a fibril expands from 10-12 kDa to 16 kDa resulting in this distinctive banding pattern (Breydo et al., 2008). Furthermore, the fibrils were

analysed using Congo red staining (figure 3.6A and 3.6B), which when observed under polarised light, shows a yellow- green birefringence indicating amyloid structures (Wolman and Bubis, 1965). The arrows in figure 3.6A and 3.6B indicate the birefringence caused by amyloid. Additionally, the fibrils were analysed using transmission electron microscopy (TEM), at two magnifications, as shown in figure 3.6C and 3.6D. The SEM images show the fibrils are long and highly structured. Taken together, these results indicate that the recPrP has adopted a fibrillar amyloid structure with a PK resistant core. The fibrils used in the cellular toxicity experiments were stored at 4 °C for up to 6 months.

Since PrP^{Sc} isolated from infected tissue is PK resistant, and the fibrils I have formed also show resistance to PK digestion, I wanted to investigate the PK resistance of the oligomers and α-helical recPrP and compare this with the fibrils. All three conformations were digested with PK for 30 minutes at 37 °C at 2 and 4 μg/ml, and analysed using SDS-PAGE and silver staining. Figure 3.7 shows the differences in PK resistance between all three conformations. The differences are particularly clear at 4 μg/ml; with the fibrils being the most PK resistant, oligomers showing some PK resistance, and the α-helical recPrP showing the least resistance. This again highlights that all three conformations have distinct structures, which confer differences in sensitivity to PK digestion. The PK sensitivity shown by the monomers and oligomers may be similar to the PK sensitivity of soluble PK sensitive PrP *in vivo*, which has also been shown to be infectious and toxic (Sajnani et al., 2012).

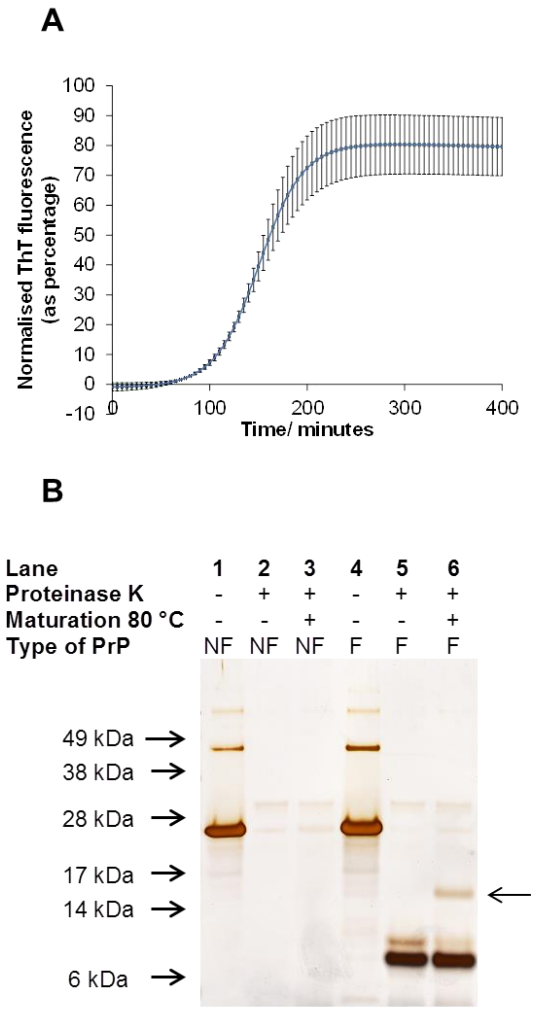

Figure 3.5 Production and characterisation of recPrP fibrils.

A) ThT average fluorescence curve, showing readings over time as the recPrP fibrils form and ThT binds (average of 4 fibrillisation reactions) ± standard deviation error bars are shown. B) Characterisation of recPrP fibrils by maturation at 80 °C and PK digestion. Lanes 1-3 show the non-fibrillar (NF) control which underwent the same conditions as the fibrils, except they were not shaken for 24 hours. Lanes 4-6 show recPrP fibrils; either with no PK, with PK but not heated to 80 °C or with PK and heated to 80 °C (maturation). The 16 kDa band present in lane 6 (highlighted by the arrow) is characteristic of amyloid fibrils. The band at approximately 40 kDa in lanes 1 and 4 is likely a dimer of recPrP and is commonly seen.

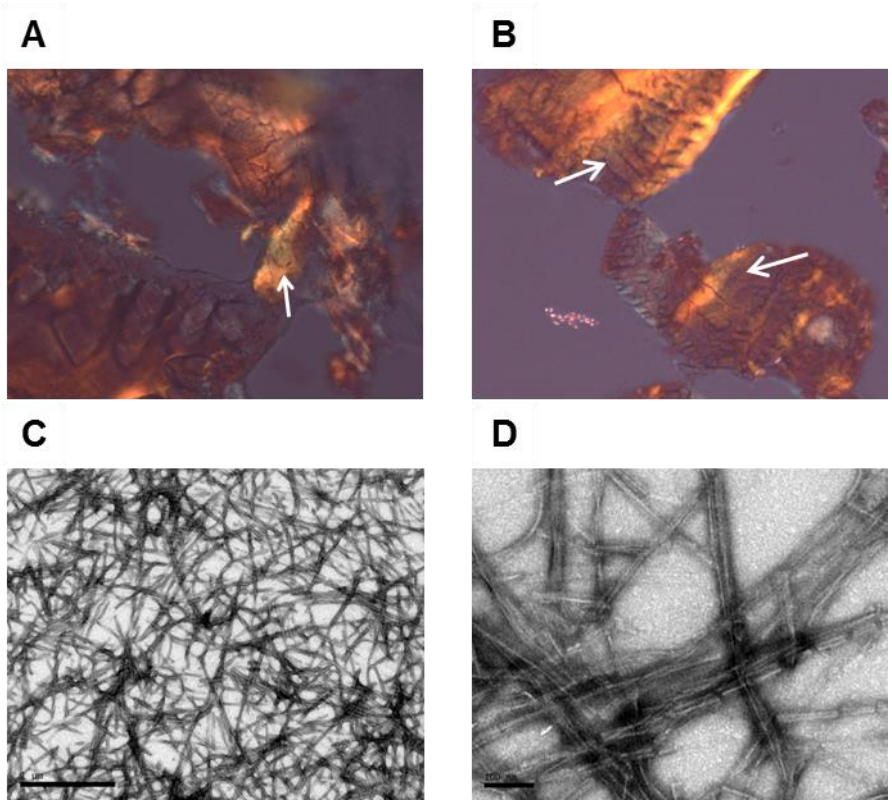

Figure 3.6 Characterisation of recPrP fibrils.

A and B show PrP fibrils with Congo red staining under polarised light, the yellow and green birefringence shows amyloid structures. C and D show scanning electron microscope pictures of recPrP fibrils, the black scale bar in the bottom left hand corner of C represents 1 µM. The scale bar in the bottom left hand corner of D represents 100 nm.

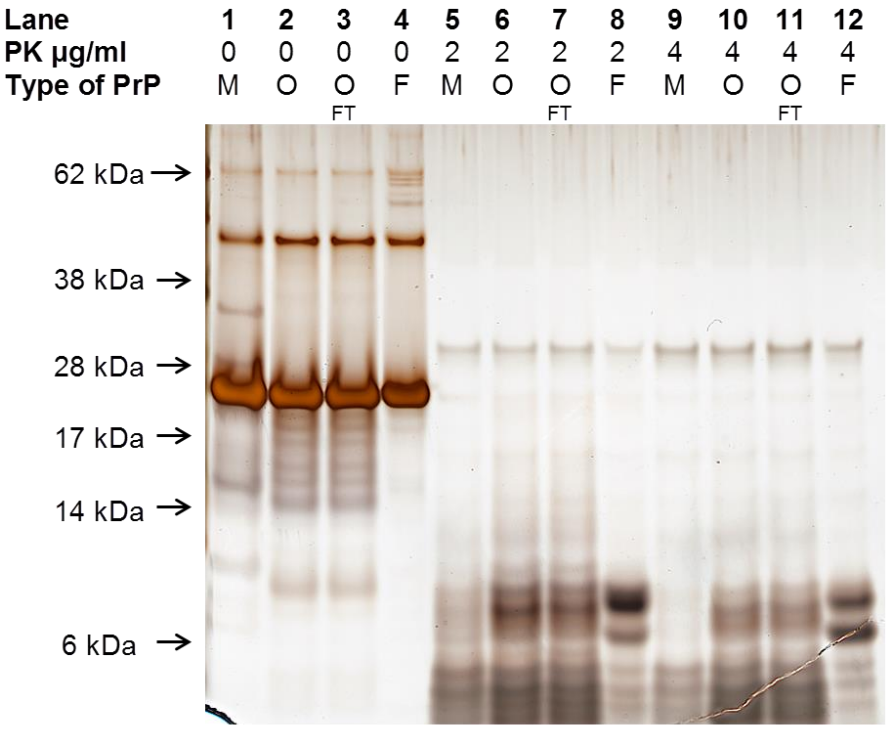

Figure 3.7 PK resistance of different recPrP conformations

SDS-PAGE gel which has been silver stained, showing differences in PK resistance between α-helical recPrP, oligomers and fibrils. Lanes 1-4 show α-helical recPrP (M), oligomers (O), oligomers which had been frozen and thawed (FT) and fibrils (F), with no PK treatment. Lanes 5-8 show the α-helical recPrP, oligomers and fibrils having been treated with PK at 2 µg/ml for 30 minutes, and lanes 9-12 shows the different recPrP conformations treated with PK at 4 µg/ml.

3.4 Production of recombinant Aβ fusion proteins

The recAβ 1-40 and recAβ 1-42 peptides were produced using the fusion protein system developed by Prof. Glockshuber's group(Finder et al., 2010), who provided plasmids containing the fusion proteins for recAβ 1-40 and recAβ 1-42. A schematic diagram of the fusion protein is shown in figure 3.8. The Aβ peptide is attached to a soluble polypeptide, linked to a histidine tag, which allows purification by immobilised metal ion affinity chromatography (IMAC). The Aβ peptide and the fusion protein are separated by a cleavage site recognised by the tobacco etch virus (TEV) protease, which was used to cleave the fusion protein from the Aβ peptide.

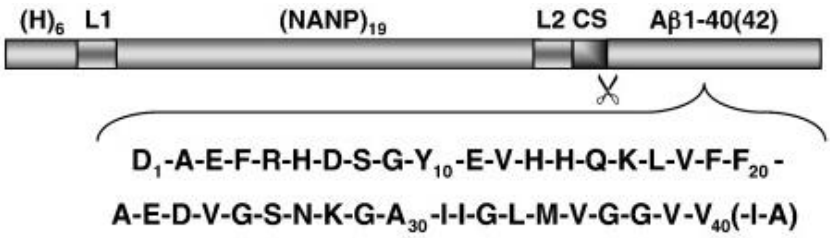

Figure 3.8 Schematic diagram of Aβ fusion protein

This schematic diagram from Finder *et al.* (Finder et al., 2010) shows the Aβ fusion protein. The Aβ peptide on the right hand side is shown to be linked to the soluble polypeptide, with a histidine tag on the left hand side. The scissors indicate the cleavage site which is recognised by TEV protease. The amino acid sequences for Aβ 1-40 and Aβ 1-42 are also shown.

E. coli transformed with the Aβ 1-40 and Aβ 1-42 fusion protein plasmids were grown in 400 ml cultures, and fusion protein expression was induced by IPTG (for more detail see materials and methods section 2.2.2). Samples were taken prior to induction and at regular intervals after induction, to assess the production of recAβ 1-40 and recAβ 1-42 fusion proteins. Theses samples were analysed by SDS-PAGE, as shown in figure 3.9A and 3.9B. The arrows show bands at the correct molecular

weight for the recAβ 1-40 and recAβ 1-42 fusion proteins, which increase in intensity over time. Following expression, the bacteria were lysed and the inclusion bodies containing the fusion proteins were solubilised using 6 M guanidine hydrochloride. The fusion proteins were purified first by immobilised metal ion affinity chromatography and then by reverse phase chromatography. Figure 3.10A shows the reverse phase chromatogram for the recAβ 1-40 fusion protein. The fractions collected from the purification were analysed using SDS-PAGE in figure 3.10B. The bands shown in lanes 11 + 12 were confirmed to be the recAβ 1-40 fusion protein by western blotting with a HIS-TAG antibody (figure 3.10C). The same procedure was carried out for the recAβ 1-42 fusion protein. The reverse phase chromatogram and corresponding fractions shown by SDS-PAGE and western blot are shown in figure 3.11A-C. The reverse phase chromatograms and SDS-PAGE gels shown are typical of other purifications of recAβ 1-40 and recAβ 1-42 fusion proteins.

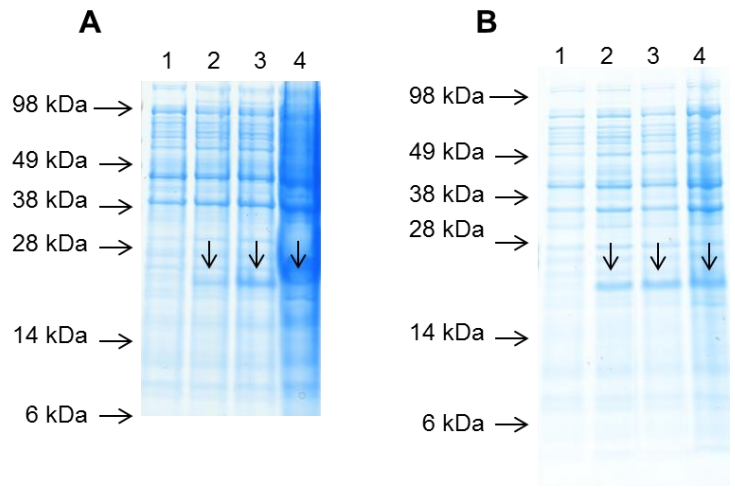

Figure 3.9 Expression of recAβ 1-40 and 1-42 fusion proteins

RecAβ 1-40 and recAβ 1-42 fusion proteins were expressed in BL21 *E.coli* and induced using IPTG. A) SDS-PAGE gel with coomassie staining, showing expression of recAβ 1-40: lane 1: un-induced bacteria, lane 2: 1 hour after induction, lane 3: 2 hours after induction and lane 4: 16 hours after induction (arrows indicate the recAβ 1-40 fusion protein bands). B) Composite SDS-PAGE gel with coomassie staining, showing expression of recAβ 1-42: lane 1: un-induced bacteria, lane 2: 1 hour after induction, lane 3: 2 hours after induction and lane 4: 16 hours after induction (arrows indicate the recAβ 1-42 fusion protein bands).

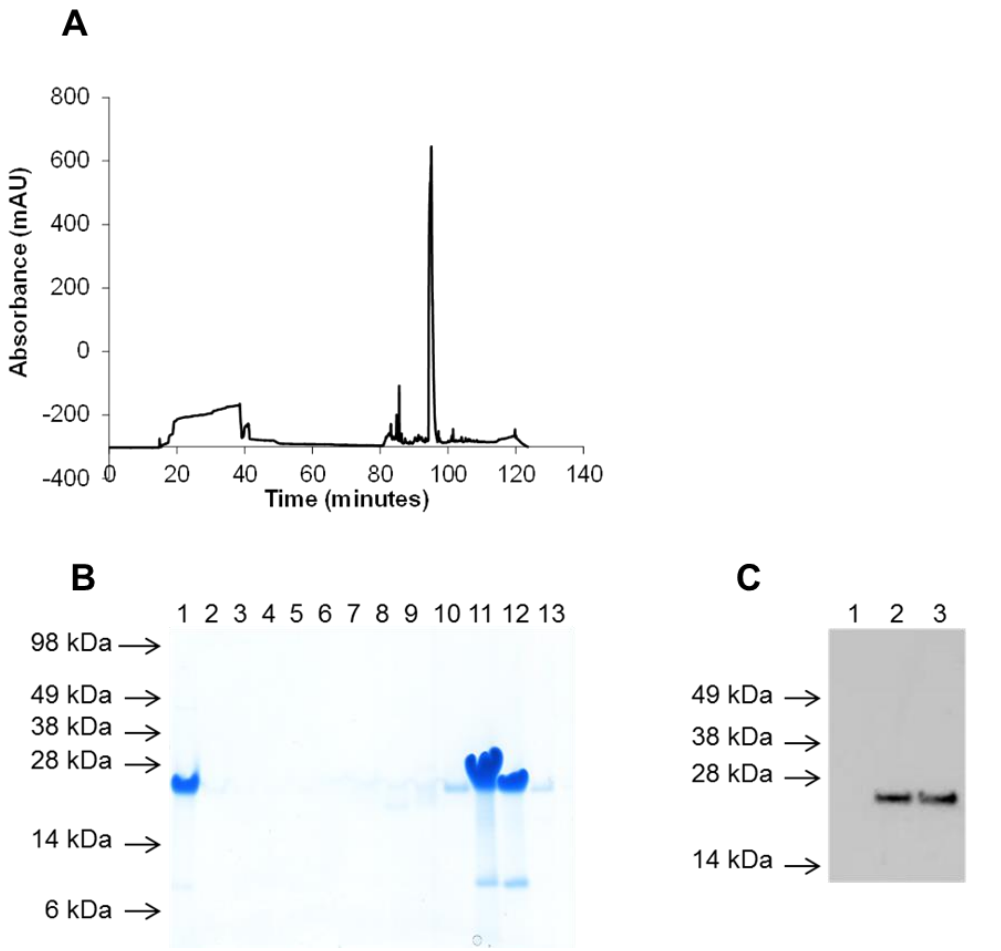

Figure 3.10 Purification of recAβ 1-40 fusion protein

A) Reverse phase chromatogram for recAβ 1-40 fusion protein purification, the large peak is the eluting fusion protein. B) SDS-PAGE gel with coomassie staining, showing fractions collected from the reverse phase chromatogram (A), lanes 11 + 12 show the recAβ 1- 40 fusion protein which corresponds to the large peak in A. C) Western blot of fractions from the recAβ 1-40 fusion protein purification. Lanes 1-3 correspond to lanes 10-12 in B; a HIS-tag antibody was used.

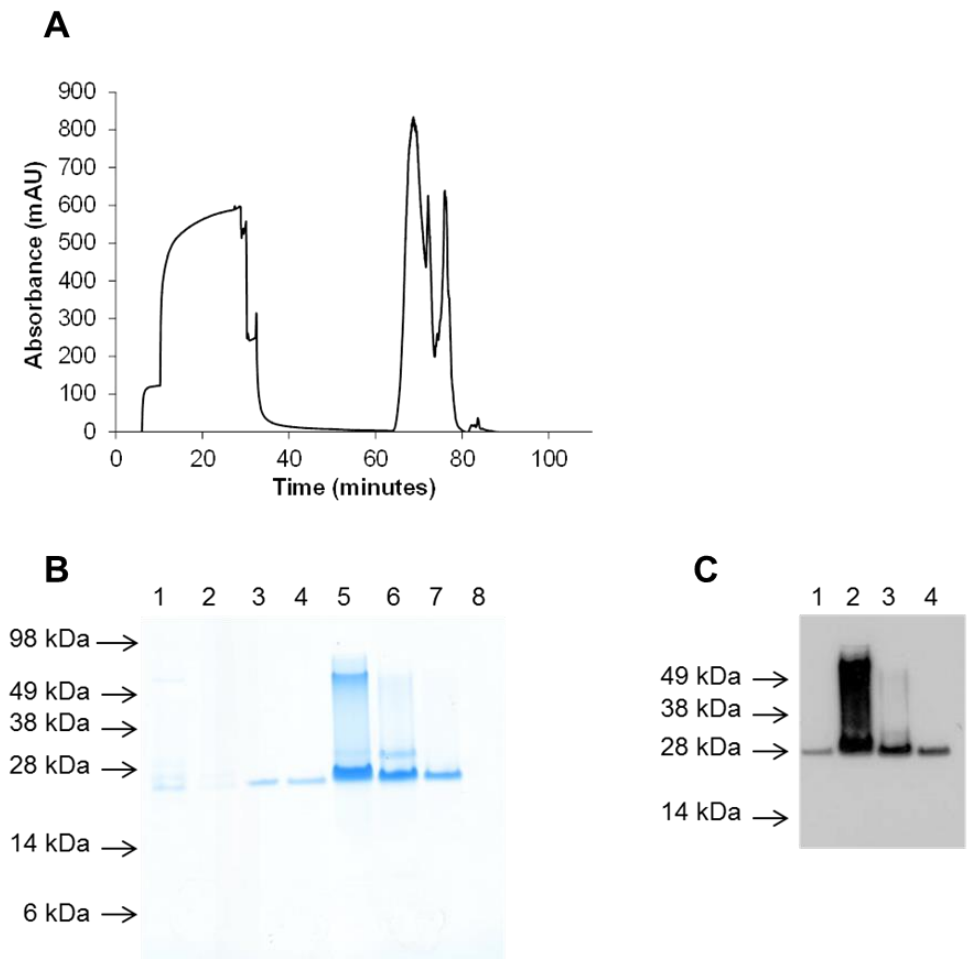

Figure 3.11 Purification of recAβ 1-42 fusion protein

A) Reverse phase chromatogram for recAβ 1-42 fusion protein purification, the large peaks correspond to the eluting fusion protein. B) SDS-PAGE gel with coomassie staining, showing fractions collected from the reverse phase chromatogram (A), lanes 4-7 show the recAβ 1-42 fusion protein which corresponds to the peaks in A. C) Western blot of fractions from the recAβ 1-42 fusion protein purification. Lanes 1-4 correspond to lanes 4-7 in B; a HIS-tag antibody was used.

3.5 Production of recombinant TEV protease

Once I had purified both fusion proteins, I needed to obtain TEV protease in order to cleave them. At the time, TEV protease was not available commercially so I

produced it as a recombinant protein. A glycerol stock of *E.coli* containing a TEV protease plasmid was available in the Gill group; this allowed me to express recTEV. TEV protease expression was induced using IPTG and samples were taken before and after induction and analysed using SDS-PAGE (figure 3.12A). The recTEV protease accumulated in inclusion bodies, which were solubilised with 8 M urea. The recTEV protease was then purified using IMAC and the resulting fractions were analysed using SDS-PAGE (figure 3.12B). The fraction shown in lane 5 was dialysed into a tris/EDTA buffer with a pH of 7.5. However, this resulted in a high degree of precipitation. This precipitation occurred despite substantial modifications to the protocol, including using purification buffers with or without reducing agent, allowing the protein to refold on the column, or changing the temperature the protein was dialysed at (4 °C or room temperature).

The recTEV protease which was still in solution after the precipitate had been pelleted was not concentrated enough, or was already beginning to precipitate further, which meant that it could not successfully cleave the fusion proteins. Figure 3.12C, shows samples taken from a cleavage reaction and analysed by SDS-PAGE, the blue arrow indicates recTEV protease, and the red arrow indicates the fusion protein. RecAβ 1-42 is approximately 4.5 kDa, and, therefore, if cleavage had been successful there would have been a protein band at this size, which is indicated by the black arrow. No low molecular weight bands were seen, showing that the recTEV protease had failed to cleave the fusion protein. Therefore, I decided that this was not a viable method for producing recTEV protease to cleave the recAβ fusion proteins. The main problem with producing recTEV protease using this method was the precipitation that occurred in the dialysis step. The dialysis step was, however, needed to dilute the urea in the purification buffers. Therefore, I wanted to use a method which did not need denaturants such as urea, which would eliminate the need for a dialysis step. Since urea was needed to solubilise the inclusion bodies that formed during expression of the protein, an alternative

method was to express TEV as a soluble protein, eliminating any need for denaturing buffers.

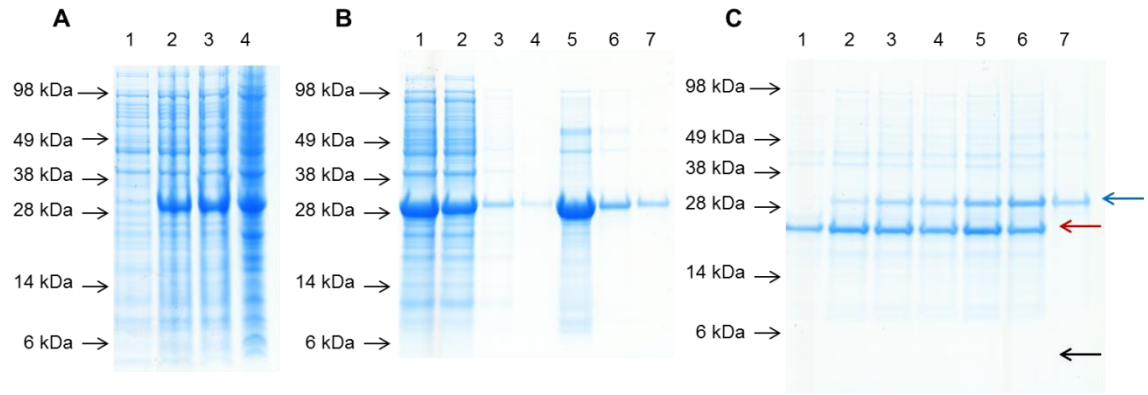

Figure 3.12 Production of recTEV protease as insoluble inclusion bodies

A) SDS-PAGE gel which has been coomassie stained, showing expression of TEV protease in *E.coli*. Lane 1: before induction, lane 2: 1 hour after induction, lane 3: 2 hours after induction and lane 4: 16 hours after induction. B) SDS-PAGE gel which has been coomassie stained, showing TEV protease fractions from IMAC purification. Lane 1: initial sample, lane 2: flow through, lane 3: wash fraction, lanes 4- 7: elution fractions. C) SDS-PAGE gel which has been coomassie stained, showing Aβ 1-42 fusion protein and TEV protease in increasing amounts, after incubation overnight. The blue arrow indicates TEV protease, the red arrow indicates un-cleaved Aβ 1-42 fusion protein, and the black arrow indicates where the Aβ 1-42 band would be if the cleavage had been successful.

When recombinant proteins are expressed at 30- 37 °C, such as in the expression system previously tested, they are produced in such abundant quantities that the protein aggregates into insoluble inclusion bodies, where the protein is not correctly folded. When producing proteins which need to be enzymatically active and, therefore, correctly folded (such as in the case of TEV protease), it is preferable to produce a soluble protein that is correctly folded in the bacteria. One way to increase the amount of soluble protein produced by expression bacteria is to

decrease the temperature, however, most *E.coli* chaperonins are very inefficient at low temperatures(Ferrer et al., 2003). The ArcticExpress competent cells from Agilent technologies contain chaperonins found in *Oleispira Antarctica*, which is a psychrophilic bacterium; these chaperonins are able to refold proteins efficiently at low temperatures, allowing soluble recombinant proteins to be produced efficiently. Therefore, I chose to use the ArcticExpress bacteria to express TEV protease as a soluble protein. The TEV protease containing plasmids were transformed into ArcticExpress bacteria and grown in 200 ml cultures, expression was then induced with IPTG. Cultures were grown for 24 hours at 12 °C, (for more detail see materials and methods section 2.2.3). Samples were taken before and after induction and analysed using SDS-PAGE, (figure 3.13A).

The protease was purified by non-denaturing IMAC and cation exchange chromatography, followed by a desalting step to exchange the imidazole containing purification buffer to an imidazole free- storage buffer. Fractions from each purification step were collected and analysed using SDS-PAGE, shown in figure 3.13B-D. The resulting protein, shown in lane 5 of figure 3.13D, was soluble and showed no precipitation. RecTEV always appeared as a doublet when analysed by SDS-PAGE, it is not clear why, however, it did not seem to affect its enzymatic capability. Following the successful purification of recTEV using this method, I tested the ability of the protease to cleave the recAβ fusion proteins. The recAβ fusion proteins were incubated with recTEV protease, which resulted in efficient cleavage of both fusion proteins. Figure 3.14A+B shows cleaved and un-cleaved fusion proteins analysed by SDS-PAGE. Figure 3.14A shows the successful cleavage of recAβ 1-40 as shown by the low molecular weight band, figure 3.14B shows the successful cleavage of recAβ 1-42.

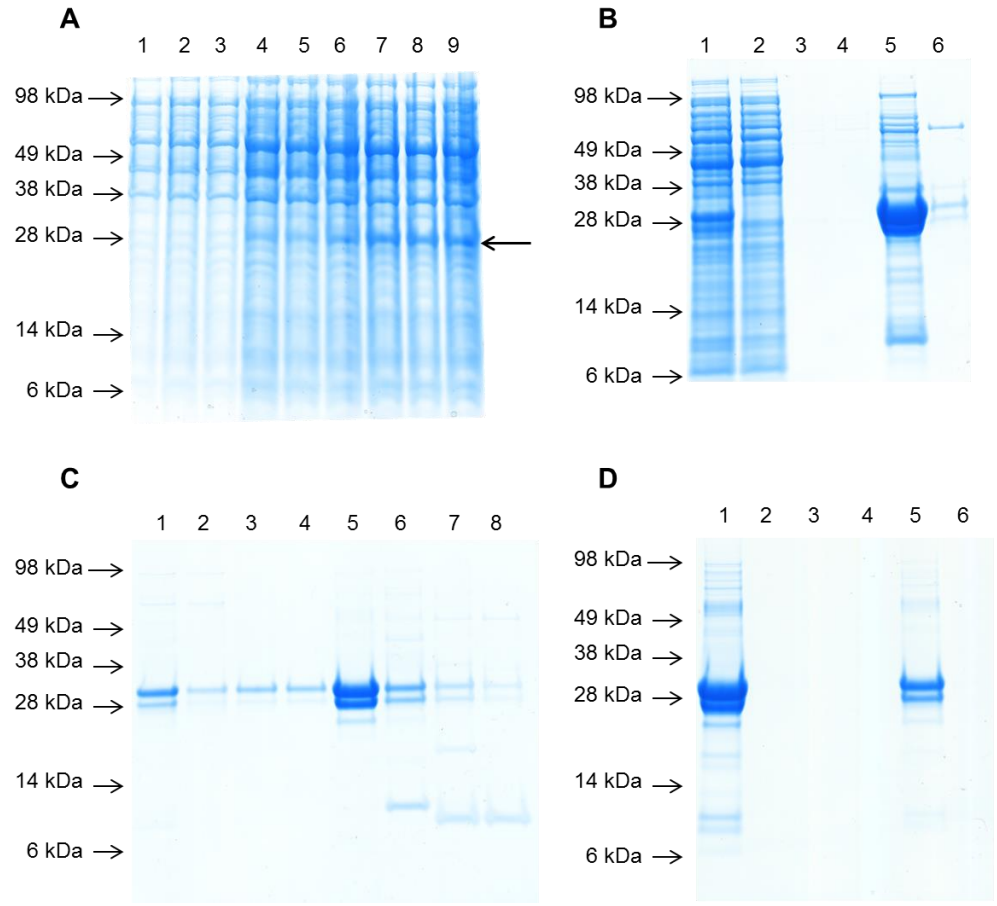

Figure 3.13 Production of recTEV as a soluble protein

A-D: SDS-PAGE gels which have been coomassie stained, showing TEV expression and purifications. A) Induction of TEV as a soluble protein, expressed at 12 °C. Lanes 1-3 show un-induced bacteria from 3 flasks, lanes 4- 6 show 3 flasks of bacteria 2 hours after induction, lanes 7- 9 show 3 flasks of bacteria 16 hours after induction. B) RecTEV protease fractions from IMAC purification, with non-denaturing buffers. Lane 1: initial sample, lane 2: flow through, lane 3: wash fraction, lanes 4- 6: elution fractions. C) Cation purification fractions, lane 1: initial sample, lane 2: flow through, lane 3: wash fraction, lanes 4- 8: elution fractions. D) Desalting of recTEV protease prior to storage, lane 1: initial sample, lanes 2- 6: elution fractions.

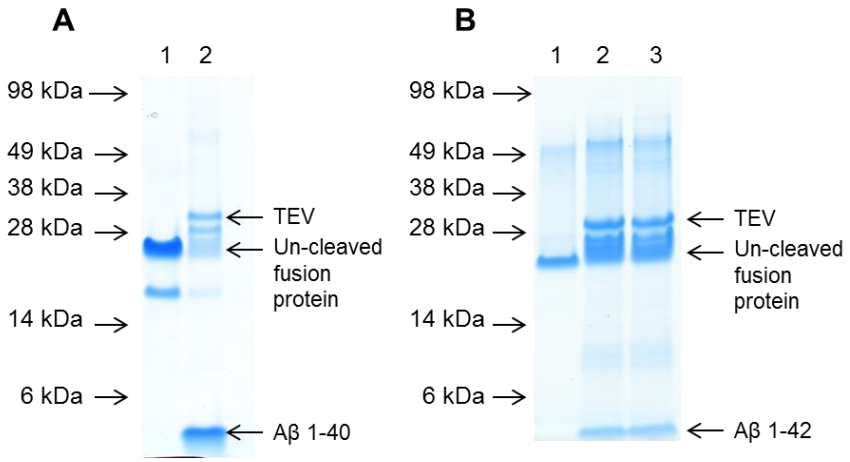

Figure 3.14 Cleavage of recAβ 1-40 and recAβ 1-42 fusion proteins

A) Coomassie stained SDS-PAGE gel showing cleavage of recAβ 1-40 with recTEV protease. B) Coomassie stained SDS-PAGE gel showing cleavage of recAβ 1-42 with recTEV protease.

3.6 Production of recAβ

Once successful cleavage of both fusion proteins had been achieved, the cleaved recAβ peptides needed to be separated from the un-cleaved fusion protein, the other half of the cleaved fusion protein, and recTEV, leaving recAβ 1-40 or 1-42 alone. This was first attempted for recAβ 1-40 using RP chromatography with a Grace VYDAC® 214TP C4 reversed phase column. However, this did not result in separation of the different components of the sample. The RP chromatogram for this purification is shown in figure 3.15A. The fractions from this purification were analysed by SDS-PAGE and are shown in figure 3.15B; lane 6 shows the fraction which corresponds to the peak highlighted by the arrow in A. It is clear that all components are in the same fraction. Following the failure of the C4 column to separate the components of the sample, I used a C8 column as shown in Finder *et al.* (Finder et al., 2010). However, as shown in figure 3.15C+D this also did not result in successful separation. The C8 column was not exactly the same as the one used in

Finder *et al.* (Finder et al., 2010), which may have affected the separation. Subsequently, separation was attempted using nickel IMAC, since both the fusion protein and TEV have a HIS-tag, while the cleaved recAβ peptides do not. However, whilst this did result in successful separation as shown in figure 3.15E (lane 6 shows pure recAβ 1-40 highlighted by *), the yield was low and when repeated the separation was variable. I therefore decided to obtain a semi-preparative Zorbax SB300 C8 column, which is the exact column used in Finder *et al.* (Finder et al., 2010), and optimise the separation using RP chromatography.

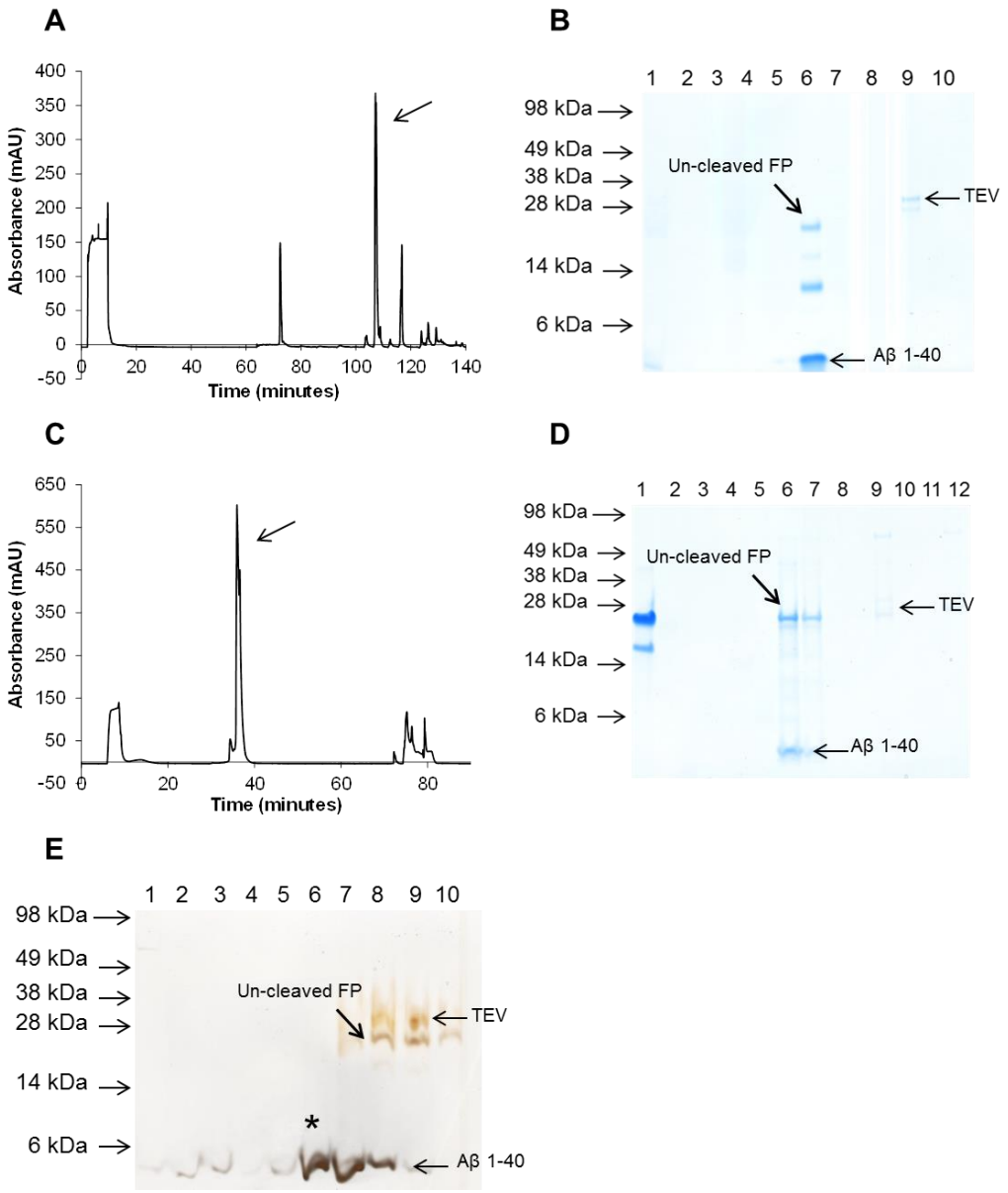

Figure 3.15 Optimisation of recAβ separation following recTEV cleavage.

A-B) Purification of recAβ 1-40 following TEV cleavage using a Grace VYDAC® 214TP C4 reversed phase column. A) RP chromatogram; the arrow indicates the elution fraction show in lane 6 (B). B) SDS-PAGE with coomassie staining of the fractions collected from A. C-D) Purification of recAβ 1-40 following TEV cleavage using a Vydac C8 228TP1010 reversed phase column. C) Reverse phase chromatogram; the arrow indicates the elution fraction shown in lanes 6 +7 of D. D) SDS-PAGE with coomassie staining of the fractions collected from C. E) SDS-PAGE with silver staining, showing separation of recAβ 1-40 following recTEV cleavage using nickel IMAC to separate recAβ 1-40 from the other cleavage products, * indicates a fraction of pure recAβ 1-40.

Separation using the SB300 C8 column was first attempted for recAβ 1-40 using a gradient of acetonitrile. Although this was not successful in fully separating recAβ 1-40 from the recTEV protease, it did show separation from the un-cleaved fusion protein. The RP chromatogram for this is shown in figure 3.16A, fractions from this purification were then analysed by SDS-PAGE and are shown in figure 3.16B: the blue arrow highlights the recTEV protease which was not separated from the recAβ 1-40. Next, I tried using a 28 % isocratic elution of acetonitrile as shown in Finder *et al.* (Finder et al., 2010). This was successful in separating recAβ 1-40 from the recTEV protease, but not the un-cleaved fusion protein. This is shown in figure 3.16C+D, the black arrow highlighting the absorbance peak in C corresponds with the fraction shown in lane 11 of D, the un-cleaved fusion protein is highlighted by the blue arrow, which is in the same fraction as Aβ 1-40. Finally, successful separation of the recAβ 1-40 peptide was achieved using a 30 % isocratic elution of acetonitrile. This is shown in figure 3.16E+F, the arrow in E points to the absorbance peak showing the eluting Aβ 1-40 peptide and the corresponding fractions are shown in lanes 8 + 9 of F, where pure Aβ 1-40 can be seen.

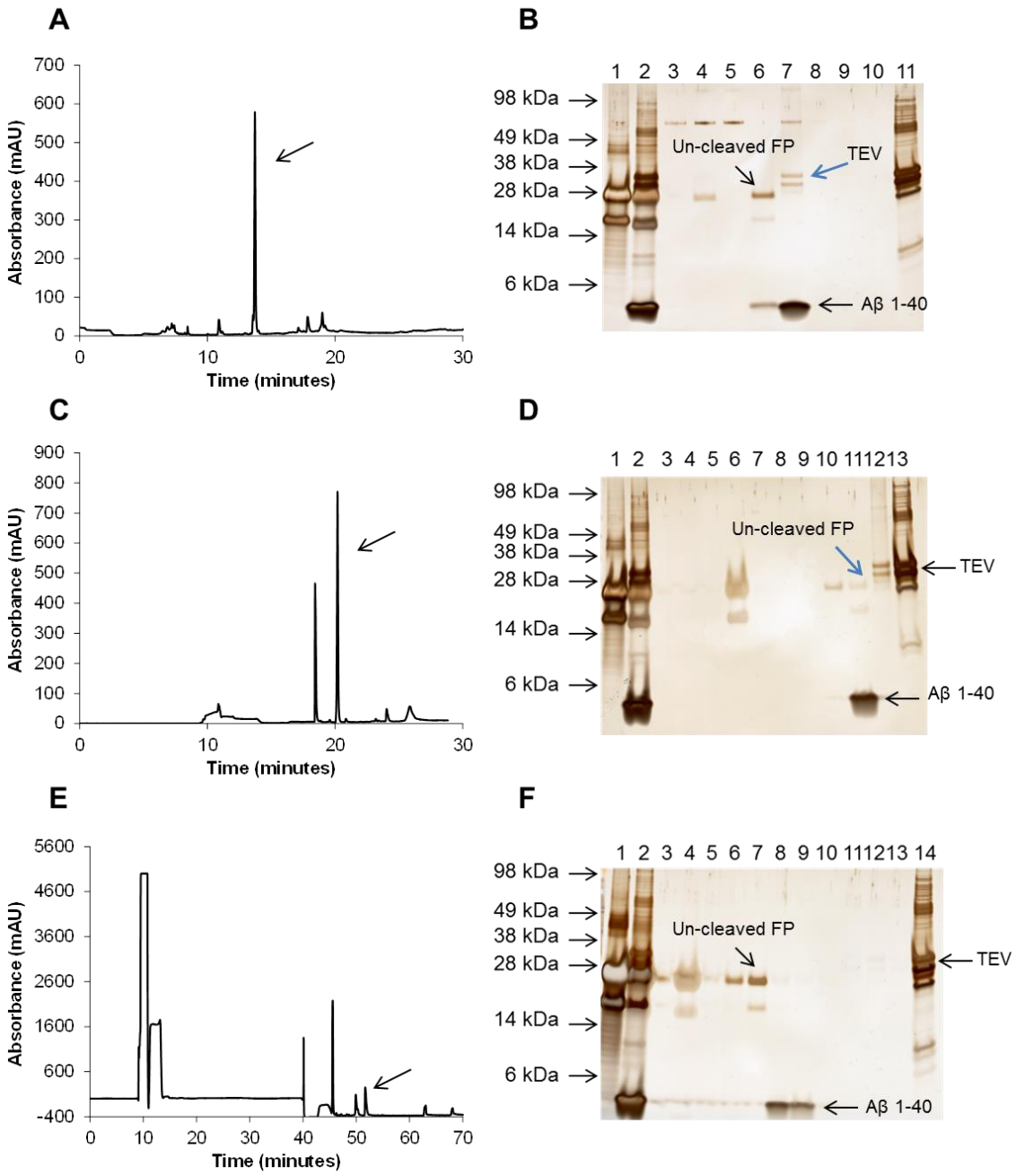
A
Absorbance (mAU)
Time (minutes)
B
1 2 3 4 5 6 7 8 9 10 11
98 kDa
49 kDa
38 kDa
28 kDa
14 kDa
6 kDa
Un-cleaved FP
TEV
Aβ 1-40
C
Absorbance (mAU)
Time (minutes)
D
1 2 3 4 5 6 7 8 9 10 111213
98 kDa
49 kDa
38 kDa
28 kDa
14 kDa
6 kDa
Un-cleaved FP
TEV
Aβ 1-40
E
Absorbance (mAU)
Time (minutes)
F
1 2 3 4 5 6 7 8 9 10 111213 14
98 kDa
49 kDa
38 kDa
28 kDa
14 kDa
6 kDa
Un-cleaved FP
TEV
Aβ 1-40

Figure 3.16 Optimisation of recAβ 1-40 separation following recTEV cleavage, with SB300 C8 reversed phase column.

A) Separation of recAβ 1-40 after cleavage with recTEV using a gradient of 0- 20 % acetonitrile in 5 minutes, 20- 40 % in 15 minutes and 40- 80 % in 10 minutes, the black arrow shows the eluting protein. B) SDS-PAGE gel which has been silver stained, showing the fractions collected from the purification shown in A (lanes 3-10), lanes 1 + 2 show un-cleaved and cleaved recAβ 1-40 respectively, and lane 11 shows recTEV protease alone. The recAβ 1-40 peptide was separated from the un-cleaved fusion protein, but not recTEV protease as shown in lane 7, highlighted by the blue arrow. C) Separation of recAβ 1-40 after cleavage with recTEV using a 28 % isocratic gradient, as shown in Finder *et al.*(Finder et al., 2010), the black arrow shows the eluting protein. D) SDS-PAGE gel which has been silver stained, showing the fractions collected from the purification shown in C (lanes 3-12), lanes 1 + 2 show un-cleaved and cleaved recAβ 1-40 respectively, and lane 13 shows recTEV protease alone. The recAβ 1-40 peptide was separated from recTEV protease as shown in lane 11, but not from the un-cleaved fusion protein, highlighted by the blue arrow. E) Separation of recAβ 1-40 after cleavage with recTEV using a 30 % isocratic gradient, the black arrow shows the eluting protein (UV absorbance was set to 214 nm). F) SDS-PAGE gel which has been silver stained, showing the fractions collected from the purification shown in E (lanes 3-13), lanes 1 + 2 show un-cleaved and cleaved recAβ 1-40 respectively, and lane 14 shows recTEV protease alone. The recAβ 1-40 peptide was separated from both recTEV protease and the un-cleaved fusion protein as shown in lanes 8 + 9.

Separating the cleaved recAβ 1-42 peptide was found to be more problematic than separating recAβ 1-40. I initially used an isocratic elution of 30.5 % acetonitrile as shown in Finder *et al.* (Finder et al., 2010). However, separation using this gradient was poor, with no separation of recAβ 1-42 from the un-cleaved fusion protein. This is shown in figure 3.17A, where it is clear from the eluting protein highlighted by the black arrow that there was little separation. The fractions from this are shown by SDS-PAGE in figure 3.17B, where lanes 7-11 all contain recAβ 1-42 and the other cleavage components. Given the failure of the isocratic elution to separate the

sample, next, I heated the column to 80 °C by resting it on a heat block, since Finder *et al.* (Finder et al., 2010) used a column heater at 80 °C to separate the recAβ peptides. However, no separation was seen (data not shown). I subsequently heated a 2.5 ml metal coil preceding the column, to heat the buffer entering the column, since I speculated that the diameter of the column was too large to successfully conduct heat from the heat block. Using the heated coil and column and the 30.5 % isocratic elution of acetonitrile resulted in better separation than previous attempts, as shown in figure 3.17C+D. The chromatogram in C shows peaks which have separated to a greater extent than in the preceding chromatogram, but the recAβ 1-42 highlighted by the black arrow is still not completely separated from the larger peak preceding it. Figure 3.17D shows the fractions from the chromatogram in C; Aβ 1-42 in lanes 10 + 11 show a much higher level of purity than seen before, but there is still a small amount of un-cleaved fusion protein present in the recAβ 1-42 fractions, which is indicated by the blue arrow. Lastly, I tried an isocratic elution of 32 % acetonitrile with heating of the column and coil at 80 °C. This method gave substantially better separation, and can be seen in figure 3.17E+F. The black arrow in E highlights the eluting peak of recAβ 1-42, which shows good separation from all other peaks. The fractions from this purification are shown in F; lane 8, which corresponds with the peak highlighted in E, containing pure recAβ 1-42.

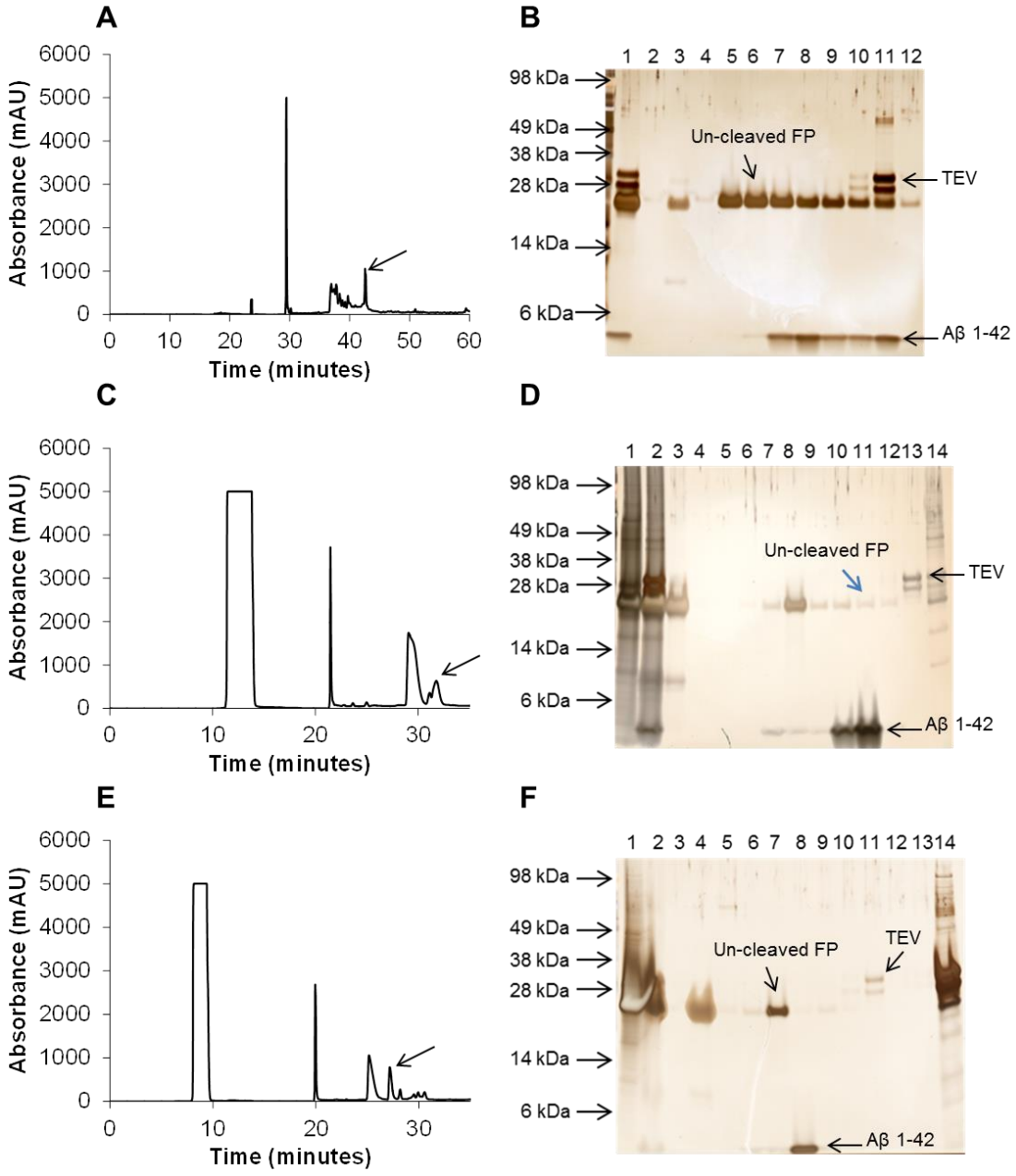
A
Absorbance (mAU)
6000
5000
4000
3000
2000
1000
0
0 10 20 30 40 50 60
Time (minutes)
B
1 2 3 4 5 6 7 8 9 10 11 12
98 kDa
49 kDa
38 kDa
28 kDa
14 kDa
6 kDa
Un-cleaved FP
TEV
Aβ 1-42
C
Absorbance (mAU)
6000
5000
4000
3000
2000
1000
0
0 10 20 30
Time (minutes)
D
1 2 3 4 5 6 7 8 9 10 11 12 13 14
98 kDa
49 kDa
38 kDa
28 kDa
14 kDa
6 kDa
Un-cleaved FP
TEV
Aβ 1-42
E
Absorbance (mAU)
6000
5000
4000
3000
2000
1000
0
0 10 20 30
Time (minutes)
F
1 2 3 4 5 6 7 8 9 10 11 12 13 14
98 kDa
49 kDa
38 kDa
28 kDa
14 kDa
6 kDa
Un-cleaved FP
TEV
Aβ 1-42

Figure 3.17 Optimisation of recAβ 1-42 separation following recTEV cleavage, with SB300 C8 reversed phase column.

A) Separation of recAβ 1-42 after cleavage with recTEV, using a 30.5 % isocratic gradient as shown in Finder *et al.* (Finder et al., 2010), the black arrow shows the eluting protein B) SDS-PAGE gel which has been silver stained, showing the fractions collected from the purification shown in A (lanes 2-12), lane 1 shows cleaved recAβ 1-42 . The recAβ 1-42 peptide was not separated from the fusion protein shown in lanes 5-11 or TEV protease shown in lanes 10 + 11. C) Separation of recAβ 1-42 after cleavage with recTEV using a 30.5% isocratic gradient as shown in Finder *et al.* (Finder et al., 2010), with the column and a 2.5 ml coil preceding it heated to 80 °C on a heat-block, the black arrow shows the eluting protein. D) SDS-PAGE gel which has been silver stained, showing the fractions collected from the purification shown in C (lanes 3-14), lanes 1 + 2 show un-cleaved and cleaved recAβ 1-42 respectively. The purification shows incomplete separation of recAβ 1-42 from the fusion protein, shown in lanes 10 + 11, highlighted by the blue arrow. E) Separation of recAβ 1-42 after cleavage with TEV using a 32 % isocratic gradient and heating the column and 2.5 ml coil to 80 °C on a heat-block, the black arrow shows the eluting protein. F) SDS-PAGE gel which has been silver stained, showing the fractions collected from the purification shown in E (lanes 3-14), lanes 1 + 2 show un-cleaved and cleaved recAβ 1-42 respectively. The recAβ 1-42 peptide was separated from both recTEV protease and the fusion protein, shown in lane 8.

3.7 Production and characterisation of recAβ disease associated isoforms

As previously stated, I wanted to investigate the toxicity of both oligomers and fibrils for recPrP and recAβ. This would allow comparisons to be made between potential important toxic species and the mechanisms leading to cell death. Therefore, once I had optimised the purification of the recAβ peptides, I wanted to develop assays to produce recAβ oligomers and fibrils. Controlling the starting conformation of recAβ 1-40 and recAβ 1-42 is crucially important in order to

compare the fibrillisation rates of the recAβ species, and to eliminate any initial aggregates from the oligomerisation preparations. I therefore needed to monomerise the recAβ peptides, since recAβ aggregates very readily and, therefore, is unlikely to be monomeric following purification. The recAβ peptides were monomerised by treating the pure lyophilised recAβ with hexafluoroisopropanol (HFIP), for 30 minutes at room temperature, and then removing the HFIP using a centrifugal vacuum. This method is widely accepted to eliminate any aggregates, leaving monomeric protein (Stine et al., 2003, Ferrão-Gonzales et al., 2005, Dahlgren et al., 2002, Young et al., 2009, Sondag et al., 2009).

Due to the propensity of Aβ to aggregate, in order to form oligomers it is necessary to stabilise the protein and slow down the fibrillisation process. I first trialled a method using a sulfonated hydrophobic molecule, 4,4'-dianilino- 1,1'-binaphthyl-5,5'-disulfonate (bis-ANS), which has been shown to bind to Aβ and stabilise it, thus slowing down fibrillisation and leading to the production of low molecular weight species (LMW) of Aβ. These LMW species were shown to be toxic to a murine monocyte-macrophage cell line (RAW) (Ferrão-Gonzales et al., 2005). I used bis-ANS at 150 μM, since at this concentration it had been shown to stabilise Aβ for more than 30 minutes (Ferrão-Gonzales et al., 2005), which I rationalised would be long enough to dose the cells before the Aβ began to aggregate. I incubated recAβ 1-42 with bis-ANS at 37 °C for 2-3 hours, and over the time course, I took samples and analysed them using SEC (a TSK3000 SWXL column). However, the chromatogram didn't change over time, and the eluting peak occurred after the bed volume of the column. In addition, the leading edge of the peak was very straight, which suggested the protein was interacting with the column. I tried to optimise this by using higher concentrations of sodium chloride in the running buffer, to reduce ionic interactions, but this did little to change the chromatograms. An example of recAβ 1-42 oligomers analysed by SEC, is shown in figure 3.18A, the bed volume of the column is 13 ml. I decided that SEC was not a reliable way to characterise the size of the oligomers formed using bis-ANS. Therefore, I used DLS instead, which is

a non-column based approach for investigating the hydrodynamic radius of a protein (for full details see methods and materials, section 2.5.2). I solubilised the monomeric Aβ in oligomerisation buffer (50 mM sodium phosphate, 100 mM sodium chloride, pH 7.4) with bis-ANS at 150 μM, and incubated the protein at room temperature for 30 minutes. I then analysed the size of the assemblies which had formed using DLS. The data showed that the recAβ species were large and of variable size, as shown in figure 3.18B (blue). Additionally, I produced oligomers and incubated these at -20 °C for 16 hours to see if the oligomers were stable when stored at -20 °C (as I did for recPrP oligomers).

The DLS data for the oligomers stored at -20 °C, showed them to be smaller and more stable than those made fresh, this is shown figure 3.18B (red). Surprisingly, the data suggested that freezing the oligomers helped stabilise the assemblies. Multiple repeats showed that a stable recAβ 1-42 oligomer population reproducibly formed under these conditions (figure 3.18C). Additionally, I found that after storage at -20 °C, the mean hydrodynamic radius for both recAβ 1-40 and recAβ 1-42 was smaller than that of fresh oligomers, which is shown in figure 3.17D. Therefore, I stored the oligomers at -20 °C prior to cellular toxicity assays. As mentioned previously, Aβ oligomers formed using bis-ANS had been found to be toxic to cells from a murine macrophage cell line, and the bis-ANS itself was found to not cause toxicity(Ferrão-Gonzales et al., 2005). Unfortunately, in initial trials bis-ANS did cause toxicity to murine primary cortical cells. The toxicity of bis-ANS, therefore, confounded the oligomer toxicity results, since it was not clear whether cellular toxicity was caused by the oligomers or the bis-ANS.

Therefore, I used an alternative method to make recAβ oligomers. This alternative method, published by Stine *et al*. (Stine et al., 2003) used ice-cold Ham's F12 cell culture medium to stabilise Aβ oligomers (Lambert et al., 1998, Stine et al., 2003). They showed the resulting Aβ species were small and globular, reminiscent of oligomers rather than resembling fibrils (Stine et al., 2003). I therefore followed this

method and analysed the resulting oligomers using DLS. The hydrodynamic radius and stability of the recAβ 1-42 oligomers were reproducible, and similar to those formed with the bis-ANS protocol (figure 3.19A). The recAβ 1-40 oligomers, however, were shown to be more heterogeneous than the recAβ 1-42 oligomers, with some much larger species suggestive of aggregation. The recAβ 1-42 and recAβ 1-40 oligomers formed using this method were used in the cellular toxicity and mechanism experiments, which are described in chapters 4 and 6.

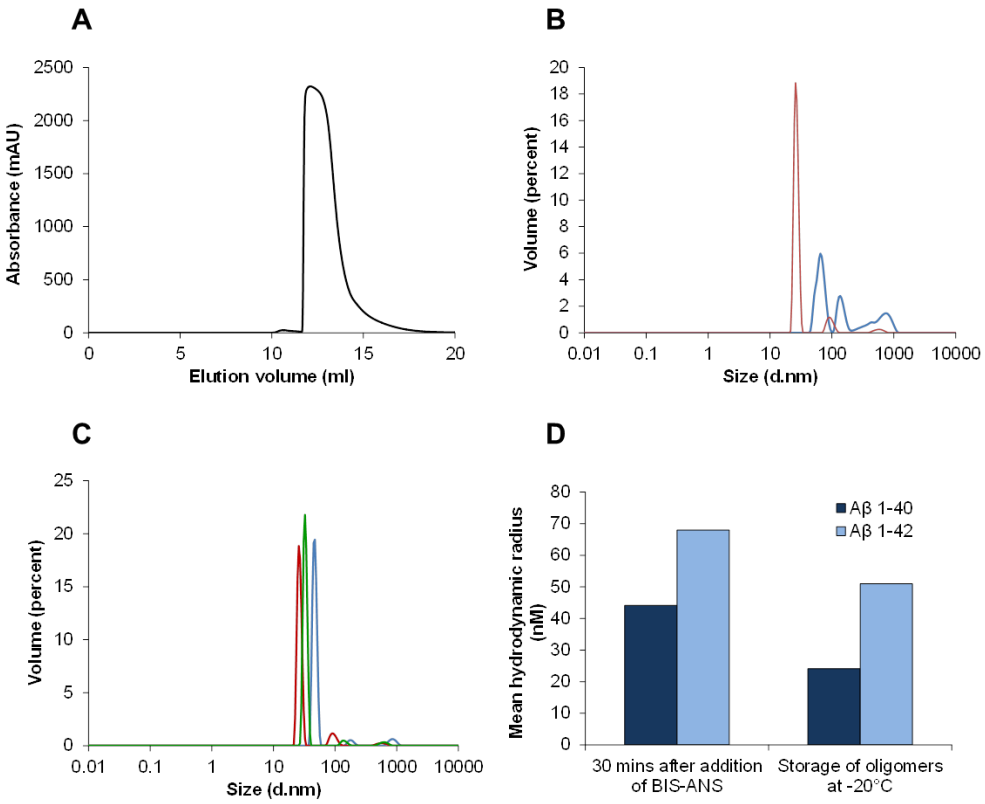

Figure 3.18 Characterisation of recAβ oligomers, using BIS-ANS.

A) SEC for recAβ 1-42 oligomers after 30 minute incubation with BIS-ANS. Protein is eluting later than bed volume of the column (absorbance 214 nm). B) DLS data; size distribution by volume of recAβ 1-42 oligomers after 30 minute incubation with bis-ANS (blue) and after 30 minute incubation with bis-ANS + storage at – 20 °C (red). C) DLS data, showing size distribution by volume of recAβ 1-42 oligomers after 30 minute incubation with bis-ANS + storage at – 20 °C, (red, blue and green show 3 repeats). D) Mean hydrodynamic radius data from DLS is shown for recAβ 1-40 and recAβ 1-42 oligomers, made after 30 minute incubation with bis-ANS + those stored at – 20 °C.

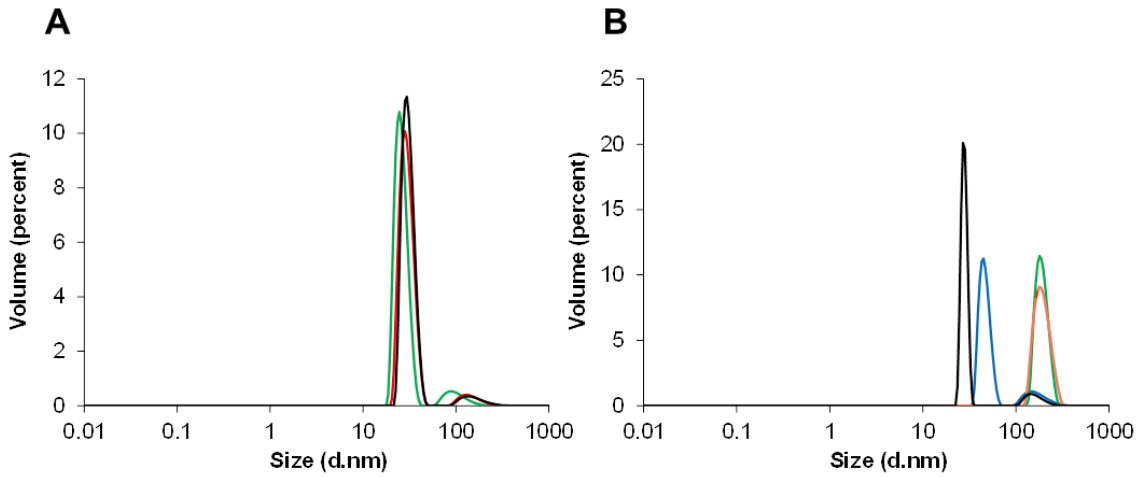

Figure 3.19 Characterisation of recAβ oligomers made in F12 media at 4 °C.

A+ B) DLS data, showing size distribution by volume of recAβ oligomers formed using Ham's F12 cell culture medium at 4 °C. A) RecAβ 1-42 oligomers with 3 repeats (green, red and black). B) RecAβ 1-40 oligomers with 4 repeats (black, blue, green and red). recAβ 1-42 oligomers showed greater stability and more reproducible data when compared to recAβ 1-40 oligomers, which showed greater variability and contained larger protein species.

In addition to oligomers, it was also important to produce an Aβ species which resembled the Aβ plaque that could be tested for toxicity on the cells. The protocol I employed was adapted from published methods(Paul and Axelsen, 2005, Finder et al., 2010) and involved fibrils being formed by solubilising recAβ in sodium hydroxide and then diluting with HEPES pH 7.4 (for full details see methods and materials, section 2.7.2). I monitored fibril formation using ThT, as I had done for recPrP fibrillisation. However, since I found recAβ to fibrillise much faster than recPrP, fluorescence readings were taken at 1 minute intervals instead of 5 minute intervals as was done for recPrP. Additionally, in the recPrP fibrillisation assay the fibrils were shaken constantly. However, the recAβ fibrillisation assay was conducted without shaking, since agitation resulted in the fibrils forming too rapidly to monitor the fibrillisation reaction.

A representative fibrillisation assay for recAβ 1-40 and recAβ 1-42 is shown in figure 3.20A. ThT data was averaged for 5 fibrillisation reactions and background fluorescence, shown by a no recAβ control reaction, was subtracted. The data was then expressed as a percentage and standard deviation error bars are shown which indicate variation between the fibrillisation reactions. The lag time (the time taken for fibrils to begin to form) is represented as a period of low fluorescence at the beginning of the assay, and is considerably longer for recAβ 1-40 (figure 3.20A: blue) when compared with recAβ 1-42 (figure 3.20A: red). These data indicate that recAβ 1-42 fibrillises more readily than recAβ 1-40. Interestingly, the increased fibrillisation rate of Aβ 1-42 may also occur *in vivo* since during disease, Aβ 1-42 forms fibrillar plaques more readily than Aβ 1-40(Lansbury and Lashuel, 2006, Suzuki et al., 1994).

The recAβ fibrils have an amyloid structure as shown by Congo red staining, where under polarised light the characteristic yellow and green birefringence can be seen (figure 3.20B). The sensitivity of the recAβ fibrils to PK digestion was also tested as it was for the recPrP fibrils. Interestingly, the recAβ fibrils were found to be PK

resistant, but no difference was seen with maturation and PK treatment. When recPrP fibrils are digested with or without maturation, a different banding pattern is seen compared to recPrP fibrils that have not been digested (figure 3.21A + B, lanes 8 + 9 compared to lane 7). The recAβ fibrils, however, looked no different when treated with or without PK, as shown in figure 3.21A for recAβ 1-40 and 3.21B for recAβ 1-42. The monomer is shown for comparison. Interestingly, the maturation step seems to increase the PK resistance of the monomer for both recAβ 1-40 and recAβ 1-42, shown in lane 3 of A and B (monomer after maturation), in comparison to lane 2 of A and B.

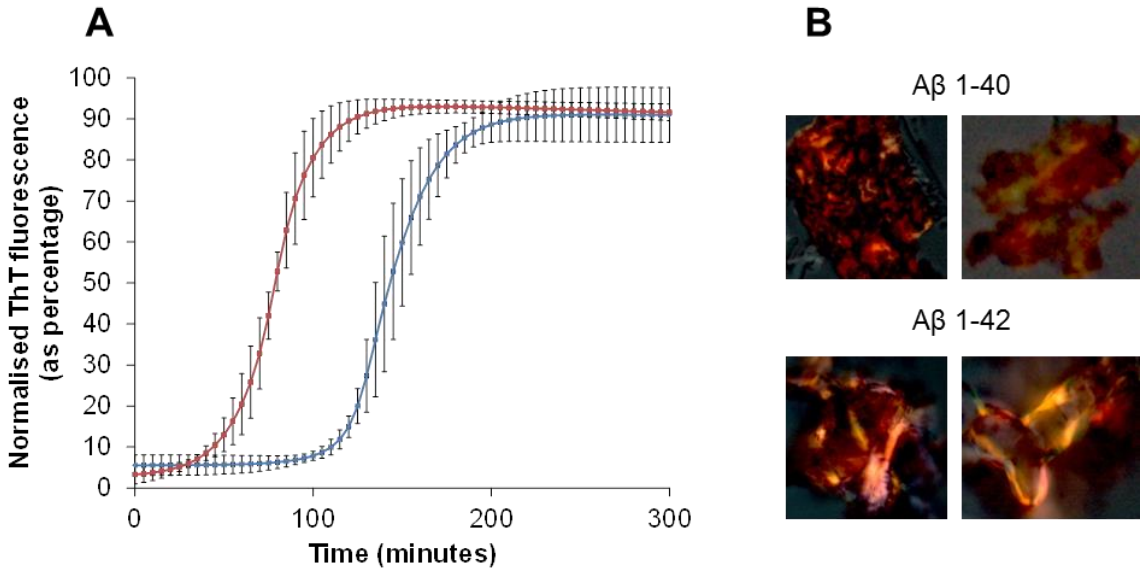

Figure 3.20 Characterisation of recAβ fibrils.

A) ThT average fluorescence curves, showing readings over time as the recAβ fibrils form and ThT binds (average of 5 fibrillisation reactions) ± standard deviation error (recAβ 1-42 is shown in red and recAβ 1-40 is shown in blue). B) RecAβ fibrils with Congo red staining under polarised light, the yellow and green birefringence shows amyloid structures.

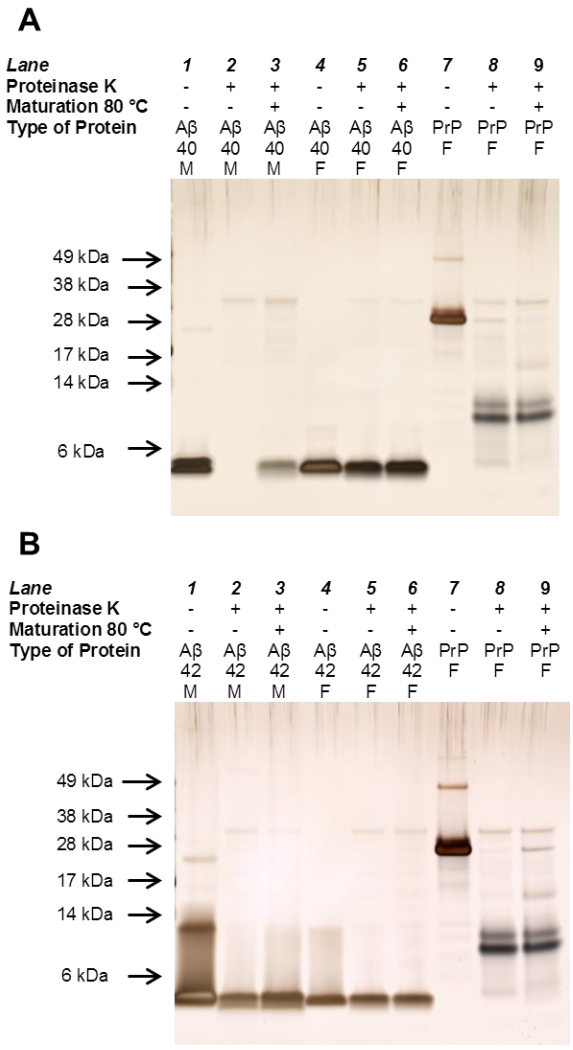

Figure 3.21 Characterisation of recAβ fibrils.

A) Characterisation of recAβ 1-40 fibrils by maturation at 80 °C and PK digestion, in A+B recPrP fibrils (PrP F) are shown as a control for PK resistance in lanes 7-9. A) Lanes 1-3 show recAβ 1-40 monomer (M) and lanes 4-6 show recAβ 1-40 fibrils (F). All were either treated with no PK, with PK but not heated to 80 °C or with PK and were heated to 80 °C (maturation). B) Characterisation of recAβ 1- 42 fibrils by maturation at 80 °C and PK digestion. Lanes 1-3 show recAβ 1-42 monomer (M) and lanes 4-6 show recAβ 1-42 fibrils (F). All were either treated with no PK, with PK but not heated to 80 °C or with PK and were heated to 80 °C (maturation).

3.8 Discussion

Most studies which have investigated protein toxicity have not compared different isoforms of multiple disease associated proteins. However, studies which have analysed the toxicity of more than one disease associated protein (Ferreiro et al., 2006, Silei et al., 1999, Brown et al., 1997, Sáez-Valero et al., 2000) rarely characterise the misfolded proteins before investigating toxicity and associated mechanisms. This makes it difficult to link protein conformation with toxicity and to compare the mechanisms leading to cell death between different proteins. In this chapter, I have optimised the production and characterisation of different isoforms of both recPrP and recAβ so that the toxicity and mechanisms leading to cell death can be investigated. These toxicity and mechanistic experiments are described in detail in chapters 4 and 6. In this chapter however, I have focused on how I produced these isoforms and how they have been characterised, since it is important to first define the structure of the misfolded proteins before testing toxicity, so that clear links between certain misfolded species and toxicity can be established.

Importantly, I have produced a protein which can be used as a negative control in toxicity experiments, since a criticism of assessing toxicity by dosing cells with misfolded proteins *in vitro*, is that exposing cells to exogenous protein will cause toxicity. The protein I produced to act as a negative control was α-helical recPrP, with a structure mimicking that of PrP^C. Since PrP^C does not cause toxicity *in vivo,* I reasoned that if I dosed the cells with an equivalent concentration of α-helical recPrP compared to oligomers or fibrils, then the lack of toxicity induced by α-helical recPrP would rule out the possibility that the toxicity was due to exogenous protein concentration. Instead, it would show that toxicity caused by oligomers or fibrils must be conformation dependent. For this reason, it was important to establish that the α-helical recPrP showed a high level of purity and was correctly folded to give an α-helical structure, which is shown in figure 3.1A+B.

Oligomers and small assemblies of misfolded proteins are thought to be fundamental in causing pathology in PMDs (Kuo et al., 1996, Naslund et al., 2000, McLean et al., 1999, Mucke et al., 2000a, Walsh et al., 2002, Quist et al., 2005, Kristiansen et al., 2007, Simoneau et al., 2007, Volles et al., 2001). Therefore, it was crucial to produce recPrP oligomers which were of a size and structure relevant to those seen in disease. It has been postulated that, *in vivo*, β-sheet rich (Glabe and Kayed, 2006, Cobb and Surewicz, 2009, Prusiner, 1998a) oligomer structures between 14 to 28 PrP monomers in size are infectious and are critical to the pathology of the disease (Silveira et al., 2005). The method which I used was adapted from Rezaei *et al*. (Rezaei et al., 2005), who demonstrated that this method produced two main populations of oligomers: a smaller population which consisted of approximately 12 PrP molecules, and a larger oligomer population which consisted of approximately 36 PrP molecules. The size of these oligomers is therefore similar to what would be relevant *in vivo,* and CD analysis showed the oligomers I had produced had a β-sheet rich structure, which is characteristic of oligomers in disease.

In addition to oligomers, I formed recPrP fibrils to mimic the large insoluble amyloid structures which are found in the brains of individuals infected with prion disease. As mentioned previously, it is widely debated whether fibrils are toxic to neurons, or if they are a protective mechanism to sequester small soluble forms of the misfolded protein (Haass and Selkoe, 2007, Treusch et al., 2009). It was therefore important to investigate the toxicity of recPrP fibrils in relation to oligomers. PrP fibrils isolated from infected tissue appear fibrillar and "rod-like" when analysed by electron microscopy (Prusiner et al., 1983), they show resistance to PK digestion (Parchi et al., 2000, Collinge et al., 1996), and, exhibit green birefringence under polarised light when stained with Congo red (Prusiner et al., 1983). The fibrils I formed *in vitro*, shared similar characteristics to fibrils found *in vivo*, with an amyloid, PK resistant structure.

In order to compare the toxicity and associated mechanisms for two important disease associated proteins, I also produced the Aβ protein, which is involved in Alzheimer's disease. With much optimisation, I produced a reproducible protocol to generate recAβ with a high degree of purity.

Before making oligomers or fibrils, I monomerised the recAβ by established methods (Stine et al., 2003, Barghorn et al., 2005, Dahlgren et al., 2002) to eliminate any aggregates so that the starting conformation of recAβ for making both oligomers and fibrils was the same. This was important to ensure reproducibility, particularly for the oligomers, since aggregates or fibrillar structures within the oligomer preparations could confound the toxicity data. It was also important that the recAβ was monomeric for the fibrillisation assays, in order to accurately compare rates of fibrillisation between recAβ 1-40 and recAβ 1-42.

Substantial optimisation of published methods (Ferrão-Gonzales et al., 2005, Stine et al., 2003) was required to produce recAβ oligomers, which could be tested for toxicity. First, I used a sulfonated hydrophobic molecule, bis-ANS, which has been shown to stabilise Aβ and slow down fibrillisation (Ferrão-Gonzales et al., 2005). However, during initial toxicity assays I found that bis-ANS was toxic to the primary cells, which meant that I could not distinguish between toxicity caused by the oligomers or by bis-ANS. I therefore had to optimise another method to make oligomers.

Next, I trialled a method using Ham's F12 cell culture media to make oligomers, which was derived from Stine *et al.* (Stine et al., 2003). This method has the advantage that the oligomerisation buffer is cell culture media and, therefore, not toxic to cells. The method had also been extensively characterised (Stine et al., 2003, Dahlgren et al., 2002, Sondag et al., 2009, Young et al., 2009), with Aβ being incubated with the Ham's F12 cell culture media and then analysed by atomic force microscopy (AFM) under various conditions, such as temperature, length of

incubation, addition of salts, and pH (Stine et al., 2003). It was shown that when Aβ was incubated at 4 °C for 24 hours in F12 media, small globular oligomers formed and larger aggregates were absent (Stine et al., 2003). Therefore, I decided that this may be a more reliable method for producing recAβ oligomers and in the absence of a toxic buffer. In the bis-ANS method, the binding of the bis-ANS molecule to recAβ results in stabilisation of the protein and slows down the formation of fibrils (Ferrão-Gonzales et al., 2005). It is likely that the F12 cell culture media method works on a similar principle, with the amino acids present in the media acting to stabilise the oligomers, since it has been shown previously that several amino acids present in F12 media, including arginine, glycine, glutamate, histidine, lysine, proline, and serine have been shown to have stabilising properties (Falconer et al., 2011, Arakawa et al., 2007) when purifying, or trying to prevent aggregation of proteins (Falconer et al., 2011, Arakawa et al., 2007).

The disease associated conformations I have formed are comparable to what has been published previously. The recPrP fibrils I have produced show comparable Congo red staining and EM analysis (Alvarez-Martinez et al., 2011, Bocharova et al., 2005, Baskakov et al., 2002, Panza et al., 2008), and the oligomers show a β-sheet rich structure consistent with several publications (Rezaei et al., 2005, Hosszu et al., 2009, Tahiri-Alaoui et al., 2006), and possess similar characteristics to those produced by Rezaei *et al*. (Rezaei et al., 2005).

There have been less papers published analysing Aβ oligomers formed *in vitro*, in comparison to PrP, likely because Aβ tends to be relatively unstable in this conformation, and, as I have found, the reproducible production of these structures is technically challenging. Most studies which have estimated the size of Aβ oligomers have done so using techniques such as AFM (Stine et al., 2003), which is a crude measure of size and gives more of a general impression as to whether small globular structures or larger aggregates are present. Studies which have used SEC seem to have chromatograms which are comparable to mine, with the protein

eluting after the bed volume (Ferrão-Gonzales et al., 2005). This observation suggests the protein was interacting with the column, which may therefore give an unreliable estimate of size. In contrast, a few papers have used light scattering techniques such as dynamic light scattering or static light scattering to investigate the size of Aβ oligomers (Bitan et al., 2003, Carrotta et al., 2006, Walsh et al., 1999). These results, however, are quite variable likely because of the different methods used to form or isolate oligomers and whether synthetic or recAβ was used. In this chapter, I have presented DLS data that reproducibly shows that there are differences between the size and stability of oligomers formed by recAβ 1-40 or recAβ 1-42.

The recAβ and recPrP fibrils both showed similar characteristics, with amyloid structures, ThT fluorescence, and resistance to PK digestion. The recAβ fibrils however, formed much more readily than recPrP fibrils. The recPrP fibrils were formed under semi-denaturing conditions with shaking. By contrast, recAβ fibrils were formed under non-denaturing conditions without shaking showing the different propensities of the proteins to form amyloid. This may have implications for the pathologies and disease processes for prion or Alzheimer's disease, and whether the fibrils are protective or harmful to the cells.

I have produced and characterised oligomers and fibrils of both recAβ and recPrP. The toxicity of these isoforms will be discussed in chapter 4. The robust characterisation of the misfolded proteins, which was carried out in this chapter, will hopefully support links between conformation and toxicity.

Chapter 4:

Toxicity of disease associated isoforms of recPrP and recAβ

4.1 Introduction

The main objective of this project was to investigate the toxicity and associated mechanisms caused by specific conformations of misfolded proteins. In chapter 3, I outlined the production and characterisation of disease associated isoforms of recPrP and recAβ. These misfolded isoforms included oligomers and fibrils. In this chapter, I will describe investigations of toxicity of these misfolded proteins. I wanted to investigate the toxicity of oligomers since they are thought to play a crucial role in the pathogenesis of many PMDs (Kuo et al., 1996, Naslund et al., 2000, McLean et al., 1999, Mucke et al., 2000a, Walsh et al., 2002, Quist et al., 2005, Kristiansen et al., 2007, Simoneau et al., 2007, Volles et al., 2001, Lue et al., 1999). Furthermore, I wanted to investigate the toxicity of fibrils, since there is much debate and controversy concerning the potential toxicity of fibrillar deposits in many PMDs (Soto, 2003, Ross and Poirier, 2004, Dobson, 2003, Haass and Selkoe, 2007, Treusch et al., 2009).

Studies investigating PMDs generally use *in vitro* or *in vivo* models, which each have advantages and disadvantages. *In vivo* experiments often use either transgenic animals overexpressing the disease associated protein, or animals with genetic mutations to mimic genetic forms of these diseases. Transgenic animals replicate some of the characteristic features and symptoms associated with naturally occurring PMDs. However, it is not known how overexpressing proteins may affect the conformation and resulting toxic species in these transgenic animals. The mechanisms and rates of protein misfolding in naturally occurring PMDs, which may take decades, may be different when compared to disease in a transgenic animal. When investigating a PMD *in vivo*, the misfolded protein deposits and associated cellular toxicity are generally analysed at specific time points within the disease process, or at the disease end point. This can make it very difficult to link specific protein conformations with toxicity and to understand which misfolded species are important. Therefore, it can be helpful to study PMDs *in vitro*. In such

experiments, proteins can be misfolded under controlled conditions into particular conformations, characterised, and subsequently tested for toxicity (Baskakov and Bocharova, 2005, Bocharova et al., 2005, Breydo et al., 2008, Ferrão-Gonzales et al., 2005, Finder et al., 2010, Simoneau et al., 2007). By studying the toxicity of well characterised isoforms we can investigate relationships between protein conformation and disease (Simoneau et al., 2007, Lambert et al., 1998, Stine et al., 2003). It is also possible to investigate mechanisms and rates of misfolding *in vitro*, which can shed light on how proteins fold or misfold under certain conditions. By studying the potential toxicity of misfolded proteins *in vitro*, it can help us to elucidate which misfolded species may be important *in vivo*. Additionally, *in vitro* studies can allow us to compare the toxicity and related mechanisms induced by misfolded proteins associated with different PMDs.

In this study, I wanted to determine what conformation of recPrP and recAβ was most toxic, and, therefore, the most likely to be important in disease pathogenesis. In order to make specific links between protein conformation and resulting toxicity, an *in vitro* approach was needed. I*n vitro* experiments allow characterisation of the misfolded proteins and controlled toxicity assays, which cannot be achieved *in vivo*. For these reasons, I used *in vitro* experimentation to investigate the toxicity of disease associated isoforms of recPrP and recAβ. I used primary cells as opposed to a cell line, since although cell lines are useful for high throughput assays they are often isolated from cancer cells or are cells which have been immortalised. This can mean that they have lost certain characteristics which would be associated with the equivalent cell *in vivo,* therefore, any toxicity data may not be representative of a normal cell (Pan et al., 2009, Burdall et al., 2003, Stansley et al., 2012). Primary cells resemble cells *in vivo* more closely since they are grown straight from the organism and not passaged or immortalised (Pan et al., 2009). Primary cells have the limitations of being grown as a monolayer, so that the architecture of the organ is lost, but they are thought to better represent cells *in vivo* than cell lines (Pan et al., 2009). Another option would have been to use organotypic slice cultures (OSCs).

OSCs have many of the advantages of primary cells (imaging and control over growth *in vitro)* but they keep much of the architecture of the organ from which they were isolated (Cho et al., 2007, Elias and Kriegstein, 2007). However, OSCs are less high throughput than primary cells for toxicity experiments. Therefore, I chose to use primary cells since they are more physiologically relevant than cell lines and they allow a more high throughput approach than OSCs. The primary cells I used were murine cortical cells. These were chosen because the cortex is a relevant brain area for both AD and prion diseases such as CJD.

Previously, studies which have looked at the toxicity of PrP or Aβ *in vitro* have generated conflicting data about whether oligomers or fibrils are more toxic (Simoneau et al., 2007, Novitskaya et al., 2006, Lorenzo and Yankner, 1994). This is likely due to different methods for producing oligomers and fibrils, which leads to discrete conformations with different toxic properties. So far there have not been any studies which have investigated the toxicity of well characterised misfolded forms of both PrP and Aβ using the same toxicity model, which allows the data to be directly compared. Previous studies have compared the toxicity of PrP fragments with Aβ fragments (Brown et al., 1997, Silei et al., 1999, Sáez-Valero et al., 2000), or with full length Aβ 1-40 (Ferreiro et al., 2006). These studies dosed either primary neurons or microglia with synthetic peptides (Ferreiro et al., 2006, Silei et al., 1999, Brown et al., 1997, Sáez-Valero et al., 2000). The results from these studies showed that fragments of PrP or Aβ can cause neuronal toxicity, which may be mediated through different pathways (Brown et al., 1997). However, since these peptide fragments had not been misfolded or characterised first, no conclusions can be drawn about the conformation of these protein fragments in relation to toxicity. In the absence of characterisation we cannot know whether the fragments were monomeric, or whether they had assembled into oligomers or fibrils prior to incubation with the cells. These considerations confound the ability to use these studies to link protein conformation and toxicity, which may be crucial to understanding these diseases.

In chapter 3 I produced full length recPrP and recAβ 1-40 and recAβ 1-42, misfolded these into oligomers and fibrils and performed extensive characterisation before undertaking any toxicity experiments. This should directly address the limitations of these previous studies. In this chapter, I will detail investigations of toxicity for these misfolded proteins using murine primary cortical cells. This will hopefully give a more complete picture of what the important toxic species are, and addresses whether they are the same for different PMDs. Additionally, it will highlight whether recPrP and recAβ elicit similar levels of toxicity.

4.2 Toxicity of disease associated isoforms of recPrP

The toxicity of recPrP was investigated using primary cortical cells, which were incubated with the recPrP isoforms for 24 hours before being fixed and stained with DAPI. Cell viability was then established by a live/dead cell count (see section 2.8.1). The recPrP cell viability data was normalised to buffer controls for each isoform, which accounted for any background toxicity caused by the buffers. If the buffer controls caused toxicity (if cell viability was less than 85 %), then the experiment was excluded since the background level of cell death was deemed unacceptably high. Firstly I tested the toxicity of all isoforms at the concentration range: 3-10 μM as shown in Simoneau *et al.* (Simoneau et al., 2007), but the volume of protein added to the cells which was needed to achieve these concentrations meant that all cells including the buffer controls showed high toxicity (data not shown). Therefore, I reduced the concentration range to: 1.3–5.2 μM (figure 4.1A), which allowed me to add lower volumes of protein or buffer to the cells. Once I had lowered the volume of buffer being added to the cells, the cell viability in the controls was above the acceptable threshold (85 %). As mentioned in chapter 3 α-helical recPrP was produced to mimic PrP^{C}, which is not toxic *in vivo*. The data shows that at the lowest concentration the α-helical recPrP caused low levels of toxicity. By contrast, the oligomers and fibrils caused a reduction in cell viability of 50 % or more. At the two higher concentrations of 2.6 μM and 5.2 μM all three conformations were toxic. In

order to demonstrate that recPrP is not in itself toxic and, therefore, any toxicity shown by the oligomers or fibrils must be conformation dependent, I wanted to select a concentration range at which α-helical recPrP causes low levels of toxicity, as PrP^C would *in vivo*. With this in mind, I next trialled a broader, lower concentration range (figure 4.1B). The data in figure 4.1B shows that all recPrP isoforms caused low levels of toxicity between 0.01- 0.29 μM. However, above 0.29 μM differences in toxicity between the isoforms are evident. Therefore, I decided to use the concentration range 0.43–1.73 μM to investigate the toxicity of the different isoforms in greater depth. At this range the α-helical recPrP shows low toxicity, and the oligomers and fibrils both elicit a toxic response from the cells.

To obtain average toxicity data, which was important to reliably determine the differences in toxicity between the isoforms, I carried out multiple experiments (minimum of n=4) at the concentration range from 0.43–1.73 μM (figure 4.2). The results show that the α-helical recPrP caused low toxicity at all concentrations, with no significant difference in toxicity when compared to the buffer control. The fibrils were shown to be significantly more toxic than α-helical recPrP at all concentrations (p value <0.05, figure 4.2) and the oligomers were shown to be significantly more toxic than α-helical recPrP at 0.87 μM and 1.73 μM. At 1.73 μM there was no significant difference in toxicity between oligomers and fibrils, however, at 0.87 μM the fibrils were significantly more toxic than the oligomers (p value <0.05). This was an unexpected finding, since oligomers are often thought to be more toxic than fibrils in PMDs (Chabry et al., 2003, Ma et al., 2002, Simoneau et al., 2007). The concentrations for the cell experiments were based on the monomer concentration. Therefore, for 12 monomers in the α-helical recPrP condition this would be equivalent to one 12 mer oligomer. If each monomer, oligomer or fibril is referred to as a unit then 1 oligomer unit would be equivalent to 12 monomer units. Fibrils are likely comprised of hundreds or thousands of monomers, therefore, one fibril unit may be equivalent to 1000 monomers and approximately 80 oligomers. This would mean that the fibrils and oligomers are even more toxic than indicated, since the

number of oligomer and fibril units are less compared to the monomer. Additionally, the number of fibril units compared to oligomer units is also considerably lower. This would suggest that the fibrils are the most toxic of the isoforms.

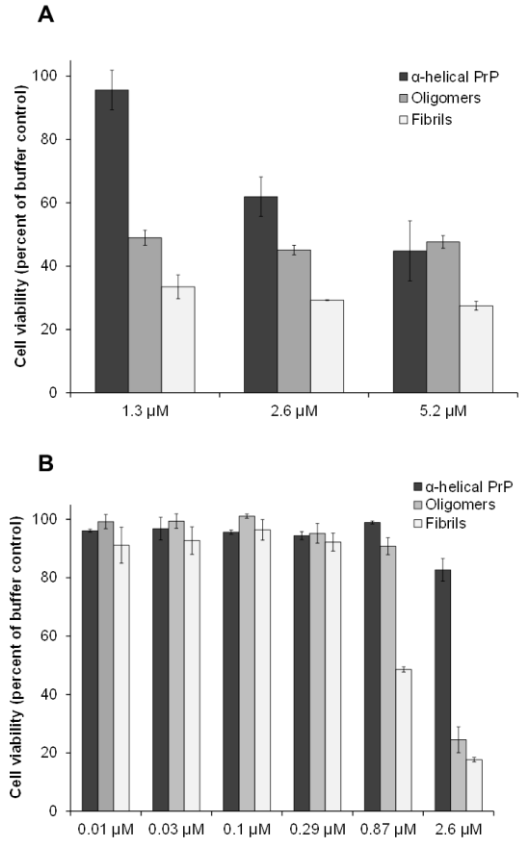

Figure 4.1 Toxicity of misfolded conformations of recPrP across a broad concentration range.

A+B) Bar charts to show the toxicity of different recPrP preparations: α-helical recPrP (dark grey), oligomers (light grey) and fibrils (white). A) Shows a concentration range from 1.3- 5.2 µM (equivalent to 30-120 µg/ml of recPrP). The cell viability is shown as a percentage of the buffer control ± standard error (SE). B) Shows a concentration range from 0.01- 2.6 µM (equivalent to 0.25- 60 µg/ml of recPrP). The cell viability is shown as a percentage of the buffer control ± standard error (SE).

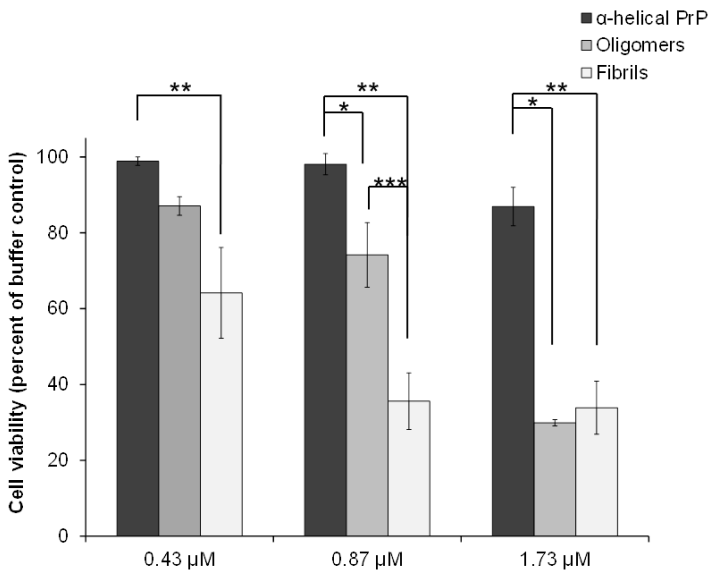

Figure 4.2 Average toxicity data for misfolded conformations of recPrP.

Bar chart to show the toxicity of different recPrP preparations: α-helical recPrP (dark grey), oligomers (light grey) and fibrils (white) at a concentration range from 0.43-1.73 µM (equivalent to 10-40 µg/ml of recPrP). Cell viability is shown as a percentage of the buffer control ± standard error (SE), a minimum of 6 readings (3-4 pictures per well with 2 wells for each) were taken for each recPrP preparation in each experiment (minimum n = 4). * indicates the oligomers or ** indicates the fibrils are significantly more toxic than the α-helical recPrP *** indicates the fibrils are significantly more toxic than the oligomers (one-way ANOVA; p value <0.05).

4.3 Toxicity of disease associated isoforms of recAβ

Once I had established the relative toxicities of the different recPrP isoforms, I wanted to compare the toxicity of recPrP oligomers and fibrils to another disease associated protein. By comparing multiple disease associated proteins, it would enable me to determine the importance of specific misfolded protein conformations in different PMDs. Therefore I investigated the toxicity of monomers, oligomers and fibrils formed from recAβ 1-40 and recAβ 1-42, which have both been shown to be

involved in AD. In chapter 3, I showed that recAβ 1-40 and recAβ 1-42 behave differently in terms of their fibrillisation kinetics and the size of oligomers which they form. It was therefore important to investigate both forms of recAβ, to see if these differences affect their relative toxicities. As with recPrP, it was important to establish a concentration range of monomeric recAβ which was not toxic to the cells. To do this, I exposed the primary cells to monomeric recAβ 1-40 and recAβ 1-42 at the range 0.11-1.73 μM (figure 4.3). They revealed that unlike recPrP which showed a dose dependent toxic effect, the cells treated with the recAβ monomers did not. Instead, the cells treated with recAβ 1-40 and recAβ 1-42 monomers showed relatively low levels of toxicity at all concentrations. However, when the results were analysed more closely, it became apparent that recAβ at 0.43 μM was more toxic than recAβ at the two higher concentrations (0.87 and 1.73 μM), suggesting an inverse dose response. However, this observation was not statistically significant. The inverse trend which was observed was investigated further, and is discussed in section 4.5.

Having established that the recAβ monomer caused low levels of toxicity, I chose to investigate the toxicity of the recAβ oligomers and fibrils at the concentration range 0.43-1.73 μM, which I used for the recPrP experiments. This allowed a direct comparison between recPrP and recAβ. I carried out multiple experiments at this concentration range to obtain reliable average toxicity data for each isoform of recAβ 1-40 and recAβ 1-42 (figure 4.4). The data revealed that cells treated with any of the recAβ 1-40 conformations showed no significant difference in viability when compared to each other at any of the concentrations tested. All cells which were treated with recAβ 1-40 showed a 20- 25 % drop in cell viability (figure 4.4A), suggesting that all conformations of recAβ 1-40 cause relatively low toxicity. By contrast, the recAβ 1-42 oligomers were shown to be significantly more toxic than the recAβ 1-42 fibrils at 0.87 μM (p value < 0.05). This shows that recAβ 1-42 oligomers are toxic to the cells, and cause a drop in cell viability of approximately 35 % at 0.87 μM. While the toxicity caused by the recAβ 1-42 monomers was not

statistically significant, the monomers do appear to cause some toxicity at the lower concentrations. However, given the propensity of recAβ 1- 42 to fibrillise, it is difficult to determine whether the toxicity was caused by recAβ 1- 42 in a monomeric state, or if toxicity could have been caused by recAβ 1- 42 assembling into oligomeric species on the pathway to forming fibrils. It is likely that if recAβ 1- 42 monomers had fibrillised during incubation with the cells, then it would be intermediates in the fibrillisation process which caused the toxicity since recAβ fibrils are not toxic. This will be investigated and discussed further in section 4.5. I presented data in chapter 3 that showed differences in the size of recAβ 1- 40 and recAβ 1- 42 oligomers. I analysed the toxicity of the different oligomers and found that there was no significant difference between the recAβ 1- 40 oligomers and the recAβ 1- 42 oligomers at any of the concentrations. The differences in the size of the oligomers must therefore not have significantly affected their toxicity.

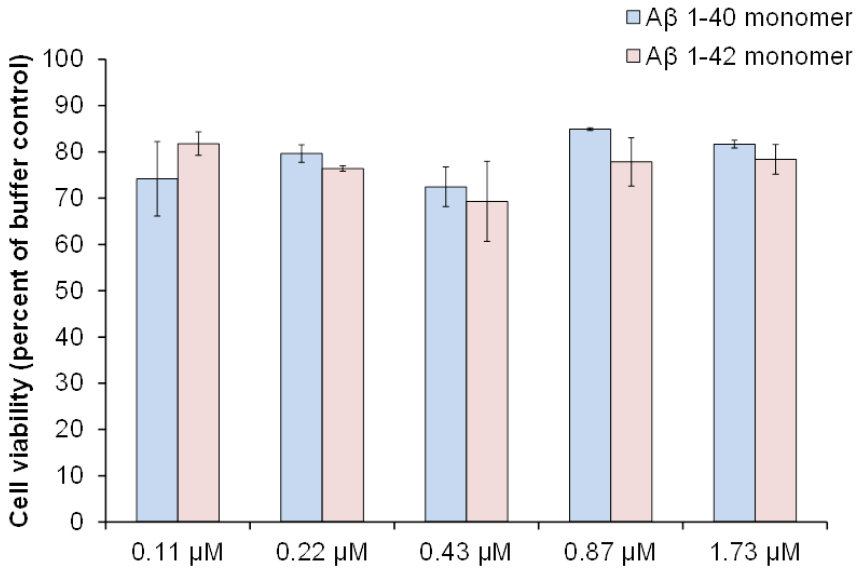

Figure 4.3 Toxicity of recAβ monomer across a broad concentration range.

Bar chart to show the toxicity of recAβ 1- 40 monomer (light blue) and recAβ 1- 42 monomer (pink), at a concentration range from 0.11-1.73 µM. Cell viability is shown as a percentage of the buffer control ± standard error (SE), a minimum of 6 readings (3- 4 pictures per well with 2 wells for each) were taken for both recAβ 1- 40 and recAβ 1- 42.

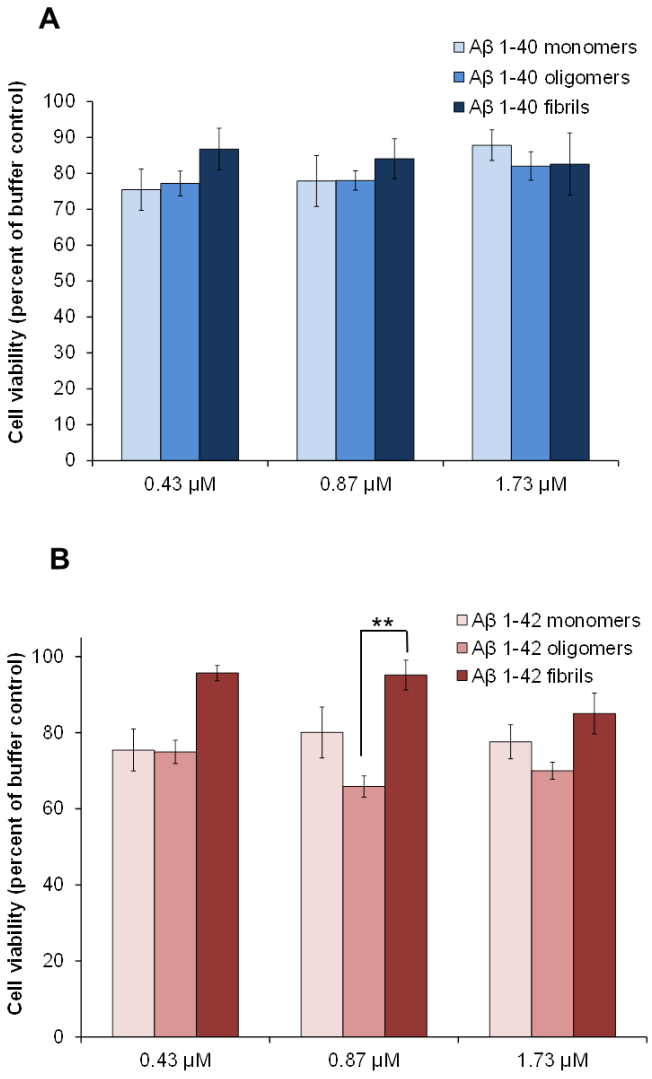

Figure 4.4 Toxicity of misfolded conformations of recAβ.

Bar chart to show the toxicity of different recAβ preparations at a concentration range from 0.43-1.73 µM. Cell viability is shown as a percentage of the buffer control ± standard error (SE), a minimum of 6 readings (3- 4 pictures per well with 2 wells for each) were taken for each recAβ preparation in each experiment (minimum of n=3 for all preparations at all concentrations). A) Shows the toxicity of different conformations of recAβ 1-40: monomers (light blue), oligomers (mid-blue) and fibrils (dark blue). B) Shows the toxicity of different conformations of recAβ 1-42: monomers (light pink), oligomers (dark pink) and fibrils (red). ** indicates the oligomers are significantly more toxic than the fibrils (one-way ANOVA; p value <0.05).

4.4 Further characterisation of recPrP fibrils

There is controversy surrounding the role of fibrils in disease, and it is unclear whether fibrillar plaques found in diseases such as AD are a protective end point in the protein misfolding pathway, or whether they are involved in causing cellular toxicity (Soto, 2003, Ross and Poirier, 2004, Dobson, 2003, Haass and Selkoe, 2007, Treusch et al., 2009, Novitskaya et al., 2006). Generally, it is thought that oligomers play a more fundamental role in causing cell death than fibrils in PMDs (Kuo et al., 1996, Naslund et al., 2000, McLean et al., 1999, Mucke et al., 2000a, Walsh et al., 2002, Quist et al., 2005, Kristiansen et al., 2007, Simoneau et al., 2007, Volles et al., 2001, Lue et al., 1999).

The cellular toxicity data for recPrP fibrils shown in section 4.2 revealed that recPrP fibrils cause high levels of toxicity to primary cortical neurons, and were found to be significantly more toxic than oligomers. This was unexpected, since as mentioned previously, fibrils are often thought to be less toxic than oligomers. The toxicity data for the recAβ fibrils shown in section 4.3 highlighted that recAβ fibrils cause very low toxicity, which coincides with this hypothesis. Therefore, I decided to further characterise the recPrP fibrils.

Oligomers are generally thought to be important in causing cell death in PMDs. In light of this, I wanted to investigate whether there were any smaller oligomer-like misfolded forms of recPrP present in the fibril preparations, which could potentially be contributing to their toxicity. I considered that since oligomers are small and soluble and fibrils are much larger and insoluble, I would be able to test for the presence of oligomer-like assemblies in the fibril preparations by centrifugation and analysis of the resulting supernatant. To do this, I pelleted the fibrils at 16100 g for differing lengths of time (between 10-60 minutes) and analysed the resulting supernatant by SDS-PAGE. Silver staining of the gel was carried out to identify low concentrations of recPrP present in the supernatant. To ensure that smaller species

of recPrP would remain in the supernatant under these centrifugation conditions, I used an oligomer sample alongside the fibrils as a control. The results (figure 4.5) show that, as expected, the oligomers are soluble and remain in the supernatant following centrifugation. This is shown by the intensity of the recPrP band in lanes 2, 4, 6 and 8, which does not decrease following centrifugation. If there was no soluble protein present in the fibril preparations then there would be an absence of a recPrP band following centrifugation. Interestingly, this was not found to be the case, the results show that soluble protein does exists in the fibril preparations. This is shown by the recPrP band in lanes 3, 5 and 7 after centrifugation, indicating that soluble recPrP is present in the supernatant of the fibril preparations.

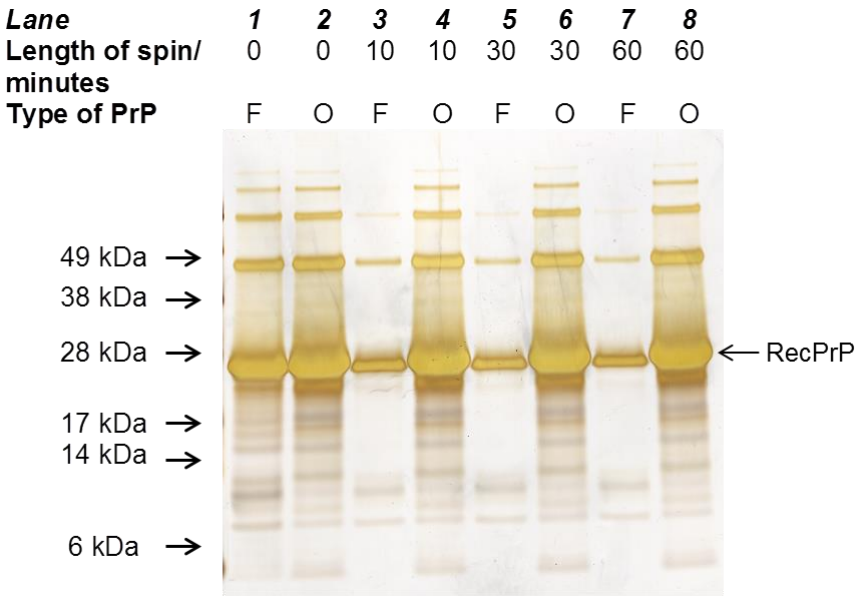

Figure 4.5 Analysis of fibril supernatant

SDS-PAGE gel which has been silver stained showing recPrP oligomers (O) and fibrils (F) before and after centrifugation for 10, 30 or 60 minutes. Only the supernatant was loaded onto the gel.

Considering that the fibril preparations were shown to contain small, soluble isoforms of recPrP I next wanted to determine the size of these soluble protein species. I first tried to do this using SEC. The storage buffer for the fibrils was 50 mM sodium acetate pH 5.5, so I used this as the running buffer for the size exclusion column. However, the fibrils seemed to interact with the column under these conditions. Even with the addition of 150 mM sodium chloride to reduce ionic interactions, the results were the same. The SEC results with 50 mM sodium acetate pH 5.5 and 150 mM sodium chloride running buffer are shown in figure 4.6A. The fibril supernatant is shown in red, and for reference oligomers are shown in blue and monomeric recPrP is shown in black. The chromatograms show the proteins are all eluting at the same time, suggesting that they are all the same size. However, I know this is not accurate since the oligomers (blue) when analysed by SEC under different buffer conditions (sodium citrate pH 3.4) elute between 6-9 ml. This indicates that with the sodium acetate buffer conditions the protein is interacting with the size exclusion column. Therefore, it is not possible to obtain a reliable estimate of size using SEC for the protein species present in the fibril supernatant.

I instead decided to use DLS to analyse the fibril supernatant, which I reasoned should provide more robust data, since DLS is a non-column based technique. Figure 4.6B shows the fibril supernatant DLS data, which clearly suggests that the protein species present in the fibril supernatant (shown in red) are much larger than monomeric recPrP (black) and the 12 mer oligomer species (blue), but smaller than the fibrils (shown in green). Some overlap in size can be seen between the fibril supernatant protein species and the fibrils, but the majority of the fibril supernatant protein does appear to be smaller. The protein present in the fibril supernatant is perhaps a pre-fibrillar species, or what is often referred to as a "protofibril", which is thought to be between an oligomer and a fibril in size(Caughey and Lansbury, 2003, Kayed et al., 2009, Ross and Poirier, 2004, Ross and Poirier, 2005, Williams et al., 2005). I decided to test the protein present in the fibril supernatant for other fibril-like characteristics such as PK resistance and whether it has an insoluble core.

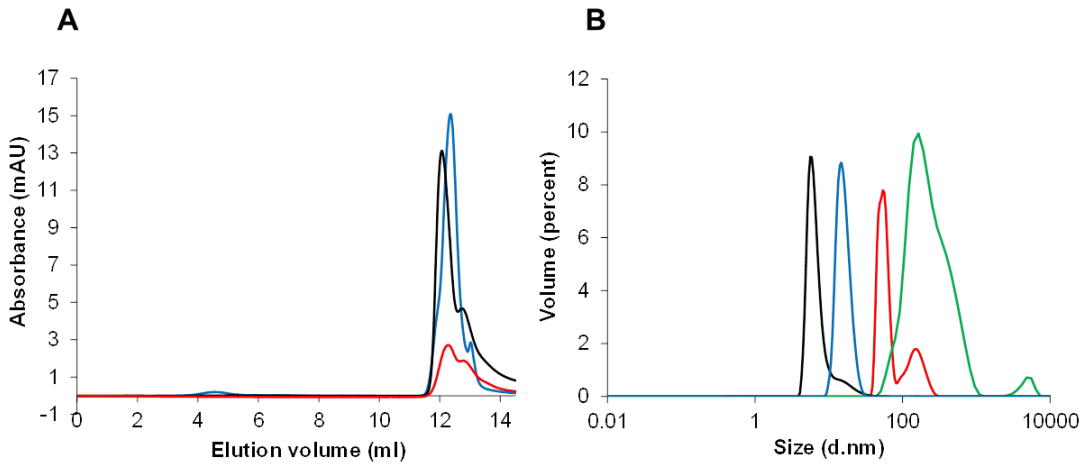

Figure 4.6 Characterisation of the size of protein species present in the fibril supernatant.

A) Size exclusion chromatogram showing recPrP monomer (black), oligomers (blue) and the supernatant from recPrP fibrils after a 45 minute spin (red). The running buffer was 50 mM sodium acetate and 150 mM sodium chloride pH 5.5. B) DLS data showing size distribution by volume of monomeric recPrP (black), recPrP oligomers (blue), recPrP fibrils (green) and the recPrP fibril supernatant (red).

In chapter 3, I showed that recPrP fibrils are resistant to PK treatment and have an insoluble core which expands under heating (maturation). In light of this, I next investigated whether the protein present in the fibril supernatant shared these characteristics. I reasoned that these characteristics would help distinguish whether the protein species present in the fibril supernatant was a smaller fibrillar species and, therefore, PK resistant, or whether it was sensitive to PK and therefore had characteristics more similar to the oligomers. To do this, I digested the fibrils, the fibril supernatant and the fibril pellet that was re-suspended after centrifugation with PK, with and without maturation. All the samples were then analysed by SDS-PAGE with silver staining, the results are shown in figure 4.7. These results show that the protein from the fibril supernatant also has an insoluble core, which expands under maturation conditions (shown in lane 9 of figure 4.7, highlighted by the arrow). The other PK resistant bands shown in lanes 8 + 9 for the fibril

supernatant, which are between 10-12 kDa, are the same as the bands seen for the fibrils or fibril pellet (lanes 2 + 3 and 5 + 6 respectively). This suggests that the protein species present in the fibril supernatant does share PK resistant properties similar to a fibril.

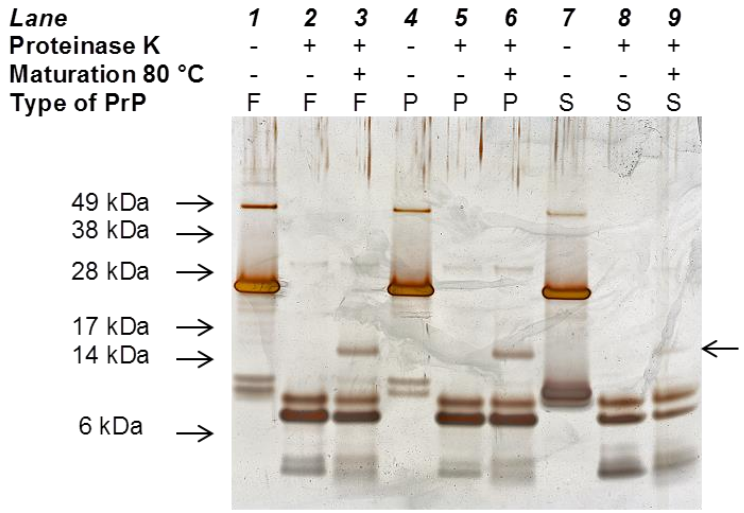

Figure 4.7 Further characterisation of fibril preparations.

SDS-PAGE gel with silver staining, lanes 1-3 show recPrP fibrils (F). Lanes 4-6 show the recPrP fibril pellet (P) following 45 minute centrifugation and re-suspension. Lanes 7-9 show the supernatant taken from the fibrils following 45 minute centrifugation. The fibrils, fibril pellet and fibril supernatant were all treated with no PK, with PK but not heated to 80 °C or with PK and heated to 80 °C (maturation). The 16 kDa band present in lanes 3, 6 and 9 shows that all fibril components have an insoluble PK resistant core, suggestive of amyloid.

Since pre-fibrillar forms of recPrP (I will refer to these as protofibrils) were found in the fibril supernatant, it was important to investigate the potential toxicity of these species to understand whether they could be contributing to the toxicity of the fibril preparations. I removed the supernatant after centrifugation of the fibrils, and tested the concentration by spectrophotometer. I then dosed the primary cortical neurons with the supernatant, the fibrils, or the re-suspended fibril pellet, at a range of

concentrations (0.22 – 0.87 μM). Multiple repeats were carried out, which allowed average toxicity data to be calculated for each of the fibril components. The average toxicity data is shown in figure 4.8. The data shows that the fibril supernatant is as toxic as the fibrils. Taking these results into consideration, it is likely that the protofibrils found in the fibril supernatant contribute to the toxicity of the fibrils. Conversely, the fibril pellet was also found to be toxic. I found no significant difference in toxicity between the fibril supernatant and the any of the fibril components. This may suggest that both the fibrils and the protofibrils are toxic to the cells.

However, it is also possible that the protofibrils may exist in equilibrium with the fibrils, and that new protofibrils may form from fibrils once they are removed. This possibility may be unlikely though, since the concentration of proteins in the supernatant of the re-suspended pellet after 24 hours was below the threshold for the spectrophotometer to analyse. This would suggest that protofibrils do not readily form from fibrils over a 24 hour period. Overall, the data suggests that protofibrils present in the fibril preparations are toxic and may, therefore, be contributing to the toxicity of the fibrils preparations. But, the fibrils alone were also shown to elicit a toxic response.

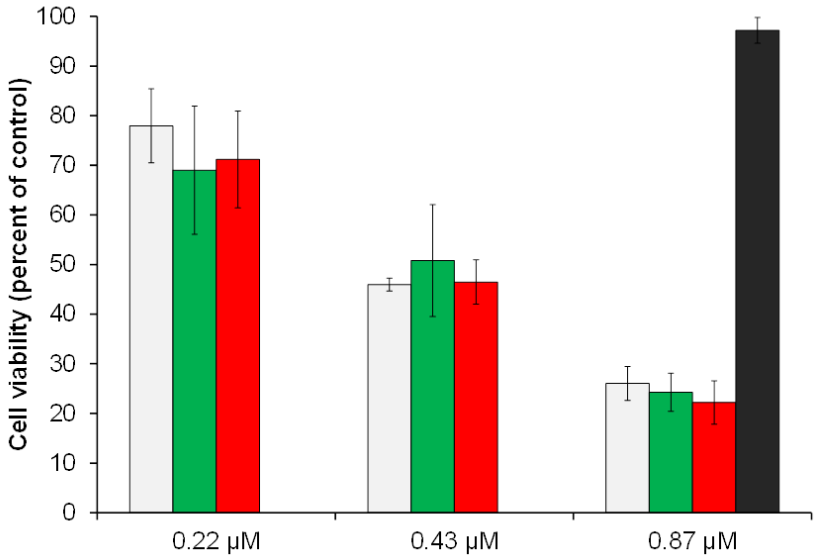

Figure 4.8 Toxicity of separated recPrP fibril components.

Bar chart to show the toxicity of separate components of recPrP fibril preparations at a concentration range from 0.22- 0.87 µM. Graph shows average data for 3 experiments, fibrils (white), the re-suspended fibril pellet following 45 minute centrifugation (green), and the supernatant taken from the fibrils following 45 minute centrifugation (red). All show high levels of toxicity when compared to the α-helical recPrP control (black) dosed at the highest concentration. There was no significant difference in toxicity between any of the fibril components.

4.5 RecAβ monomer fibrillises in cell culture media

As shown in figure 4.9A, the toxicity of the recAβ 1-40 monomer is suggestive of an inverse dose response. Although the differences are not statistically significant, there is a definite trend, and it is possible that with more replications the differences would reach statistical significance. In light of this I next investigated the factors which underpinned this inverse dose response, which I hypothesised may be due to the monomer fibrillising in the cell culture media in a concentration dependent manner. It is likely that lower concentrations of monomer would take longer to interact in the solution and begin to assemble and fibrillise, since there are fewer

molecules to interact. This would imply that the higher concentrations of monomer would fibrillise more quickly. The fibrillisation of monomers into fibrils would be expected to reduce toxicity, since as shown in figure 4.4, recAβ fibrils cause low toxicity. The slower rate of recAβ fibrillisation at lower concentrations may mean that the cells are exposed to smaller pre-fibrillar assemblies for longer, such as oligomers, which may be more toxic than the fibrils. To investigate this, I incubated the recAβ 1-40 monomers in cell culture media (with no supplements or serum) at 37 °C for 24 hours, to mimic the conditions the proteins are exposed to when incubated with the cells. I did this at a range of concentrations and monitored any fibril formation using ThT, as I did for the fibrillisation assays (see section 3.3). The lower concentrations of 0.43 and 0.87 μM were too dilute to detect any ThT fluorescence. However, a concentration range from 1.73 – 7 μM did show an increase in ThT fluorescence (suggestive of fibrils forming) in a concentration and time- dependent manner (figure 4.9B).

The ThT data would suggest that recAβ monomers fibrillise in a dose-dependent fashion, however, since the lower concentrations were too dilute to be investigated by ThT fluorescence, I investigated the possibility that fibrils had formed using native PAGE. To do this, I analysed fibrils concurrently on native and denaturing gels. I discovered that whilst fibrils could be seen in denaturing gels, they were not soluble enough to resolve on a native gel. Therefore, the presence of protein on a denaturing gel with a corresponding absence of protein resolved on a native gel was indicative of fibrils. Figure 4.9D shows a denaturing gel with the recAβ 1-40 monomer in lane 1 and recAβ 1-40 fibrils in lane 2. In figure 4.9C, the same samples were run on a native gel: recAβ 1-40 monomer in lane 1 and recAβ 1-40 fibrils in lane 2. In lane 2 there is a clear lack of protein, since there is protein in the sample (shown by lane 2, figure 4.9D), the absence of protein in the native gel suggests the size or insoluble nature of the fibrils prevents it from being resolved by the gel. The native gel shown in figure 4.9E, shows recAβ 1-40 monomer in lane 1, oligomers in lane 2 and recAβ 1-40 fibrils in lane 3. Lanes 4–8 are samples from recAβ 1-40

monomer kept in cell culture media at 37 °C for 24 hours at 0.43 μM, 0.87 μM, 1.73 μM, 3.5 μM and 7 μM respectively. The absence of any protein bands in lanes 4-8 suggests that the recAβ 1-40 monomer had fibrillised at all concentrations. Taken together, this data suggests that the recAβ 1-40 monomer does fibrillise even at low concentrations. But the more concentrated the solution is the more quickly this will occur, thus making the higher concentrations less toxic. The fibrillisation of recAβ 1-42 monomer was also investigated. However, the ThT experiments showed that the recAβ 1-42 monomer fibrillised very quickly at all concentrations. This meant that it was not possible to identify a dose and time dependent pattern of fibrillisation, as I have done for recAβ 1-40. But it is likely that the fibrillisation process of the recAβ 1-42 monomer contributes to its toxicity.

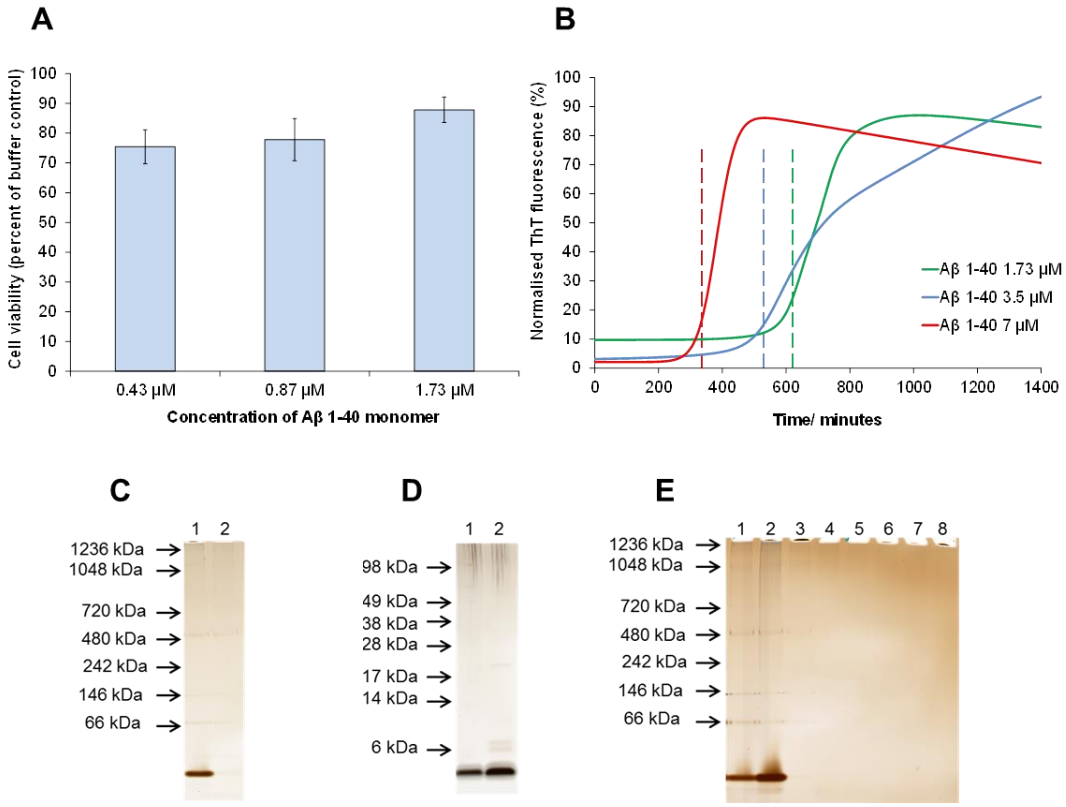

Figure 4.9 Analysis of recAβ 1-40 monomer fibrillisation in cell culture media.

A) Bar chart to show the toxicity of recAβ 1-40 monomer at a concentration range from 0.43-1.73 μM. Cell viability is shown as a percentage of the buffer control ± standard error (SE), a minimum of 6 readings (3- 4 pictures per well with 2 wells for each) were taken for each concentration in each experiment (minimum of n=3 for all concentrations). B) RecAβ 1-40 monomer at 1.73 μM (green), 3.5 μM (blue) and 7 μM (red) in cell culture media, with ThT to monitor fibrillisation over 24 hours with fluorescence readings taken at 5 minute intervals. Dashed lines show the point at which ThT fluorescence starts to rise for each concentration, showing the formation of fibrils. C) Silver stained native gel, lane 1: recAβ 1-40 monomer, lane 2: recAβ 1-40 fibrils. No band can be seen for the recAβ 1-40 fibrils. D) Silver stained denaturing SDS-PAGE gel, with the same samples loaded as shown in C. In lane 2 there is recAβ 1-40 fibril band, showing the absence of a band on the native gel is not from a lack of protein in the sample. E) Silver stained native gel; lane 1: recAβ 1-40 monomer, lane 2: recAβ 1-40 oligomers made with bis-ANS, lane 3: recAβ 1-40 fibrils, lanes 4-8: recAβ 1-40 monomer after overnight incubation in cell culture media, at the following concentrations: lane 4: 0.43 μM, lane 5: 0.87 μM, lane 6: 1.73 μM, lane 7: 3.5 μM and lane 8: 7 μM. No bands can be seen for the recAβ 1-40 fibrils in lanes 3-8.

4.6 Comparison of toxicity caused by misfolded isoforms of recPrP and recAβ

I further analysed the differences in toxicity caused by recPrP and recAβ isoforms. Figure 4.10 shows the comparative toxicity data for recPrP and recAβ monomers, oligomers and fibrils. There was no significant difference in toxicity found between monomeric recAβ and recPrP (figure 4.10A), additionally, there was no significant difference in toxicity between recAβ oligomers and recPrP oligomers at 0.43 μM or 0.87 μM. Interesting, at 1.73 μM recPrP oligomers were significantly more toxic than both recAβ oligomers (p value <0.05). This is perhaps not surprising since recPrP oligomers cause a distinct dose-response and the recPrP oligomers show

considerable toxicity at 1.73 μM. This means that recPrP oligomers are significantly more toxic than recAβ oligomers at increasing concentration.

The difference in toxicity between the recPrP and recAβ fibrils was striking. The recAβ fibrils cause low toxicity, while the recPrP fibrils cause extensive toxicity to the cells. The recPrP fibrils were shown to be significantly more toxic than the recAβ 1-40 and recAβ 1-42 fibrils at all concentrations tested (p value <0.05, figure 4.1C). This may be a result of the structure of the fibrils formed *in vitro*, which causes the recPrP fibrils to be significantly more toxic than the recAβ fibrils. However, it could be suggestive of the type of fibrillar plaques which form during disease and their involvement in causing cellular toxicity. Aβ may form fibrillar plaques, which cause little toxicity. By contrast, PrP may form fibrils which can cause considerable toxicity and cell damage. These findings may be important when understanding what the important toxic species are in these PMDs.

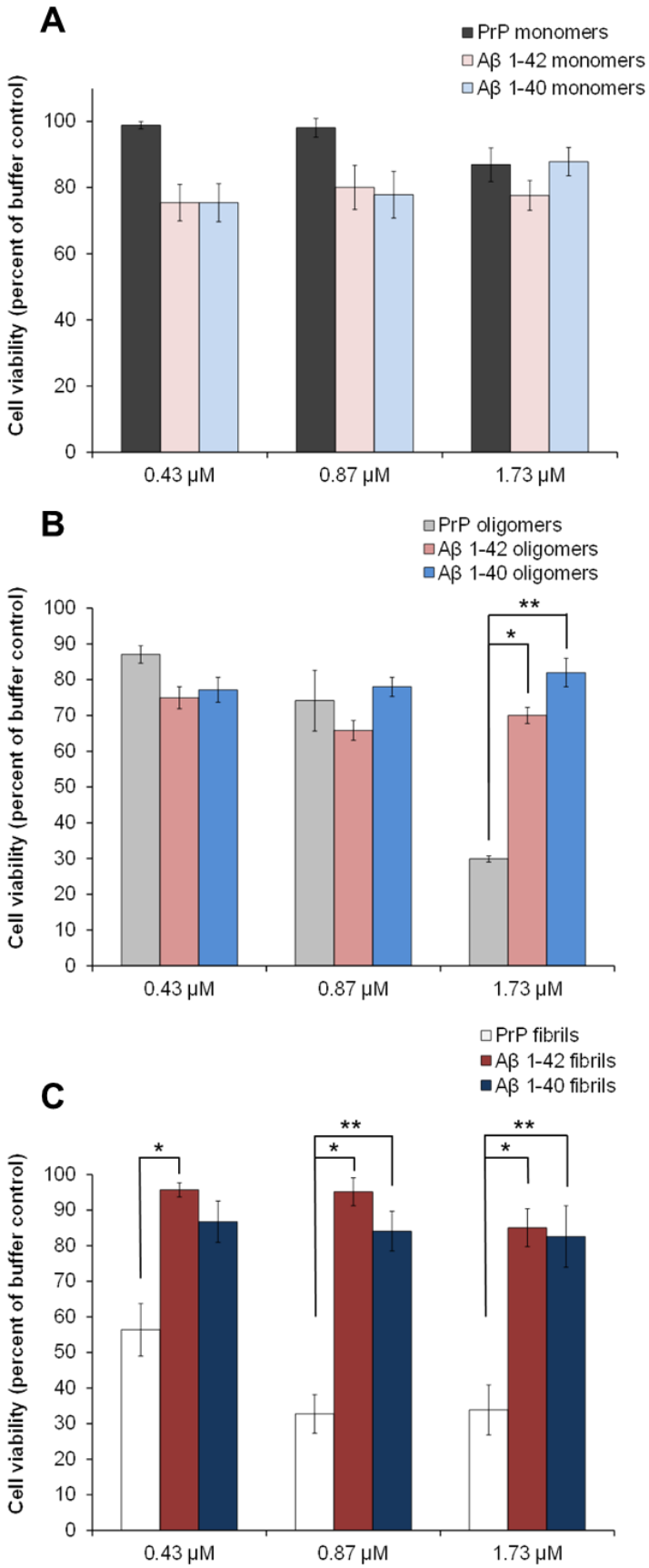
A
PrP monomers
Aβ 1-42 monomers
Aβ 1-40 monomers
Cell viability (percent of buffer control)
0
20
40
60
80
100
0.43 μM
0.87 μM
1.73 μM
B
PrP oligomers
Aβ 1-42 oligomers
Aβ 1-40 oligomers
Cell viability (percent of buffer control)
0
10
20
30
40
50
60
70
80
90
100
**
*
0.43 μM
0.87 μM
1.73 μM
C
PrP fibrils
Aβ 1-42 fibrils
Aβ 1-40 fibrils
Cell viability (percent of buffer control)
0
10
20
30
40
50
60
70
80
90
100
*
**
*
**
*
0.43 μM
0.87 μM
1.73 μM

Figure 4.10 Comparison of toxicity caused by misfolded isoforms of recPrP and recAβ

Bar charts to compare the toxicity of recPrP with recAβ 1-40 and recAβ 1-42 monomers, oligomers and fibrils. A-C show cell viability as a percentage of the buffer control ± standard error (SE), a minimum of 6 readings (3- 4 pictures per well with 2 wells for each) were taken for each concentration in each experiment (minimum of n=3 for all concentrations). * indicates a significant difference in cell viability between cells treated with recPrP and recAβ 1-42, ** indicates a significant difference in cell viability between cells treated with recPrP or recAβ 1-40 (one-way ANOVA; p value <0.05). A) Bar chart to compare the toxicity of recPrP monomers with recAβ 1-40 and recAβ 1-42 monomers B) Bar chart to compare the toxicity of recPrP oligomers with recAβ 1-40 and recAβ 1-42 oligomers C) Bar chart to compare the toxicity of recPrP fibrils with recAβ 1-40 and recAβ 1-42 fibrils.

4.6 Discussion

In this chapter, I have investigated the toxicity of well characterised disease associated conformations of recPrP and recAβ. These included fibrils, to mimic the fibrillar plaques found in both prion disease and AD. In addition, I produced oligomers to assess the toxicity of smaller, soluble assemblies of the misfolded proteins. I found that recPrP oligomers and fibrils both caused significant toxicity to primary cortical cells, while α-helical recPrP at the same concentration range (0.43–1.73 μM) caused no significant toxicity. This demonstrates that recPrP is not in itself toxic, but suggests that toxicity is conformation dependent. Furthermore, at 0.87 μM the recPrP fibrils were found to be significantly more toxic than the oligomers. This finding was unexpected, since fibrils are often thought to be less toxic than oligomers and, therefore, less important in the pathogenesis of PMDs (Simoneau et al., 2007, Kuo et al., 1996, Naslund et al., 2000, McLean et al., 1999, Mucke et al., 2000a, Walsh et al., 2002, Quist et al., 2005, Kristiansen et al., 2007, Volles et al., 2001, Lue et al., 1999). With this in mind, I decided to further characterise the recPrP fibrils to identify any characteristics which could be contributing to their toxicity.

Additional characterisation of the recPrP fibrils showed that the fibril preparations contained smaller isoforms of recPrP that remained in solution following centrifugation. DLS analysis revealed that these isoforms are larger than a monomer or an oligomer, but smaller than the true fibril population. Intriguingly these smaller isoforms have some "fibril-like" characteristics; they are PK resistant and have an insoluble core. Therefore, this smaller protein species present in the fibril preparations may represent a "pre-fibril" or "protofibril". Investigating the toxicity of the protofibrils revealed that these assemblies caused cell death at a level comparable with the fibrils, with no significant difference between the fibrils and protofibrils. This may suggest that the smaller protofibrils present in the fibril preparations contribute to the toxicity caused by the recPrP fibrils. However, my data also suggest that the fibrils are themselves toxic, since the fibril pellet which was re-suspended following centrifugation and removal of the supernatant was as toxic as the protofibrils. Overall these data show that the recPrP fibrils contain smaller protofibrils, which have fibril-like characteristics and are highly toxic to the cells. It is possible that these protofibrils may form during the fibrillisation assay on the pathway to becoming a fibril, or they may form through a separate distinct pathway. Alternatively, these protofibrils may have broken off from the main fibrils. It is possible that these protofibrils may contribute to the toxicity of the fibril preparations, which could help explain why the recPrP fibrils are so toxic.

Previously, there has been much controversy surrounding whether oligomers or fibrils are more toxic and, therefore, more important in the pathogenesis of prion disease. It seems likely that both may play a part, oligomers are soluble and much smaller than fibrils and are able to diffuse throughout the extracellular space allowing more widespread toxicity (Aguzzi and Falsig, 2012). In addition, it has been shown that PrP can cause toxicity *in vivo* in the absence of fibrillar deposits or fibrils. Oligomeric PrP present in the cytosol of a cell has been shown to be highly toxic (Ma et al., 2002), and non-fibrillar fragments of PrP (118-135) also elicit a very strong toxic response *in vivo* and *in vitro* (Chabry et al., 2003). However, it has also

been shown that the process of fibrillisation and sites surrounding fibrils in the brain show tissue damage (Jeffrey et al., 1997), which suggests that fibrils can cause toxicity *in vivo*. Interestingly, this observation seems to be dependent on brain area with some areas showing more vulnerability to fibril deposition compared with other regions (Jeffrey et al., 1997). In Novitskaya *et al.* fibrils were shown to cause toxicity *in vitro*, in this study the same method which I used for producing fibrils was employed (Novitskaya et al., 2006). This may suggest that the type of fibrils produced from this method have a particularly toxic structure, or are perhaps prone to shearing; producing small protofibrils which contribute to toxicity. Fibrils are perhaps more variable than oligomers in their toxicity due to their more heterogeneous size and structure, ranging from small fibrils made up of ~100 molecules up to large plaques made up of 1000s of molecules (Silveira et al., 2005, Prusiner et al., 1983). Their insoluble nature may also mean that access to cells during disease is more limited, without the ability to diffuse between cells. Therefore, although I have shown that recPrP fibrils are more toxic than recPrP oligomers, during disease the fibrils may play less of a fundamental role in causing toxicity due to their insolubility. Furthermore, it may be possible that the structure of some PrP fibrils gives rise to smaller isoforms of misfolded PrP. These smaller pre-fibrillar structures may then contribute to the oligomer burden and toxicity.

In stark contrast to the recPrP fibril toxicity data, the recAβ fibrils were shown to cause low toxicity at all concentrations tested. They were found to be significantly less toxic than the recPrP fibrils at all concentrations. This could indicate structural differences between the fibrils formed *in vitro* for recPrP and recAβ, or it may suggest that the function of fibrillar plaque deposition in disease differs between PMDs. For example, in AD if fibrillar plaques are non-toxic then they may be a protective mechanism to sequester more harmful oligomeric species. However, in prion diseases it is possible that fibrillar plaques may be the end point in a toxic fibrillisation process. Together, the toxicity data in this chapter suggest that fibrils may play different roles in the pathogenesis of different PMDs.

In addition to the fibrillisation toxicity data, I have shown that recAβ monomers fibrillise in cell culture media which reduces toxicity; suggesting that the propensity of Aβ to fibrillise may be protective. The illustration in figure 4.11 demonstrates how recAβ monomers may fibrillise in the cell culture media. I have shown that recAβ monomers fibrillise in a concentration and time dependent manner, and that the faster the recAβ fibrillised the less toxic it was to the cells. It is possible that the monomers will first form oligomers and protofibrils before becoming non-toxic fibrils (figure 4.11). The greater the concentration of monomers the faster this process will happen, therefore, the less toxic the recAβ sample would be. This would also mean that the lower the concentration of monomers, the slower the process meaning that the recAβ could spend more time in a pre-fibrillar state which would likely be more toxic. This would explain the inverse dose response that was seen for the recAβ monomers and support the hypothesis that the fibrillisation process in AD is protective.

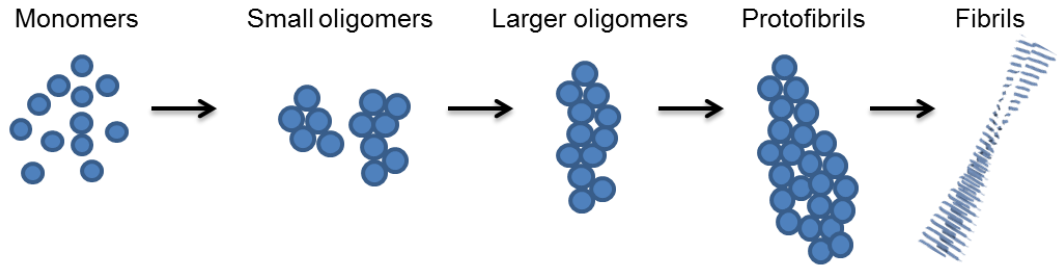

Figure 4.11 Illustration showing the potential fibrillisation process of recAβ

Illustration demonstrating how recAβ monomers may fibrillise in cell culture media

Previously Aβ oligomers have been shown to be more toxic than fibrils (Kuo et al., 1996, Naslund et al., 2000, McLean et al., 1999, Mucke et al., 2000a, Manzoni et al., 2011, Haass and Selkoe, 2007, El-Agnaf et al., 2000, Cleary et al., 2005, Texido et al., 2011) and, therefore, are thought to be more important in disease pathogenesis. This would coincide with my data, which shows that recAβ 1-42 oligomers are

significantly more toxic than recAβ 1-42 fibrils at 0.87 μM. Previously, Aβ 1-42 has been shown to be more toxic than Aβ 1-40 (El-Agnaf et al., 2000), however, my data demonstrated that there was no significant difference in toxicity between the recAβ 1-40 oligomers and the recAβ 1-42 oligomers. Studies which have used the same methods I have to produce Aβ 1-42 oligomers also found them to be toxic (Sondag et al., 2009, Young et al., 2009, Lambert et al., 1998). The toxicity data published previously has shown these oligomers to cause toxicity to neuronal cell lines, primary cells and microglia (Sondag et al., 2009, Young et al., 2009, Lambert et al., 1998). Therefore, it is likely that Aβ oligomers produced using this method have a structure which is toxic and, therefore, is perhaps similar in conformation to Aβ oligomers seen in disease.

The clinical phase in AD compared to most human prion diseases is much longer. On average, the clinical phase of AD is between 3 and 10 years (Zanetti et al., 2009). If the patient is diagnosed in their 60s or 70s then it is more likely to be 7-10 years (Zanetti et al., 2009). By contrast, the clinical phase of CJD, the most common human prion disease, is only 3 months (personal communication Dr M.W. Head). It is possible that this may be due to the comparative toxicities of the causative misfolded proteins. I have shown that at higher concentrations (1.73 μM), recPrP oligomers are significantly more toxic than recAβ 1-40 and recAβ 1-42 oligomers. At the clinical stage of disease the concentration of misfolded protein would likely be at its highest, since levels build up during the pre-clinical phase (Selkoe, 2003). This may mean that high levels of PrP oligomers would cause widespread cell death and mortality earlier than in AD, where the oligomers are less toxic and so the process may be slower.

The toxicity data from this chapter provides insights into how the structure of misfolded proteins can cause toxicity. However, the misfolded protein conformers were formed *in vitro* meaning that they may not replicate the conformation of misfolded proteins in disease. I have tried to account for these limitations by

characterising the proteins to try and produce conformations with similar properties to those found in disease, however, there may be differences. Furthermore, the *in vitro* system I have used for testing toxicity is also artificial and does not replicate the same chronic process that occurs during disease. Therefore, while I cannot draw conclusions about how misfolded proteins lead to neurodegeneration in PMDs, I can suggest that certain conformations of proteins have the ability to cause toxicity and may therefore be important in causing neuronal cell death in these diseases.

In this chapter, I have shown that both recPrP oligomers and fibrils cause significant toxicity to primary cortical cells in a dose dependent fashion. Interestingly, recPrP fibrils were found to be significantly more toxic than recPrP oligomers. Further analysis revealed that the recPrP fibril preparations contained small soluble protofibril-like isoforms, which were smaller than the main fibril population but had fibril-like characteristics. These protofibrils were found to be as toxic as the fibrils and may contribute to the toxicity of the fibril preparations. In addition, recAβ 1-42 oligomers were found to be significantly more toxic than recAβ 1-42 fibrils. However, recAβ 1-40 oligomers were not found to be significantly more toxic than Aβ 1-40 monomers or fibrils. The mechanisms leading to recPrP and recAβ induced cell death will be investigated in chapter 6. In the next chapter, I will explore the importance of the disulphide bond in recPrP in relation to oligomerisation and associated toxicity.

Chapter 5:

The presence of the disulphide bond in recPrP determines oligomer size and toxicity

5.1 Introduction

In prion diseases, the disease process appears to be driven by the conformational conversion of PrP^{C} into an abnormal isoform, designated PrP^{Sc}. While the presence of PrP^{Sc} is diagnostic of prion disease, there is considerable doubt as to whether PrP^{Sc} is itself toxic to cells (Aguzzi and Falsig, 2012, Radford and Mallucci, 2010, Sandberg et al., 2014, Krasemann et al., 2013, Collinge and Clarke, 2007). PrP^{Sc} can be detected in infected brains prior to overt neuronal loss (Sandberg et al., 2014, Aguzzi and Falsig, 2012, Collinge and Clarke, 2007), however, there can be a lack of correlation between the temporal and spatial distribution of protein deposition and neuronal cell death (Sandberg et al., 2014, Aguzzi and Falsig, 2012, Collinge and Clarke, 2007). Instead, small soluble oligomeric assemblies of prion protein represent a plausible alternative species that causes neuronal toxicity (Harris and True, 2006, Simoneau et al., 2007). Whilst there has been some evidence to suggest that the size of oligomers is important in toxicity (Silveira et al., 2005), very little is known about what causes different sized oligomers to form.

Post-translational modifications of proteins occur in the endoplasmic reticulum (ER), where there is a high concentration of chaperones to assist in folding proteins into their correct tertiary structure (Kleizen and Braakman, 2004). These include oxidising components to support disulphide bond formation (Kleizen and Braakman, 2004), which is an important component of PrP^{C}. In addition, other post-translational modifications are made such as cleavage of the N-terminal signal peptide (Harris, 2003), attachment of the GPI-anchor and addition of N-linked glycans to residues 180 and 196 (Wiseman et al., 2005). *In vivo*, the glycosylation of PrP is variable; the protein can be un-, mono- or di- glycosylated (Tuzi et al., 2008, Wiseman et al., 2005).

All post-translational modifications are thought to be important for the normal folding and functioning of PrP^{C} (Wiseman et al., 2005, Tuzi et al., 2008, Jackson et al.,

1999, Sang et al., 2012) and, therefore, changes to these could be important in the conversion of PrP^{C} to PrP^{Sc}. Glycosylation is thought to be important for stability of the protein, but as yet it has not been proven to play a major determining role in conversion of PrP^{C} to PrP^{Sc} or in propagation of PrP^{Sc} (Wiseman et al., 2005, Tuzi et al., 2008). The GPI anchor is thought to play a part in increasing susceptibility to prion infection, since the cell surface is thought to be a possible site of conversion for PrP^{C} to PrP^{Sc}. However, animals expressing anchorless protein are still susceptible to prion infection, although these show altered pathology and are less likely to exhibit clinical signs (Chesebro et al., 2005, Klingeborn et al., 2011). It is thought that the GPI anchor may be important for neuroinvasion and spread of PrP^{Sc} (Klingeborn et al., 2011), which may go some way to explain why clinical signs are less frequently seen in infected GPI-anchorless mice. However, studies using the N-terminal and middle domain of the yeast prion protein Sup35 (Sup35NM) have shown that aggregates of cytosolic Sup35NM can spread to other cells (Hofmann et al., 2013). This shows that membrane anchoring is not required for cell to cell infection of prions (Hofmann et al., 2013). Thus it is likely that the GPI anchor is important, but not essential for infection.

The disulphide bond is important for the normal folding of the protein, although it is unclear how the absence of the disulphide bond in PrP may impact on misfolding during disease. Studies to date have shown that reduction of the disulphide bond results in a switch from the mainly α-helical structure of PrP with an intact disulphide bond, to one composed primarily of β-sheets (Jackson et al., 1999, Sang et al., 2012). It has also been demonstrated that a free thiol group may be needed for conversion of PrP^{C} to PrP^{Sc} (Lucassen et al., 2003), which would suggest that the oxidation state of PrP is important in disease. Transgenic mice with C-terminal deletions of PrP, meaning that they lack the disulphide bond, develop a neurodegenerative disease with symptoms similar to a neuronal storage disorder (Muramoto et al., 1997). Whilst this finding may not be entirely attributable to the loss of the disulphide bond, since the disulphide bond was not all that was deleted,

it does suggest that PrP without a disulphide bond can be neurotoxic and capable of causing disease.

In this chapter, I will explore how the oxidative state of recPrP is important in oligomerisation and is deterministic of the size of oligomers which subsequently form. I will investigate how the presence or absence of the disulphide bond in recPrP can alter its biophysical properties when prepared under the same conditions. Furthermore, I will analyse the differences in toxicity caused by oligomers formed from recPrP with or without the disulphide bond. This will help elucidate how changes to post-translational modifications such as the disulphide bond can affect how a protein misfolds and causes toxicity. Henceforth, I will refer to recPrP with an intact disulphide bond as oxidised recPrP and recPrP without a disulphide bond as disulphide-reduced recPrP.

5.2 Reverse phase chromatography produces purification fractions with different oligomerisation properties

In this study, recPrP was purified from bacteria before being refolded into disease associated conformations. The final stage when purifying recPrP is RP chromatography. RP chromatography is a purification method which separates proteins in a sample by their hydrophobicity. A concentration gradient of acetonitrile is used to elute proteins from the column. The more hydrophobic a protein is, the higher the percentage of acetonitrile needed to elute it. When purifying recPrP by preparative RP chromatography, a broad UV peak seen at an absorbance of 280 nm represents the protein eluting and is collected as one fraction or as multiple fractions. To obtain recPrP with a very high purity, I decided to collect multiple fractions across the eluting peak. This gave a better chance of separating recPrP from any impurities, which may elute around the same time as recPrP. This protocol resulted in the collection of multiple fractions containing recPrP.

When I performed oligomerisation reactions on separate recPrP fractions, I observed that oligomers which formed from fractions collected across the RP peak were different. The oligomerisation assay (heating at 45 °C for 2.5 hours at pH 3.4), which I have used is adapted from Rezaei *et al*. (Rezaei et al., 2005) and produces two main populations of oligomers. The proportions of these two populations, which Rezaei *et al.* showed to consist of 12 recPrP molecules (12 mer) and 36 recPrP molecules (36 mer), seemed to be affected by where in the RP peak they had been collected. Figure 5.1A shows a RP chromatogram with the different fractions which were collected separately highlighted as F1 and F2. These fractions were oligomerised and analysed by SEC (figure 5.1C+D). Fraction 1, which was collected from the left hand side of the RP peak, produced oligomers which were almost all P2 (smaller 12 mer population). Fraction 2, which was collected from the right hand side of the RP peak, produced oligomers which had a high proportion of P1 (larger 36 mer population). The differences between the two chromatograms are distinct. The fractions were analysed by SDS-PAGE to examine purity (figure 5.1B), fraction 1 is shown in lane 7 and fraction 2 is shown in lane 9. The purity of the two fractions is similar and not likely to account for such stark differences in oligomerisation profiles. Therefore, the differences in oligomerisation profiles for the different RP fractions must be caused by another variable.

To investigate what this unknown variable could be, I had the samples analysed by mass spectrometry. Mass spectrometry can identify very small changes in mass, including the loss or addition of side chains and the loss or addition of specific bonds. The purification protocol I used to purify recPrP involves an oxidation step, in which oxidised glutathione is added to the recPrP sample and left overnight. This step is crucial for normal folding of the protein, since it allows the disulphide bond found in the C-terminal to form. Oxidised glutathione is used to slow down disulphide-bond formation, which encourages intramolecular disulphide bonds instead of intermolecular bonds. This procedure results in five possible oxidation states. The most abundant is oxidised recPrP with an intact disulphide bond. RecPrP

can also occur with a glutathione attached to each cysteine, so it is reduced but has no free thiol groups. RecPrP can occur with no disulphide bond and with one glutathione attached to either of the cysteines. Lastly, recPrP can exist with no disulphide bond and no glutathione attached (disulphide-reduced recPrP). Figure 5.2 shows the total ion count (TIC) chromatogram from liquid chromatography mass spectrometry (LC-MS) analysis. The TIC chromatogram shows a recPrP fraction containing all of the possible oxidation states. The chromatogram shows that the oxidised recPrP elutes first, followed by those with glutathione attached and the disulphide-reduced recPrP elutes last.

The mass spectrometry data showed that the RP fraction collected from the leading edge of the eluting peak was comprised of oxidised recPrP (figure 5.3A). By contrast, the RP fraction collected from the right hand side of the eluting peak had a large proportion of disulphide-reduced recPrP (figure 5.3C). The RP fraction collected from the top of the RP peak was also analysed, it showed a combination of all oxidation states of recPrP. These results suggest that the presence or absence of the disulphide bond in recPrP may be responsible for causing such different oligomerisation profiles. This led to the hypothesis that the oxidation state of recPrP, whether it has an intact disulphide bond or not, can determine the size of the oligomers which will form.

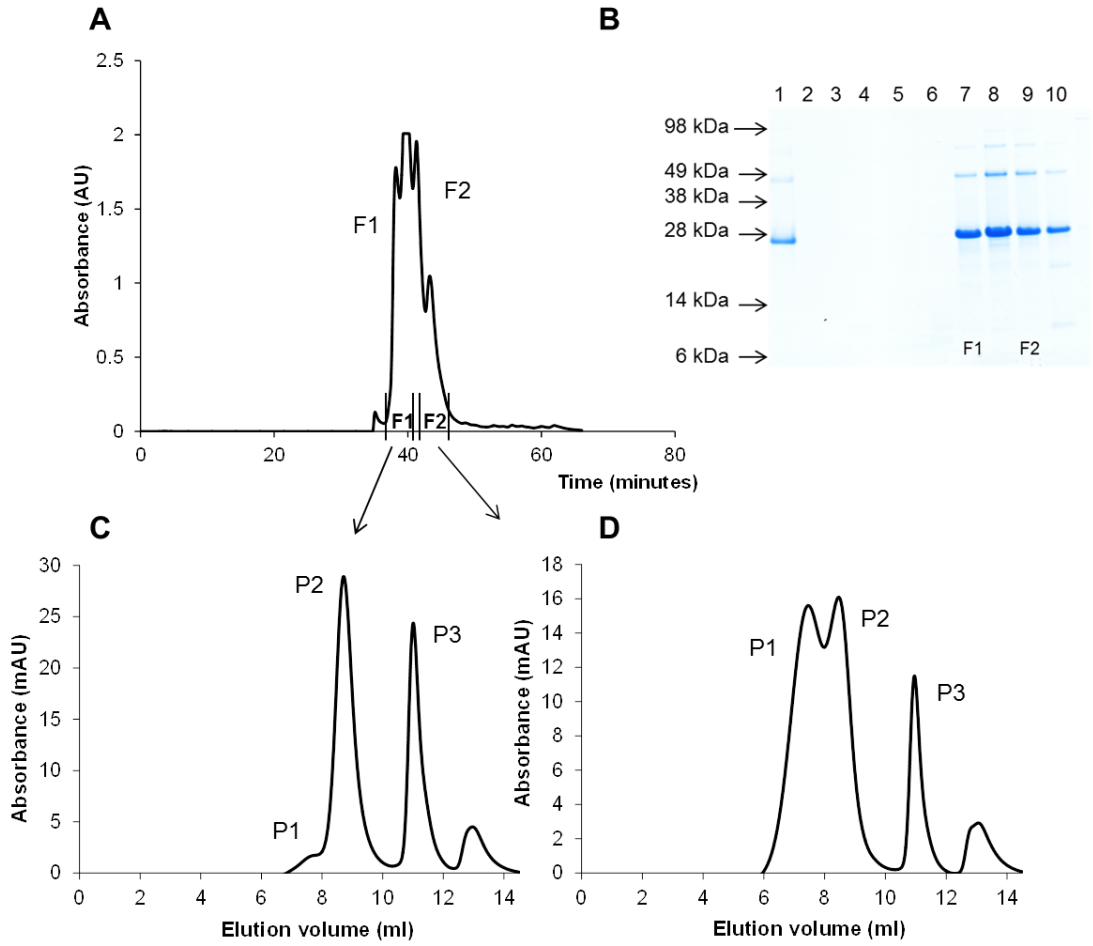

Figure 5.1 Sequential purification fractions show different oligomerisation profiles.

A) RP chromatogram for recPrP: fractions were collected from the left-hand side, top and right-hand side of the eluting peak. The left and right-hand fractions are labelled as F1 and F2, missing out the fraction collected from the top of the peak. B) SDS-PAGE gel with coomassie staining, showing the fractions collected from the RP chromatogram in A. F1 and F2 are shown in lanes 7 and 9 respectively, both show equal levels of purity. The higher molecular weight band at approximately 46 kDa shows recPrP dimer. C) Oligomerisation chromatogram of fraction 1 (F1) collected from the left-hand side of the RP peak shown in A. D) Oligomerisation chromatogram of fraction 2 (F2) collected from the right-hand side of the RP peak shown in A. C+D) P1 shows the larger 36 mer oligomer population, P2 highlights the smaller 12 mer oligomer population and P3 shows the monomer.

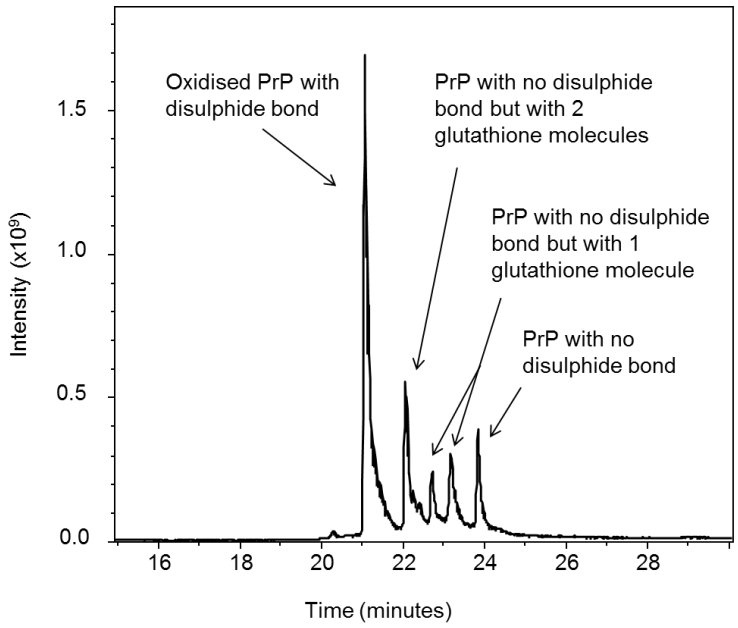

Figure 5.2 Mass spectrometry data showing the different oxidation states of recPrP.

TIC chromatogram from LC-MS analysis showing the different oxidation states of recPrP which can form from the protocol used. Arrows highlight which peaks correspond with which form of recPrP.

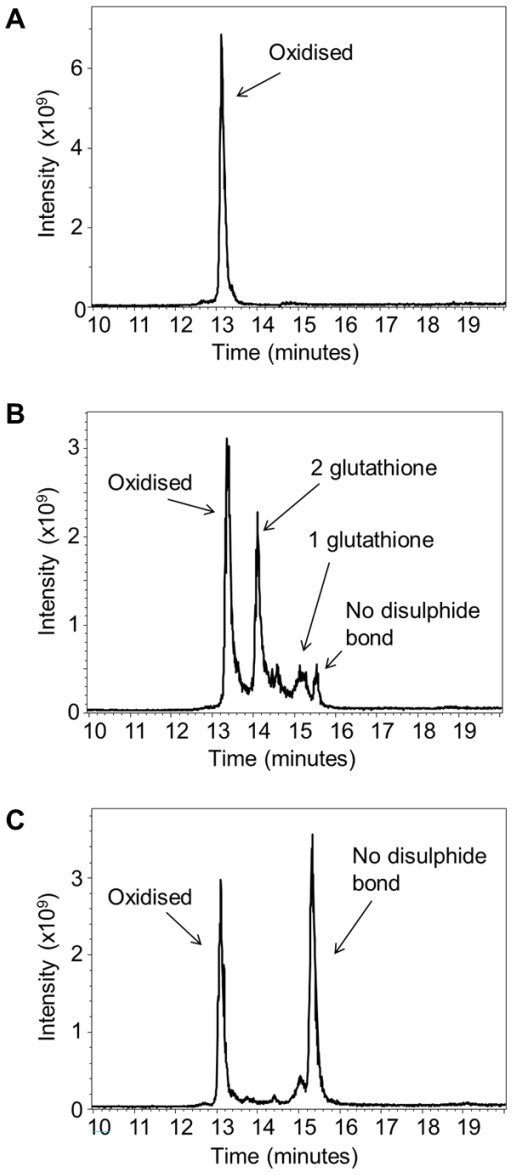

Figure 5.3 TIC chromatograms of different RP chromatography fractions.

A) TIC chromatogram from LC-MS analysis of RP purification fraction collected from the left- hand side of the eluting peak, all recPrP is shown to have the disulphide bond. B) TIC chromatogram from LC-MS analysis of RP purification fraction collected from the top of the eluting peak, arrows indicate the different oxidised states of recPrP present in the fraction. C) TIC chromatogram from LC-MS analysis of RP purification fraction collected from the right-hand side of the eluting peak, arrows indicate the different oxidised states of recPrP present in the fraction, the largest proportion of recPrP has no disulphide bond.

5.3 Disulphide-reduced recPrP drives the formation of larger oligomers

The results in section 5.2, demonstrate that oligomers formed from recPrP collected from the left hand side of the RP elution peak consist almost entirely of the smaller 12 mer oligomer species. Alternatively, recPrP collected from the right hand side of the RP peak formed oligomers with a high proportion of the large 36 mer population. Mass spectrometry data shows that the recPrP from the left hand side of the RP peak had an intact disulphide bond, and recPrP from the right hand side of the elution peak had a high proportion of disulphide-reduced recPrP.

In light of this, I wanted to investigate whether the presence or absence of the disulphide bond was causing the differences in oligomerisation profiles. To do this, I first purified recPrP and analysed it using mass spectrometry to determine the oxidation state of the protein (figure 5.4A+B). RecPrP shown to be completely oxidised was oligomerised. The oxidised recPrP oligomers were shown to be comprised of almost entirely the 12 mer species (P2), with less than 3 % 36 mer oligomers (P1), (figure 5.4C). To ensure that the oligomer peaks shown by SEC were recPrP, I collected fractions to analyse by SDS-PAGE. The fractions which corresponded to the SEC peaks were shown to contain protein at the correct molecular weight for recPrP (figure 5.4D), demonstrating that the SEC peaks are recPrP oligomers. Next, I wanted to investigate the size of the oligomers which would form from disulphide-reduced recPrP.

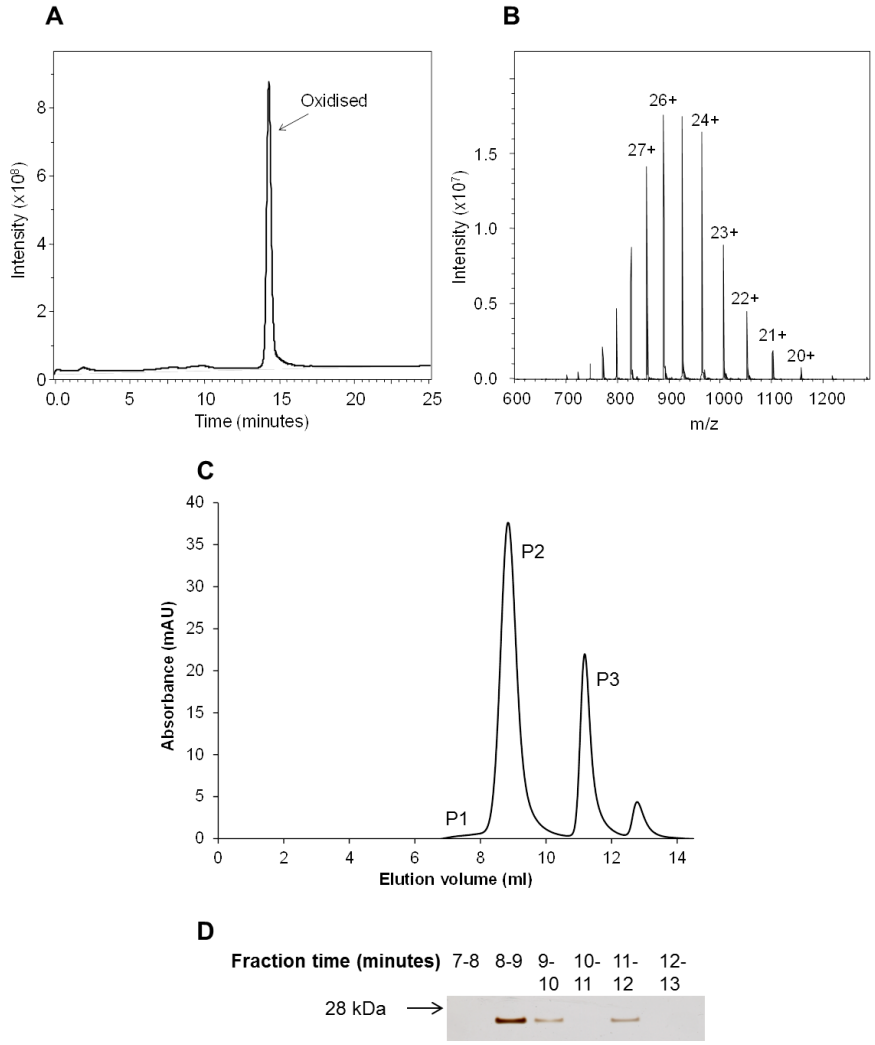

Figure 5.4 Oligomer profile for oxidised recPrP.

A) TIC chromatogram from LC-MS analysis showing only oxidised recPrP which was used for oligomerisation in C. B) Mass spectrum of the protein shown in A. The various peaks all correspond to full length recPrP but with different charges (as labelled). Multiplying each peak's m/z value with the charge and then subtracting the charge, gives a measure of mass. The average of all the peaks was calculated, which generated the mass of the protein. The mass was shown to be 23,061.8 Da, which corresponds to oxidised recPrP. C) Oligomerisation chromatogram of 100 % oxidised recPrP. P1 shows the larger 36 mer oligomer population, P2 highlights the smaller 12 mer oligomer population and P3 shows the monomer. D) SDS-PAGE gel with silver staining, showing fractions collected from the chromatogram in C. The bands correspond to the peaks in C and are the correct molecular weight for recPrP.

To analyse how disulphide-reduced recPrP would behave in the oligomerisation assay, I took recPrP which was shown by mass spectrometry to be completely oxidised (did not contain recPrP with other oxidation states) and treated this with the reducing agent DTT. Following reduction, recPrP was re-purified by RP chromatography to remove the DTT. The recPrP was analysed by mass spectrometry to ensure that the reduction reaction had been successful. The data show that the reduced recPrP samples contained only disulphide-reduced recPrP (figure 5.5A+B).

The disulphide-reduced recPrP was oligomerised and analysed by SEC (figure 5.5C). The disulphide-reduced recPrP oligomers had a very high proportion of the large 36 mer species (P1) and much less of the smaller 12 mer species (P2). In addition, the monomer peak (shown as P3) was less intense in the reduced state than in the oxidised oligomer chromatogram (figure 5.4C), suggesting that oligomerisation was more complete. To confirm that the SEC oligomer peaks were recPrP, fractions were collected and analysed by SDS-PAGE (figure 5.5D). The fractions which corresponded to the oligomer peaks were shown to contain protein with the correct molecular weight to be recPrP.

The data shows that the presence or absence of the disulphide bond in recPrP impacts the size of the oligomers which subsequently form. RecPrP with no disulphide bond will result in oligomers with a high proportion of the large 36 mer species. By contrast, oxidised recPrP forms oligomers which consist almost entirely of the smaller 12 mer oligomer population. Next, I wanted to investigate how much disulphide-reduced recPrP was necessary to instigate 36 mer production.

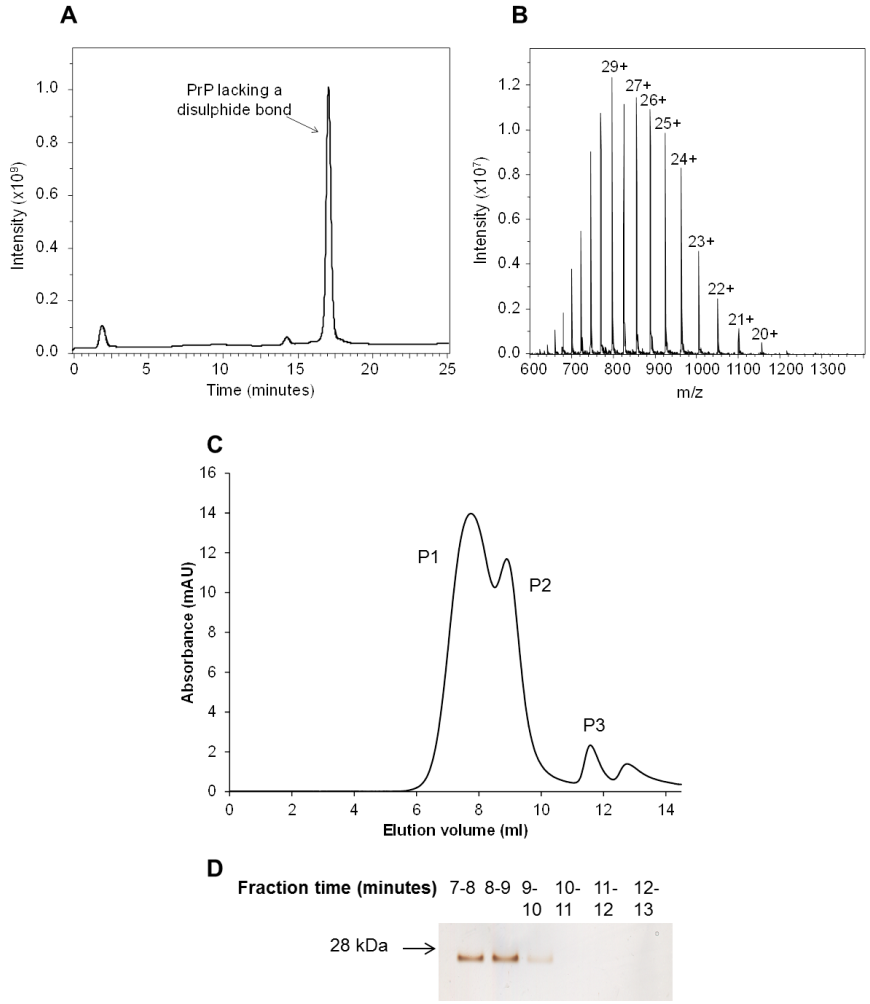

Figure 5.5 Oligomer profile for disulphide-reduced recPrP.

A) TIC chromatogram from LC-MS analysis showing disulphide-reduced recPrP which was used for oligomerisation in C. B) Mass spectrum of the protein shown in A. The peaks all correspond to full length recPrP but with different charges (as labelled). The average mass was calculated, which was shown to be 23,063,5 Da, which corresponds with disulphide-reduced recPrP. It is approximately 2 Da more than oxidised recPrP, because there are 2 extra hydrogen atoms attached to the cysteine residues. C) Oligomerisation chromatogram of disulphide-reduced recPrP. P1 shows the larger 36 mer oligomer population, P2 highlights the smaller 12 mer oligomer population and P3 shows the monomer. D) SDS-PAGE gel with silver staining, showing fractions collected from the chromatogram in C. The bands correspond to the peaks in A and are the correct molecular weight for recPrP.

5.4 Investigating the proportion of disulphide-reduced recPrP needed to drive the formation of the larger oligomer species

I have demonstrated that the presence or absence of the disulphide bond in recPrP affects the size of the oligomers which form, with disulphide-reduced recPrP driving the formation of the larger 36 mer species. With this in mind, I wanted to investigate what percentage of disulphide-reduced recPrP was needed to instigate a significant increase in 36 mer production. To do this, I solubilised both oxidised recPrP and disulphide-reduced recPrP in the acidic oligomerisation buffer and mixed a controlled percentage of the disulphide-reduced recPrP with the oxidised recPrP. This was then oligomerised by heating at 45 °C for 2.5 hours. Following oligomerisation, all samples were analysed by SEC. Figure 5.6 shows oligomers formed with 0-100 % disulphide-reduced recPrP. The results clearly show that the 36 mer (P1) peak increases with the increasing percentage of disulphide-reduced recPrP. The area under each peak was calculated and expressed as a percentage of total protein; multiple repeats were carried out to obtain average data as shown in figure 5.7.

The integration data shows that when 1 % disulphide-reduced recPrP was oligomerised, there was no significant increase in 36 mer production when compared to 0 % disulphide-reduced recPrP oligomers (t-test p value > 0.05). However, there was a significant increase in 36 mer production with 5 % disulphide-reduced recPrP when compared to 0 % disulphide-reduced oligomers (t-test p value < 0.01). This suggests that a 5 % or greater proportion of disulphide-reduced recPrP is needed in order to produce a significant amount of the 36 mer species. At this concentration (1 mg/ml) the proportion of the P1 oligomer species does not reach 100 % even with 100 % disulphide-reduced recPrP, this may be because the 12 mer and 36 mer oligomers exist in equilibrium. Therefore, it may not be possible to produce 100 % P1 oligomers if 12 mer oligomers assemble to become 36 mer oligomers and 36 mer oligomers disassemble to produce 12 mer oligomers.

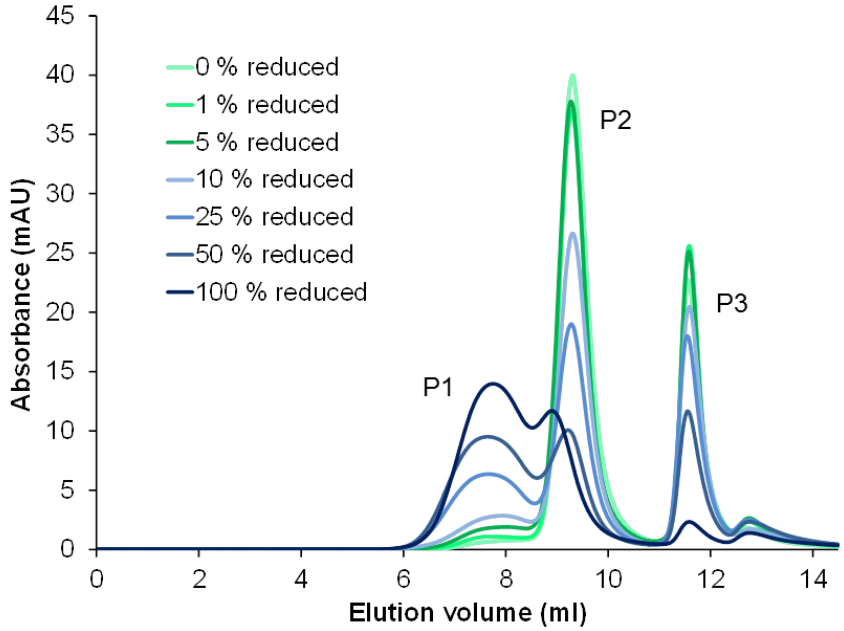

Figure 5.6 Size exclusion chromatograms for oligomers formed with 0-100 % disulphide-reduced recPrP.

Size exclusion chromatograms for oligomers formed with 0 % disulphide-reduced recPrP (100 % oxidised, lightest green) up to 100 % disulphide-reduced recPrP (dark blue). P1 shows the larger 36 mer oligomer population, P2 highlights the smaller 12 mer oligomer population and P3 shows the monomer.

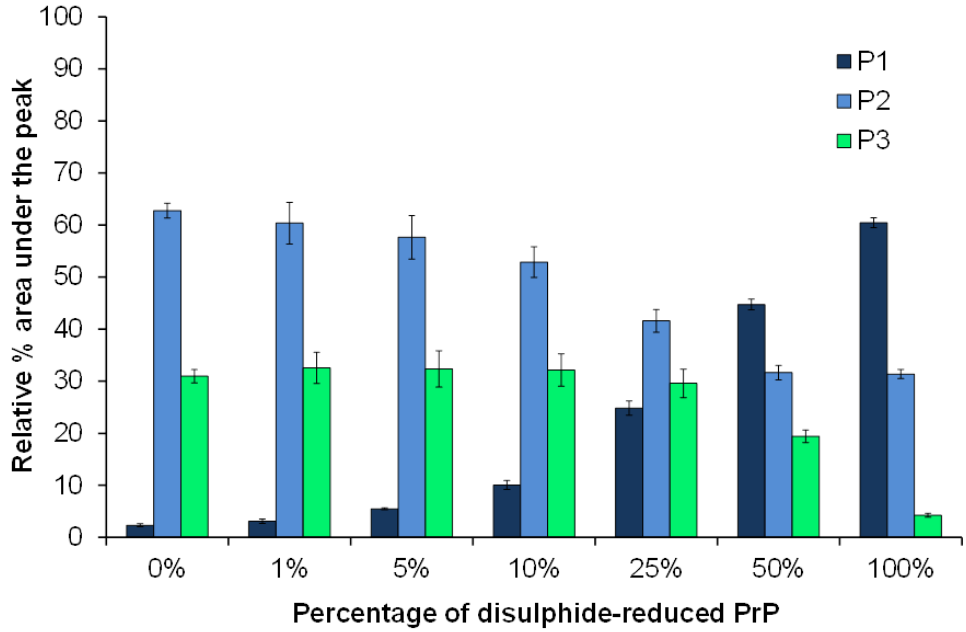

Figure 5.7 Integration data for oligomers formed with 0-100 % disulphide-reduced recPrP.

Bar chart to show the average integration data from oligomers formed from 0-100 % disulphide-reduced recPrP. The area under each peak from the size exclusion chromatograms was calculated as a percentage of the total area under all peaks, for oligomers formed from 0, 1, 5, 10, 25, 50 and 100 % disulphide-reduced recPrP, with a minimum of n=3 for each, ± standard error (SE) bars are shown. P1 shows the larger 36 mer oligomer population, P2 shows the smaller 12 mer oligomer population and P3 shows the monomer.

The concept that disulphide-reduced recPrP was driving the formation of the larger P1 oligomer species, was strengthened by data collected in the Gill group for the mutant S169N recPrP. The S169N mutant is murine recPrP with a point mutation at residue 169. Oxidised and disulphide-reduced S169N recPrP were mixed so that the final sample contained 25 % disulphide-reduced recPrP, this was oligomerised and fractions were collected for each peak (figure 5.8A). The fractions were then analysed by mass spectrometry to investigate the proportion of oxidised and disulphide-reduced recPrP present in each of the oligomer species. The data show

that the P1 oligomers contain the most disulphide-reduced recPrP, with much less in the P2 oligomers and very little in the monomer. Interestingly, the P1 peak contained both disulphide-reduced recPrP and oxidised recPrP. This would suggest that the disulphide-reduced recPrP is recruiting the oxidised recPrP into the larger oligomer species and, therefore, is driving 36 mer production. Although this analysis was carried out using S169N recPrP, there are no indicators that would suggest this mutant would behave differently to wild type recPrP.

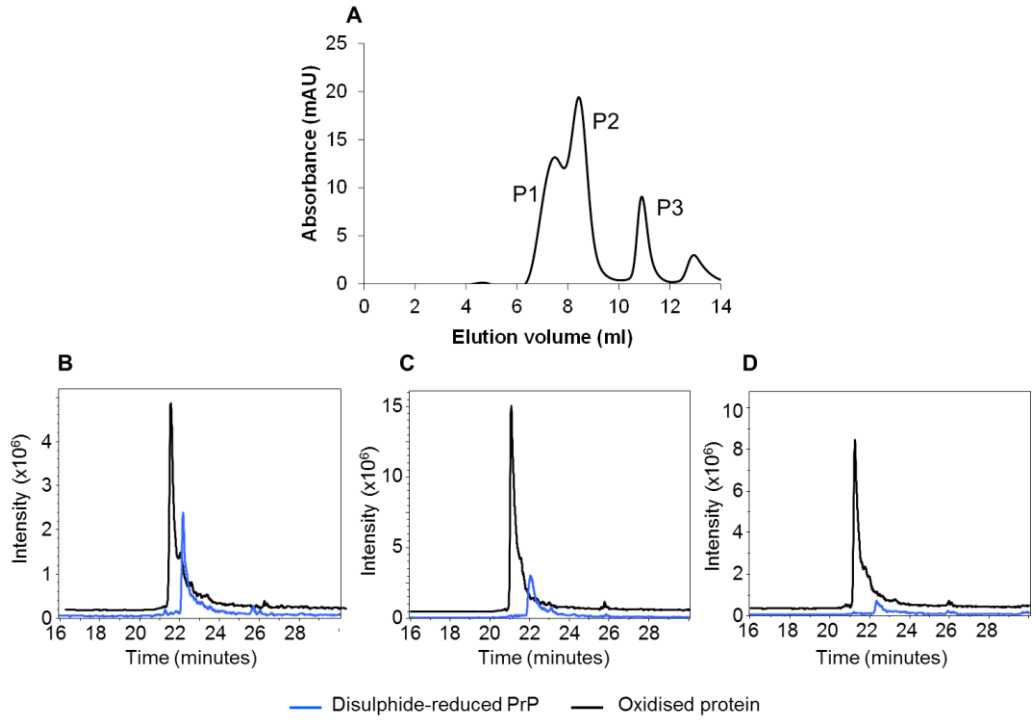

Figure 5.8 Mass spectrometry data for oligomer fractions

A) Oligomerisation chromatogram of S169N mutant recPrP. P1 shows the larger 36 mer oligomer population, P2 highlights the smaller 12 mer oligomer population and P3 shows the monomer. Fractions were collected and analysed by mass spectrometry. B) TIC chromatogram from LC-MS analysis from the P1 peak in A. C) TIC chromatogram from LC-MS analysis from the P2 peak in A. D) TIC chromatogram from LC-MS analysis from the P3 peak in A.

5.5 Oligomers formed from disulphide-reduced recPrP are significantly more toxic than oxidised oligomers

Once I had established that the absence of the disulphide bond in recPrP affected the size of the oligomers which formed, I wanted to explore whether this would also affect the toxicity of the oligomers. With this in mind, I produced oligomers with 100 % oxidised recPrP and 100 % disulphide-reduced recPrP. The oligomers formed with oxidised recPrP were made up almost solely of the 12 mer species, while the oligomers formed with the disulphide-reduced recPrP had a high proportion of the 36 mer species (figures 5.4 and 5.5 respectively). The toxicity of both oligomer preparations was investigated using murine primary cortical cells. The oligomers were diluted into cell culture media to give a final concentration of 0.65 or 1.3 μM. These concentrations were used since they fall within the range I showed causes toxicity (chapter 4). The cells were incubated with the oligomers for 24 hours before being fixed and stained with DAPI. Once the cells were stained they were imaged and a live/dead cell count was carried out, allowing toxicity to be assessed.

The viability data for the cells following treatment with the oligomers is shown in figure 5.9. Interestingly, the data shows that at 0.65 μM the oxidised recPrP oligomers, which consisted of the 12 mer species, were significantly less toxic than the oligomers formed with the disulphide reduced recPrP, which contained a high proportion of the 36 mer species (p value <0.05). This would suggest that at this concentration the larger 36 mer oligomers are more toxic than the smaller 12 mer species. At the higher concentration of 1.3 μM there was not a significant difference in toxicity between the two oligomer preparations, however, a suggestive p value of 0.071 was observed, which may indicate that with further repeats a significant difference would have been seen. The cells were also treated with α-helical recPrP at the higher concentration of 1.3 μM. There was no significant difference in toxicity between the α-helical recPrP and the buffer control, which demonstrates that recPrP

is not in itself toxic and that any toxicity seen in the oligomer treated cells must be conformation dependent.

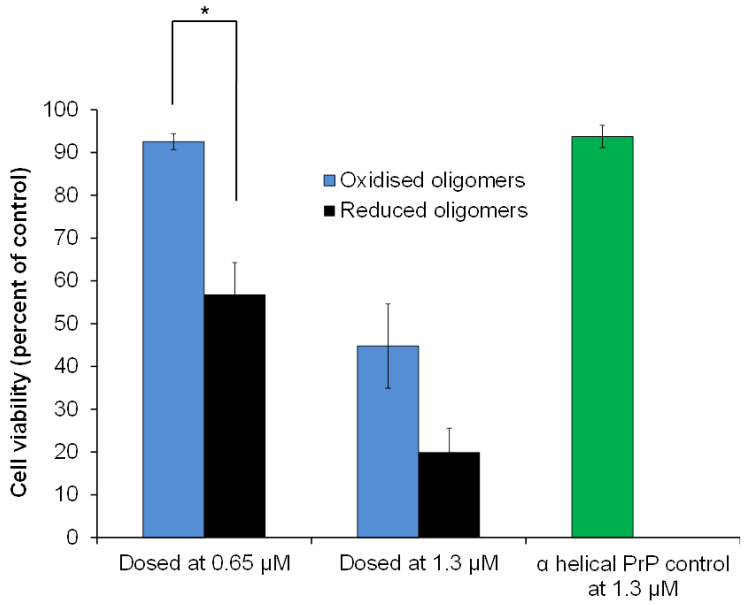

Figure 5.9 Toxicity of oligomers formed from oxidised or disulphide-reduced recPrP.

Bar chart to show the toxicity of oligomers formed with 100 % oxidised recPrP (blue) or 100 % disulphide-reduced recPrP (black) at 0.65 and 1.3 µM, α-helical monomeric recPrP (green) is shown at the higher concentration for comparison. Cell viability is shown as a percentage of the buffer control, a minimum of 6 readings (3-4 pictures per well with 2 wells for each) were taken for each recPrP preparation in each experiment (n=4) ± standard error (SE) bars are shown. * indicates a significant difference (ANOVA: p value <0.05).

I have shown that the larger 36 mer oligomer species formed from disulphide-reduced recPrP are significantly more toxic than the oxidised oligomers at least at 0.65 µM. With this in mind, I decided next to investigate whether it was the size of the oligomers formed from disulphide-reduced recPrP which was making them more toxic or whether the absence of the disulphide bond was increasing toxicity. I wanted to determine whether disulphide-reduced recPrP was itself intrinsically

toxic, or if the ability for disulphide-reduced recPrP to drive the formation of larger oligomers increased its toxicity. To do this, I solubilised both oxidised and disulphide-reduced recPrP in buffer typically used to produce monomeric recPrP (sodium acetate pH 5.5). Under these conditions oxidised recPrP is monomeric and α-helical. Therefore I assumed that disulphide-reduced recPrP would also be monomeric. If both oxidised and disulphide-reduced recPrP were monomeric, then any differences in toxicity would be due to the different oxidation states rather than differences in size. Therefore, I tested the toxicity of oxidised and disulphide-reduced recPrP under neutral "monomeric" buffer conditions. Intriguingly, the disulphide-reduced recPrP was found to be significantly more toxic than the oxidised recPrP under neutral buffer conditions (p-value < 0.05, figure 5.10), at both 0.65 and 1.3 μM. However, before drawing the conclusion that disulphide-reduced recPrP is intrinsically more toxic than oxidised recPrP, I wanted to ensure that the disulphide-reduced recPrP was monomeric under these buffer conditions. Since if disulphide-reduced recPrP is not monomeric at pH 5.5, then the differences in toxicity between disulphide-reduced recPrP and oxidised recPrP are not necessarily due to disulphide-reduced recPrP being intrinsically toxic, but could be due to size.

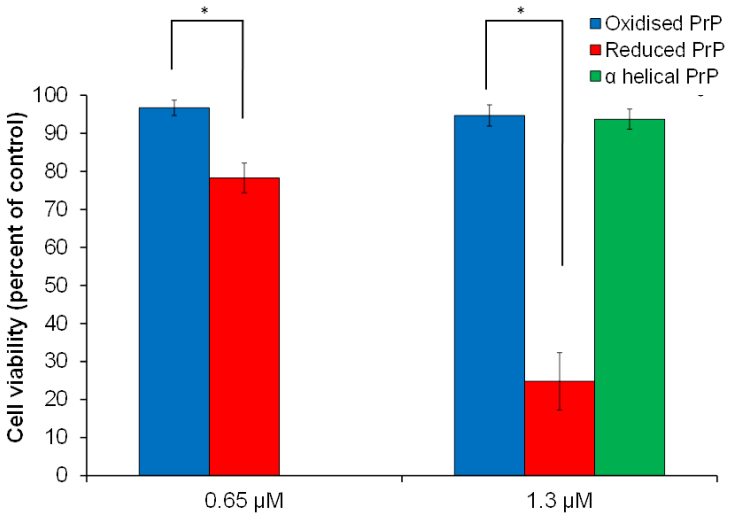

.

Figure 5.10 Toxicity of oxidised or disulphide-reduced recPrP prepared under "monomeric" conditions.

Bar chart to show the toxicity caused by oxidised (blue) or disulphide-reduced (red) recPrP conformations formed in sodium acetate buffer at pH 5.5 at 0.65 and 1.3 µM. α-helical monomeric recPrP (green) is shown at the higher concentration for comparison. Cell viability is shown as a percentage of the buffer control, a minimum of 6 readings (3- 4 pictures per well with 2 wells for each) were taken for each recPrP preparation in each experiment (n=4) ± standard error (SE) bars are shown. * indicates a significant difference (ANOVA: p value <0.05).

5.6 Structural comparison of oxidised and disulphide-reduced recPrP under neutral and acidic conditions

I have shown that disulphide-reduced recPrP is more toxic than oxidised recPrP, both under neutral monomeric conditions and under acidic oligomeric conditions. Under oligomeric conditions, I have shown that disulphide-reduced recPrP forms oligomers which are larger than those formed from oxidised recPrP and significantly more toxic. Under neutral "monomeric" buffer conditions (pH 5.5), disulphide-reduced recPrP was also found to be more toxic than oxidised recPrP. I

wanted to investigate the size of disulphide-reduced recPrP at pH 5.5 to determine whether it was monomeric, like oxidised recPrP, or if it forms oligomers.

In chapter 4, I explored the size of soluble misfolded species of recPrP in the fibril preparations and found that SEC was not reliable when using sodium acetate pH 5.5 as the running buffer. The monomeric buffer conditions are the same as the fibril storage buffer, therefore, I knew that SEC would not be a robust method to investigate the size of disulphide-reduced recPrP under these conditions. In light of this, I decided to use DLS to analyse the size of disulphide-reduced recPrP in sodium acetate pH 5.5. For comparison, I also analysed the size of oxidised recPrP under the same buffer conditions and oxidised and disulphide-reduced oligomers (formed at pH 3.4).

The DLS data shows that disulphide reduced recPrP under "monomeric" buffer conditions (pH 5.5) is not a monomer. The hydrodynamic radius of disulphide-reduced recPrP at pH 5.5 was significantly greater than oxidised recPrP under the same conditions (figure 5.11B). Additionally, the hydrodynamic radius of disulphide-reduced recPrP at pH 5.5 was significantly greater than oxidised recPrP under oligomeric conditions (pH 3.4). The SEC data I have for the oxidised oligomers (figure 5.4A) shows them to be almost entirely the P2 species, which as Rezaei *et al.* showed, relates to approximately 12 PrP molecules(Rezaei et al., 2005). Therefore, this would suggest that disulphide-reduced recPrP at pH 5.5 exists as an oligomer which is larger than a 12 mer (figure 5.11). Furthermore, the DLS data shows that there was no significant difference in hydrodynamic radius between disulphide-reduced recPrP at pH 5.5 and disulphide-reduced recPrP that had been oligomerised at pH 3.4 (figure 5.11B). This would suggest that disulphide-reduced recPrP forms oligomers even at pH 5.5, and that the size of the oligomers are not significantly different to those formed at pH 3.4. The DLS percentage volume data (figure 5.11A) suggests that disulphide-reduced recPrP at pH 5.5 forms oligomers which are less heterogeneous than those formed at pH 3.4. This is shown by the

narrow peak for disulphide-reduced recPrP at pH 5.5 in figure 5.11A (red), showing spread of oligomer size, in comparison to disulphide-reduced recPrP at pH 3.4 (black) which is much broader. Therefore, while the oligomers formed from disulphide-reduced recPrP at pH 3.4 are a mixture of both 36 mer and 12 mer species, those formed from disulphide-reduced recPrP at pH 5.5 may exist as a more homogenous population.

In light of this, the toxicity data presented in figure 5.10 did not compare the toxicity of oxidised and disulphide-reduced monomers. Instead, the toxicity of oxidised monomers was compared to oligomers produced from disulphide-reduced recPrP under neutral conditions. Without toxicity data for the disulphide-reduced monomer, it is very difficult to determine whether disulphide-reduced recPrP is in itself toxic or if it is its ability to form large oligomers which makes it highly toxic. Therefore, it is impossible to say whether oligomers formed from disulphide-reduced recPrP are more toxic because they are larger, or because disulphide-reduced recPrP is in itself toxic. However, if disulphide-reduced recPrP does not exist as a monomer even under relatively neutral buffer conditions, then perhaps the two are linked.

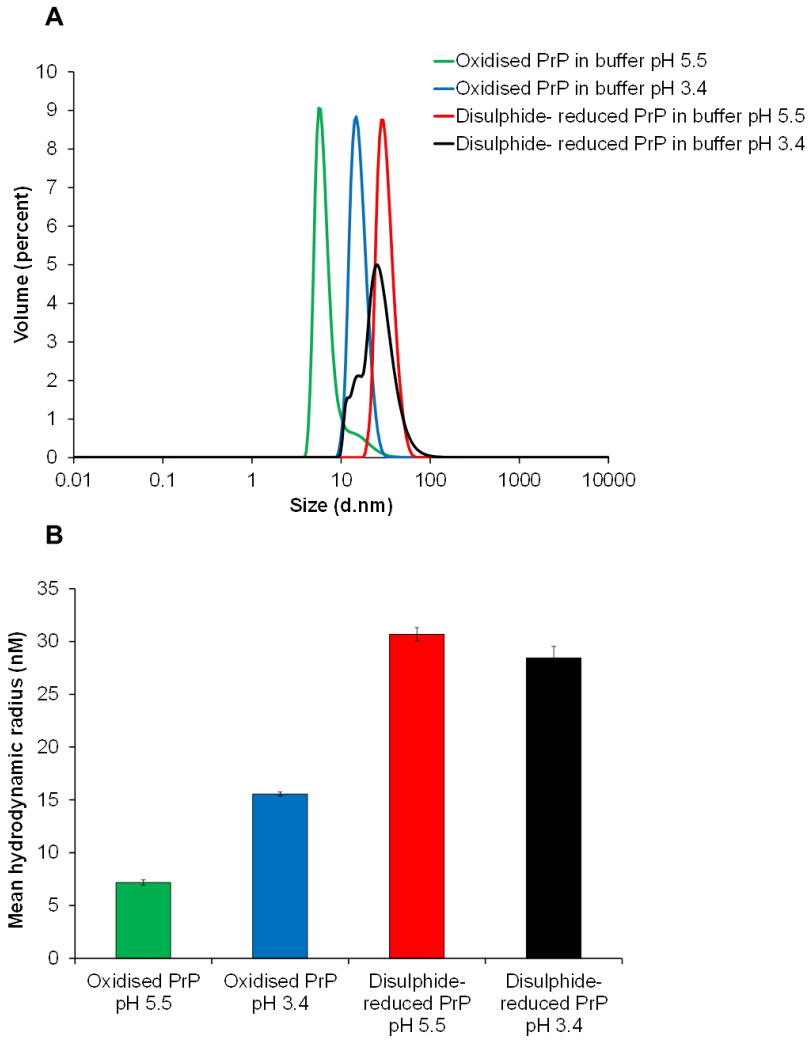

Figure 5.11 Dynamic light scattering data for oxidised and disulphide-reduced recPrP conformations formed under "monomeric" or "oligomeric" conditions.

A) DLS data showing size distribution by volume of both oxidised and disulphide-reduced recPrP under either "monomeric" conditions (sodium acetate pH 5.5, green for oxidised and red for reduced) or "oligomeric" conditions (sodium citrate pH 3.4, blue for oxidised and black for reduced). B) Average mean hydrodynamic radius DLS data, for both oxidised and disulphide-reduced recPrP under either "monomeric" conditions (sodium acetate pH 5.5, green for oxidised and red for reduced) or "oligomeric" conditions (sodium citrate pH 3.4, blue for oxidised and black for reduced). N=3 for each recPrP conformation, ± standard error (SE) bars are shown.

The toxicity of oligomers *in vivo* and *in vitro* is often ascribed to their β-sheet rich structures (Glabe and Kayed, 2006, Cobb and Surewicz, 2009, Prusiner, 1998a). Therefore, I wanted to investigate whether oligomers formed from disulphide-reduced recPrP under neutral buffer conditions had a β-sheet rich structure, which may contribute to their toxicity. I investigated the secondary structure of disulphide-reduced recPrP at pH 5.5 using CD. The secondary structure of disulphide-reduced recPrP at pH 5.5 was found to have a high β-sheet content (figure 5.12, red). The CD spectrum for disulphide-reduced recPrP oligomers formed at pH 5.5 was similar to that of disulphide-reduced oligomers formed at pH 3.4 (figure 5.12, black). This suggests that oligomers formed from disulphide-reduced recPrP whether they form at a more neutral or an acidic pH, have a β-sheet rich structure. By contrast, oxidised recPrP at pH 5.5 has an α-helical structure (figure 5.12, green) showing a conformation similar to that of PrP^{C}. Lastly, oligomers formed from oxidised recPrP at pH 3.4 have a secondary structure in between that of the oxidised α-helical monomer and the disulphide-reduced oligomers. This would suggest that the oxidised oligomers have a higher β-sheet content than the oxidised monomer at pH 5.5, but a lower β-sheet content than the disulphide-reduced oligomers.

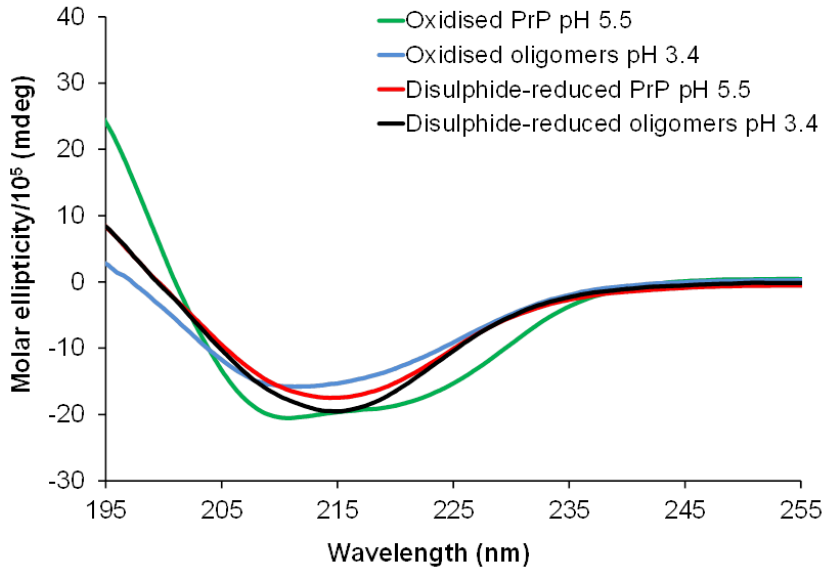

Figure 5.12 Secondary structure of oxidised and disulphide-reduced recPrP shown by circular dichroism.

CD spectra for both oxidised and disulphide-reduced recPrP, under monomeric conditions (sodium acetate pH 5.5, green for oxidised and red for reduced) and under oligomeric conditions (sodium citrate pH 3.4, blue for oxidised and black for reduced).

I wanted to investigate whether there were any differences in toxicity between oligomers formed at pH 3.4 or pH 5.5. Interestingly, disulphide-reduced oligomers formed at pH 3.4 were found to be significantly more toxic than disulphide-reduced oligomers formed at pH 5.5 at 0.65 μM (p value <0.05, figure 5.13). This would suggest that the oligomers formed under different pH buffer conditions must have some structural differences, which confer different toxicities. Additionally, oxidised oligomers made at pH 3.4 were found to be significantly more toxic than oxidised monomers made at pH 5.5 (p value <0.05, figure 5.13). This was not surprising since oxidised recPrP under these conditions is monomeric and α-helical and I have previously shown it to be non-toxic.

Overall, the data show that disulphide-reduced recPrP can form oligomers with β-sheet rich structures at both pH 5.5 and 3.4. The DLS data suggests that there is no significant difference in hydrodynamic radius between the oligomers which form at pH 5.5 and pH 3.4 (figure 5.11B). However, the volume percentage data (figure 5.11A) suggests that the oligomers formed at pH 5.5 are more homogenous than those formed at pH 3.4. It is possible that the more heterogeneous nature of the oligomers formed at pH 3.4 contribute to their toxicity, or there may be other structural differences between the oligomers. Further investigation would be needed to explore this further.

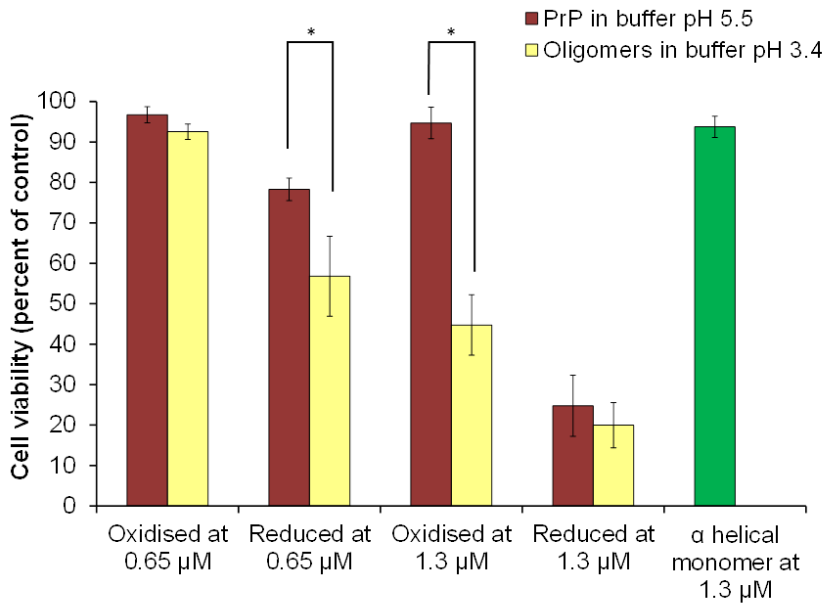

Figure 5.13 Toxicity of oxidised and disulphide reduced recPrP conformations formed under "monomeric" or "oligomeric" conditions.

Bar chart to show the toxicity of oxidised or disulphide-reduced recPrP conformations formed under either "monomeric" conditions (sodium acetate pH 5.5, red) or "oligomeric" conditions (sodium citrate pH 3.4, yellow) at 0.65 and 1.3 µM. The α-helical monomeric control (green) is shown at the higher concentration for comparison. Cell viability is shown as a percentage of the buffer control, a minimum of 6 readings (3- 4 pictures per well with 2 wells for each) were taken for each recPrP preparation in each experiment (n=4) ± standard error (SE) bars are shown. * indicates a significant difference; ANOVA: p value <0.05.

5.7 Discussion

The importance and involvement of small, soluble oligomeric forms of misfolded proteins in PMDs is widely accepted (Kuo et al., 1996, Naslund et al., 2000, McLean et al., 1999, Mucke et al., 2000a, Walsh et al., 2002, Quist et al., 2005, Kristiansen et al., 2007, Simoneau et al., 2007, Volles et al., 2001, Lue et al., 1999). However, the pathways leading to the production of oligomers and the factors which affect their size and toxicity are not well defined. In this chapter, I have demonstrated that the presence or absence of the disulphide bond in recPrP is crucial in determining the size of the oligomers which will form and, importantly, their toxicity. I found that recPrP lacking the disulphide bond (disulphide-reduced) formed oligomers with a high proportion of the large 36 mer species. This was in stark contrast to oligomers formed from oxidised recPrP, which consisted almost entirely of the smaller 12 mer oligomers. The differences in the size of the oligomers also affected their toxicity, with the larger disulphide-reduced oligomers causing significantly more toxicity than the smaller oxidised oligomers. In addition, the disulphide-reduced oligomers were shown to have a more β-sheet rich structure when compared to the oxidised oligomers. Under relatively neutral buffer conditions with a pH of 5.5, oxidised recPrP is monomeric, α-helical, and non-toxic to the cells. Under the same buffer conditions I discovered that disulphide-reduced recPrP forms highly toxic oligomers. This highlights how the absence of the disulphide bond can dramatically affect the ability of recPrP to form oligomers and cause toxicity.

Previous studies show conflicting evidence relating to how disulphide-reduced recPrP behaves under different buffer conditions, and whether it exists as a monomer or an oligomer (Jackson et al., 1999, Hosszu et al., 2009, Maiti and Surewicz, 2001, Sasaki et al., 2008). It has been postulated that disulphide-reduced recPrP can exist as a β-sheet rich monomer (Jackson et al., 1999), however, various studies dispute this finding and instead show disulphide-reduced recPrP to be oligomeric (Maiti and Surewicz, 2001, Hosszu et al., 2009, Sasaki et al., 2008). Some

studies have shown that lowering the pH or increasing the concentration of salts is needed to instigate oligomerisation (Trevitt et al., 2014, Maiti and Surewicz, 2001), while others have shown an oligomeric structure is possible even under neutral conditions (Hosszu et al., 2009, Sang et al., 2012). The differences in techniques used to analyse the structure of the protein and differences in the recPrP species used may all contribute to these inconsistencies. Additionally, some papers analysed the structure of truncated disulphide-reduced PrP (amino acids 91-231) instead of full length PrP (Jackson et al., 1999, Hosszu et al., 2009), which behaves differently as shown by Trevitt *et al.* (Trevitt et al., 2014). This is also likely to account for some of the disparity seen between studies.

There has been some speculation about whether oligomers during disease are formed through intermolecular disulphide bonds (Knaus et al., 2001, Lee and Eisenberg, 2003). If this was the case, then disulphide-reduced PrP could recruit oxidised PrP and reform disulphide bonds between molecules. This may be possible in some cases, however, my data would suggest that the oligomers formed by disulphide-reduced recPrP do not contain intermolecular disulphide bonds, since when they are analysed by mass spectrometry they appear as monomers. If they were assembled and linked by disulphide bonds, then they would remain oligomeric during mass spectrometry. Additionally, Sang *et al.* (Sang et al., 2012) showed that oligomers formed by mutant PrP containing no disulphide bonds were not assembled by intermolecular disulphide bonds, since oligomerisation was the same even under DTT reducing conditions.

When studying the importance of the disulphide bond in PrP and how it might relate to disease, it is important to establish whether disulphide-reduced PrP can occur naturally *in vivo*. It has been shown that PrP has a "weak" signal peptide, which can cause it to not be transported into the ER. Instead it can be translocated to the cytosol (Orsi et al., 2006), since it has not been through the ER this form of PrP has no disulphide bond and an intact signal peptide (Orsi et al., 2006). Under ER

stress conditions, it has been shown that levels of this cytosolic PrP increases (Orsi et al., 2006) and that it is likely toxic (Ma et al., 2002). Another potential source of disulphide-reduced PrP in the cell is termed PrP^{CTM}, which spans the ER membrane and is not processed and refolded properly. PrP^{CTM} has been shown to be translocated away from the ER to either the Golgi or the cytosol, where it is thought to cause toxicity (Orsi et al., 2006, Lisa et al., 2012). Both these sources of cytosolic PrP lack a disulphide bond and would normally be degraded by the proteasome. However, in some cases where the proteasome is inhibited or working less efficiently, such as in aged individuals or during an infection, there could be a build- up in the cytosol. It has also been shown that ER stress or inhibition of the proteasome can lead to PrP aggregation in the cell (Nunziante et al., 2011), and that these aggregates can be transported to the cell membrane (Nunziante et al., 2011). This could lead to a seeding event and spontaneous disease (Ma and Lindquist, 1999).

In mice, it has been shown that various mutations in the *Prnp* gene can cause an up regulation of PrP^{CTM}, which causes neurodegeneration (Hegde et al., 1998, Stewart and Harris, 2005). Mutations which caused the highest levels of PrP^{CTM} had the shortest life span, and those with lower levels took significantly longer to develop disease (Hegde et al., 1999). It was shown that if PrP^{CTM} was down regulated then disease no longer occurred, indicating that PrP^{CTM} was directly involved in toxicity (Hegde et al., 1998). During a prion infection it has been shown that levels of PrP^{CTM} increase as the disease progresses (Hegde et al., 1999), so it is possible that PrP^{CTM} could be responsible for the cellular toxicity seen in these diseases. Once formed, PrP^{CTM} has been shown to exit the ER (Yedidia et al., 2001, Hegde et al., 1998) and by an unknown mechanism cause toxicity (Hegde et al., 1998). Additionally, mice with mutations which cause increased levels of PrP^{CTM} were shown to have an absence of PK resistant fibrillar deposits (Hegde et al., 1998) suggesting that the toxic species was perhaps soluble and oligomeric. It has been found that there is an increase in PrP^{CTM} found in the brains of those affected with GSS disease caused by the A117V

mutation(Hegde et al., 1998). Similar to the mice with increased levels of PrP^{CTM}, patients with this mutation have little or no PK resistant PrP^{Sc} (Hegde et al., 1998). This would indicate that PrP^{CTM} is playing a role in causing disease.

It has been suggested that PrP^{CTM} may play a role in causing neurodegeneration in prion diseases. If this hypothesis is correct and disulphide-reduced PrP^{CTM} is upregulated under prion infection or because of a mutation, then there is the question of how PrP^{CTM} causes toxicity once it has exited the ER. One possibility is that the disulphide-reduced PrP forms oligomers either through association with other disulphide-reduced PrP or with oxidised, normally folded PrP. I have shown that disulphide-reduced recPrP can oligomerise with oxidised recPrP, and that as little as 5 % disulphide-reduced recPrP can drive the formation of large highly toxic oligomers. If the disulphide-reduced PrP did go on to form oligomers in the cytosol, then it is yet to be established how these might cause toxicity. One explanation is that they may insert into the cell membrane, causing disruption to the calcium homeostasis of the cell. It has been demonstrated that when PrP has been disulphide reduced, it binds strongly to membranes (Kazlauskaite et al., 2003, Kazlauskaite et al., 2005) and causes disruption potentially by membrane insertion (Shin et al., 2008, Shin et al., 2009, Caughey and Lansbury, 2003). Therefore, this may be a potential pathway for how toxicity may occur in disease (Kazlauskaite et al., 2005, Caughey and Lansbury, 2003).

The diagram in figure 5.14A illustrates how the disulphide-reduced oligomers may cause toxicity in the primary cell experiments. The model demonstrates that the oligomers may cause toxicity through membrane insertion externally, or after being taken up by the cell, and that the larger oligomers may insert deeper into the membrane and cause greater toxicity. The model in figure 5.14B shows how disulphide-reduced PrP may cause toxicity during disease *in vivo*. The model proposes that if during infection PrP^{Sc} causes ER stress and the up-regulation of PrP^{CTM}, then the PrP^{CTM} could be translocated to the cytosol where it could

oligomerise. These oligomers could then insert into the cell membrane and cause cellular disruption and death, or go on to form fibrils. Alternatively, under ER stress disulphide-reduced PrP could remain in the ER and potentially oligomerise and insert into the ER membrane causing apoptosis. If PrP^{CTM} is directly involved in causing cellular toxicity during prion infection, then this may account for why the PrP^{Sc} titre does not always correlate with cell death and why PrP^{Sc} itself is not thought to be the toxic entity (Hill et al., 2000, Sandberg et al., 2014, Krasemann et al., 2013).

In summary, I have shown that the oxidation state of PrP is crucial in determining the size and potential toxicity of oligomers which will form. I have shown that disulphide-reduced recPrP forms oligomers at pH 5.5 and pH 3.4, and that these oligomers have different structures and confer different levels of toxicity. Disulphide-reduced PrP does exist *in vivo* and may be involved in instigating spontaneous prion infection, or it may play a part in causing toxicity during disease.

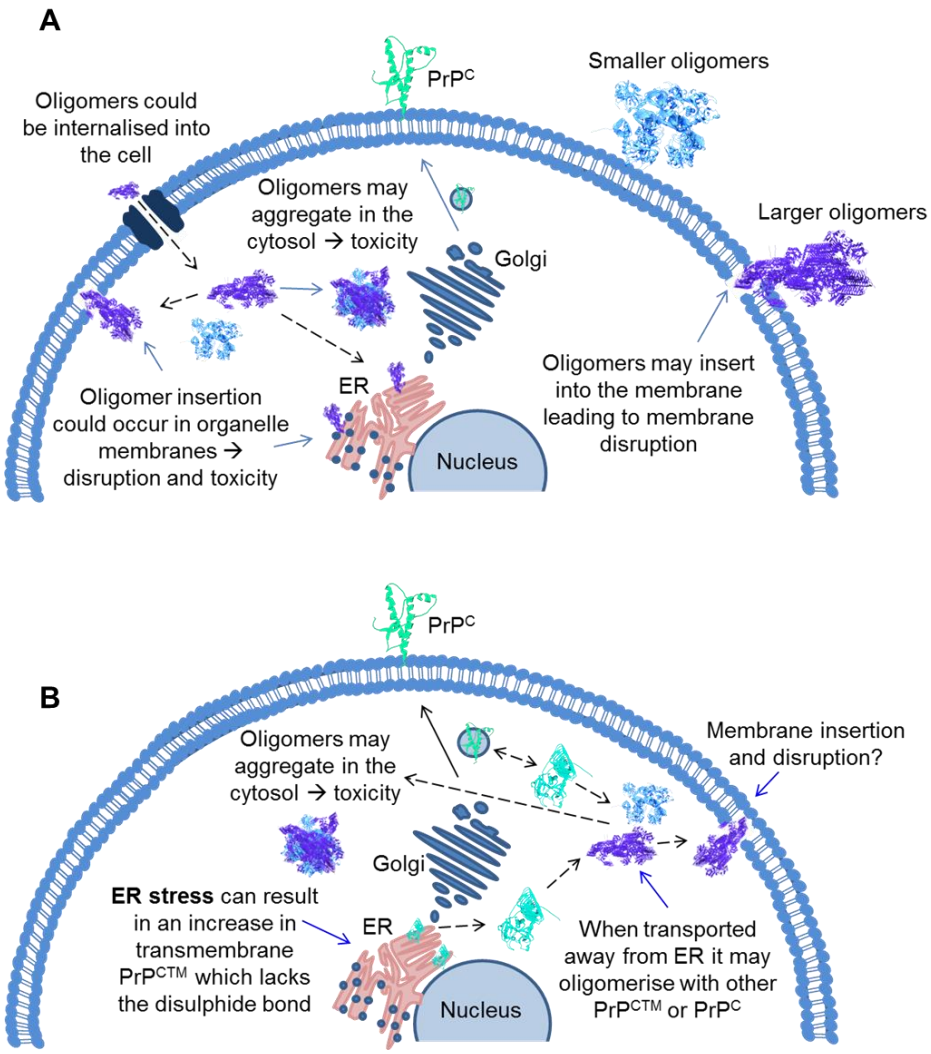

Figure 5.14 Toxicity models.

A) Representation of a mammalian cell exposed to recPrP oligomers *in vitro*, the image shows how oligomers may cause cellular toxicity which leads to apoptosis. B) Representation of a mammalian cell *in vivo* which is under ER stress, potentially from a neurodegenerative disease. The image illustrates how under ER stress recPrP lacking a disulphide bond can form, and potentially be given the chance to oligomerise and cause toxicity.

Chapter 6:

Mechanisms leading to cell death associated with misfolded isoforms of recPrP and recAβ

6.1 Introduction

In order to better understand the pathology of PMDs, it is important to investigate mechanisms and pathways leading to cell death caused by the misfolded proteins implicated in these diseases. A better understanding of the pathways leading to cell death may help in the development of drugs or therapies for these diseases, which are not presently available. The hypothesis that there may be common mechanisms leading to cellular toxicity across PMDs has been widely debated (Glabe, 2006, Kayed et al., 2003, Haass and Selkoe, 2007, Quist et al., 2005). It is thought that small oligomeric forms of the misfolded proteins may activate common pathways leading to cell death (Glabe, 2006, Kayed et al., 2003, Haass and Selkoe, 2007, Quist et al., 2005). If this was the case, then therapies could be developed which target these pathways meaning they could be effective in multiple PMDs.

Previous studies have shown that both PrP and Aβ oligomers can induce apoptotic cell death (Novitskaya et al., 2006, Simoneau et al., 2007, Youssef et al., 2008, Yang et al., 2009). Additionally, apoptotic cells have been found around lesions in the brains of those affected with CJD (Jesionek-Kupnicka et al., 1997). Apoptosis is an energy dependent form of programmed cell death in which cellular organelles break down and the DNA in the nucleus fragments (Elmore, 2007). Apoptotic cells have shrunken nuclei and can undergo blebbing, where small portions of the cellular membrane containing cytoplasm can break off from the cell body (Elmore, 2007). The process of apoptosis is normal within an organism and the balance between cell division and apoptosis is integral to maintaining properly functioning tissues. However, during disease the balance between cell division and cell death can be altered. In cancer the rate of apoptosis is less than that of cell division, which is thought to be vitally important in the process of tumour growth (Elmore, 2007). In neurodegenerative diseases such as AD, Huntington's and prion disease misfolded proteins are thought to instigate apoptosis (Elmore, 2007, Hickey and Chesselet, 2003, Shimohama, 2000, Rohn, 2010, Jesionek-Kupnicka et al., 1997), which results in

the death of large numbers of cells. This process results in the loss of neurons and atrophy of the brain, which ultimately causes the symptoms seen in these diseases (Hickey and Chesselet, 2003, Shimohama, 2000, Rohn, 2010).

In addition to apoptosis, excitotoxic cell death has previously been implicated in several PMDs, including AD (Molinuevo et al., 2005, Esposito et al., 2013, Di et al., 2010, Dong et al., 2009), ALS (Van Damme et al., 2005) and Huntington's disease (Tabrizi et al., 1999, Chiarlone et al., 2014, Dong et al., 2009). Excitotoxic cell death occurs when NMDA receptors, which are calcium gated ion channels activated by glutamate, are overly stimulated (Dong et al., 2009). This results in excessive calcium influx, which downstream causes cell death (Dong et al., 2009). Previously, Aβ oligomers have been shown to activate NMDA receptors leading to excitotoxic cell death (Dong et al., 2009, Li et al., 2009, Alberdi et al., 2010, Li et al., 2011, Rammes et al., 2011, Rönicke et al., 2011). Fewer studies have been published which have found this to be the case for PrP induced cell death (Muller et al., 1993, Sassoon et al., 2004, Thellung et al., 2013).

As outlined in chapter 5, the ER is the site within a cell where secreted proteins undergo post-translational modifications and are correctly folded with the aid of chaperones (Kleizen and Braakman, 2004). When proteins are folded incorrectly they are transported to the cytosol and degraded by the proteasome (Dobson, 2003, Wickner et al., 1999). Under certain circumstances the proteasome can become overloaded, such as in aged individuals or during infection (Dobson, 2003, Wickner et al., 1999, Kristiansen et al., 2007). This can mean that the production of incorrectly folded proteins can overtake their degradation, which can be toxic to the cell (Dobson, 2003, Wickner et al., 1999, Kristiansen et al., 2007). The presence of unfolded proteins in the ER causes the unfolded protein response (UPR) to be activated (Bukau et al., 2006). This causes a cascade of proteins to be up-regulated, which in the first instance will try to re-establish the balance between protein formation and degradation by the production of chaperones (Bukau et al., 2006,

Voisine et al., 2010). In addition the ER-associated degradation pathway (ERAD) is activated, which translocates misfolded proteins to the cytosol for degradation (Bukau et al., 2006). However, if the balance between protein production and degradation cannot be corrected then the cell will undergo apoptosis (Bukau et al., 2006). It has been shown previously that misfolded proteins found in neurodegenerative conditions such as AD or prion diseases can cause ER stress (Lindholm et al., 2006, Yoshida, 2007) which, when unresolved, can lead to cell death (Lindholm et al., 2006, Yoshida, 2007).

I chose to explore apoptosis, excitotoxicity and ER stress as potential mechanisms leading to cell death caused by the recPrP and recAβ isoforms. I chose these pathways since they had all been previously implicated in PMDs. Additionally there were reagents available to investigate these pathways, such as inhibitors or specific proteins which could be probed for in the case of ER stress. There are many other pathways which may be involved in causing cell death when cells come into contact with misfolded proteins. These include both autophagy (Mizushima et al., 2008, Martinez-Vicente and Cuervo, 2007) and oxidative stress (Nakamura and Lipton, 2010, Youssef et al., 2008).

In chapter 4, I described work that investigated the toxicity caused by misfolded isoforms of recPrP and recAβ. I found that both recPrP oligomers and fibrils caused significant toxicity to primary cortical cells, while α-helical recPrP at the same concentration did not. Additionally, I discovered that while recAβ 1-42 oligomers cause significant toxicity, all recAβ 1-40 isoforms caused low toxicity and both recAβ 1-40 and recAβ 1-42 fibrils were found to be non-toxic. In light of this, I wanted to investigate how recPrP oligomers and fibrils and recAβ 1-42 oligomers were causing toxicity. In this chapter, I will explore the mechanisms which are activated in the cells when they are incubated with these misfolded proteins.

6.2 Misfolded isoforms of recPrP and recAβ cause apoptosis

Both recPrP oligomers and fibrils caused significant toxicity to the cells, with the recPrP fibrils eliciting the greatest toxic response. By contrast, both recAβ 1-40 and recAβ 1-42 fibrils caused no significant toxicity. However, the recAβ 1-42 oligomers did cause significant toxicity when compared to the buffer control or the recAβ 1-42 fibrils. In this chapter, I will explore the pathways and mechanisms which are activated by these misfolded proteins, which ultimately lead to cell death.

Firstly, I wanted investigate whether recPrP oligomers or fibrils could be causing cell death *via* apoptosis. To do this, I used a pan-caspase inhibitor which blocks apoptosis by inhibiting the three major caspase pathways (caspases 9/3, 8/10 and 12)(Caserta et al., 2003). The toxin staurosporine is known to cause apoptosis(Léveillé et al., 2010), however, when cells are treated with the pan-caspase inhibitor prior to exposure to staurosporine, cell viability is dramatically and significantly increased (figure 6.1A). Therefore, staurosporine was used as a positive control for these assays. Subsequently, I compared cell death between those treated with recPrP oligomers or fibrils alone, and those treated with oligomers or fibrils and the caspase inhibiter. The cells were incubated with the caspase inhibitor for 1 hour prior to the addition of recPrP, once the recPrP isoforms had been added, the cells were incubated at 37 °C for 24 hours. Interestingly, I found a significant recovery in cell viability when cells were treated with recPrP oligomers and the caspase inhibitor (paired t-test; p value <0.05, figure 6.1A), suggesting that recPrP oligomers activate the programmed cell death pathway and cause apoptosis. By contrast, no significant difference was seen in cell viability between cells treated with fibrils alone and those treated with fibrils and the caspase inhibiter (figure 6.1A). This suggests that recPrP fibrils do not cause cell death by apoptosis. Importantly, this also indicates that recPrP oligomers and fibrils are activating different cellular pathways to cause toxicity.

To further analyse the role of apoptosis in oligomer induced cell death, I probed for the presence of activated caspase 3. Caspase 3 is an executioner caspase and, once cleaved, it becomes active and causes the cell to undergo programmed cell death(Brentnall et al., 2013). I detected activated caspase 3 by western blotting. I found there was an up-regulation of activated caspase 3 in cells treated with recPrP oligomers (figure 6.1B+C), which confirms that recPrP oligomers induce apoptosis. The western blot shown in figure 6.1B is a representative example of 4 western blots, in which activated caspase 3 was detected. All of the western blots were analysed by densitometry for activated caspase 3 protein expression. β-actin was used as a control for the amount of protein loaded, hence the activated caspase 3 expression was normalised to β-actin expression. The data presented in figure 6.1C is the average western blot data expressed as a percentage of the high and low controls. The untreated cells acted as a low control and staurosporine treated cells acted as a high control. By presenting the data this way, it takes into account background cell death (untreated low control) and the maximum amount of activated caspase 3 that could be produced in this assay (staurosporine, high control). The oligomer treated cells at 1.3 μM show the greatest expression of activated caspase 3 (figure 6.1C). However, the fibril treated cells also showed activated caspase 3 expression (figure 6.1B+C). This was surprising, since there was no recovery with the caspase inhibitor. The activated caspase 3 expression seen in the fibril treated cells is lower than that seen for oligomer treated cells. Therefore, perhaps there was a subset of fibril treated cells which were dying by apoptosis. The small soluble protofibrils found in the fibril preparations could be causing apoptosis in these cells. However, the main fibril population may be causing cell death by a different pathway, which is why no recovery was seen with the caspase inhibitor. Further studies would be needed to test this hypothesis. Nevertheless, the data strongly suggests that recPrP oligomers cause apoptosis.

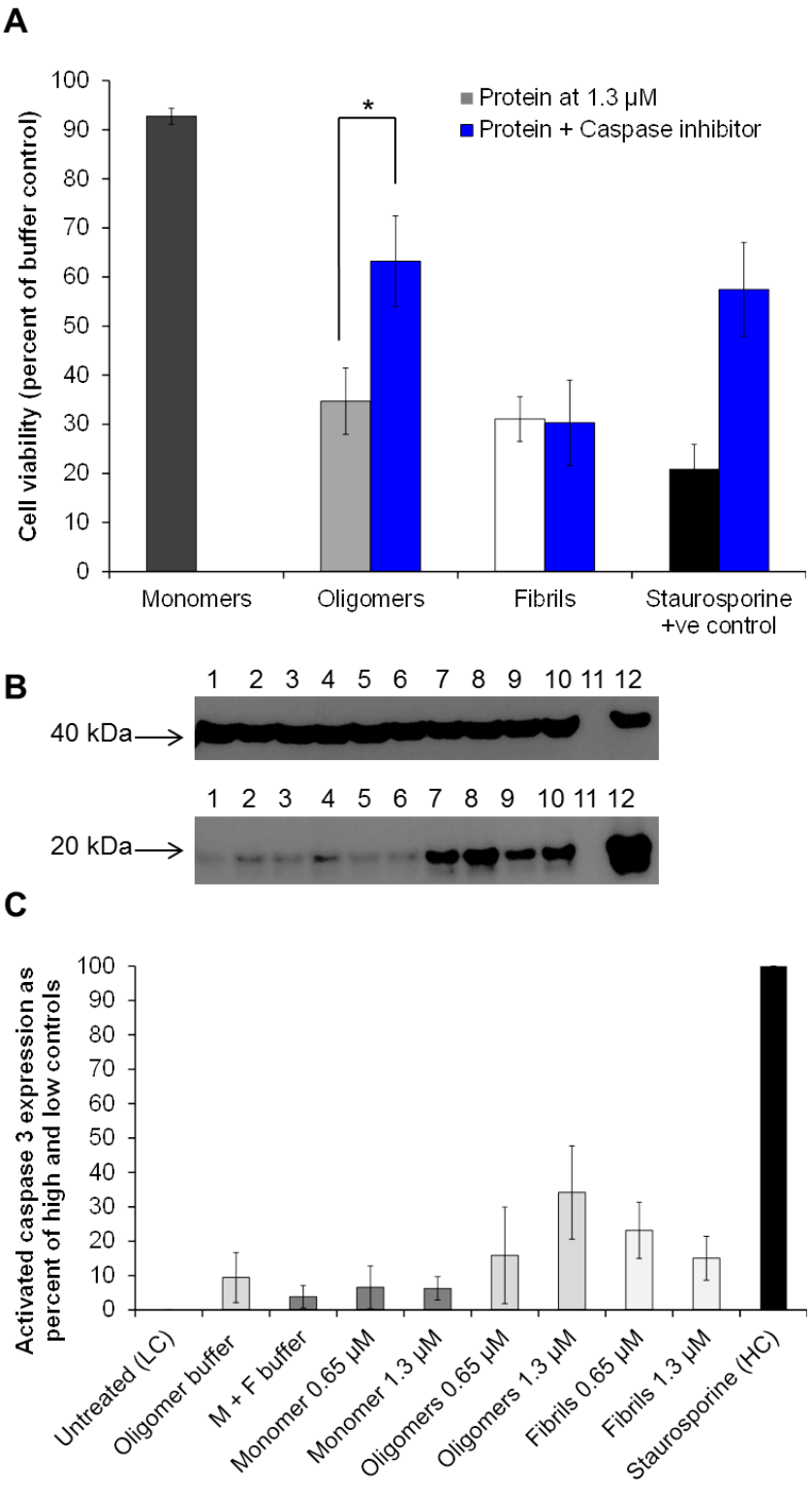
A
Cell viability (percent of buffer control)
100
90
80
70
60
50
40
30
20
10
0
*
Protein at 1.3 µM
Protein + Caspase inhibitor
Monomers
Oligomers
Fibrils
Staurosporine +ve control
B
1 2 3 4 5 6 7 8 9 10 11 12
40 kDa
1 2 3 4 5 6 7 8 9 10 11 12
20 kDa
C
Activated caspase 3 expression as percent of high and low controls
100
90
80
70
60
50
40
30
20
10
0
Untreated (LC)
Oligomer buffer
M + F buffer
Monomer 0.65 µM
Monomer 1.3 µM
Oligomers 0.65 µM
Oligomers 1.3 µM
Fibrils 0.65 µM
Fibrils 1.3 µM
Staurosporine (HC)

Figure 6.1 RecPrP oligomers cause apoptosis.

A) Bar chart to show viability of the primary cells when treated with recPrP oligomers (mid grey) or fibrils (white) at 1.3 µM alone or in addition to the caspase inhibitor Q-VD-OPh (50 µM), the cells were also treated with recPrP monomers (dark grey) at 1.3 µM as a negative control and staurosporine (200 nM) as a positive control. Cell viability is shown as a percentage of the buffer control, a minimum of 6 readings (3-4 pictures per well with 2 wells for each) were taken for each experiment (n=4) ± standard error (SE). * indicates a significant recovery in cell viability for cells treated with oligomers and the caspase inhibitor when compared to oligomers alone (paired t-test; p value <0.05). B) Western blot to show the presence of activated caspase 3 in the cells, the blot is representative of 4 blots. Top: shows β-actin loading control, bottom: shows activated caspase 3. Lanes 1-12 show cells treated with: lane 1: untreated, lane 2:, oligomer buffer control, lane 3: monomer and fibril buffer control, lane 4: monomer at 0.65 µM, lane 5: monomer at 1.3 µM, lane 6: α-helical PrP at 0.65 µM, lane 7: oligomers at 0.65 µM, lane 8: oligomers at 1.3 µM, lane 9: fibrils at 0.65 µM, lane 10: fibrils at 1.3 µM, lane 11: blank, lane 12: staurosporine (positive control) at 200 nM. C) Bar chart to show the average western blot results for activated caspase 3 (for 2 independent experiments with 2 wells of cells and 2 blots in each experiment), blots were analysed by image J and normalised to the β-actin control. Results were then expressed as a percentage of the high control (staurosporine) and low control (untreated).

When the primary cells were visualised under a microscope following incubation with the recPrP isoforms, the cells appeared morphologically different from each other. Bright-field microscopy images of the primary cells after a 24 hour incubation with either α-helical recPrP, recPrP oligomers or recPrP fibrils are shown in figure 6.2. Cells treated with α-helical recPrP appear similar to untreated cells, however, cells treated with oligomers or fibrils do not share the same morphology as the untreated cells. The cells treated with the oligomers are more spread out across the plate, with obvious neurite loss. Conversely, the fibril treated cells are clumped together, with large areas of the plate showing no cells. These morphological

differences further suggest that the recPrP oligomers and fibrils are activating different cellular pathways leading to cell death.

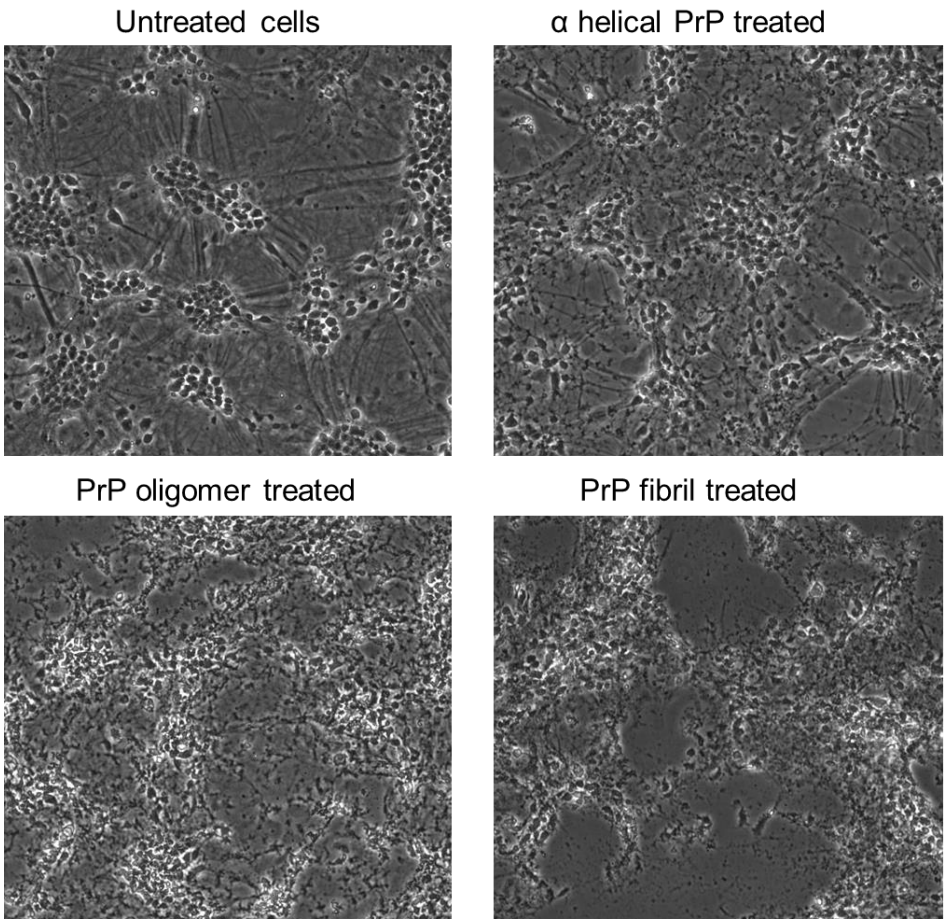

Figure 6.2 Bright-field images of recPrP treated cells

Bright-field microscopy images of murine primary cortical cells treated with different isoforms of recPrP. Top left image shows untreated cells. Top right image shows cells treated with α-helical recPrP at 1.3 µM. Bottom left image shows cells treated with recPrP oligomers at 1.3 µM and the bottom right image shows cells treated with recPrP fibrils at 1.3 µM. All images are shown at 10x magnification.

In chapter 4, I showed that both the recAβ 1-42 monomers and oligomers caused significantly more toxicity that the recAβ 1-42 fibrils. Therefore, I investigated the mechanisms leading to cell death for both recAβ 1-42 monomers and oligomers.

After establishing that recPrP oligomers cause apoptosis to primary cortical cells (figure 6.1), I wanted to investigate whether toxic isoforms of recAβ 1-42 also induce apoptosis. I again investigated this using a pan-caspase inhibiter to block apoptosis. The average cell viability results are shown in figure 6.3A. There was some recovery in the cells treated with the caspase inhibitor and the Aβ 1-42 oligomers (figure 6.3A). However, the recovery was not significant (paired t-test p value = 0.089). It is likely that the difference was not significant because in one of the three repeats the cell density was very high, which meant that the oligomer toxicity was reduced (figure 6.3D). The three independent repeats are shown in figure 6.3 B-D, the caspase inhibitor seemed to reduce toxicity in the oligomer treated cells in B and C. However, further repeats would be needed in order to see if the recovery with the caspase inhibitor would reach statistical significance. If the recAβ oligomers were found to also cause apoptosis this would be very interesting when put in context with the recPrP oligomer data, and could suggest a common mechanism leading to cell death caused by oligomers. The recAβ 1-42 monomer treated cells showed no significant recovery when treated with the caspase inhibitor. This is likely due to the recAβ 1-42 monomer not causing high enough levels of toxicity to be significantly recovered, since there was some recovery seen but not a significant difference.

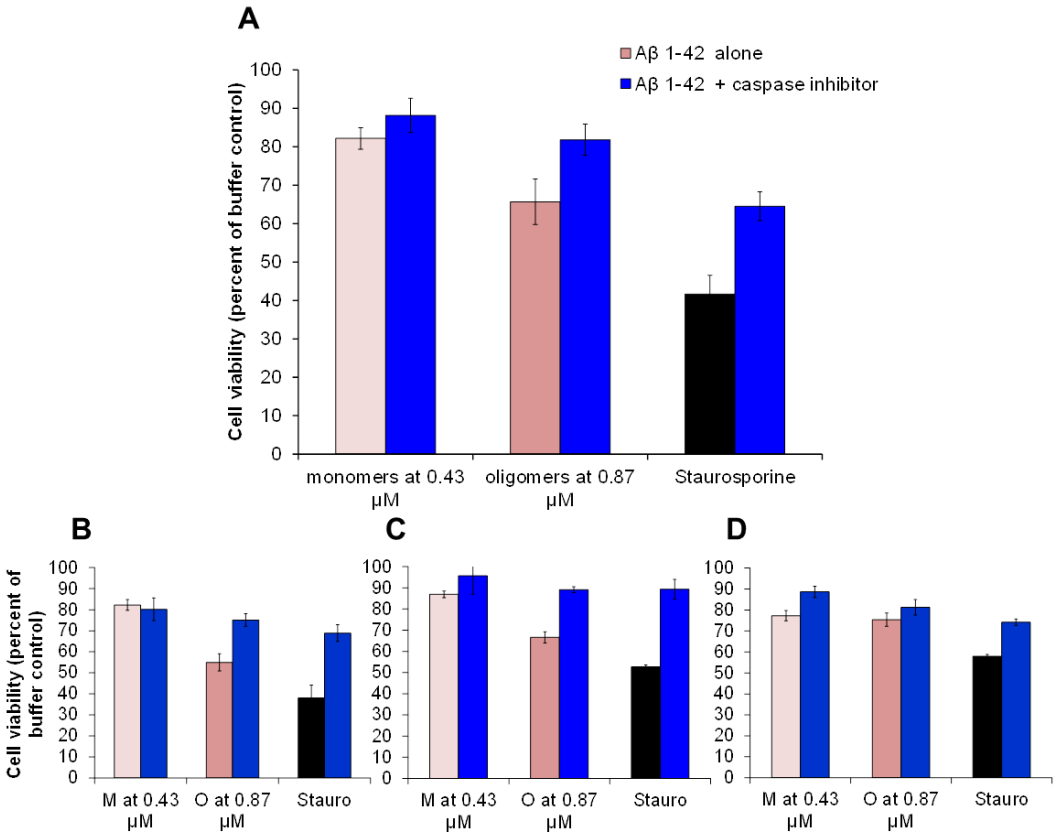

Figure 6.3 RecAβ 1-42 oligomers cause apoptosis.

A-D) Bar charts to show viability of the primary cells when treated with recAβ 1-42 oligomers at 0.87 µM (dark pink) or recAβ 1-42 monomers at 0.43 µM (pale pink) alone or in addition to the caspase inhibitor Q-VD-OPh (50 µM, blue). Staurosporine (200 nM) acted as a positive control. Cell viability is shown as a percentage of the buffer control, a minimum of 6 readings (3- 4 pictures per well with 2 wells for each) were taken for each experiment ± standard error (SE). A) Average cell viability data for 3 independent experiments (shown separately B-D) B-D) Independent cell viability experiments, M: recAβ 1-42 monomers, O: recAβ 1-42 oligomers, Stauro: staurosporine.

6.3 The role of excitotoxicity in oligomer induced cell death

I have demonstrated that recPrP oligomers induce apoptosis in primary cortical cells. Additionally, I have shown that recAβ 1-42 oligomers may also induce apoptosis. I wanted to further investigate the mechanisms leading to apoptosis, instigated by the oligomers. It has been shown that over stimulation of NMDA receptors can lead to excitotoxicity, which causes an influx of calcium into the cell and can lead to apoptosis. Excitotoxic cell death has been implicated in many PMDs (Molinuevo et al., 2005, Esposito et al., 2013, Di et al., 2010, Dong et al., 2009, Tabrizi et al., 1999, Chiarlone et al., 2014, Muller et al., 1993, Sassoon et al., 2004, Thellung et al., 2013, Alberdi et al., 2010). Therefore, I wanted to investigate whether the apoptosis induced by the oligomers could be caused by excitotoxicity. To investigate this, I used an NMDA receptor antagonist which blocks excitotoxicity. I first investigated the role of excitotoxicity in recPrP induced cell death. The cells were incubated with the NMDA receptor antagonist for 1 hour prior to the recPrP isoforms being added to the cell culture media. Cells were also treated with the recPrP isoforms alone, so that cell viability could be compared. There was no recovery seen in cells treated with the NMDA receptor antagonist and either recPrP oligomers or recPrP fibrils (figure 6.4). I repeated the experiment, and again no recovery was seen for cells treated with the NMDA receptor antagonist and oligomers or fibrils. Therefore, I decided not to carry out further repeats since even with an n =2 the result seemed conclusive. I think that since no recovery was seen with the NMDA receptor antagonist it is very unlikely that the oligomers cause excitotoxicity. Therefore, the oligomers must be activating a different pathway, which is leading to apoptosis. The data also suggests that recPrP fibrils do not cause excitotoxicity, therefore, the mechanisms causing fibril induced cell death are still unknown. NMDA was used as a positive control, which causes excitotoxicity and is recovered by the NMDA receptor antagonist (figure 6.4).

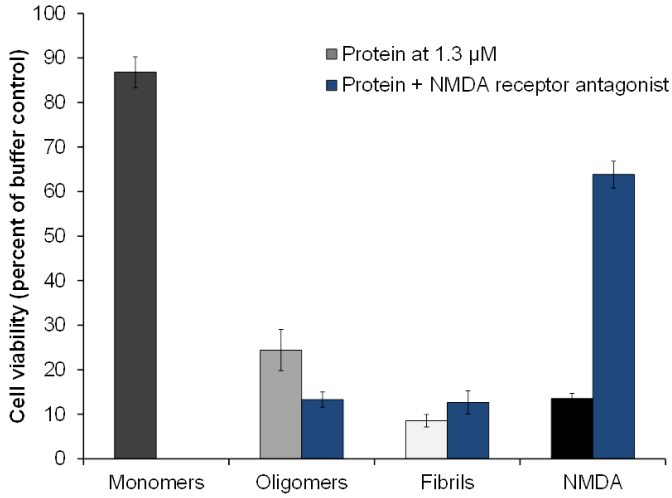

Figure 6.4 RecPrP oligomers and fibrils are not inducing excitotoxicity.

Bar chart to show viability of the primary cells when treated with recPrP oligomers (mid grey) or fibrils (white) at 1.3 µM alone or in addition to the NMDA receptor antagonist MK-801. The cells were also treated with monomers (dark grey) at 1.3 µM as a negative control and NMDA (50 µM) as a positive control. Cell viability is shown as a percentage of the buffer control, a minimum of 6 readings (3- 4 pictures per well with 2 wells for each) were taken for each experiment (n=2) ± standard error (SE).

Having established that recPrP oligomers do not cause excitotoxicity, I wanted to investigate whether recAβ 1-42 oligomers induce excitotoxic cell death. I used a NMDA receptor antagonist to block excitotoxicity, as I did for the recPrP assays. The average cell viability results can be seen in figure 6.5A. The cells treated with the NMDA receptor antagonist and the recAβ 1-42 oligomers show an increase in viability, however, this increase was not significant (figure 6.5A). This was again likely due to the cells being highly confluent in one of the repeats, so that the oligomers caused less toxicity (figure 6.5D). The three independent repeats are shown in figure 6.5 B-D. The NMDA receptor antagonist seemed to increase cell viability in the oligomer treated cells in B and C, however, overall the recovery was not significant for the average data. It is possible that with further repeats the recovery with the NMDA receptor antagonist may reach statistical significance. If this was found to be the case then this could indicate that the recAβ 1-42 oligomers cause excitotoxicity, which then leads to apoptosis. If the recAβ 1-42 oligomers cause excitotoxicity, then this would suggest that recPrP oligomers and recAβ oligomers trigger different pathways leading to cell death.

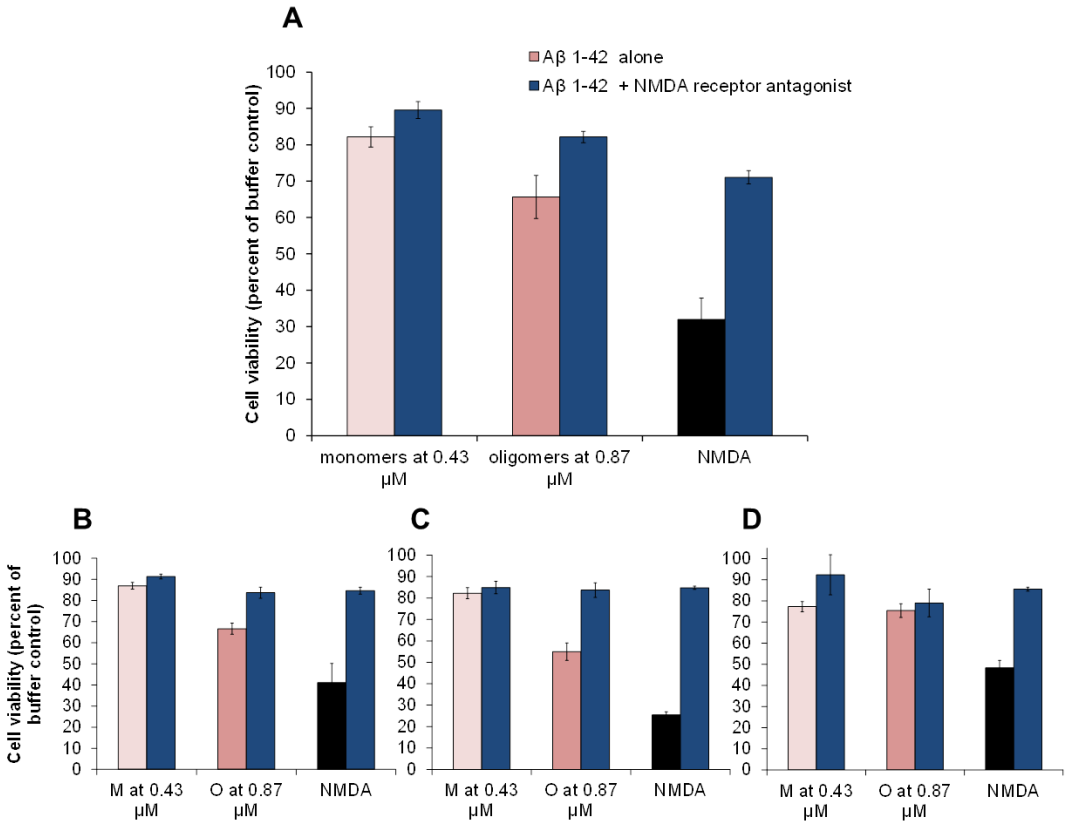

Figure 6.5 RecAβ 1-42 oligomers may induce excitotoxicity.

A-D) Bar charts to show viability of the primary cells when treated with recAβ 1-42 oligomers at 0.87 µM (dark pink) or recAβ 1-42 monomers at 0.43 µM (pale pink) alone or in addition to the NMDA receptor antagonist MK801 (blue). NMDA (50 µM) acted as a positive control. Cell viability is shown as a percentage of the buffer control, a minimum of 6 readings (3- 4 pictures per well with 2 wells for each) were taken for each experiment ± standard error (SE). A) Average cell viability data for 3 independent experiments (shown separately B-D) B-D) Independent cell viability experiments, M: recAβ 1-42 monomers, O: recAβ 1-42 oligomers.

6.4 Investigating the role of ER stress in recPrP induced toxicity

The endoplasmic reticulum (ER) is the site within a cell where secreted proteins undergo post-translational modifications and are correctly folded. The process

within a cell of translating proteins and then folding them correctly, so they are functional, is based on a fine balance of protein production and protein degradation. Misfolded proteins in the ER cause the UPR and ERAD systems to be activated. The ERAD pathway translocates misfolded proteins to the cytosol for degradation by the proteasome. The UPR pathway causes the upregulation of chaperones to aid in protein folding. However, certain conditions such as aging or disease can put the ER under stress and cause the amount of incorrectly folded proteins to rise, this can lead to apoptosis through an ER stress related pathway. Additionally, a rise in the concentration of misfolded proteins can put a greater burden on the proteasome and lead to cell death potentially through autophagy. ER stress is thought to be involved in some PMDs, where the misfolded protein assemblies can cause ER stress leading to cellular toxicity and death. In light of this, I wanted to investigate if the recPrP oligomers could be causing ER stress. To investigate the involvement of ER stress in oligomer induced toxicity, I probed for the up-regulation of proteins associated with ER stress and the UPR pathway (figure 6.6).

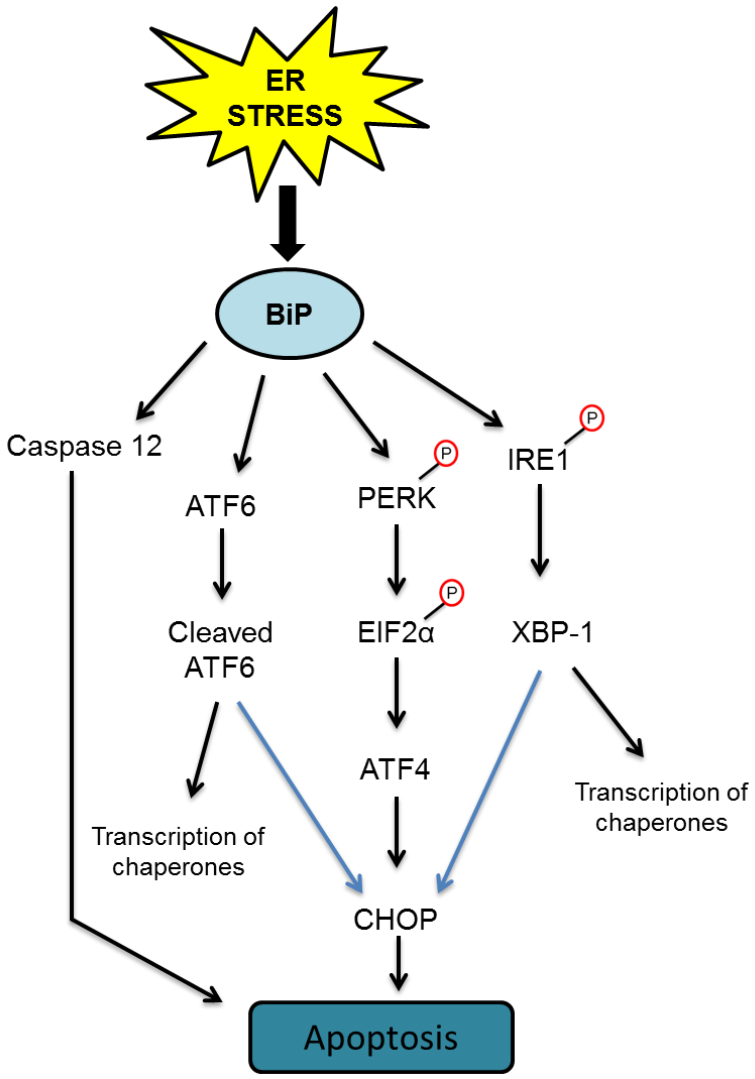

Figure 6.6 ER stress illustration

Illustration showing the unfolded protein response (UPR) pathways downstream of ER stress.

The cells were incubated with the different recPrP isoforms, lysed, and the cell lysates were used for western blotting. Initially I incubated the cells with recPrP for 24 hours prior to lysis, since this was the length of incubation used in all cell viability assays. I first probed for the ER chaperone BiP, which is upstream of the other ER stress related proteins and is produced at the early stages of ER stress(Lee,

2005) (figure 6.6). I found no significant up-regulation of BiP at the 24 hour time point in cells treated with any of the recPrP isoforms (figure 6.7). I also incubated the cells with tunicamycin, which causes ER stress and acted as a positive control. Cells treated with tunicamycin showed an up-regulation in BiP expression. I decided to also probe for the presence of CHOP which is downstream of BiP and promotes apoptosis(Moreno et al., 2013). I found no CHOP expression for cells treated with any of the recPrP isoforms (figure 6.8, lane 11 shows the positive control). Additionally, I tested for the presence of phosphorylated EIF2α. EIF2α, as shown in figure 6.6 is downstream of BiP and upstream of CHOP. During ER stress EIF2α is phosphorylated, so the presence of the phosphorylated form is indicative of ER stress. I probed for the presence of phosphorylated EIF2α and normalised this to total EIF2α expression. I saw no up-regulation of phosphorylated EIF2α in cells treated with any of the recPrP isoforms (figure 6.9). Figure 6.6 depicts the various ER stress related pathways; caspase 12 is shown to be separate from the other UPR pathways and can cause apoptosis independently of CHOP. With this is mind, I decided to probe for the presence of caspase 12 to see if oligomer induced apoptosis could be triggered through this pathway. There was an up-regulation of caspase 12 in oligomer and fibril treated cells, however, this was not significant.

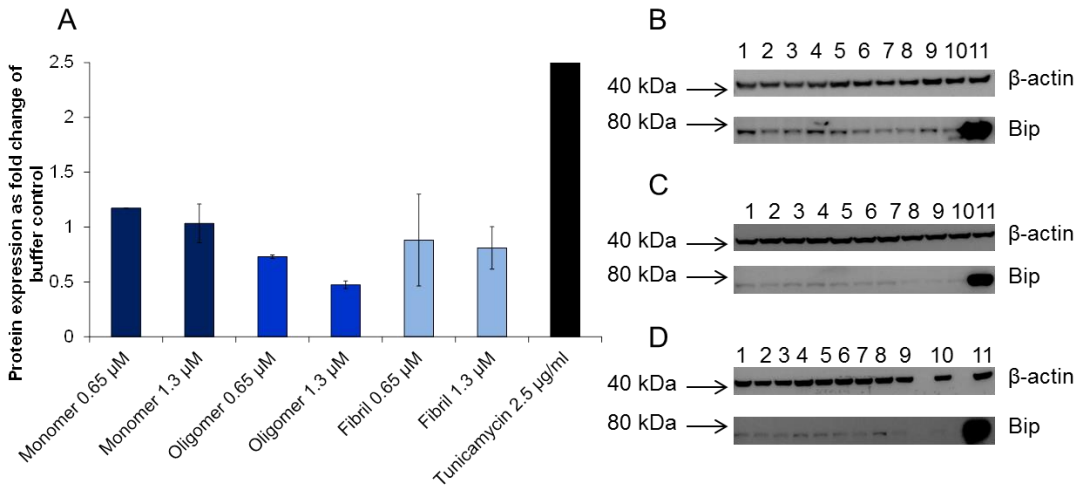

Figure 6.7 ER stress data for BiP after 24 hour incubation with recPrP isoforms

A) Bar chart to show the average BiP western blot data for cells treated with recPrP isoforms for 24 hours (for 2 independent experiments with 2 wells of cells in each experiment), blots were analysed by image J and normalised to the β-actin control. The data is expressed as fold change over the buffer controls (the buffer controls would be 1). B+C western blots are from the same experiment but different wells of cells, D shows an independent experiment (all after 24 hour incubation). B+C) Lane 1: untreated, lane 2: oligomer buffer control, lane 3: monomer and fibril buffer control, lane 4: monomer at 0.65 µM, lane 5: monomer at 1.3 µM, lane 6: α-helical control at 0.65 µM, lane 7: oligomers at 0.65 µM, lane 8: oligomers at 1.3 µM, lane 9: fibrils at 0.65 µM, lane 10: fibrils at 1.3 µM, lane 11: tunicamycin (2.5 µg/ml). D) Lane 1: untreated, lane 2: oligomer buffer control, lane 3: monomer and fibril buffer control, lane 4: monomer at 0.65 µM, lane 5: monomer at 1.3 µM, lane 6: oligomers at 0.65 µM, lane 7: oligomers at 1.3 µM, lane 8: fibrils at 0.65 µM, lane 9: fibrils at 1.3 µM, lane 10: staurosporine (200 nM), lane 11: tunicamycin (2.5 µg/ml).

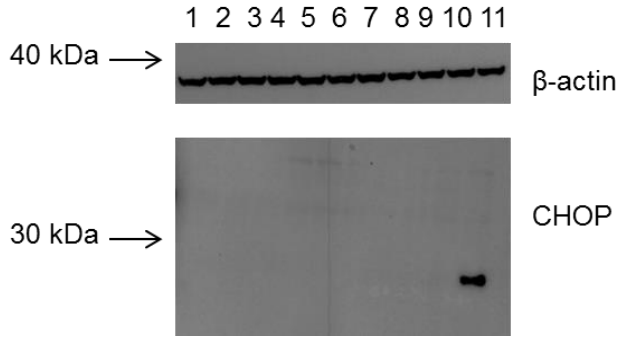

Figure 6.8 ER stress data for CHOP after 24 hour incubation with recPrP isoforms

Western blot from cell lysates after a 24 hour incubation with recPrP isoforms. Lane 1: untreated, lane 2: oligomer buffer control, lane 3: monomer and fibril buffer control, lane 4: monomer at 0.65 µM, lane 5: monomer at 1.3 µM, lane 6: α-helical control at 0.65 µM, lane 7: oligomers at 0.65 µM, lane 8: oligomers at 1.3 µM, lane 9: fibrils at 0.65 µM, lane 10: fibrils at 1.3 µM, lane 11: tunicamycin (2.5 µg/ml). The CHOP band at 27 kDa can be seen in lane 11.

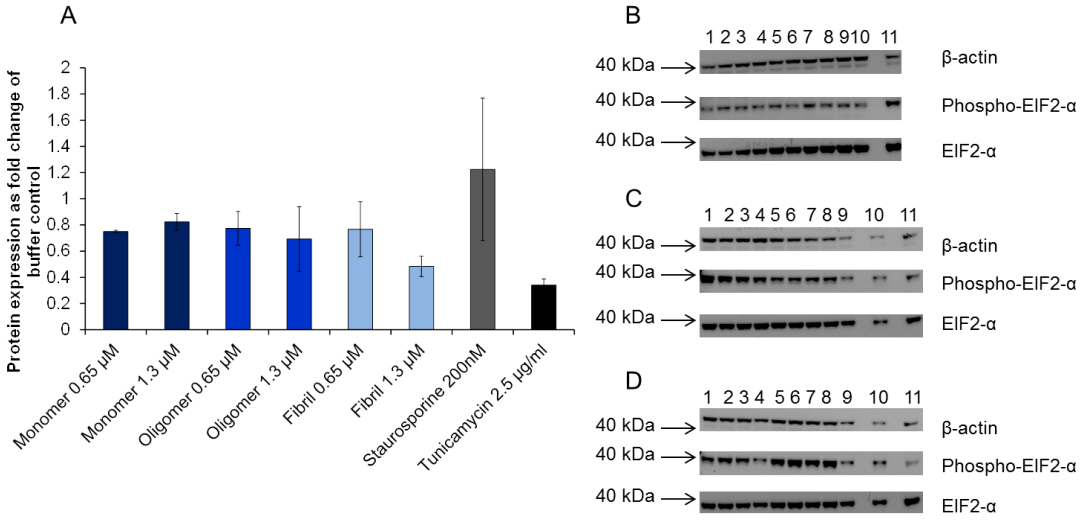

Figure 6.9 ER stress data for phosphorylated EIF2α after 24 hour incubation with recPrP isoforms

A) Bar chart to show the average phosphorylated EIF2α western blot data for cells treated with PrP isoforms for 24 hours (for 2 independent experiments with 2 wells of cells in each experiment), blots were analysed by image J and normalised first to the β-actin control and then phosphorylated EIF2α was normalised to total EIF2α expression. The data is expressed as fold change over the buffer controls (the buffer controls would be 1). C+D show western blots from the same experiment but different wells of cells, B shows an independent experiment (all after 24 hour incubation). B) Lane 1: untreated, lane 2: oligomer buffer control, lane 3: monomer and fibril buffer control, lane 4: monomer at 0.65 µM, lane 5: monomer at 1.3 µM, lane 6: α-helical control at 0.65 µM, lane 7: oligomers at 0.65 µM, lane 8: oligomers at 1.3 µM, lane 9: fibrils at 0.65 µM, lane 10: fibrils at 1.3 µM, lane 11: tunicamycin (2.5 µg/ml). C+D) Lane 1: untreated, lane 2: oligomer buffer control, lane 3: monomer and fibril buffer control, lane 4: monomer at 0.65 µM, lane 5: monomer at 1.3 µM, lane 6: oligomers at 0.65 µM, lane 7: oligomers at 1.3 µM, lane 8: fibrils at 0.65 µM, lane 9: fibrils at 1.3 µM, lane 10: staurosporine (200 nM), lane 11: tunicamycin (2.5 µg/ml).

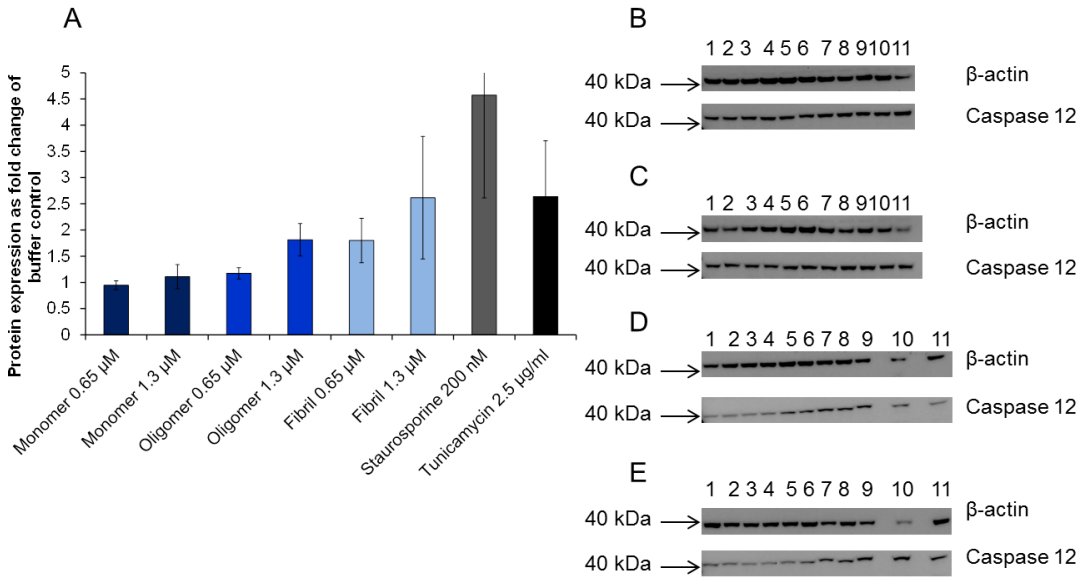

Figure 6.10 ER stress data for caspase 12 after 24 hour incubation with recPrP isoforms

A) Bar chart to show the average caspase 12 western blot data for cells treated with recPrP isoforms for 24 hours (for 2 independent experiments with 2 wells of cells in each experiment), blots were analysed by image J and normalised to the β-actin control. The data is expressed as fold change over the buffer controls (the buffer controls would be 1). B+C show western blots from the same experiment but different wells of cells, D+E show western blots from the same experiment but different wells of cells (all after 24 hour incubation). B+C) Lane 1: untreated, lane 2: oligomer buffer control, lane 3: monomer and fibril buffer control, lane 4: monomer at 0.65 µM, lane 5: monomer at 1.3 µM, lane 6: α-helical control at 0.65 µM, lane 7: oligomers at 0.65 µM, lane 8: oligomers at 1.3 µM, lane 9: fibrils at 0.65 µM, lane 10: fibrils at 1.3 µM, lane 11: staurosporine (200 nM). C+D) Lane 1: untreated, lane 2: oligomer buffer control, lane 3: monomer and fibril buffer control, lane 4: monomer at 0.65 µM, lane 5: monomer at 1.3 µM, lane 6: oligomers at 0.65 µM, lane 7: oligomers at 1.3 µM, lane 8: fibrils at 0.65 µM, lane 9: fibrils at 1.3 µM, lane 10: staurosporine (200 nM), lane 11: tunicamycin (2.5 µg/ml).

I hypothesised that the lack of ER stress related markers at the 24 hour time point could be due to a high proportion of the cells being dead. Therefore, I decided to investigate the expression of ER stress related proteins in the cells after a six hour incubation with the recPrP isoforms. I hypothesised that an earlier time point may show early stages of toxicity and increased expression of ER stress proteins, if ER stress was being induced.

After a six hour incubation, cells treated with the recPrP oligomers did show an up-regulation of BiP above the buffer control (figure 6.11). Although this up-regulation was not significant (t-test, $p = 0.07$). BiP was also not significantly upregulated in cells treated with α-helical recPrP or recPrP fibrils, showing that neither were causing ER stress.

In addition to BiP, I also probed for the presence of CHOP (figure 6.12). After a six hour incubation, no CHOP expression was seen in cells treated with any of the recPrP isoforms (figure 6.12). CHOP can be seen in the tunicamycin treated cells in lane 10 (27 kDa), showing that the CHOP antibody was working. There was some up-regulation of caspase 12 seen at the 24 hour time point in oligomer and fibril treated cells. Therefore, I wanted to see if there was greater caspase 12 expression at an earlier time point when the level of cell death would be lower. However, after a six hour incubation I saw no up-regulation of caspase 12 in any of the recPrP treated cells when compared to the buffer control cells (figure 6.13).

Taken together, it seems that the recPrP oligomers and fibrils are not causing ER stress through an EIF2α/ CHOP related pathway or through the caspase 12 ER stress pathway. The recPrP oligomers must be causing apoptosis independently of ER stress. Further study would be needed to identify other pathways which may be involved.

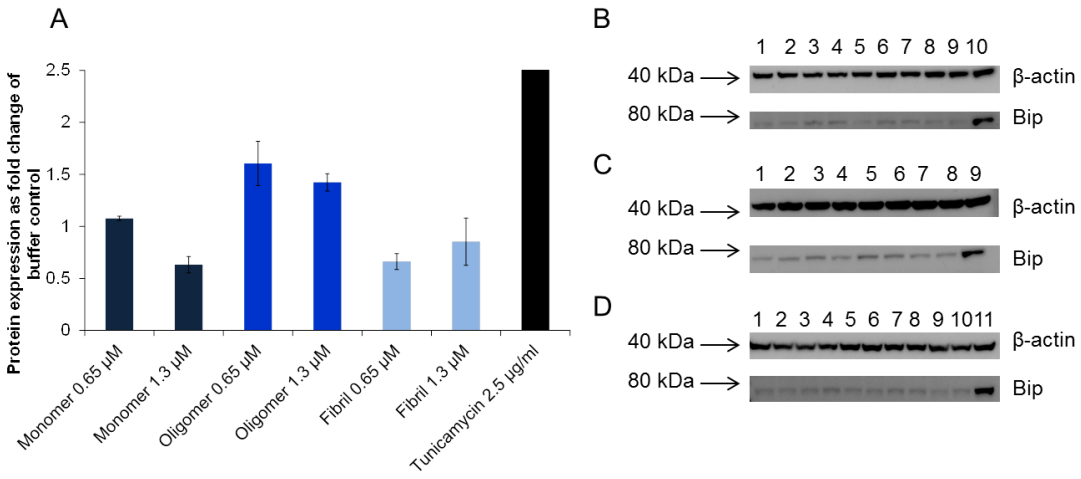

Figure 6.11 ER stress data for BiP after six hour incubation with PrP isoforms

A) Bar chart to show the average BiP western blot data for cells treated with PrP isoforms for six hours (for 2 independent experiments with 2 wells of cells in each experiment), blots were analysed by image J and normalised to the β-actin control. The data is expressed as fold change over the buffer controls (the buffer controls would be 1, t-test showed a p value of 0.07 for oligomers at 0.65 µM compared to the buffer control). B + C western blots are from the same experiment but different wells of cells, D shows an independent experiment (all after 6 hour incubation). B) Lane 1: untreated, lane 2: oligomer buffer control, lane 3: monomer and fibril buffer control, lane 4: monomer at 0.65 µM, lane 5: monomer at 1.3 µM, lane 6: oligomers at 0.65 µM, lane 7: oligomers at 1.3 µM, lane 8: fibrils at 0.65 µM, lane 9: fibrils at 1.3 µM, lane 10: tunicamycin (2.5 µg/ml). C) Lane 1: oligomer buffer control, lane 2: monomer and fibril buffer control, lane 3: monomer at 0.65 µM, lane 4: monomer at 1.3 µM, lane 5: oligomers at 0.65 µM, lane 6: oligomers at 1.3 µM, lane 7: fibrils at 0.65 µM, lane 8: fibrils at 1.3 µM, lane 9: tunicamycin (2.5 µg/ml). D) Lane 1: untreated, lane 2: oligomer buffer control, lane 3: monomer and fibril buffer control, lane 4: monomer at 0.65 µM, lane 5: monomer at 1.3 µM, lane 6: α-helical control at 0.65 µM, lane 7: oligomers at 0.65 µM, lane 8: oligomers at 1.3 µM, lane 9: fibrils at 0.65 µM, lane 10: fibrils at 1.3 µM, lane 11: tunicamycin (2.5 µg/ml).

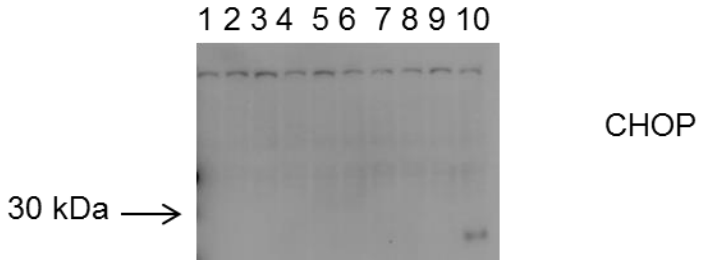

Figure 6.12 ER stress data for CHOP after six hour incubation with recPrP isoforms

Western blot for cell lysates after a six hour incubation with recPrP isoforms. Lane 1: untreated, lane 2: oligomer buffer control, lane 3: monomer and fibril buffer control, lane 4: monomer at 0.65 µM, lane 5: monomer at 1.3 µM, lane 6: oligomers at 0.65 µM, lane 7: oligomers at 1.3 µM, lane 8: fibrils at 0.65 µM, lane 9: fibrils at 1.3 µM, lane 10: tunicamycin (2.5 µg/ml). CHOP can be seen as a faint band at 27 kDa in lane 10.

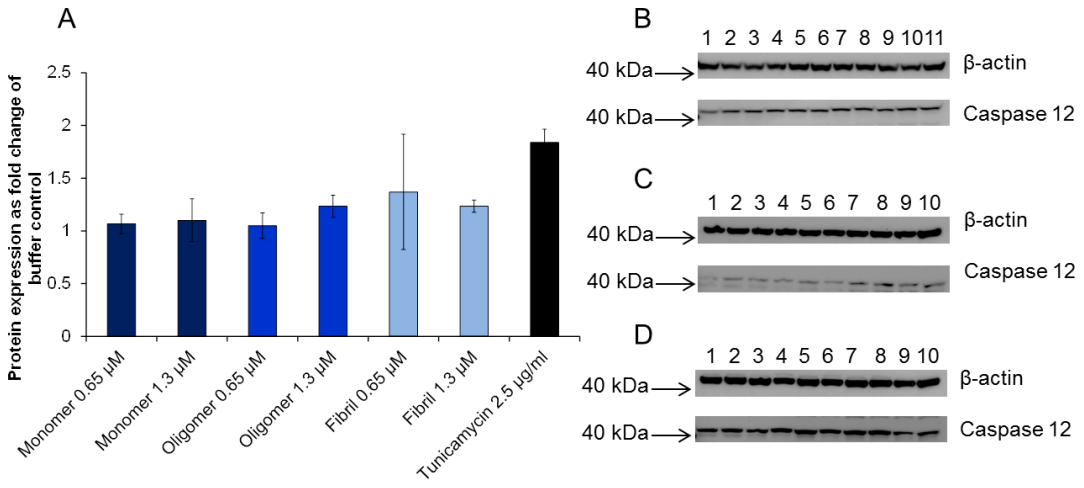

Figure 6.13 ER stress data for caspase 12 after six hour incubation with recPrP isoforms

A) Bar chart to show the average caspase 12 western blot data for cells treated with recPrP isoforms for six hours (for 2 independent experiments with 2 wells of cells in each experiment), blots were analysed by image J and normalised to the β-actin control. The data is expressed as fold change over the buffer controls (the buffer controls would be 1). C+D blots are from the same experiment but different wells of cells, B shows an independent experiment (all after 6 hour incubation). B) Lane 1: untreated, lane 2: oligomer buffer control, lane 3: monomer and fibril buffer control, lane 4: monomer at 0.65 µM, lane 5: monomer at 1.3 µM, lane 6: α-helical control at 0.65 µM, lane 7: oligomers at 0.65 µM, lane 8: oligomers at 1.3 µM, lane 9: fibrils at 0.65 µM, lane 10: fibrils at 1.3 µM, lane 11: tunicamycin (2.5 µg/ml). C+D) Lane 1: untreated, lane 2: oligomer buffer control, lane 3: monomer and fibril buffer control, lane 4: monomer at 0.65 µM, lane 5: monomer at 1.3 µM, lane 6: oligomers at 0.65 µM, lane 7: oligomers at 1.3 µM, lane 8: fibrils at 0.65 µM, lane 9: fibrils at 1.3 µM, lane 10: tunicamycin (2.5 µg/ml).

6.6 Discussion

Methods for studying pathways and mechanisms associated with cell death often involve the use of inhibitors to block specific pathways, or the detection of specific markers associated with a cellular pathway (Oslowski and Urano, 2011, Moreno et al., 2013, Hetz et al., 2003, Léveillé et al., 2010). In this chapter, when investigating the mechanisms associated with recPrP and recAβ induced cell death, I have employed the use of both methods. I have used inhibitors to test for apoptosis and excitotoxicity induced by the misfolded proteins. Additionally, I have detected the presence of activated proteins associated with ER stress. I also probed for the up-regulation of activated caspase 3 to complement the apoptosis inhibitor data. In all of these experiments it was very important to have the correct controls. For the inhibitor experiments a positive control was needed, which was recovered by the inhibitor. Without this, it would be impossible to know whether the inhibitor was effectively blocking the pathway under investigation.

In this chapter, I have investigated potential pathways which may be involved in recPrP or recAβ induced cell death. I found that recPrP oligomers cause apoptosis, which is not mediated through excitotoxic mechanisms or ER stress. I have shown that recPrP oligomers and fibrils activate different pathways and the mechanisms leading to fibril induced cell death are still to be determined. Interestingly, I found that recAβ 1-42 oligomers may also induce apoptosis. However, by contrast, this could be caused by excitotoxicity. These potential differences are intriguing, and may be important when developing therapies which target PMDs.

Previous studies have shown many pathways to be activated in cells treated with misfolded forms of PrP including apoptosis (Simoneau et al., 2007, Novitskaya et al., 2006), excitotoxicity (Muller et al., 1993, Sassoon et al., 2004, Thellung et al., 2013), ER stress(Lindholm et al., 2006, Yoshida, 2007) and autophagy (Wong and Cuervo, 2010, Heiseke et al., 2010). My data show that primary cells treated with recPrP

oligomers were recovered by a caspase inhibitor, indicating apoptotic cell death. By contrast, while recPrP fibrils elicited a strong toxic response from the cells and were shown to cause some up-regulation of activated caspase 3, fibril treated cells were not recovered by a caspase inhibitor. This indicated that the majority of fibril treated cells were not dying by apoptosis. These differences between fibril and oligomer treated cells may have important implications for the pathology of prion diseases, and for targeting certain pathways for therapeutic purposes.

Relatively few papers have demonstrated that misfolded forms of PrP induce excitotoxicity (Muller et al., 1993, Sassoon et al., 2004, Thellung et al., 2013). The recPrP treated cells in this study were not recovered by a NMDA receptor antagonist, demonstrating that neither the oligomers nor fibrils were inducing excitotoxicity. Studies which have found excitotoxicity in PrP treated cells used fragments of PrP (Thellung et al., 2013, Sassoon et al., 2004), which may behave differently to full length PrP. In addition, one study showed excitotoxicity in cells treated with PrP^{Sc} (Muller et al., 1993). PrP^{Sc}, isolated from hamster brain, was incubated with liposomes and it was this PrP^{Sc}/ liposome material that was used to dose the cells (Muller et al., 1993). No structural information for the PrP^{Sc}/ liposome mixture is available, which makes it difficult to determine the toxic species and how this might stimulate excitotoxicity. Taken together, it is unclear from these studies how much of a role excitotoxicity would play *in vivo*. When undertaking *in vitro* experiments, it is important to remember that the conditions are artificial and, therefore, not a direct comparison for prion disease mechanisms *in vivo*. Evidence for excitotoxicity acting as a mechanism of disease in prion diseases, *in vivo*, is tentative (Marandi et al., 2012). Further investigations will be needed to understand whether excitotoxicity does play a role in prion related pathology, as it seems to in other PMDs (Molinuevo et al., 2005, Esposito et al., 2013, Di et al., 2010, Dong et al., 2009, Tabrizi et al., 1999, Chiarlone et al., 2014).

ER stress is associated with many neurodegenerative conditions with misfolded proteins causing the UPR and ERAD systems to be activated (Bukau et al., 2006, Voisine et al., 2010, Lindholm et al., 2006, Yoshida, 2007), leading to apoptosis if balance is not resumed (Bukau et al., 2006, Voisine et al., 2010, Lindholm et al., 2006, Yoshida, 2007). Therefore, I hypothesised that the recPrP oligomers may be causing ER stress which was leading to apoptosis. However, I found no significant up-regulation of ER stress related proteins in cells treated with recPrP oligomers. Therefore, in this *in vitro* system, ER stress was not the mechanism of cell death. For ER stress to be activated by misfolded exogenous protein, such as in this *in vitro* system, the recPrP oligomers would have had to be endocytosed and trafficked to the ER. I found no evidence for this, since no ER stress proteins were up-regulated. This may mean that *in vivo*, extracellular oligomers may also not be endocytosed, however, if oligomers were formed within a cell then this may lead to ER stress. For example, PrP^{CTM} as discussed in chapter 5 could oligomerise within a cell and cause ER stress. Therefore, *in vivo* ER stress could be involved in toxicity and disease pathology.

In chapter 5, I discussed the possibility that the oligomers may be causing cell death by membrane insertion. It has been shown previously that oligomers can insert into phospholipid membranes (Kayed et al., 2004, Demuro et al., 2005), causing membrane disruption and affecting the calcium homeostasis of the cell (Demuro et al., 2005), which can lead to apoptosis. If the recPrP oligomers in this study are causing apoptosis independently of ER stress or excitotoxicity, then it is perhaps plausible that the oligomers may be inducing apoptosis through membrane insertion. Further study would be needed to explore this pathway.

The toxicity of fibrils in prion diseases and also other PMDs has long been debated (Novitskaya et al., 2006, Novitskaya et al., 2007, Simoneau et al., 2007, Kuo et al., 1996, Naslund et al., 2000, McLean et al., 1999, Mucke et al., 2000a, Walsh et al., 2002,

Quist et al., 2005, Kristiansen et al., 2007, Volles et al., 2001, Lue et al., 1999). Whether fibrillar plaques are a non-toxic endpoint or a toxic species important in disease pathology is yet to be proved. The toxicity data for recPrP fibrils has been variable, with some studies showing high levels of toxicity (Novitskaya et al., 2006, Novitskaya et al., 2007) while others show them to cause relatively low levels of toxicity (Simoneau et al., 2007, Kuo et al., 1996, Naslund et al., 2000, McLean et al., 1999, Mucke et al., 2000a, Walsh et al., 2002, Quist et al., 2005, Kristiansen et al., 2007, Volles et al., 2001, Lue et al., 1999). As mentioned in chapter 4, some of the variability in toxicity associated with fibrils may be due to the variable structure of fibrils and amyloid plaques. Additionally, since fibrils are insoluble their availability *in vivo* to cause toxicity to neurons may be substantially less than soluble oligomers. These are important limitations to keep in mind when interpreting *in vitro* data, since *in vivo* only a subset of neurons would be in close proximity with fibrillar plaques. Therefore, other misfolded protein species such as oligomers are likely responsible for cell death seen in the wider population of cells. In this study, I was not able to identify how the fibrils were causing toxicity. Previous studies have shown that autophagy may be involved (Levine and Kroemer, 2008, Martinez-Vicente and Cuervo, 2007, Wong and Cuervo, 2010, Heiseke et al., 2010), since large aggregated proteins cannot pass through the narrow pore of the proteasomal barrel making them good candidates for lysosomal degradation (Levine and Kroemer, 2008). Therefore, the fibrils may be causing cell death by activating lysosomal degradation and autophagy. Further work would be required to explore these pathways and determine their involvement.

Aβ oligomers and their involvement in AD is widely accepted (Haass and Selkoe, 2007, El-Agnaf et al., 2000, Cleary et al., 2005, Texido et al., 2011). Aβ fibrils are thought to be relatively non-toxic (Dahlgren et al., 2002, Ahmed et al., 2010, Lesné et al., 2008) but potentially act as a reservoir of smaller oligomeric forms of Aβ, which can form a halo around the fibrillar plaque (Koffie et al., 2009). Many *in vitro* studies have shown Aβ 1-42 oligomers to be cytotoxic (Manzoni et al., 2011, El-Agnaf et al.,

2000, Texido et al., 2011). Therefore, it is likely that oligomers play an important role in causing neuronal loss during disease. *In vivo* studies have complemented the *in vitro* work and also show an important role for Aβ oligomers in causing toxicity (Walsh et al., 2002, Klyubin et al., 2005, Cleary et al., 2005, Oddo et al., 2006). My data show that recAβ 1-42 oligomers caused a significant level of toxicity in primary cortical cells. Caspase inhibitor and NMDA receptor antagonist experiments showed that this toxicity was likely mediated through excitotoxic induced apoptosis, since the cells showed some recovery with both inhibitors. However, as I have shown in sections 6.2 and 6.3, in one of the inhibitor recovery experiments the recAβ 1-42 oligomers did not cause a significant level of toxicity due to the cells being highly confluent. Therefore, in that one experiment there was not a significant recovery with the inhibitor or receptor antagonist. This meant that the average recovery data was not significant. However, in the other two experiments recovery with both inhibitors was seen. Therefore, the data suggests that both apoptosis and excitotoxicity are likely activated in cells treated with recAβ 1-42 oligomers, but further experiments are needed to confirm this. The mechanism data I have presented for recAβ 1-42 oligomers is substantiated by previous work (Yang et al., 2009, Youssef et al., 2008, Molinuevo et al., 2005, Esposito et al., 2013, Di et al., 2010, Dong et al., 2009, Alberdi et al., 2010). Studies have shown that Aβ 1-42 oligomers induce both apoptosis and excitotoxicity both *in vitro* and *in vivo* (Yang et al., 2009, Youssef et al., 2008, Molinuevo et al., 2005, Esposito et al., 2013, Di et al., 2010, Dong et al., 2009, Alberdi et al., 2010). These previous findings strengthen the validity of my data.

While there are similarities in potential toxic species between PMDs and, therefore, some potential shared mechanisms leading to cell death such as apoptosis, during disease it is likely to be a lot more complicated with multiple pathways and mechanisms being activated. It is likely that toxicity in these diseases is caused by a multitude of toxic misfolded protein species. It is unlikely that oligomers occur as one species, and instead are probably a heterogeneous mixture of isoforms that are

different sizes and have different abilities to induce toxicity. With this in mind, it is plausible that they would stimulate different pathways. In prion disease the majority of oligomers may cause apoptosis by membrane insertion, but in some instances they may cause ER stress (Lindholm et al., 2006, Yoshida, 2007) or autophagy(Levine and Kroemer, 2008, Mizushima et al., 2008, Wong and Cuervo, 2010, Heiseke et al., 2010). Therefore, it is too simplistic to identify one pathway which is causing cell death in PMDs. It is much more likely that an array of pathways are activated and lead to cellular toxicity.

In this study, the oligomers which were formed from recPrP and recAβ likely represent one set of oligomeric isoforms that could potentially form during disease. Therefore, the pathways that I have shown to be activated would correspond to potential pathways that could be important during neurodegeneration. However, due to the *in vitro* conditions in which this study was conducted, it is hard to determine the relevance of these findings for disease. Conclusions which can be drawn are that if oligomers or fibrils were to occur in disease with structures similar to those demonstrated, then they would likely cause cell death by the mechanisms I have presented.

Chapter 7:

Conclusions and future directions

7.1 Conclusions

Protein misfolding diseases (PMDs) are thought to be caused by misfolded, aggregated proteins which accumulate in the brain. These misfolded proteins can exist as small soluble assemblies or large insoluble fibrillar deposits. There is still some debate surrounding whether fibrils are involved in causing toxicity in these diseases(Soto, 2003, Ross and Poirier, 2004, Dobson, 2003, Haass and Selkoe, 2007, Treusch et al., 2009), or whether they may be protective (Haass and Selkoe, 2007, Treusch et al., 2009). However, there is a general consensus that smaller assemblies of misfolded proteins, such as oligomers or protofibrils, are more toxic than fibrils and, consequently, more important in disease (Kuo et al., 1996, Lue et al., 1999, Naslund et al., 2000, McLean et al., 1999, Mucke et al., 2000a, Walsh et al., 2002, Quist et al., 2005, Kristiansen et al., 2007, Simoneau et al., 2007, Volles et al., 2001). Therefore, it is possible there may be a common pathological protein species which underpins multiple PMDs.

Although similarities between PrP and Aβ have been previously demonstrated, their toxicity and mechanisms of their pathogenicity have not previously been compared. PrP^{Sc} is known to spread and replicate by a templating process, converting normal PrP^{C} to PrP^{Sc} (Collinge and Clarke, 2007). It has now been shown that Aβ behaves in a similar manner during disease (Jucker and Walker, 2011). Aβ injected into the brains of transgenic APP mice, which overexpress the amyloid precursor protein, spreads to other axonally connected areas of the brain in a manner reminiscent of PrP^{Sc} (Jucker and Walker, 2011, Walker et al., 2002). Interestingly, it has also been shown that intraperitoneal (IP) injection of Aβ can cause Aβ pathology in the brains of transgenic mice after a prolonged incubation (Eisele et al., 2010). This is very similar to how PrP^{Sc} behaves after peripheral inoculation, through IP, subcutaneous, or intravenous injection (Eklund et al., 1967, Kimberlin and Walker, 1979). Additionally, oligomers of the two proteins are thought be important in causing toxicity during disease. Therefore, this led to the

hypothesis that these two proteins may be eliciting cell death by the same mechanisms.

In this thesis I have demonstrated the production of two disease associated proteins and their subsequent misfolding into disease associated conformations. These misfolded isoforms were extensively characterised before toxicity experiments were carried out using primary cortical cells. The toxicity of the different misfolded protein species were robustly analysed and compared. The mechanisms underlying the toxicity caused by these misfolded proteins were then investigated. Additionally, I have shown that the oxidative state of recPrP, whether it has an intact disulphide bond, is crucially important in determining the size of oligomers which will form and how this impacts on toxicity. This work has built upon the existing body of research which has investigated the molecular mechanisms underlying PMDs.

Previous studies that have sought to investigate the mechanisms underlying PMDs have often analysed the toxicity and associated mechanisms of partially-uncharacterised misfolded proteins (Alberdi et al., 2010, El-Agnaf et al., 2000, Li et al., 2011, Rammes et al., 2011, Muller et al., 1993). This has made it difficult to link specific protein species with toxicity and define the mechanisms which lead to cell death in these diseases. To address these limitations, I have produced misfolded protein species for both recPrP and recAβ and extensively characterised them prior to any toxicity experiments. By producing well characterised misfolded protein species, it is possible to have confidence in the resulting experimental data and this allows us to directly correlate specific protein species with toxicity.

I have shown that while oligomers of recPrP and recAβ are both toxic to murine cortical cells, there are distinct differences in the toxicity of the fibrils composed of each protein. The data in chapter 4 shows that recPrP fibrils are not only significantly more toxic than recPrP oligomers, they are also significantly more toxic

than all of the recAβ isoforms. By contrast, the recAβ fibrils do not cause significant toxicity to the cells. These differences may be due to the structure of the fibrils formed *in vitro*, the differences in toxicity caused by these fibrils could be an artefact of the fact they were formed in the laboratory under artificial conditions. However, I do not believe this is the case, since the fibrils I have formed *in vitro* have properties similar to those found in disease. These include an amyloid structure as shown by Congo red staining, resistance to PK digestion and they bind to thioflavin T. Therefore, the differences in toxicity may instead indicate that PrP fibrils are toxic and important in the pathology of prion disease. The size distribution of PrP fibrils *in vivo* is not well studied, making it difficult to compare to the proteins produced *in vitro*, but it is thought that PrP^{Sc} exists as a heterogeneous mixture of sizes (Silveira et al., 2005, Prusiner et al., 1983). These likely range from hundreds to thousands of PrP molecules (Silveira et al., 2005, Prusiner et al., 1983). The toxicity I have shown for the recAβ fibrils fits with the general consensus that fibrils are not toxic and may be protective; sequestering small toxic oligomers into a less toxic form. The size of Aβ fibrils in disease are not well defined, but seem to be very heterogeneous and vary from small protofibrils up to large plaques ranging in size from 100- 1500 μm^2 (Hyman et al., 1995).

Furthermore, at higher concentrations, the recPrP oligomers are significantly more toxic than the recAβ oligomers. If this were the case *in vivo*, then it is possible that these differences in toxicity may impact on how quickly neurons are killed and, therefore, how quickly the disease progresses. It is possible that this could explain why prion diseases have a much shorter clinical phase than AD. These data suggest that there may be significant differences in which protein species are important in different PMDs.

Previous studies have highlighted a variety of pathways and mechanisms which may be activated by misfolded proteins (Elmore, 2007, Lindholm et al., 2006, Martinez-Vicente and Cuervo, 2007, Youssef et al., 2008). However, in many of these

studies the misfolded proteins were not characterised prior to investigating toxicity and associated mechanisms (Elmore, 2007, Lindholm et al., 2006, Martinez-Vicente and Cuervo, 2007, Youssef et al., 2008). Therefore, it is difficult to interpret the resulting data and to correlate specific protein species with particular mechanisms of toxicity. In this study, I sought to address many of these issues by producing and characterising misfolded forms of recPrP and recAβ before investigating their toxicity and associated mechanisms. Previous studies have indicated many pathways that may be involved in cell death associated with misfolded proteins including apoptosis, excitotoxicity, ER stress, autophagy and oxidative stress (Elmore, 2007, Hickey and Chesselet, 2003, Shimohama, 2000, Rohn, 2010, Jesionek-Kupnicka et al., 1997, Dong et al., 2009, Li et al., 2009, Alberdi et al., 2010, Li et al., 2011, Rammes et al., 2011, Rönicke et al., 2011, Lindholm et al., 2006, Yoshida, 2007, Mizushima et al., 2008, Martinez-Vicente and Cuervo, 2007, Nakamura and Lipton, 2010, Youssef et al., 2008). My data indicates that recPrP oligomers cause apoptosis and recAβ oligomers may cause apoptosis but more repeats are needed to confirm this. These findings are supported by many studies that have shown apoptosis to be important in these diseases (Elmore, 2007, Hickey and Chesselet, 2003, Shimohama, 2000, Rohn, 2010, Jesionek-Kupnicka et al., 1997, Youssef et al., 2008, Yang et al., 2009, Novitskaya et al., 2006, Simoneau et al., 2007). However, the data in chapter 6 indicates that recPrP oligomers are not inducing apoptosis through an excitotoxic pathway, therefore, they must be causing apoptosis through an independent and, as yet, undefined pathway. The recAβ oligomer data suggested that the oligomers may be causing excitotoxicity but, like the apoptosis data, more repeats are needed to confirm this. If this was found to be the case, then this would suggest that recPrP and recAβ oligomers potentially activate different pathways. These findings may further highlight that recAβ and recPrP oligomers have different structures, which not only confer different abilities to cause toxicity but also potentially affect how they interact with the cells, activating different pathways. These differences may be fundamental to understanding the pathogenesis of PMDs, and how assemblies of different proteins may cause toxicity by activating different mechanisms.

At the highest concentration tested, recPrP oligomers were found to be significantly more toxic than recAβ oligomers this may be due to differences in the structure of these protein assemblies. However, as I demonstrated in chapter 5, there is considerable variation in the structure and size of oligomers which can form from recPrP. These differences were shown to be caused by the presence or absence of the disulphide bond, with disulphide-reduced recPrP forming larger oligomers than those formed from oxidised recPrP (with an intact disulphide bond). The disulphide-reduced recPrP oligomers were also significantly more toxic than oligomers formed from oxidised recPrP. It is possible that other post-translational modifications could also affect the structure and toxicity of recPrP oligomers. This adds another layer of complexity, since it means that during disease the oligomers formed from PrP may vary considerably in their structure and toxicity.

Aβ fibrillises more readily than PrP, therefore, Aβ oligomers may be more transient than PrP oligomers. However, Aβ does vary in its length, according to where the γ-secretase complex cleaves the APP, which affects its readiness to fibrillise. I found that recAβ 1-40 oligomers were not toxic; only the recAβ 1-42 oligomers elicited a toxic response from the cells. The ratio of the different forms of Aβ varies in the brain, with Aβ 1-42 found at lower concentrations than Aβ 1-40, although it is often upregulated in LOAD and in certain types of FAD (Thinakaran and Koo, 2008, Hansson et al., 2007). The lower concentration of the toxic Aβ 1-42 form may impact on how long it takes for harmful oligomers to cause cell death and may suggest why AD has such a long clinical phase.

As previously suggested, the extreme toxic effect of the recPrP fibrils may be due to the structure of the fibrils formed from this method (Breydo et al., 2008), or it may be that fibrils formed from different proteins may have different abilities to cause toxicity. However, whilst in some cases fibrils may be toxic, the large insoluble plaques seen in many PMDs are insoluble and, therefore, not able to diffuse throughout the brain in the same way as oligomers or soluble protofibrils. This

would mean that only cells within the vicinity of a fibrillar plaque would likely be damaged. In AD it has been suggested that fibrils can act as a reservoir of small soluble oligomers and that oligomers can form a halo around a plaque (Koffie et al., 2009). This would likely be more of a chronic effect caused by fibrils which would not be detected during a 24 hour incubation period with the cells. Further experiments with longer incubation periods, which could assess more chronic damage, may be useful in investigating this. Therefore, while I have demonstrated that recPrP fibrils elicit a very strong toxic response *in vitro*, it is still difficult to determine how important fibrils are in causing cell death in disease.

In this study, I have sought to investigate how the structure and conformation of the PrP and Aβ proteins are related to toxicity, and the subsequent mechanisms that lead to cell death. To do this an *in vitro* approach was needed, since this allows controlled misfolding and extensive characterisation of the proteins. Toxicity can then be tested in a controlled manner eliminating many other variables, which allows direct links to be made between protein conformation and toxicity. However, while an *in vitro* approach allows these direct links to be made between conformation and toxicity, there are several limitations to this type of experimental approach.

Firstly, producing proteins recombinantly in bacteria has limitations which may affect the ability to extrapolate results to native proteins. Proteins which are produced in bacteria may not have the same post-translational modifications as those produced natively in mammalian cells, for example, recPrP lacks the N-terminal signal peptide which is present in native PrP (murine recPrP starts at residue 23 leaving out the signal peptide residues). This signal peptide is necessary for the translocation of the protein into the ER prior to secretion into the cellular membrane, therefore, this effect may not impact my study since I did not address the cellular processing of PrP. However, as discussed in chapter 5, it is possible that PrP may misfold spontaneously before entering the ER, preventing the signal

peptide from being cleaved. In this case, the conformation of the resultant oligomers or fibrils could be affected by the presence of the signal peptide. Therefore, the conformation of oligomers and fibrils produced from recombinant PrP may not be the same as those containing the signal peptide.

Furthermore, there are limitations to testing the toxicity of proteins by incubating cells with exogenously added conformations. The main criticism of this type of study is that it is not representative of real physiological conditions or that there may be some kind of toxic response caused by adding any exogenous protein to cells. While these points are valid, it is possible to try and control for some of these variables by using control proteins such as α- helical recPrP. If the control protein causes no toxicity at the same concentration as the misfolded proteins, then the toxicity seen in the cells treated with misfolded proteins is likely conformation specific. This type of study will never be as physiologically relevant as an *in vivo* study, however, by using primary cells the biological model is as close to cells *in vivo* as possible.

Other approaches such as transfecting mammalian cells with plasmids encoding specific protein fragments, which are more likely to form oligomers or fibrils, may be useful. Toxicity can then be monitored in the transfected cells. However, this also has limitations since it is difficult to control the amount of misfolded protein produced in the cells, or how this is processed or degraded. It would also be difficult to analyse the conformation of the proteins which were produced in the cells, making it harder to directly link conformation with toxicity.

Using animal models is another valuable approach. Transgenic animals which overexpress a protein, or animals which are injected with misfolded protein such as PrP^{Sc}, can be used to investigate neurodegeneration and various aspects of the disease process. However, as I have mentioned in previous chapters, *in vivo* animal experiments make it very difficult to directly link protein conformation and toxicity.

Studies using animal models can cull the animals at set time points (pre-symptomatic, symptomatic etc.) and then analyse pathology, protein deposition etc. however, if pathological changes have already occurred it is hard to define which protein species may be important in causing toxicity.

Natural disease models also have advantages and disadvantages, patients with PMDs or animals with natural scrapie, BSE etc. present an opportunity to study the disease process is in its most natural form. However, even with more advanced imaging techniques, which are now available, tissue from patients is not available until post-mortem. This means that the disease has already run its course, and makes it impossible to understand the disease mechanisms which occurred prior to cell death. There are still limitations even with animals with naturally occurring disease. While the animal can be culled and tissues taken as soon as symptoms are observed, it may still be too late to investigate how misfolded protein species are causing cell death since once the onset of symptoms has occurred, cellular toxicity and pathological changes in the brain have already started to happen.

In light of this, it is likely that both *in vivo* and *in vitro* studies will be needed to fully elucidate the disease processes in PMDs. *In vivo* studies are needed to investigate the more complex chronic effects of neurodegeneration caused by the presence misfolded proteins, whilst *in vitro* studies allow us to directly investigate the toxicity of certain protein conformations. If the data from both types of studies are combined, then this will give us a better understanding of these diseases.

There are limitations to all of these experimental approaches. In this study, I set out to try and understand how the conformation of a misfolded protein can affect toxicity and to try and compare the toxicity of different disease associated proteins. Therefore, I think the *in vitro* model which I have used, whilst it has limitations, was the most appropriate approach for the questions I wanted to investigate.

7.2 Possible future directions

The are many areas of this thesis which could be developed and explored further, to possibly lead to a more complete picture of the mechanisms underlying neurodegeneration in AD and prion disease. Potential areas to investigate further would include:

Further investigations of how the recPrP oligomers are causing apoptosis, since they were shown to cause apoptosis by a pathway independent of ER stress and excitotoxicity. A potential candidate could be membrane insertion. Further experiments could include fluorescently tagging the recPrP oligomers and investigating how the oligomers interact with the cells by confocal microscopy. This may show whether the oligomers are inserting into the cell membrane. Furthermore, experiments could be carried out to investigate whether the membrane potential of the cells is affected by the oligomers.

Whilst my data suggest that recAβ oligomers are causing both apoptosis and excitotoxicity, more repeats are needed in order to confirm this observation. Further repeats are needed for both the caspase inhibitor and NMDA receptor antagonist experiments, in order to see if the recovery of cells treated with recAβ oligomers and the inhibitors is significant. If the caspase inhibitor and NMDA receptor antagonist data was confirmed for the recAβ oligomers, then it would be interesting to explore these pathways further. How the oligomers are interacting with the cells and causing excitotoxicity could be investigated. Firstly it would be important to understand if the recAβ oligomers are endocytosed. If they are taken up by the cell then it would be interesting to see how this may be mediated. Furthermore, it would be important to understand if the recAβ oligomers cause excitotoxicity directly by interacting with the NMDA receptors or if they instigate a cascade which indirectly causes excitotoxicity.

The recAβ fibrils did not cause toxicity to the cells over a 24 hour incubation period. It would be interesting to investigate more chronic effects which the fibrils may cause by incubating the fibrils with the cells for longer incubation periods. Previous studies have demonstrated that Aβ fibrils can be a reservoir for Aβ oligomers suggesting that the fibrils might cause toxicity if the incubation time was longer.

Further investigations could be carried out to look at how the recAβ monomer fibrillises in the cell culture media. I demonstrated in chapter 4 that the recAβ monomer fibrillises in a concentration and time dependent manner in cell culture media. It would be valuable to understand the process that the recAβ monomer goes through to become a fibril. Different time points could be taken during the 24 hour period in which the fibrillisation takes place and experiments could be done to assess the size of the assemblies which have formed. This could be done using DLS and native gels. This may help us understand the process of plaque formation in AD and how smaller assemblies which are more toxic can form.

Additionally, it would be important to try and elucidate how the recPrP fibrils are causing toxicity. Pathways which may potentially be involved include autophagy and oxidative stress. To fully understand the importance of the different misfolded PrP species in disease, it would be important to reveal how the fibrils cause toxicity.

Furthermore, it would be interesting to try and determine the physiological relevance of the data I have presented. One approach would be to purify PrP^{Sc} oligomers and fibrils from infected tissue, and test their toxicity using the same primary cell culture model I have used in this study. This would identify what the toxic species of PrP^{Sc} are, and show if they are the same as for misfolded recPrP.

The work I have presented concerning the importance of the disulphide bond in oligomerisation and toxicity could be developed further. Transgenic mice could be engineered, which have PrP with no disulphide bond (one of the cysteine residues

could be mutated to a methionine). The mice could then be analysed for any build-up of oligomeric protein, reduction in lifespan and potentially the development of any neurological disease.

In this study, I have investigated the toxicity and associated mechanisms of misfolded forms of recPrP and recAβ. It would be interesting to explore this further with other disease associated proteins such as α-synuclein, associated with Parkinson's, or huntingtin, associated with Huntington's disease. This would provide a more comprehensive picture of whether there are common toxic species between PMDs and if they activate the same pathways.

In conclusion, I have shown that both recPrP and recAβ oligomers cause toxicity but potentially by activating independent pathways. Additionally, I have demonstrated differences in the toxicity of fibrils formed from recPrP and recAβ. I have also shown that the presence or absence of the disulphide-bond in recPrP is critically important in determining the size of oligomers which will form and their toxicity. This demonstrates how important post-translational modifications can be in modifying the misfolding of a protein and how this may have important implications during disease. The differences I have presented between these two important disease associated proteins may indicate that the molecular mechanisms that underlie PMDs are not as similar as was thought.

References

Aguzzi, A. & Falsig, J. 2012. Prion propagation, toxicity and degradation. *Nat Neurosci,* 15**,** 936-939.

Aguzzi, A., Heikenwalder, M. & Polymenidou, M. 2007. Mechanisms of disease - Insights into prion strains and neurotoxicity. *Nature Reviews Molecular Cell Biology,* 8**,** 552-561.

Ahmed, M., Davis, J., Aucoin, D., Sato, T., Ahuja, S., Aimoto, S., Elliott, J. I., Van Nostrand, W. E. & Smith, S. O. 2010. Structural conversion of neurotoxic amyloid-[beta]1-42 oligomers to fibrils. *Nat Struct Mol Biol,* 17**,** 561-567.

Aizenstein, H. J., Nebes, R. D., Saxton, J. A., Price, J. C., Mathis, C. A., Tsopelas, N. D., Ziolko, S. K., James, J. A., Snitz, B. E., Houck, P. R., Bi, W., Cohen, A. D., Lopresti, B. J., DeKosky, S. T., Halligan, E. M. & Klunk, W. E. 2008. Frequent amyloid deposition without significant cognitive impairment among the elderly. *Arch Neurol,* 65**,** 1509-17.

Alberdi, E., Sánchez-Gómez, M. V., Cavaliere, F., Pérez-Samartín, A., Zugaza, J. L., Trullas, R., Domercq, M. & Matute, C. 2010. Amyloid β oligomers induce Ca2+ dysregulation and neuronal death through activation of ionotropic glutamate receptors. *Cell Calcium,* 47**,** 264-272.

Allan Butterfield, D. 2002. Amyloid β-peptide (1-42)-induced Oxidative Stress and Neurotoxicity: Implications for Neurodegeneration in Alzheimer's Disease Brain. A Review. *Free Radical Research,* 36**,** 1307-1313.

Alper, T., Cramp, W. A., Haig, D. A. & Clarke, M. C. 1967. DOES AGENT OF SCRAPIE REPLICATE WITHOUT NUCLEIC ACID. *Nature,* 214**,** 764-&.

Alvarez-Martinez, M. T., Fontes, P., Zomosa-Signoret, V., Arnaud, J. D., Hingant, E., Pujo-Menjouet, L. & Liautard, J. P. 2011. Dynamics of polymerization shed light on the mechanisms that lead to multiple amyloid structures of the prion protein. *Biochim Biophys Acta,* 1814**,** 1305-17.

Alzheimer, A. 1907. Uber eine eigenartige Erkrankung der Hirnrinde. *Allgemeine Zeitschrife Psychiatrie,* 64**,** 146-148.

Alzheimer, A. 1911. über eigenartige Krankheitsfälle des späteren Alters. *Zeitschrift für die gesamte Neurologie und Psychiatrie,* 4**,** 356-385.

Arakawa, T., Tsumoto, K., Kita, Y., Chang, B. & Ejima, D. 2007. Biotechnology applications of amino acids in protein purification and formulations. *Amino Acids,* 33**,** 587-605.

Aronoff-Spencer, E., Burns, C. S., Avdievich, N. I., Gerfen, G. J., Peisach, J., Antholine, W. E., Ball, H. L., Cohen, F. E., Prusiner, S. B. & Millhauser, G. L. 2000. Identification of the Cu2+ Binding Sites in the N-Terminal Domain of the Prion Protein by EPR and CD Spectroscopy†. *Biochemistry,* 39**,** 13760-13771.

Baeten, L. A., Powers, B. E., Jewell, J. E., Spraker, T. R. & Miller, M. W. 2007. A Natural Case of Chronic Wasting Disease in a Free-ranging Moose (Alces alces shirasi). *Journal of Wildlife Diseases,* 43**,** 309-314.

Barghorn, S., Nimmrich, V., Striebinger, A., Krantz, C., Keller, P., Janson, B., Bahr, M., Schmidt, M., Bitner, R. S., Harlan, J., Barlow, E., Ebert, U. & Hillen, H. 2005. Globular amyloid β-peptide1−42 oligomer − a homogenous and stable neuropathological protein in Alzheimer's disease. *Journal of Neurochemistry,* 95**,** 834-847.

Barnes, D. E. & Yaffe, K. 2011. The projected effect of risk factor reduction on Alzheimer's disease prevalence. *The Lancet Neurology,* 10**,** 819-828.

Baskakov, I. V. & Bocharova, O. V. 2005. In vitro conversion of mammalian prion protein into amyloid fibrils displays unusual features. *Biochemistry,* 44**,** 2339-2348.

Baskakov, I. V., Legname, G., Baldwin, M. A., Prusiner, S. B. & Cohen, F. E. 2002. Pathway Complexity of Prion Protein Assembly into Amyloid. *Journal of Biological Chemistry,* 277**,** 21140-21148.

Baylis, M., Chihota, C., Stevenson, E., Goldmann, W., Smith, A., Sivam, K., Tongue, S. & Gravenor, M. B. 2004. Risk of scrapie in British sheep of different prion protein genotype. *Journal of General Virology,* 85**,** 2735-2740.

Belay, E. D., Blase, J., Sehulster, L. M., Maddox, R. A. & Schonberger, L. B. 2013. Management of Neurosurgical Instruments and Patients Exposed to Creutzfeldt-Jakob Disease. *Infection Control & Hospital Epidemiology,* 34**,** 1272-1280

M3 - 10.1086/673986.

Beranger, F., Mange, A., Goud, B. & Lehmann, S. 2002. Stimulation of PrPC retrograde transport toward the endoplasmic reticulum increases accumulation of PrPSc in prion-infected cells. *Journal of Biological Chemistry,* 277**,** 38972-38977.

Bhimani, R. 2014. Understanding the Burden on Caregivers of People with Parkinson's: A Scoping Review of the Literature. *Rehabil Res Pract,* 2014**,** 718527.

Bitan, G., Kirkitadze, M. D., Lomakin, A., Vollers, S. S., Benedek, G. B. & Teplow, D. B. 2003. Amyloid β-protein (Aβ) assembly: Aβ40 and Aβ42 oligomerize through distinct pathways. *Proceedings of the National Academy of Sciences,* 100**,** 330-335.

Bocharova, O. V., Breydo, L., Parfenov, A. S., Salnikov, V. V. & Baskakov, I. V. 2005. In vitro conversion of full-length mammalian prion protein produces amyloid form with physical properties of PrPSc. *Journal of Molecular Biology,* 346**,** 645-659.

.

Borchelt, D. R., Thinakaran, G., Eckman, C. B., Lee, M. K., Davenport, F., Ratovitsky, T., Prada, C.-M., Kim, G., Seekins, S., Yager, D., Slunt, H. H., Wang, R., Seeger, M., Levey, A. I., Gandy, S. E., Copeland, N. G., Jenkins, N. A., Price, D. L., Younkin, S. G. & Sisodia, S. S. 1996. Familial Alzheimer's Disease–Linked Presenilin 1 Variants Elevate Aβ1–42/1–40 Ratio In Vitro and In Vivo. *Neuron,* 17**,** 1005-1013.

Bousset, L., Pieri, L., Ruiz-Arlandis, G., Gath, J., Jensen, P. H., Habenstein, B., Madiona, K., Olieric, V., Böckmann, A., Meier, B. H. & Melki, R. 2013. Structural and functional characterization of two alpha-synuclein strains. *Nat Commun,* 4.

Braak, H. & Braak, E. 1991. NEUROPATHOLOGICAL STAGING OF ALZHEIMER-RELATED CHANGES. *Acta Neuropathologica,* 82**,** 239-259.

Braak, H., Del Tredici, K., Rub, U., de Vos, R. A. I., Steur, E. & Braak, E. 2003. Staging of brain pathology related to sporadic Parkinson's disease. *Neurobiology of Aging,* 24**,** 197-211.

Bradley, R. 1991. Bovine spongiform encephalopathy (BSE): The current situation and research. *European Journal of Epidemiology,* 7**,** 532-544.

Bremer, J., Baumann, F., Tiberi, C., Wessig, C., Fischer, H., Schwarz, P., Steele, A. D., Toyka, K. V., Nave, K.-A., Weis, J. & Aguzzi, A. 2010. Axonal prion protein is required for peripheral myelin maintenance. *Nat Neurosci,* 13**,** 310-318.

Brentnall, M., Rodriguez-Menocal, L., De Guevara, R. L., Cepero, E. & Boise, L. H. 2013. Caspase-9, caspase-3 and caspase-7 have distinct roles during intrinsic apoptosis. *BMC Cell Biol,* 14**,** 32.

Breydo, L., Makarava, N. & Baskakov, I. V. 2008. Methods for conversion of prion protein into amyloid fibrils. *Methods in Molecular Biology***,** 105-115.

Brotherston, J. G., Renwick, C. C., Stamp, J. T., Zlotnik, I. & Pattison, I. H. 1968. Spread of scrapie by contact to goats and sheep. *Journal of Comparative Pathology,* 78**,** 9-17.

Brown, D. R., Herms, J. W., Schmidt, B. & Kretzschmar, H. A. 1997. PrP and β-Amyloid Fragments Activate Different Neurotoxic Mechanisms in Cultured Mouse Cells. *European Journal of Neuroscience,* 9**,** 1162-1169.

Brown, D. R., Schmidt, B. & Kretzschmar, H. A. 1996. Role of microglia and host prion protein in neurotoxicity of a prion protein fragment. *Nature,* 380**,** 345-347.

Brown, P., Preece, M., Brandel, J. P., Sato, T., McShane, L., Zerr, I., Fletcher, A., Will, R. G., Pocchiari, M., Cashman, N. R., d'Aignaux, J. H., Cervenáková, L., Fradkin, J., Schonberger, L. B. & Collins, S. J. 2000. Iatrogenic Creutzfeldt–Jakob disease at the millennium. *Neurology,* 55**,** 1075-1081.

Bruce, M. E. 2003. TSE strain variation: An investigation into prion disease diversity. *British Medical Bulletin,* 66**,** 99-108.

Bucciantini, M., Giannoni, E., Chiti, F., Baroni, F., Formigli, L., Zurdo, J., Taddei, N., Ramponi, G., Dobson, C. M. & Stefani, M. 2002. Inherent toxicity of aggregates implies a common mechanism for protein misfolding diseases. *Nature,* 416**,** 507-11.

Bueler, H., Aguzzi, A., Sailer, A., Greiner, R. A., Autenried, P., Aguet, M. & Weissmann, C. 1993. MICE DEVOID OF PRP ARE RESISTANT TO SCRAPIE. *Cell,* 73**,** 1339-1347.

Bukau, B., Weissman, J. & Horwich, A. 2006. Molecular Chaperones and Protein Quality Control. *Cell,* 125**,** 443-451.

Burdall, S. E., Hanby, A. M., Lansdown, M. R. & Speirs, V. 2003. Breast cancer cell lines: friend or foe? *Breast Cancer Res,* 5**,** 89-95.

Burns, C. S., Aronoff-Spencer, E., Legname, G., Prusiner, S. B., Antholine, W. E., Gerfen, G. J., Peisach, J. & Millhauser, G. L. 2003. Copper Coordination in the Full-Length, Recombinant Prion Protein. *Biochemistry,* 42**,** 6794-6803.

Caetano, F. A., Lopes, M. H., Hajj, G. N. M., Machado, C. F., Pinto Arantes, C., Magalhães, A. C., Vieira, M. D. P. B., Américo, T. A., Massensini, A. R., Priola, S. A., Vorberg, I., Gomez, M. V., Linden, R., Prado, V. F., Martins, V. R. & Prado, M. A. M. 2008. Endocytosis of Prion Protein Is Required for ERK1/2 Signaling Induced by Stress-Inducible Protein 1. *The Journal of Neuroscience,* 28**,** 6691-6702.

Carrasquillo, M. M., Belbin, O., Hunter, T. A., Ma, L., Bisceglio, G. D., Zou, F., Crook, J. E., Pankratz, V. S., Dickson, D. W., Graff-Radford, N. R., Petersen, R. C., Morgan, K. & Younkin, S. G. 2010. Replication of CLU, CR1, and PICALM Associations With Alzheimer Disease. *Archives of Neurology,* 67**,** 961-964.

Carrotta, R., Di Carlo, M., Manno, M., Montana, G., Picone, P., Romancino, D. & San Biagio, P. L. 2006. Toxicity of recombinant beta-amyloid prefibrillar oligomers on the morphogenesis of the sea urchin Paracentrotus lividus. *Faseb Journal,* 20**,** 1916-+.

Caserta, T. M., Smith, A. N., Gultice, A. D., Reedy, M. A. & Brown, T. L. 2003. Q-VD-OPh, a broad spectrum caspase inhibitor with potent antiapoptotic properties. *Apoptosis,* 8**,** 345-52.

Caughey, B. & Lansbury, P. T. 2003. Protofibrils, pores, fibrils, and neurodegeneration: Separating the responsible protein aggregates from the innocent bystanders. *Annual Review of Neuroscience,* 26**,** 267-298.

Chabry, J., Ratsimanohatra, C., Sponne, I., Elena, P.-P., Vincent, J.-P. & Pillot, T. 2003. In Vivo and In Vitro Neurotoxicity of the Human Prion Protein (PrP) Fragment P118–135 Independently of PrP Expression. *The Journal of Neuroscience,* 23**,** 462-469.

Chandler, R. L. 1961. ENCEPHALOPATHY IN MICE PRODUCED BY INOCULATION WITH SCRAPIE BRAIN MATERIAL. *The Lancet,* 277**,** 1378-1379.

Chesebro, B., Trifilo, M., Race, R., Meade-White, K., Teng, C., LaCasse, R., Raymond, L., Favara, C., Baron, G., Priola, S., Caughey, B., Masliah, E. & Oldstone, M. 2005. Anchorless prion protein results in infectious amyloid disease without clinical scrapie. *Science,* 308**,** 1435-1439.

Chiarlone, A., Bellocchio, L., Blázquez, C., Resel, E., Soria-Gómez, E., Cannich, A., Ferrero, J. J., Sagredo, O., Benito, C., Romero, J., Sánchez-Prieto, J., Lutz, B., Fernández-Ruiz, J., Galve-Roperh, I. & Guzmán, M. 2014. A restricted population of CB1 cannabinoid receptors with neuroprotective activity. *Proceedings of the National Academy of Sciences,* 111**,** 8257-8262.

Cho, S., Wood, A. & Bowlby, M. R. 2007. Brain Slices as Models for Neurodegenerative Disease and Screening Platforms to Identify Novel Therapeutics. *Current Neuropharmacology,* 5**,** 19-33.

Clavaguera, F., Bolmont, T., Crowther, R. A., Abramowski, D., Frank, S., Probst, A., Fraser, G., Stalder, A. K., Beibel, M., Staufenbiel, M., Jucker, M., Goedert, M.

& Tolnay, M. 2009. Transmission and spreading of tauopathy in transgenic mouse brain. *Nat Cell Biol,* 11**,** 909-13.

Cleary, J. P., Walsh, D. M., Hofmeister, J. J., Shankar, G. M., Kuskowski, M. A., Selkoe, D. J. & Ashe, K. H. 2005. Natural oligomers of the amyloid-[beta] protein specifically disrupt cognitive function. *Nat Neurosci,* 8**,** 79-84.

Cobb, N. J. & Surewicz, W. K. 2009. Prion Diseases and Their Biochemical Mechanisms. *Biochemistry,* 48**,** 2574-2585.

Colby, D. W., Giles, K., Legname, G., Wille, H., Baskakov, I. V., DeArmond, S. J. & Prusiner, S. B. 2009. Design and construction of diverse mammalian prion strains. *Proceedings of the National Academy of Sciences,* 106**,** 20417-20422.

Collinge, J. 2001. PRION DISEASES OF HUMANS AND ANIMALS: Their Causes and Molecular Basis. *Annual Review of Neuroscience,* 24**,** 519-550.

Collinge, J. & Clarke, A. R. 2007. A General Model of Prion Strains and Their Pathogenicity. *Science,* 318**,** 930-936.

Collinge, J., Sidle, K. C. L., Meads, J., Ironside, J. & Hill, A. F. 1996. Molecular analysis of prion strain variation and the aetiology of 'new variant' CJD. *Nature,* 383**,** 685-690.

Collinge, J., Whitfield, J., McKintosh, E., Beck, J., Mead, S., Thomas, D. J. & Alpers, M. P. 2006. Kuru in the 21st century--an acquired human prion disease with very long incubation periods. *Lancet,* 367**,** 2068-74.

Collins, S., McLean, C. A. & Masters, C. L. 2001. Gerstmann-Sträussler-Scheinker syndrome,fatal familial insomnia, and kuru: a review ofthese less common human transmissiblespongiform encephalopathies. *Journal of Clinical Neuroscience,* 8**,** 387-397.

Corder, E. H., Saunders, A. M., Strittmatter, W. J., Schmechel, D. E., Gaskell, P. C., Small, G. W., Roses, A. D., Haines, J. L. & Pericak-Vance, M. A. 1993. Gene Dose of Apolipoprotein E Type 4 Allele and the Risk of Alzheimer's Disease in Late Onset Families. *Science,* 261**,** 921-923.

Cruts, M. & Van Broeckhoven, C. 1998. Presenilin mutations in Alzheimer's disease. *Hum Mutat,* 11**,** 183-90.

Cunningham, C., Deacon, R., Wells, H., Boche, D., Waters, S., Diniz, C. P., Scott, H., Rawlins, J. N. P. & Perry, V. H. 2003. Synaptic changes characterize early behavioural signs in the ME7 model of murine prion disease. *European Journal of Neuroscience,* 17**,** 2147-2155.

Curtis, J., Errington, M., Bliss, T., Voss, K. & MacLeod, N. 2003. Age-dependent loss of PTP and LTP in the hippocampus of PrP-null mice. *Neurobiol Dis,* 13**,** 55-62.

Dahlgren, K. N., Manelli, A. M., Stine, W. B., Baker, L. K., Krafft, G. A. & LaDu, M. J. 2002. Oligomeric and Fibrillar Species of Amyloid-β Peptides Differentially Affect Neuronal Viability. *Journal of Biological Chemistry,* 277**,** 32046-32053.

Danzer, K. M., Krebs, S. K., Wolff, M., Birk, G. & Hengerer, B. 2009. Seeding induced by alpha-synuclein oligomers provides evidence for spreading of alpha-synuclein pathology. *Journal of Neurochemistry,* 111**,** 192-203.

de Villemeur, T. B., Gelot, A., Deslys, J. P., Dormont, D., Duyckaerts, C., Jardin, L., Denni, J. & Robain, O. 1994. Iatrogenic Creutzfeldt—Jakob disease in three

growth hormone recipients: a neuropathological study. *Neuropathology and Applied Neurobiology,* 20**,** 111-117.

Deighton, R. F., Márkus, N. M., Al-Mubarak, B., Bell, K. F. S., Papadia, S., Meakin, P. J., Chowdhry, S., Hayes, J. D. & Hardingham, G. E. 2014. Nrf2 target genes can be controlled by neuronal activity in the absence of Nrf2 and astrocytes. *Proceedings of the National Academy of Sciences,* 111**,** E1818-E1820.

Deleault, N. R., Walsh, D. J., Piro, J. R., Wang, F., Wang, X., Ma, J., Rees, J. R. & Supattapone, S. 2012. Cofactor molecules maintain infectious conformation and restrict strain properties in purified prions. *Proceedings of the National Academy of Sciences,* 109**,** E1938-E1946.

Demuro, A., Mina, E., Kayed, R., Milton, S. C., Parker, I. & Glabe, C. G. 2005. Calcium Dysregulation and Membrane Disruption as a Ubiquitous Neurotoxic Mechanism of Soluble Amyloid Oligomers. *Journal of Biological Chemistry,* 280**,** 17294-17300.

Devanand, D., Lee, J., Luchsinger, J., Manly, J., Marder, K., Mayeux, R., Scarmeas, N., Schupf, N. & Stern, Y. 2013. Lessons from Epidemiologic Research about Risk Factors, Modifiers, and Progression of Late Onset Alzheimer's Disease in New York City at Columbia University Medical Center. *Journal of Alzheimer's Disease,* 33**,** S447-S455.

Di, X., Yan, J., Zhao, Y., Zhang, J., Shi, Z., Chang, Y. & Zhao, B. 2010. l-theanine protects the APP (Swedish mutation) transgenic SH-SY5Y cell against glutamate-induced excitotoxicity via inhibition of the NMDA receptor pathway. *Neuroscience,* 168**,** 778-786.

Diack, A. B., Head, M. W., McCutcheon, S., Boyle, A., Knight, R., Ironside, J. W., Manson, J. C. & Will, R. G. 2014. Variant CJD. *Prion,* 8**,** 286-295.

Dimcheff, D. E., Portis, J. L. & Caughey, B. 2003. Prion proteins meet protein quality control. *Trends in Cell Biology,* 13**,** 337-340.

Dobson, C. M. 2003. Protein folding and misfolding. *Nature,* 426**,** 884-890.

Dolev, I., Fogel, H., Milshtein, H., Berdichevsky, Y., Lipstein, N., Brose, N., Gazit, N. & Slutsky, I. 2013. Spike bursts increase amyloid-[beta] 40/42 ratio by inducing a presenilin-1 conformational change. *Nat Neurosci,* 16**,** 587-595.

Dong, X. X., Wang, Y. & Qin, Z. H. 2009. Molecular mechanisms of excitotoxicity and their relevance to pathogenesis of neurodegenerative diseases. *Acta Pharmacol Sin,* 30**,** 379-87.

Eisele, Y. S., Obermüller, U., Heilbronner, G., Baumann, F., Kaeser, S. A., Wolburg, H., Walker, L. C., Staufenbiel, M., Heikenwalder, M. & Jucker, M. 2010. Peripherally Applied Aβ-Containing Inoculates Induce Cerebral β-Amyloidosis. *Science,* 330**,** 980-982.

Eklund, C. M., Kennedy, R. C. & Hadlow, W. J. 1967. Pathogenesis of Scrapie Virus Infection in the Mouse. *The Journal of Infectious Diseases,* 117**,** 15-22.

El-Agnaf, O. M. A., Mahil, D. S., Patel, B. P. & Austen, B. M. 2000. Oligomerization and Toxicity of β-Amyloid-42 Implicated in Alzheimer's Disease. *Biochemical and Biophysical Research Communications,* 273**,** 1003-1007.

Elias, L. & Kriegstein, A. 2007. Organotypic Slice Culture of E18 Rat Brains. *Journal of Visualized Experiments : JoVE***,** 235.

Elmore, S. 2007. Apoptosis: a review of programmed cell death. *Toxicol Pathol,* 35**,** 495-516.

Elsen, J. M., Amigues, Y., Schelcher, F., Ducrocq, V., Andreoletti, O., Eychenne, F., Tien Khang, J. V., Poivey, J. P., Lantier, F. & Laplanche, J. L. 1999. Genetic susceptibility and transmission factors in scrapie: detailed analysis of an epidemic in a closed flock of Romanov. *Archives of Virology,* 144**,** 431-445.

Esposito, Z., Belli, L., Toniolo, S., Sancesario, G., Bianconi, C. & Martorana, A. 2013. Amyloid β, Glutamate, Excitotoxicity in Alzheimer's Disease: Are We on the Right Track? *CNS Neuroscience & Therapeutics,* 19**,** 549-555.

Falconer, R. J., Chan, C., Hughes, K. & Munro, T. P. 2011. Stabilization of a monoclonal antibody during purification and formulation by addition of basic amino acid excipients. *Journal of Chemical Technology & Biotechnology,* 86**,** 942-948.

Ferreiro, E., Resende, R., Costa, R., Oliveira, C. R. & Pereira, C. M. F. 2006. An endoplasmic-reticulum-specific apoptotic pathway is involved in prion and amyloid-beta peptides neurotoxicity. *Neurobiology of Disease,* 23**,** 669-678.

Ferrer, M., Chernikova, T. N., Yakimov, M. M., Golyshin, P. N. & Timmis, K. N. 2003. Chaperonins govern growth of Escherichia coli at low temperatures. *Nat Biotech,* 21**,** 1266-1267.

Ferrão-Gonzales, A. D., Robbs, B. K., Moreau, V. H., Ferreira, A., Juliano, L., Valente, A. P., Almeida, F. C. L., Silva, J. L. & Foguel, D. 2005. Controlling β-Amyloid Oligomerization by the Use of Naphthalene Sulfonates: TRAPPING LOW MOLECULAR WEIGHT OLIGOMERIC SPECIES. *Journal of Biological Chemistry,* 280**,** 34747-34754.

.

Finder, V. H., Vodopivec, I., Nitsch, R. M. & Glockshuber, R. 2010. The Recombinant Amyloid-beta Peptide A beta 1-42 Aggregates Faster and Is More Neurotoxic than Synthetic A beta 1-42. *Journal of Molecular Biology,* 396**,** 9-18.

Forloni, G., Angeretti, N., Chiesa, R., Monzani, E., Salmona, M., Bugiani, O. & Tagliavini, F. 1993. Neurotoxicity of a prion protein fragment. *Nature,* 362**,** 543-6.

Fratiglioni, L., De Ronchi, D. & Aguero-Torres, H. 1999. Worldwide prevalence and incidence of dementia. *Drugs & Aging,* 15**,** 365-375.

Fuhrmann, M., Mitteregger, G., Kretzschmar, H. & Herms, J. 2007. Dendritic Pathology in Prion Disease Starts at the Synaptic Spine. *The Journal of Neuroscience,* 27**,** 6224-6233.

Furukawa, K., Sopher, B. L., Rydel, R. E., Begley, J. G., Pham, D. G., Martin, G. M., Fox, M. & Mattson, M. P. 1996. Increased activity-regulating and neuroprotective efficacy of alpha-secretase-derived secreted amyloid precursor protein conferred by a C-terminal heparin-binding domain. *J Neurochem,* 67**,** 1882-96.

Gambetti, P., Cali, I., Notari, S., Kong, Q., Zou, W. Q. & Surewicz, W. K. 2011. Molecular biology and pathology of prion strains in sporadic human prion diseases. *Acta Neuropathol,* 121**,** 79-90.

Gambetti, P., Kong, Q., Zou, W., Parchi, P. & Chen, S. G. 2003. Sporadic and familial CJD: classification and characterisation. *British Medical Bulletin,* 66**,** 213-239.

Garai, K., Crick, S. L., Mustafi, S. M. & Frieden, C. 2009. Expression and purification of amyloid-β peptides from Escherichia coli. *Protein Expression and Purification,* 66**,** 107-112.

Gesine, L., Anne, B., Horst, B., Martin, E., Martin, H. G. & Georg, E. 2007. Epidemiological and genetical differences between classical and atypical scrapie cases. *Vet. Res.,* 38**,** 65-80.

Giles, K., Glidden, D. V., Beckwith, R., Seoanes, R., Peretz, D., DeArmond, S. J. & Prusiner, S. B. 2008. Resistance of Bovine Spongiform Encephalopathy (BSE) Prions to Inactivation. *Plos Pathogens,* 4**,** 9.

Gill, S. C. & von Hippel, P. H. 1989. Calculation of protein extinction coefficients from amino acid sequence data. *Anal Biochem,* 182**,** 319-26.

Glabe, C. G. 2006. Common mechanisms of amyloid oligomer pathogenesis in degenerative disease. *Neurobiology of Aging,* 27**,** 570-575.

Glabe, C. G. & Kayed, R. 2006. Common structure and toxic function of amyloid oligomers implies a common mechanism of pathogenesis. *Neurology,* 66**,** S74-S78.

Goldgaber, D., Goldfarb, L. G., Brown, P., Asher, D. M., Brown, W. T., Lin, S., Teener, J. W., Feinstone, S. M., Rubenstein, R., Kascsak, R. J., Boellaard, J. W. & Gajdusek, D. C. 1989. Mutations in familial Creutzfeldt-Jakob disease and Gerstmann-Sträussler-Scheinker's syndrome. *Experimental Neurology,* 106**,** 204-206.

Gong, Y., Chang, L., Viola, K. L., Lacor, P. N., Lambert, M. P., Finch, C. E., Krafft, G. A. & Klein, W. L. 2003. Alzheimer's disease-affected brain: presence of oligomeric A beta ligands (ADDLs) suggests a molecular basis for reversible memory loss. *Proc Natl Acad Sci U S A,* 100**,** 10417-22.

Goold, R., Rabbanian, S., Sutton, L., Andre, R., Arora, P., Moonga, J., Clarke, A. R., Schiavo, G., Jat, P., Collinge, J. & Tabrizi, S. J. 2011. Rapid cell-surface prion protein conversion revealed using a novel cell system. *Nature Communications,* 2.

Gouix, E., Léveillé, F., Nicole, O., Melon, C., Had-Aissouni, L. & Buisson, A. 2009. Reverse glial glutamate uptake triggers neuronal cell death through extrasynaptic NMDA receptor activation. *Molecular and Cellular Neuroscience,* 40**,** 463-473.

Gralle, M. & Ferreira, S. T. 2007. Structure and functions of the human amyloid precursor protein: The whole is more than the sum of its parts. *Progress in Neurobiology,* 82**,** 11-32.

Greig, J. R. 1950. Scrapie in sheep. *Journal of Comparative Pathology and Therapeutics,* 60**,** 263-266.

Guo, Jing L., Covell, Dustin J., Daniels, Joshua P., Iba, M., Stieber, A., Zhang, B., Riddle, Dawn M., Kwong, Linda K., Xu, Y., Trojanowski, John Q. & Lee, Virginia M. Y. 2013. Distinct α-Synuclein Strains Differentially Promote Tau Inclusions in Neurons. *Cell,* 154**,** 103-117.

Guo, J. L. & Lee, V. M. Y. 2014. Cell-to-cell transmission of pathogenic proteins in neurodegenerative diseases. *Nat Med,* 20**,** 130-138.

Haass, C. & Selkoe, D. J. 2007. Soluble protein oligomers in neurodegeneration: lessons from the Alzheimer's amyloid [beta]-peptide. *Nat Rev Mol Cell Biol,* 8**,** 101-112.

Hansson, O., Zetterberg, H., Buchhave, P., Andreasson, U., Londos, E., Minthon, L. & Blennow, K. 2007. Prediction of Alzheimer's disease using the CSF Abeta42/Abeta40 ratio in patients with mild cognitive impairment. *Dementia and geriatric cognitive disorders,* 23**,** 316-320.

Hardy, J. & Selkoe, D. J. 2002. Medicine - The amyloid hypothesis of Alzheimer's disease: Progress and problems on the road to therapeutics. *Science,* 297**,** 353-356.

Hardy, J. A. & Higgins, G. A. 1992. Alzheimer's disease: the amyloid cascade hypothesis. *Science,* 256**,** 184-5.

Harold, D., Abraham, R., Hollingworth, P., Sims, R., Gerrish, A., Hamshere, M. L., Pahwa, J. S., Moskvina, V., Dowzell, K., Williams, A., Jones, N., Thomas, C., Stretton, A., Morgan, A. R., Lovestone, S., Powell, J., Proitsi, P., Lupton, M. K., Brayne, C., Rubinsztein, D. C., Gill, M., Lawlor, B., Lynch, A., Morgan, K., Brown, K. S., Passmore, P. A., Craig, D., McGuinness, B., Todd, S., Holmes, C., Mann, D., Smith, A. D., Love, S., Kehoe, P. G., Hardy, J., Mead, S., Fox, N., Rossor, M., Collinge, J., Maier, W., Jessen, F., Schurmann, B., Heun, R., van den Bussche, H., Heuser, I., Kornhuber, J., Wiltfang, J., Dichgans, M., Frolich, L., Hampel, H., Hull, M., Rujescu, D., Goate, A. M., Kauwe, J. S. K., Cruchaga, C., Nowotny, P., Morris, J. C., Mayo, K., Sleegers, K., Bettens, K., Engelborghs, S., De Deyn, P. P., Van Broeckhoven, C., Livingston, G., Bass, N. J., Gurling, H., McQuillin, A., Gwilliam, R., Deloukas, P., Al-Chalabi, A., Shaw, C. E., Tsolaki, M., Singleton, A. B., Guerreiro, R., Muhleisen, T. W., Nothen, M. M., Moebus, S., Jockel, K.-H., Klopp, N., Wichmann, H. E., Carrasquillo, M. M., Pankratz, V. S., Younkin, S. G., Holmans, P. A., O'Donovan, M., Owen, M. J. & Williams, J. 2009. Genome-wide association study identifies variants at CLU and PICALM associated with Alzheimer's disease. *Nat Genet,* 41**,** 1088-1093.

Harper, J. D. & Lansbury, P. T. 1997. Models of amyloid seeding in Alzheimier's disease and scrapie: Mechanistic truths and physiological consequences of the time-dependent solubility of amyloid proteins. *Annual Review of Biochemistry,* 66**,** 385-407.

Harris, D. A. 2003. Trafficking, turnover and membrane topology of PrP. *British Medical Bulletin,* 66**,** 71-+.

Harris, D. A. & True, H. L. 2006. New Insights into Prion Structure and Toxicity. *Neuron,* 50**,** 353-357.

Hartmann, T., Bieger, S. C., Bruhl, B., Tienari, P. J., Ida, N., Allsop, D., Roberts, G. W., Masters, C. L., Dotti, C. G., Unsicker, K. & Beyreuther, K. 1997. Distinct sites of intracellular production for Alzheimer's disease A[beta]40/42 amyloid peptides. *Nat Med,* 3**,** 1016-1020.

Hayashi, H. K., Yokoyama, T., Takata, M., Iwamaru, Y., Imamura, M., Ushiki, Y. K. & Shinagawa, M. 2005. The N-terminal cleavage site of PrPSc from BSE differs from that of PrPSc from scrapie. *Biochemical and Biophysical Research Communications,* 328**,** 1024-1027.

Head, M. W., Yull, H. M., Ritchie, D. L., Bishop, M. T. & Ironside, J. W. 2009. Pathological investigation of the first blood donor and recipient pair linked by transfusion-associated variant Creutzfeldt-Jakob disease transmission. *Neuropathology and Applied Neurobiology,* 35**,** 433-436.

Hegde, R. S., Mastrianni, J. A., Scott, M. R., DeFea, K. A., Tremblay, P., Torchia, M., DeArmond, S. J., Prusiner, S. B. & Lingappa, V. R. 1998. A Transmembrane Form of the Prion Protein in Neurodegenerative Disease. *Science,* 279**,** 827-834.

Hegde, R. S., Tremblay, P., Groth, D., DeArmond, S. J., Prusiner, S. B. & Lingappa, V. R. 1999. Transmissible and genetic prion diseases share a common pathway of neurodegeneration. *Nature,* 402**,** 822-826.

Heiseke, A., Aguib, Y. & Schatzl, H. M. 2010. Autophagy, prion infection and their mutual interactions. *Curr Issues Mol Biol,* 12**,** 87-97.

Hetz, C., Russelakis-Carneiro, M., Maundrell, K., Castilla, J. & Soto, C. 2003. Caspase-12 and endoplasmic reticulum stress mediate neurotoxicity of pathological prion protein. *Embo j,* 22**,** 5435-45.

Hickey, M. A. & Chesselet, M. F. 2003. Apoptosis in Huntington's disease. *Prog Neuropsychopharmacol Biol Psychiatry,* 27**,** 255-65.

Hill, A. F., Joiner, S., Linehan, J., Desbruslais, M., Lantos, P. L. & Collinge, J. 2000. Species-barrier-independent prion replication in apparently resistant species. *Proceedings of the National Academy of Sciences,* 97**,** 10248-10253.

Hofmann, J. P., Denner, P., Nussbaum-Krammer, C., Kuhn, P.-H., Suhre, M. H., Scheibel, T., Lichtenthaler, S. F., Schätzl, H. M., Bano, D. & Vorberg, I. M. 2013. Cell-to-cell propagation of infectious cytosolic protein aggregates. *Proceedings of the National Academy of Sciences,* 110**,** 5951-5956.

Hope, J., Reekie, L. J. D., Hunter, N., Multhaup, G., Beyreuther, K., White, H., Scott, A. C., Stack, M. J., Dawson, M. & Wells, G. A. H. 1988. FIBRILS FROM BRAINS OF COWS WITH NEW CATTLE DISEASE CONTAIN SCRAPIE-ASSOCIATED PROTEIN. *Nature,* 336**,** 390-392.

Hornemann, S., Korth, C., Oesch, B., Riek, R., Wider, G., Wüthrich, K. & Glockshuber, R. 1997. Recombinant full-length murine prion protein, mPrP(23–231): purification and spectroscopic characterization. *FEBS Letters,* 413**,** 277-281.

Hosszu, L. L. P., Trevitt, C. R., Jones, S., Batchelor, M., Scott, D. J., Jackson, G. S., Collinge, J., Waltho, J. P. & Clarke, A. R. 2009. Conformational Properties of β-PrP. *Journal of Biological Chemistry,* 284**,** 21981-21990.

Hsia, A. Y., Masliah, E., McConlogue, L., Yu, G. Q., Tatsuno, G., Hu, K., Kholodenko, D., Malenka, R. C., Nicoll, R. A. & Mucke, L. 1999. Plaque-independent disruption of neural circuits in Alzheimer's disease mouse models. *Proc Natl Acad Sci U S A,* 96**,** 3228-33.

Hu, X., Pickering, E., Liu, Y. C., Hall, S., Fournier, H., Katz, E., Dechairo, B., John, S., Van Eerdewegh, P., Soares, H. & the Alzheimer's Disease Neuroimaging, I. 2011. Meta-Analysis for Genome-Wide Association Study Identifies Multiple Variants at the BIN1 Locus Associated with Late-Onset Alzheimer's Disease. *PLoS ONE,* 6**,** e16616.

Hyman, B. T., West, H. L., Rebeck, G. W., Buldyrev, S. V., Mantegna, R. N., Ukleja, M., Havlin, S. & Stanley, H. E. 1995. Quantitative analysis of senile plaques in Alzheimer disease: observation of log-normal size distribution and molecular epidemiology of differences associated with apolipoprotein E genotype and trisomy 21 (Down syndrome). *Proc Natl Acad Sci U S A,* 92**,** 3586-90.

Imran, M. & Mahmood, S. 2011. An overview of human prion diseases. *Virol J,* 8**,** 559.

Ironside, J. W., Ritchie, D. L. & Head, M. W. 2005. Phenotypic variability in human prion diseases. *Neuropathology and Applied Neurobiology,* 31**,** 565-579.

Itkin, A., Dupres, V., Dufrêne, Y. F., Bechinger, B., Ruysschaert, J.-M. & Raussens, V. 2011. Calcium Ions Promote Formation of Amyloid β-Peptide (1–40) Oligomers Causally Implicated in Neuronal Toxicity of Alzheimer's Disease. *PLoS ONE,* 6**,** e18250.

Jackson, G. S., Hosszu, L. L. P., Power, A., Hill, A. F., Kenney, J., Saibil, H., Craven, C. J., Waltho, J. P., Clarke, A. R. & Collinge, J. 1999. Reversible Conversion of Monomeric Human Prion Protein Between Native and Fibrilogenic Conformations. *Science,* 283**,** 1935-1937.

Jeffrey, M., Goodsir, C. M., Bruce, M. E., McBride, P. A. & Fraser, J. R. 1997. In vivo toxicity of prion protein in murine scrapie: ultrastructural and immunogold studies. *Neuropathology and Applied Neurobiology,* 23**,** 93-101.

Jeffrey, M., Halliday, W. G., Bell, J., Johnston, A. R., MacLeod, N. K., Ingham, C., Sayers, A. R., Brown, D. A. & Fraser, J. R. 2000. Synapse loss associated with abnormal PrP precedes neuronal degeneration in the scrapie-infected murine hippocampus. *Neuropathol Appl Neurobiol,* 26**,** 41-54.

Jesionek-Kupnicka, D., Buczynski, J., Kordek, R., Sobow, T., Kloszewska, I., Papierz, W. & Liberski, P. P. 1997. Programmed cell death (apoptosis) in Alzheimer's disease and Creutzfeldt-Jakob disease. *Folia Neuropathol,* 35**,** 233-5.

Jobling, M. F., Stewart, L. R., White, A. R., McLean, C., Friedhuber, A., Maher, F., Beyreuther, K., Masters, C. L., Barrow, C. J., Collins, S. J. & Cappai, R. 1999. The Hydrophobic Core Sequence Modulates the Neurotoxic and Secondary Structure Properties of the Prion Peptide 106-126. *Journal of Neurochemistry,* 73**,** 1557-1565.

Jucker, M. & Walker, L. C. 2011. Pathogenic protein seeding in alzheimer disease and other neurodegenerative disorders. *Annals of Neurology,* 70**,** 532-540.

Kaden, D., Munter, L. M., Reif, B. & Multhaup, G. 2012. The amyloid precursor protein and its homologues: Structural and functional aspects of native and pathogenic oligomerization. *European Journal of Cell Biology,* 91**,** 234-239.

Kamenetz, F., Tomita, T., Hsieh, H., Seabrook, G., Borchelt, D., Iwatsubo, T., Sisodia, S. & Malinow, R. 2003. APP Processing and Synaptic Function. *Neuron,* 37**,** 925-937.

Kane, M. D., Lipinski, W. J., Callahan, M. J., Bian, F., Durham, R. A., Schwarz, R. D., Roher, A. E. & Walker, L. C. 2000. Evidence for seeding of beta-amyloid by intracerebral infusion of Alzheimer brain extracts in beta-amyloid precursor protein-transgenic mice. *Journal of Neuroscience,* 20**,** 3606-3611.

Kayed, R., Head, E., Thompson, J. L., McIntire, T. M., Milton, S. C., Cotman, C. W. & Glabe, C. G. 2003. Common structure of soluble amyloid oligomers implies common mechanism of pathogenesis. *Science,* 300**,** 486-489.

Kayed, R., Pensalfini, A., Margol, L., Sokolov, Y., Sarsoza, F., Head, E., Hall, J. & Glabe, C. 2009. Annular Protofibrils Are a Structurally and Functionally Distinct Type of Amyloid Oligomer. *Journal of Biological Chemistry,* 284**,** 4230-4237.

Kayed, R., Sokolov, Y., Edmonds, B., McIntire, T. M., Milton, S. C., Hall, J. E. & Glabe, C. G. 2004. Permeabilization of lipid bilayers is a common conformation-dependent activity of soluble amyloid oligomers in protein misfolding diseases. *Journal of Biological Chemistry,* 279**,** 46363-46366.

Kazlauskaite, J., Sanghera, N., Sylvester, I., Vénien-Bryan, C. & Pinheiro, T. J. T. 2003. Structural Changes of the Prion Protein in Lipid Membranes Leading to Aggregation and Fibrillization†. *Biochemistry,* 42**,** 3295-3304.

Kazlauskaite, J., Young, A., Gardner, C. E., Macpherson, J. V., Vénien-Bryan, C. & Pinheiro, T. J. T. 2005. An unusual soluble β-turn-rich conformation of prion is involved in fibril formation and toxic to neuronal cells. *Biochemical and Biophysical Research Communications,* 328**,** 292-305.

Kimberlin, R. H. & Walker, C. A. 1979. Pathogenesis of mouse scrapie: Dynamics of agent replication in spleen, spinal cord and brain after infection by different routes. *Journal of Comparative Pathology,* 89**,** 551-562.

Kirby, L., Agarwal, S., Graham, J. F., Goldmann, W. & Gill, A. C. 2010. Inverse Correlation of Thermal Lability and Conversion Efficiency for Five Prion Protein Polymorphic Variants. *Biochemistry,* 49**,** 1448-1459.

Kleizen, B. & Braakman, I. 2004. Protein folding and quality control in the endoplasmic reticulum. *Current Opinion in Cell Biology,* 16**,** 343-349.

Klingeborn, M., Race, B., Meade-White, K. D., Rosenke, R., Striebel, J. F. & Chesebro, B. 2011. Crucial Role for Prion Protein Membrane Anchoring in the Neuroinvasion and Neural Spread of Prion Infection. *Journal of Virology,* 85**,** 1484-1494.

Klyubin, I., Walsh, D. M., Lemere, C. A., Cullen, W. K., Shankar, G. M., Betts, V., Spooner, E. T., Jiang, L., Anwyl, R., Selkoe, D. J. & Rowan, M. J. 2005. Amyloid [beta] protein immunotherapy neutralizes A[beta] oligomers that disrupt synaptic plasticity in vivo. *Nat Med,* 11**,** 556-561.

Knaus, K. J., Morillas, M., Swietnicki, W., Malone, M., Surewicz, W. K. & Yee, V. C. 2001. Crystal structure of the human prion protein reveals a mechanism for oligomerization. *Nature Structural Biology,* 8**,** 770-774.

Knowles, T. P. J., Vendruscolo, M. & Dobson, C. M. 2014. The amyloid state and its association with protein misfolding diseases. *Nat Rev Mol Cell Biol,* 15**,** 384-396.

Knowles, T. P. J., Waudby, C. A., Devlin, G. L., Cohen, S. I. A., Aguzzi, A., Vendruscolo, M., Terentjev, E. M., Welland, M. E. & Dobson, C. M. 2009. An Analytical Solution to the Kinetics of Breakable Filament Assembly. *Science,* 326**,** 1533-1537.

Kocisko, D. A., Priola, S. A., Raymond, G. J., Chesebro, B., Lansbury, P. T. & Caughey, B. 1995. Species specificity in the cell-free conversion of prion protein to protease-resistant forms: a model for the scrapie species barrier. *Proceedings of the National Academy of Sciences of the United States of America,* 92**,** 3923-3927.

Koffie, R. M., Meyer-Luehmann, M., Hashimoto, T., Adams, K. W., Mielke, M. L., Garcia-Alloza, M., Micheva, K. D., Smith, S. J., Kim, M. L., Lee, V. M., Hyman, B. T. & Spires-Jones, T. L. 2009. Oligomeric amyloid beta associates with postsynaptic densities and correlates with excitatory synapse loss near senile plaques. *Proc Natl Acad Sci U S A,* 106**,** 4012-7.

Kong, Q., Huang, S., Zou, W., Vanegas, D., Wang, M., Wu, D., Yuan, J., Zheng, M., Bai, H., Deng, H., Chen, K., Jenny, A. L., O'Rourke, K., Belay, E. D., Schonberger, L. B., Petersen, R. B., Sy, M.-S., Chen, S. G. & Gambetti, P. 2005. Chronic Wasting Disease of Elk: Transmissibility to Humans Examined by Transgenic Mouse Models. *The Journal of Neuroscience,* 25**,** 7944-7949.

Kovács, G., Puopolo, M., Ladogana, A., Pocchiari, M., Budka, H., van Duijn, C., Collins, S., Boyd, A., Giulivi, A., Coulthart, M., Delasnerie-Laupretre, N., Brandel, J., Zerr, I., Kretzschmar, H., de Pedro-Cuesta, J., Calero-Lara, M., Glatzel, M., Aguzzi, A., Bishop, M., Knight, R., Belay, G., Will, R. & Mitrova, E. 2005. Genetic prion disease: the EUROCJD experience. *Human Genetics,* 118**,** 166-174.

Krasemann, S., Neumann, M., Szalay, B., Stocking, C. & Glatzel, M. 2013. Protease-sensitive prion species in neoplastic spleens of prion-infected mice with uncoupling of PrPSc and prion infectivity. *Journal of General Virology,* 94**,** 453-463.

Kristiansen, M., Deriziotis, P., Dimcheff, D. E., Jackson, G. S., Ovaa, H., Naumann, H., Clarke, A. R., van Leeuwen, F. W. B., Menéndez-Benito, V., Dantuma, N. P., Portis, J. L., Collinge, J. & Tabrizi, S. J. 2007. Disease-Associated Prion Protein Oligomers Inhibit the 26S Proteasome. *Molecular Cell,* 26**,** 175-188.

Kumar-Singh, S., Theuns, J., Van Broeck, B., Pirici, D., Vennekens, K., Corsmit, E., Cruts, M., Dermaut, B., Wang, R. & Van Broeckhoven, C. 2006. Mean age-of-onset of familial alzheimer disease caused by presenilin mutations correlates with both increased Abeta42 and decreased Abeta40. *Hum Mutat,* 27**,** 686-95.

Kuo, Y.-M., Emmerling, M. R., Vigo-Pelfrey, C., Kasunic, T. C., Kirkpatrick, J. B., Murdoch, G. H., Ball, M. J. & Roher, A. E. 1996. Water-soluble A(N-40, N-42) Oligomers in Normal and Alzheimer Disease Brains. *Journal of Biological Chemistry,* 271**,** 4077-4081.

Lakhan, S. E., Sabharanjak, S. & De, A. 2009. Endocytosis of glycosylphosphatidylinositol-anchored proteins. *Journal of Biomedical Science,* 16.

Lambert, M. P., Barlow, A. K., Chromy, B. A., Edwards, C., Freed, R., Liosatos, M., Morgan, T. E., Rozovsky, I., Trommer, B., Viola, K. L., Wals, P., Zhang, C., Finch, C. E., Krafft, G. A. & Klein, W. L. 1998. Diffusible, nonfibrillar ligands derived from Aβ1–42 are potent central nervous system neurotoxins. *Proceedings of the National Academy of Sciences,* 95**,** 6448-6453.

Lansbury, P. T. & Lashuel, H. A. 2006. A century-old debate on protein aggregation and neurodegeneration enters the clinic. *Nature,* 443**,** 774-779.

Lee, A. S. 2005. The ER chaperone and signaling regulator GRP78/BiP as a monitor of endoplasmic reticulum stress. *Methods,* 35**,** 373-81.

Lee, E. K., Hwang, J. H., Shin, D. Y., Kim, D. I. & Yoo, Y. J. 2005. Production of recombinant amyloid-β peptide 42 as an ubiquitin extension. *Protein Expression and Purification,* 40**,** 183-189.

Lee, S. & Eisenberg, D. 2003. Seeded conversion of recombinant prion protein to a disulfide-bonded oligomer by a reduction-oxidation process. *Nat Struct Mol Biol,* 10**,** 725-730.

Legname, G., Baskakov, I. V., Nguyen, H.-O. B., Riesner, D., Cohen, F. E., DeArmond, S. J. & Prusiner, S. B. 2004. Synthetic Mammalian Prions. *Science,* 305**,** 673-676.

Lemere, C. A., Blusztajn, J. K., Yamaguchi, H., Wisniewski, T., Saido, T. C. & Selkoe, D. J. 1996. Sequence of deposition of heterogeneous amyloid beta-peptides and APO E in Down syndrome: Implications for initial events in amyloid plaque formation. *Neurobiology of Disease,* 3**,** 16-32.

Lesné, S., Kotilinek, L. & Ashe, K. H. 2008. Plaque-bearing mice with reduced levels of oligomeric amyloid-β assemblies have intact memory function. *Neuroscience,* 151**,** 745-749.

Levine, B. & Kroemer, G. 2008. Autophagy in the Pathogenesis of Disease. *Cell,* 132**,** 27-42.

Lewis, J., Dickson, D. W., Lin, W. L., Chisholm, L., Corral, A., Jones, G., Yen, S. H., Sahara, N., Skipper, L., Yager, D., Eckman, C., Hardy, J., Hutton, M. & McGowan, E. 2001. Enhanced neurofibrillary degeneration in transgenic mice expressing mutant tau and APP. *Science,* 293**,** 1487-91.

Li, S., Hong, S., Shepardson, N. E., Walsh, D. M., Shankar, G. M. & Selkoe, D. 2009. Soluble Oligomers of Amyloid β Protein Facilitate Hippocampal Long-Term Depression by Disrupting Neuronal Glutamate Uptake. *Neuron,* 62**,** 788-801.

Li, S., Jin, M., Koeglsperger, T., Shepardson, N. E., Shankar, G. M. & Selkoe, D. J. 2011. Soluble Aβ Oligomers Inhibit Long-Term Potentiation through a Mechanism Involving Excessive Activation of Extrasynaptic NR2B-Containing NMDA Receptors. *The Journal of Neuroscience,* 31**,** 6627-6638.

Lindholm, D., Wootz, H. & Korhonen, L. 2006. ER stress and neurodegenerative diseases. *Cell Death Differ,* 13**,** 385-392.

Lisa, S., Domingo, B., Martinez, J., Gilch, S., Llopis, J. F., Schatzl, H. M. & Gasset, M. 2012. Failure of Prion Protein Oxidative Folding Guides the Formation of

Toxic Transmembrane Forms. *Journal of Biological Chemistry,* 287**,** 36693-36701.

Llewelyn, C. A., Hewitt, P. E., Knight, R. S. G., Amar, K., Cousens, S., Mackenzie, J. & Will, R. G. 2004. Possible transmission of variant Creutzfeldt-Jakob disease by blood transfusion. *The Lancet,* 363**,** 417-421.

Lorenzo, A. & Yankner, B. A. 1994. Beta-amyloid neurotoxicity requires fibril formation and is inhibited by congo red. *Proceedings of the National Academy of Sciences,* 91**,** 12243-12247.

Lucassen, R., Nishina, K. & Supattapone, S. 2003. In vitro amplification of protease-resistant prion protein requires free sulfhydryl groups. *Biochemistry,* 42**,** 4127-4135.

Luchsinger, J. A., Cheng, D., Tang, M. X., Schupf, N. & Mayeux, R. 2012. Central obesity in the elderly is related to late onset Alzheimer's disease. *Alzheimer Disease and Associated Disorders,* 26**,** 101-105.

Lue, L. F., Kuo, Y. M., Roher, A. E., Brachova, L., Shen, Y., Sue, L., Beach, T., Kurth, J. H., Rydel, R. E. & Rogers, J. 1999. Soluble amyloid beta peptide concentration as a predictor of synaptic change in Alzheimer's disease. *Am J Pathol,* 155**,** 853-62.

Luk, K. C., Kehm, V., Carroll, J., Zhang, B., O'Brien, P., Trojanowski, J. Q. & Lee, V. M. 2012. Pathological alpha-synuclein transmission initiates Parkinson-like neurodegeneration in nontransgenic mice. *Science,* 338**,** 949-53.

Luk, K. C., Song, C., O'Brien, P., Stieber, A., Branch, J. R., Brunden, K. R., Trojanowski, J. Q. & Lee, V. M. Y. 2009. Exogenous alpha-synuclein fibrils seed the formation of Lewy body-like intracellular inclusions in cultured cells. *Proceedings of the National Academy of Sciences of the United States of America,* 106**,** 20051-20056.

Léveillé, F., Papadia, S., Fricker, M., Bell, K. F. S., Soriano, F. X., Martel, M.-A., Puddifoot, C., Habel, M., Wyllie, D. J., Ikonomidou, C., Tolkovsky, A. M. & Hardingham, G. E. 2010. Suppression of the Intrinsic Apoptosis Pathway by Synaptic Activity. *The Journal of Neuroscience,* 30**,** 2623-2635.

Ma, J. Y. & Lindquist, S. 1999. De novo generation of a PrPSc-like conformation in living cells. *Nature Cell Biology,* 1**,** 358-361.

Ma, J. Y., Wollmann, R. & Lindquist, S. 2002. Neurotoxicity and neurodegeneration when PrP accumulates in the cytosol. *Science,* 298**,** 1781-1785.

Macao, B., Hoyer, W., Sandberg, A., Brorsson, A. C., Dobson, C. M. & Hard, T. 2008. Recombinant amyloid beta-peptide production by coexpression with an affibody ligand. *BMC Biotechnol,* 8**,** 82.

Maglio, L. E., Martins, V. R., Izquierdo, I. & Ramirez, O. A. 2006. Role of cellular prion protein on LTP expression in aged mice. *Brain Res,* 1097**,** 11-8.

Maglio, L. E., Perez, M. F., Martins, V. R., Brentani, R. R. & Ramirez, O. A. 2004. Hippocampal synaptic plasticity in mice devoid of cellular prion protein. *Brain Res Mol Brain Res,* 131**,** 58-64.

Maiti, N. R. & Surewicz, W. K. 2001. The Role of Disulfide Bridge in the Folding and Stability of the Recombinant Human Prion Protein. *Journal of Biological Chemistry,* 276**,** 2427-2431.

Makarava, N. & Baskakov, I. V. 2008. Expression and purification of full-length recombinant PrP of high purity. *Methods Mol Biol,* 459**,** 131-43.

.

Mallucci, G. R., Ratte, S., Asante, E. A., Linehan, J., Gowland, I., Jefferys, J. G. R. & Collinge, J. 2002. Post-natal knockout of prion protein alters hippocampal CA1 properties, but does not result in neurodegeneration (vol 21, pg 202, 2002). *Embo Journal,* 21**,** 1240-1240.

Mancuso, C. & Gaetani, S. 2014. Preclinical and clinical issues in Alzheimer's disease drug research and development. *Frontiers in Pharmacology,* 5**,** 234.

Mandelkow, E. M. & Mandelkow, E. 1998. Tau in Alzheimer's disease. *Trends in Cell Biology,* 8**,** 425-427.

Manzoni, C., Colombo, L., Bigini, P., Diana, V., Cagnotto, A., Messa, M., Lupi, M., Bonetto, V., Pignataro, M., Airoldi, C., Sironi, E., Williams, A. & Salmona, M. 2011. The Molecular Assembly of Amyloid Aβ Controls Its Neurotoxicity and Binding to Cellular Proteins. *PLoS ONE,* 6**,** e24909.

Marandi, Y., Farahi, N., Sadeghi, A. & Sadeghi-Hashjin, G. 2012. Prion diseases - current theories and potential therapies: a brief review. *Folia Neuropathol,* 50**,** 46-9.

Martinez-Vicente, M. & Cuervo, A. M. 2007. Autophagy and neurodegeneration: when the cleaning crew goes on strike. *The Lancet Neurology,* 6**,** 352-361.

Mastrianni, J. A. 2010. The genetics of prion diseases. *Genet Med,* 12**,** 187-195.

Masuda-Suzukake, M., Nonaka, T., Hosokawa, M., Oikawa, T., Arai, T., Akiyama, H., Mann, D. M. & Hasegawa, M. 2013. Prion-like spreading of pathological alpha-synuclein in brain. *Brain,* 136**,** 1128-38.

Mathiason, C. K., Powers, J. G., Dahmes, S. J., Osborn, D. A., Miller, K. V., Warren, R. J., Mason, G. L., Hays, S. A., Hayes-Klug, J., Seelig, D. M., Wild, M. A., Wolfe, L. L., Spraker, T. R., Miller, M. W., Sigurdson, C. J., Telling, G. C. & Hoover, E. A. 2006. Infectious Prions in the Saliva and Blood of Deer with Chronic Wasting Disease. *Science,* 314**,** 133-136.

Mattson, M. P. 1997. Cellular actions of beta-amyloid precursor protein and its soluble and fibrillogenic derivatives. *Physiol Rev,* 77**,** 1081-132.

McCutcheon, S., Alejo Blanco, A. R., Houston, E. F., de Wolf, C., Tan, B. C., Smith, A., Groschup, M. H., Hunter, N., Hornsey, V. S., MacGregor, I. R., Prowse, C. V., Turner, M. & Manson, J. C. 2011. All Clinically-Relevant Blood Components Transmit Prion Disease following a Single Blood Transfusion: A Sheep Model of vCJD. *PLoS ONE,* 6**,** e23169.

McLean, C. A., Cherny, R. A., Fraser, F. W., Fuller, S. J., Smith, M. J., Beyreuther, K., Bush, A. I. & Masters, C. L. 1999. Soluble pool of Abeta amyloid as a determinant of severity of neurodegeneration in Alzheimer's disease. *Ann Neurol,* 46**,** 860-6.

Mead, S., Stumpf, M. P., Whitfield, J., Beck, J. A., Poulter, M., Campbell, T., Uphill, J. B., Goldstein, D., Alpers, M., Fisher, E. M. & Collinge, J. 2003. Balancing selection at the prion protein gene consistent with prehistoric kurulike epidemics. *Science,* 300**,** 640-3.

Medeiros, R., Baglietto-Vargas, D. & LaFerla, F. M. 2011. The Role of Tau in Alzheimer's Disease and Related Disorders. *CNS Neuroscience & Therapeutics,* 17**,** 514-524.

Medina, M. & Avila, J. 2014. New perspectives on the role of tau in Alzheimer's disease. Implications for therapy. *Biochem Pharmacol,* 88**,** 540-7.

Meyer-Luehmann, M., Coomaraswamy, J., Bolmont, T., Kaeser, S., Schaefer, C., Kilger, E., Neuenschwander, A., Abramowski, D., Frey, P., Jaton, A. L., Vigouret, J. M., Paganetti, P., Walsh, D. M., Mathews, P. M., Ghiso, J., Staufenbiel, M., Walker, L. C. & Jucker, M. 2006. Exogenous induction of cerebral beta-amyloidogenesis is governed by agent and host. *Science,* 313**,** 1781-4.

Millhauser, G. L. 2007. Copper and the prion protein: Methods, structures, function, and disease. *Annual Review of Physical Chemistry,* 58**,** 299-320.

Mizushima, N., Levine, B., Cuervo, A. M. & Klionsky, D. J. 2008. Autophagy fights disease through cellular self-digestion. *Nature,* 451**,** 1069-1075.

Moechars, D., Dewachter, I., Lorent, K., Reverse, D., Baekelandt, V., Naidu, A., Tesseur, I., Spittaels, K., Haute, C. V., Checler, F., Godaux, E., Cordell, B. & Van Leuven, F. 1999. Early phenotypic changes in transgenic mice that overexpress different mutants of amyloid precursor protein in brain. *J Biol Chem,* 274**,** 6483-92.

Molinuevo, J. L., Lladó, A. & Rami, L. 2005. Memantine: Targeting glutamate excitotoxicity in Alzheimer's disease and other dementias. *American Journal of Alzheimer's Disease and Other Dementias,* 20**,** 77-85.

Moreno, J. A., Halliday, M., Molloy, C., Radford, H., Verity, N., Axten, J. M., Ortori, C. A., Willis, A. E., Fischer, P. M., Barrett, D. A. & Mallucci, G. R. 2013. Oral treatment targeting the unfolded protein response prevents neurodegeneration and clinical disease in prion-infected mice. *Sci Transl Med,* 5**,** 206ra138.

Mucke, L., Masliah, E., Yu, G. Q., Mallory, M., Rockenstein, E. M., Tatsuno, G., Hu, K., Kholodenko, D., Johnson-Wood, K. & McConlogue, L. 2000a. High-level neuronal expression of A beta(1-42) in wild-type human amyloid protein precursor transgenic mice: Synaptotoxicity without plaque formation. *Journal of Neuroscience,* 20**,** 4050-4058.

Mucke, L., Masliah, E., Yu, G. Q., Mallory, M., Rockenstein, E. M., Tatsuno, G., Hu, K., Kholodenko, D., Johnson-Wood, K. & McConlogue, L. 2000b. High-level neuronal expression of abeta 1-42 in wild-type human amyloid protein precursor transgenic mice: synaptotoxicity without plaque formation. *J Neurosci,* 20**,** 4050-8.

Muller, W. E. G., Ushijima, H., Schroder, H. C., Forrest, J. M. S., Schatton, W. F. H., Rytik, P. G. & Heffnerlauc, M. 1993. Cytoprotective Effect of Nmda Receptor Antagonists on Prion Protein (Prion(Sc))-Induced Toxicity in Rat Cortical Cell-Cultures. *European Journal of Pharmacology-Molecular Pharmacology Section,* 246**,** 261-267.

Muramoto, T., DeArmond, S. J., Scott, M., Telling, G. C., Cohen, F. E. & Prusiner, S. B. 1997. Heritable disorder resembling neuronal storage disease in mice

expressing prion protein with deletion of an alpha-helix. *Nature Medicine,* 3**,** 750-755.

Naj, A. C., Jun, G., Reitz, C., Kunkle, B. W., Perry, W., Park, Y., Beecham, G. W., Rajbhandary, R. A., Hamilton-Nelson, K. L., Wang, L.-S., Kauwe, J. S. K., Huentelman, M. J., Myers, A. J., Bird, T. D., Boeve, B. F., Baldwin, C. T., Jarvik, G. P., Crane, P. K., Rogaeva, E., Barmada, M. M., Demirci, F. Y., Cruchaga, C., Kramer, P., Alzheimer's Disease Genetics, C., Ertekin-Taner, N., Hardy, J., Graff-Radford, N. R., Green, R. C., Larson, E. B., St George-Hyslop, P., Buxbaum, J. D., Evans, D., Schneider, J. A., Lunetta, K. L., Kamboh, M. I., Saykin, A. J., Reiman, E. M., De Jager, P. L., Bennett, D. A., Morris, J. C., Montine, T. J., Goate, A. M., Blacker, D., Tsuang, D. W., Hakonarson, H., Kukull, W. A., Foroud, T. M., Martin, E. R., Haines, J. L., Mayeux, R., Farrer, L. A., Schellenberg, G. D. & Pericak-Vance, M. A. 2014. Age-at-Onset in Late Onset Alzheimer Disease is Modified by Multiple Genetic Loci. *JAMA neurology,* 71**,** 1394-1404.

Nakamura, T. & Lipton, S. 2010. Redox regulation of mitochondrial fission, protein misfolding, synaptic damage, and neuronal cell death: potential implications for Alzheimer's and Parkinson's diseases. *Apoptosis,* 15**,** 1354-1363.

Naslund, J., Haroutunian, V., Mohs, R., Davis, K. L., Davies, P., Greengard, P. & Buxbaum, J. D. 2000. Correlation between elevated levels of amyloid beta-peptide in the brain and cognitive decline. *Jama-Journal of the American Medical Association,* 283**,** 1571-1577.

Novitskaya, V., Bocharova, O. V., Bronstein, I. & Baskakov, I. V. 2006. Amyloid fibrils of mammalian prion protein are highly toxic to cultured cells and primary neurons. *Journal of Biological Chemistry,* 281**,** 13828-13836.

Novitskaya, V., Makarava, N., Sylvester, I., Bronstein, I. B. & Baskakov, I. V. 2007. Amyloid fibrils of mammalian prion protein induce axonal degeneration in NTERA2-derived terminally differentiated neurons. *Journal of Neurochemistry,* 102**,** 398-407.

Nunziante, M., Ackermann, K., Dietrich, K., Wolf, H., Gädtke, L., Gilch, S., Vorberg, I., Groschup, M. & Schätzl, H. M. 2011. Proteasomal Dysfunction and Endoplasmic Reticulum Stress Enhance Trafficking of Prion Protein Aggregates through the Secretory Pathway and Increase Accumulation of Pathologic Prion Protein. *Journal of Biological Chemistry,* 286**,** 33942-33953.

O'Donovan, C. N., Tobin, D. & Cotter, T. G. 2001. Prion Protein Fragment PrP-(106–126) Induces Apoptosis via Mitochondrial Disruption in Human Neuronal SH-SY5Y Cells. *Journal of Biological Chemistry,* 276**,** 43516-43523.

Oddo, S., Billings, L., Kesslak, J. P., Cribbs, D. H. & LaFerla, F. M. 2004. Abeta immunotherapy leads to clearance of early, but not late, hyperphosphorylated tau aggregates via the proteasome. *Neuron,* 43**,** 321-32.

Oddo, S., Caccamo, A., Cheng, D., Jouleh, B., Torp, R. & LaFerla, F. M. 2007. Genetically augmenting tau levels does not modulate the onset or progression of A beta pathology in transgenic mice. *Journal of Neurochemistry,* 102**,** 1053-1063.

Oddo, S., Caccamo, A., Tran, L., Lambert, M. P., Glabe, C. G., Klein, W. L. & LaFerla, F. M. 2006. Temporal Profile of Amyloid-β (Aβ) Oligomerization in an in Vivo Model of Alzheimer Disease: A LINK BETWEEN Aβ AND TAU PATHOLOGY. *Journal of Biological Chemistry,* 281**,** 1599-1604.

Orsi, A., Fioriti, L., Chiesa, R. & Sitia, R. 2006. Conditions of Endoplasmic Reticulum Stress Favor the Accumulation of Cytosolic Prion Protein. *Journal of Biological Chemistry,* 281**,** 30431-30438.

Oslowski, C. M. & Urano, F. 2011. Measuring ER stress and the unfolded protein response using mammalian tissue culture system. *Methods Enzymol,* 490**,** 71-92.

Pan, C., Kumar, C., Bohl, S., Klingmueller, U. & Mann, M. 2009. Comparative Proteomic Phenotyping of Cell Lines and Primary Cells to Assess Preservation of Cell Type-specific Functions. *Molecular & Cellular Proteomics,* 8**,** 443-450.

Pan, K. M., Baldwin, M., Nguyen, J., Gasset, M., Serban, A., Groth, D., Mehlhorn, I., Huang, Z., Fletterick, R. J., Cohen, F. E. & et al. 1993. Conversion of alpha-helices into beta-sheets features in the formation of the scrapie prion proteins. *Proc Natl Acad Sci U S A,* 90**,** 10962-6.

Panza, G., Stöhr, J., Dumpitak, C., Papathanassiou, D., Weiß, J., Riesner, D., Willbold, D. & Birkmann, E. 2008. Spontaneous and BSE-prion-seeded amyloid formation of full length recombinant bovine prion protein. *Biochemical and Biophysical Research Communications,* 373**,** 493-497.

Papadia, S., Soriano, F. X., Leveille, F., Martel, M. A., Dakin, K. A., Hansen, H. H., Kaindl, A., Sifringer, M., Fowler, J., Stefovska, V., McKenzie, G., Craigon, M., Corriveau, R., Ghazal, P., Horsburgh, K., Yankner, B. A., Wyllie, D. J. A., Ikonomidou, C. & Hardingham, G. E. 2008. Synaptic NMDA receptor activity boosts intrinsic antioxidant defenses. *Nature Neuroscience,* 11**,** 476-487.

Parchi, P., Zou, W., Wang, W., Brown, P., Capellari, S., Ghetti, B., Kopp, N., Schulz-Schaeffer, W. J., Kretzschmar, H. A., Head, M. W., Ironside, J. W., Gambetti, P. & Chen, S. G. 2000. Genetic influence on the structural variations of the abnormal prion protein. *Proceedings of the National Academy of Sciences,* 97**,** 10168-10172.

Parry, H. B. 1962. Scrapie: A transmissible and hereditary disease of sheep. *Heredity,* 17**,** 75-105.

Pattison, J. 1998. The emergence of bovine spongiform encephalopathy and related diseases. *Emerging Infectious Diseases,* 4**,** 390-394.

Paul, C. & Axelsen, P. H. 2005. β Sheet Structure in Amyloid β Fibrils and Vibrational Dipolar Coupling. *Journal of the American Chemical Society,* 127**,** 5754-5755.

Peden, A. H., Head, M. W., Diane, L. R., Jeanne, E. B. & James, W. I. 2004. Preclinical vCJD after blood transfusion in a PRNP codon 129 heterozygous patient. *The Lancet,* 364**,** 527-529.

Peretz, D., Supattapone, S., Giles, K., Vergara, J., Freyman, Y., Lessard, P., Safar, J. G., Glidden, D. V., McCulloch, C., Nguyen, H. O. B., Scott, M., DeArmond, S.

J. & Prusiner, S. B. 2006. Inactivation of prions by acidic sodium dodecyl sulfate. *Journal of Virology,* 80**,** 322-331.

Petrakis, S. & Sklaviadis, T. 2006. Identification of proteins with high affinity for refolded and native PrPC. *Proteomics,* 6**,** 6476-84.

Price, D. L., Tanzi, R. E., Borchelt, D. R. & Sisodia, S. S. 1998. Alzheimer's disease: genetic studies and transgenic models. *Annu Rev Genet,* 32**,** 461-93.

Prusiner, S. B. 1998a. Prions. *Proceedings of the National Academy of Sciences of the United States of America,* 95**,** 13363-13383.

Prusiner, S. B. 1998b. The prion diseases. *Brain Pathology,* 8**,** 499-513.

Prusiner, S. B. & Hsiao, K. K. 1994. Human prion diseases. *Ann Neurol,* 35**,** 385-95.

Prusiner, S. B., McKinley, M. P., Bowman, K. A., Bolton, D. C., Bendheim, P. E., Groth, D. F. & Glenner, G. G. 1983. Scrapie prions aggregate to form amyloid-like birefringent rods. *Cell,* 35**,** 349-358.

Prusiner, S. B., Scott, M. R., DeArmond, S. J. & Cohen, F. E. 1998. Prion protein biology. *Cell,* 93**,** 337-348.

Quist, A., Doudevski, L., Lin, H., Azimova, R., Ng, D., Frangione, B., Kagan, B., Ghiso, J. & Lal, R. 2005. Amyloid ion channels: A common structural link for protein-misfolding disease. *Proceedings of the National Academy of Sciences of the United States of America,* 102**,** 10427-10432.

Race, B., Meade-White, K. D., Phillips, K., Striebel, J., Race, R. & Chesebro, B. 2014. Chronic Wasting Disease Agents in Nonhuman Primates. *Emerging Infectious Diseases,* 20**,** 833-837.

Radford, H. E. & Mallucci, G. R. 2010. The role of GPI-anchored PrP C in mediating the neurotoxic effect of scrapie prions in neurons. *Curr Issues Mol Biol,* 12**,** 119-27.

Rammes, G., Hasenjäger, A., Sroka-Saidi, K., Deussing, J. M. & Parsons, C. G. 2011. Therapeutic significance of NR2B-containing NMDA receptors and mGluR5 metabotropic glutamate receptors in mediating the synaptotoxic effects of β-amyloid oligomers on long-term potentiation (LTP) in murine hippocampal slices. *Neuropharmacology,* 60**,** 982-990.

.

Rezaei, H., Eghiaian, F., Perez, J., Doublet, B., Choiset, Y., Haertle, T. & Grosclaude, J. 2005. Sequential generation of two structurally distinct ovine prion protein soluble oligomers displaying different biochemical reactivities. *J Mol Biol,* 347**,** 665-79.

Rezaei, H., Marc, D., Choiset, Y., Takahashi, M., Hui Bon Hoa, G., Haertlé, T., Grosclaude, J. & Debey, P. 2000. High yield purification and physico-chemical properties of full-length recombinant allelic variants of sheep prion protein linked to scrapie susceptibility. *European Journal of Biochemistry,* 267**,** 2833-2839.

Ridley, R. M., Baker, H. F., Windle, C. P. & Cummings, R. M. 2006. Very long term studies of the seeding of beta-amyloidosis in primates. *Journal of Neural Transmission,* 113**,** 1243-1251.

Rogaeva, E. A., Fafel, K. C., Song, Y. Q., Medeiros, H., Sato, C., Liang, Y., Richard, E., Rogaev, E. I., Frommelt, P., Sadovnick, A. D., Meschino, W., Rockwood,

K., Boss, M. A., Mayeux, R. & St. George–Hyslop, P. 2001. Screening for PS1 mutations in a referral-based series of AD cases: 21 Novel mutations. *Neurology,* 57**,** 621-625.

Rohn, T. 2010. The role of caspases in Alzheimer's disease; potential novel therapeutic opportunities. *Apoptosis,* 15**,** 1403-1409.

Ross, C. A. & Poirier, M. A. 2004. Protein aggregation and neurodegenerative disease. *Nature Medicine,* 10**,** S10-S17.

Ross, C. A. & Poirier, M. A. 2005. What is the role of protein aggregation in neurodegeneration? *Nat Rev Mol Cell Biol,* 6**,** 891-898.

Rossetti, G., Cong, X., Caliandro, R., Legname, G. & Carloni, P. 2011. Common Structural Traits across Pathogenic Mutants of the Human Prion Protein and Their Implications for Familial Prion Diseases. *Journal of Molecular Biology,* 411**,** 700-712.

Roucou, X. & LeBlanc, A. C. 2005. Cellular prion protein neuroprotective function: implications in prion diseases. *J Mol Med (Berl),* 83**,** 3-11.

Rönicke, R., Mikhaylova, M., Rönicke, S., Meinhardt, J., Schröder, U. H., Fändrich, M., Reiser, G., Kreutz, M. R. & Reymann, K. G. 2011. Early neuronal dysfunction by amyloid β oligomers depends on activation of NR2B-containing NMDA receptors. *Neurobiology of Aging,* 32**,** 2219-2228.

Safar, J. G., Lessard, P., Tamgüney, G., Freyman, Y., Deering, C., Letessier, F., DeArmond, S. J. & Prusiner, S. B. 2008. Transmission and Detection of Prions in Feces. *Journal of Infectious Diseases,* 198**,** 81-89.

Sajnani, G., Silva, C. J., Ramos, A., Pastrana, M. A., Onisko, B. C., Erickson, M. L., Antaki, E. M., Dynin, I., Vázquez-Fernández, E., Sigurdson, C. J., Carter, J. M. & Requena, J. R. 2012. PK-sensitive PrP^{Sc} Is Infectious and Shares Basic Structural Features with PK-resistant PrP^{Sc}. *PLoS Pathog,* 8**,** e1002547.

Sandberg, M. K., Al-Doujaily, H., Sharps, B., De Oliveira, M. W., Schmidt, C., Richard-Londt, A., Lyall, S., Linehan, J. M., Brandner, S., Wadsworth, J. D. F., Clarke, A. R. & Collinge, J. 2014. Prion neuropathology follows the accumulation of alternate prion protein isoforms after infective titre has peaked. *Nat Commun,* 5.

Sang, J. C., Lee, C. Y., Luh, F. Y., Huang, Y. W., Chiang, Y. W. & Chen, R. P. Y. 2012. Slow spontaneous alpha-to-beta structural conversion in a non-denaturing neutral condition reveals the intrinsically disordered property of the disulfide-reduced recombinant mouse prion protein. *Prion,* 6**,** 9.

.

Sasaki, K., Gaikwad, J., Hashiguchi, S., Kubota, T., Sugimura, K., Kremer, W., Kalbitzer, H. R. & Akasaka, K. 2008. Reversible monomer-oligomer transition in human prion protein. *Prion,* 2**,** 118-122.

Sassoon, J., Daniels, M. & Brown, D. R. 2004. Astrocytic regulation of NMDA receptor subunit composition modulates the toxicity of prion peptide PrP106–126. *Molecular and Cellular Neuroscience,* 25**,** 181-191.

Saunders, G. C., Cawthraw, S., Mountjoy, S. J., Hope, J. & Windl, O. 2006. PrP genotypes of atypical scrapie cases in Great Britain. *J Gen Virol,* 87**,** 3141-9.

Scarmeas, N., Luchsinger, J. A., Schupf, N., Brickman, A. M., Cosentino, S., Tang, M. X. & Stern, Y. 2009. Physical Activity, Diet, and Risk of Alzheimer Disease. *Jama-Journal of the American Medical Association,* 302**,** 627-637.

Selkoe, D. J. 2001. Alzheimer's disease: Genes, proteins, and therapy. *Physiological Reviews,* 81**,** 741-766.

Selkoe, D. J. 2003. Folding proteins in fatal ways. *Nature,* 426**,** 900-904.

Selvaggini, C., Degioia, L., Cantu, L., Ghibaudi, E., Diomede, L., Passerini, F., Forloni, G., Bugiani, O., Tagliavini, F. & Salmona, M. 1993. Molecular Characteristics of a Protease-Resistant, Amyloidogenic and Neurotoxic Peptide Homologous to Residues 106-126 of the Prion Protein. *Biochemical and Biophysical Research Communications,* 194**,** 1380-1386.

Shepherd, C., McCann, H. & Halliday, G. M. 2009. Variations in the neuropathology of familial Alzheimer's disease. *Acta Neuropathol,* 118**,** 37-52.

Shimohama, S. 2000. Apoptosis in Alzheimer's disease--an update. *Apoptosis,* 5**,** 9-16.

Shin, J., Shin, J., Kim, J., Yang, Y., Shin, Y.-K., Kim, K., Lee, S. & Kweon, D.-H. 2009. Disulfide bond as a structural determinant of prion protein membrane insertion. *Molecules and Cells,* 27**,** 673-680.

Shin, J. I., Shin, J. Y., Kim, J. S., Yang, Y. S., Shin, Y. K. & Kweon, D. H. 2008. Deep membrane insertion of prion protein upon reduction of disulfide bond. *Biochemical and Biophysical Research Communications,* 377**,** 995-1000.

Shyng, S. L., Heuser, J. E. & Harris, D. A. 1994. A GLYCOLIPID-ANCHORED PRION PROTEIN IS ENDOCYTOSED VIA CLATHRIN-COATED PITS. *Journal of Cell Biology,* 125**,** 1239-1250.

Silei, V., Fabrizi, C., Venturini, G., Salmona, M., Bugiani, O., Tagliavini, F. & Lauro, G. M. 1999. Activation of microglial cells by PrP and β-amyloid fragments raises intracellular calcium through L-type voltage sensitive calcium channels. *Brain Research,* 818**,** 168-170.

Silveira, J. R., Raymond, G. J., Hughson, A. G., Race, R. E., Sim, V. L., Hayes, S. F. & Caughey, B. 2005. The most infectious prion protein particles. *Nature,* 437**,** 257-261.

Simoneau, S., Rezaei, H., Sales, N., Kaiser-Schulz, G., Lefebvre-Roque, M., Vidal, C., Fournier, J. G., Comte, J., Wopfner, F., Grosclaude, J., Schatzl, H. & Lasmezas, C. I. 2007. In vitro and in vivo neurotoxicity of prion protein oligomers. *Plos Pathogens,* 3**,** 1175-1186.

Sondag, C. M., Dhawan, G. & Combs, C. K. 2009. Beta amyloid oligomers and fibrils stimulate differential activation of primary microglia. *J Neuroinflammation,* 6**,** 1.

Soto, C. 2003. Unfolding the role of protein misfolding in neurodegenerative diseases. *Nat Rev Neurosci,* 4**,** 49-60.

Stansley, B., Post, J. & Hensley, K. 2012. A comparative review of cell culture systems for the study of microglial biology in Alzheimer's disease. *J Neuroinflammation,* 9**,** 115.

Stewart, R. S. & Harris, D. A. 2005. A Transmembrane Form of the Prion Protein Is Localized in the Golgi Apparatus of Neurons. *Journal of Biological Chemistry,* 280**,** 15855-15864.

Stine, W. B., Dahlgren, K. N., Krafft, G. A. & LaDu, M. J. 2003. In Vitro Characterization of Conditions for Amyloid-β Peptide Oligomerization and Fibrillogenesis. *Journal of Biological Chemistry,* 278**,** 11612-11622.

Suzuki, N., Cheung, T. T., Cai, X.-D., Odaka, A., Jr, L. O., Eckman, C., Golde, T. E. & Younkin, S. G. 1994. An Increased Percentage of Long Amyloid β Protein Secreted by Familial Amyloid β Protein Precursor (βAPP717) Mutants. *Science,* 264**,** 1336-1340.

Sáez-Valero, J., Angeretti, N. & Forloni, G. 2000. Caspase-3 activation by β-amyloid and prion protein peptides is independent from their neurotoxic effect. *Neuroscience Letters,* 293**,** 207-210.

Tabrizi, S. J., Cleeter, M. W. J., Xuereb, J., Taanman, J. W., Cooper, J. M. & Schapira, A. H. V. 1999. Biochemical abnormalities and excitotoxicity in Huntington's disease brain. *Annals of Neurology,* 45**,** 25-32.

Tahiri-Alaoui, A., Sim, V. L., Caughey, B. & James, W. 2006. Molecular heterosis of prion protein beta-oligomers. A potential mechanism of human resistance to disease. *J Biol Chem,* 281**,** 34171-8.

Tamaoka, A., Odaka, A., Ishibashi, Y., Usami, M., Sahara, N., Suzuki, N., Nukina, N., Mizusawa, H., Shoji, S., Kanazawa, I. & et al. 1994. APP717 missense mutation affects the ratio of amyloid beta protein species (A beta 1-42/43 and a beta 1-40) in familial Alzheimer's disease brain. *J Biol Chem,* 269**,** 32721-4.

Tanaka, M., Collins, S. R., Toyama, B. H. & Weissman, J. S. 2006. The physical basis of how prion conformations determine strain phenotypes. *Nature,* 442**,** 585-9.

Texido, L., Martin-Satue, M., Alberdi, E., Solsona, C. & Matute, C. 2011. Amyloid beta peptide oligomers directly activate NMDA receptors. *Cell Calcium,* 49**,** 184-90.

.

Thadani, V., Penar, P. L., Partington, J., Kalb, R., Janssen, R., Schonberger, L. B., Rabkin, C. S. & Prichard, J. W. 1988. Creutzfeldt-Jakob disease probably acquired from a cadaveric dura mater graft. *Journal of Neurosurgery,* 69**,** 766-769.

Thal, D. R., Rub, U., Orantes, M. & Braak, H. 2002. Phases of A beta-deposition in the human brain and its relevance for the development of AD. *Neurology,* 58**,** 1791-1800.

Thellung, S., Gatta, E., Pellistri, F., Corsaro, A., Villa, V., Vassalli, M., Robello, M. & Florio, T. 2013. Excitotoxicity through NMDA receptors mediates cerebellar granule neuron apoptosis induced by prion protein 90-231 fragment. *Neurotox Res,* 23**,** 301-14.

Thinakaran, G. & Koo, E. H. 2008. Amyloid Precursor Protein Trafficking, Processing, and Function. *Journal of Biological Chemistry,* 283**,** 29615-29619.

Tobler, I., Deboer, T. & Fischer, M. 1997. Sleep and Sleep Regulation in Normal and Prion Protein-Deficient Mice. *The Journal of Neuroscience,* 17**,** 1869-1879.

Tobler, I., Gaus, S. E., Deboer, T., Achermann, P., Fischer, M., Rulicke, T., Moser, M., Oesch, B., McBride, P. A. & Manson, J. C. 1996. Altered circadian activity rhythms and sleep in mice devoid of prion protein. *Nature,* 380**,** 639-642.

Tomic, J. L., Pensalfini, A., Head, E. & Glabe, C. G. 2009. Soluble fibrillar oligomer levels are elevated in Alzheimer's disease brain and correlate with cognitive dysfunction. *Neurobiol Dis,* 35**,** 352-8.

Torres, M., Castillo, K., Armisen, R., Stutzin, A., Soto, C. & Hetz, C. 2010. Prion Protein Misfolding Affects Calcium Homeostasis and Sensitizes Cells to Endoplasmic Reticulum Stress. *Plos One,* 5.

Toyama, B. H., Kelly, M. J., Gross, J. D. & Weissman, J. S. 2007. The structural basis of yeast prion strain variants. *Nature,* 449**,** 233-7.

Treusch, S., Cyr, D. M. & Lindquist, S. 2009. Amyloid deposits Protection against toxic protein species? *Cell Cycle,* 8**,** 1668-1674.

Trevitt, C. R., Hosszu, L. L. P., Batchelor, M., Panico, S., Terry, C., Nicoll, A. J., Risse, E., Taylor, W. A., Sandberg, M. K., Al-Doujaily, H., Linehan, J. M., Saibil, H. R., Scott, D. J., Collinge, J., Waltho, J. P. & Clarke, A. R. 2014. N-terminal Domain of Prion Protein Directs its Oligomeric Association. *Journal of Biological Chemistry*.

Tuzi, N. L., Cancellotti, E., Baybutt, H., Blackford, L., Bradford, B., Plinston, C., Coghill, A., Hart, P., Piccardo, P., Barron, R. M. & Manson, J. C. 2008. Host PrP glycosylation: A major factor determining the outcome of prion infection. *Plos Biology,* 6**,** 872-882.

Tyan, S.-H., Shih, A. Y.-J., Walsh, J. J., Maruyama, H., Sarsoza, F., Ku, L., Eggert, S., Hof, P. R., Koo, E. H. & Dickstein, D. L. 2012. Amyloid precursor protein (APP) regulates synaptic structure and function. *Molecular and Cellular Neuroscience,* 51**,** 43-52.

Urbanc, B., Cruz, L., Le, R., Sanders, J., Ashe, K. H., Duff, K., Stanley, H. E., Irizarry, M. C. & Hyman, B. T. 2002. Neurotoxic effects of thioflavin S-positive amyloid deposits in transgenic mice and Alzheimer's disease. *Proceedings of the National Academy of Sciences of the United States of America,* 99**,** 13990-13995.

Van Damme, P., Dewil, M., Robberecht, W. & Van Den Bosch, L. 2005. Excitotoxicity and amyotrophic lateral sclerosis. *Neurodegener Dis,* 2**,** 147-59.

van Oijen, M., Hofman, A., Soares, H. D., Koudstaal, P. J. & Breteler, M. M. B. 2006. Plasma Aβ1–40 and Aβ1–42 and the risk of dementia: a prospective case-cohort study. *The Lancet Neurology,* 5**,** 655-660.

Voisine, C., Pedersen, J. S. & Morimoto, R. I. 2010. Chaperone networks: Tipping the balance in protein folding diseases. *Neurobiology of Disease,* 40**,** 12-20.

Volles, M. J., Lee, S.-J., Rochet, J.-C., Shtilerman, M. D., Ding, T. T., Kessler, J. C. & Lansbury, P. T. 2001. Vesicle Permeabilization by Protofibrillar α-Synuclein: Implications for the Pathogenesis and Treatment of Parkinson's Disease†. *Biochemistry,* 40**,** 7812-7819.

Wadia, J. S., Schaller, M., Williamson, R. A. & Dowdy, S. F. 2008. Pathologic Prion Protein Infects Cells by Lipid-Raft Dependent Macropinocytosis. *PLoS ONE,* 3**,** e3314.

Walker, L. C., Callahan, M. J., Bian, F., Durham, R. A., Roher, A. E. & Lipinski, W. J. 2002. Exogenous induction of cerebral beta-amyloidosis in beta APP-transgenic mice. *Peptides,* 23**,** 1241-1247.

Walsh, D. M., Hartley, D. M., Kusumoto, Y., Fezoui, Y., Condron, M. M., Lomakin, A., Benedek, G. B., Selkoe, D. J. & Teplow, D. B. 1999. Amyloid β-Protein Fibrillogenesis: STRUCTURE AND BIOLOGICAL ACTIVITY OF PROTOFIBRILLAR INTERMEDIATES. *Journal of Biological Chemistry,* 274**,** 25945-25952.

Walsh, D. M., Klyubin, I., Fadeeva, J. V., Cullen, W. K., Anwyl, R., Wolfe, M. S., Rowan, M. J. & Selkoe, D. J. 2002. Naturally secreted oligomers of amyloid beta protein potently inhibit hippocampal long-term potentiation in vivo. *Nature,* 416**,** 535-9.

Wang, F., Wang, X., Yuan, C.-G. & Ma, J. 2010. Generating a Prion with Bacterially Expressed Recombinant Prion Protein. *Science,* 327**,** 1132-1135.

Weissmann, C. 2004. The state of the prion. *Nature Reviews Microbiology,* 2**,** 861-871.

Westergard, L., Christensen, H. M. & Harris, D. A. 2007. The cellular prion protein (PrPC): Its physiological function and role in disease. *Biochimica et Biophysica Acta (BBA) - Molecular Basis of Disease,* 1772**,** 629-644.

Wickner, S., Maurizi, M. R. & Gottesman, S. 1999. Posttranslational Quality Control: Folding, Refolding, and Degrading Proteins. *Science,* 286**,** 1888-1893.

Wijsman, E. M., Pankratz, N. D., Choi, Y., Rothstein, J. H., Faber, K. M., Cheng, R., Lee, J. H., Bird, T. D., Bennett, D. A., Diaz-Arrastia, R., Goate, A. M., Farlow, M., Ghetti, B., Sweet, R. A., Foroud, T. M., Mayeux, R. & The, N. I. A. L. N. F. S. G. 2011. Genome-Wide Association of Familial Late-Onset Alzheimer's Disease Replicates <italic>BIN1</italic> and <italic>CLU</italic> and Nominates <italic>CUGBP2</italic> in Interaction with <italic>APOE</italic>. *PLoS Genet,* 7**,** e1001308.

Will, R. G. 2003. Acquired prion disease: iatrogenic CJD, variant CJD, kuru. *British Medical Bulletin,* 66**,** 255-265.

Williams, A. D., Sega, M., Chen, M., Kheterpal, I., Geva, M., Berthelier, V., Kaleta, D. T., Cook, K. D. & Wetzel, R. 2005. Structural properties of Aβ protofibrils stabilized by a small molecule. *Proceedings of the National Academy of Sciences of the United States of America,* 102**,** 7115-7120.

Williams, E. S. & Miller, M. W. 2002. Chronic wasting disease in deer and elk in North America. *Revue Scientifique Et Technique De L Office International Des Epizooties,* 21**,** 305-316.

Williams, E. S., Miller, M. W., Kreeger, T. J., Kahn, R. H. & Thorne, E. T. 2002. Chronic Wasting Disease of Deer and Elk: A Review with Recommendations for Management. *The Journal of Wildlife Management,* 66**,** 551-563.

Williams, E. S. & Young, S. 1980. CHRONIC WASTING DISEASE OF CAPTIVE MULE DEER: A SPONGIFORM ENCEPHALOPATHY. *Journal of Wildlife Diseases,* 16**,** 89-98.

Winner, B., Jappelli, R., Maji, S. K., Desplats, P. A., Boyer, L., Aigner, S., Hetzer, C., Loher, T., Vilar, M., Campioni, S., Tzitzilonis, C., Soragni, A., Jessberger, S., Mira, H., Consiglio, A., Pham, E., Masliah, E., Gage, F. H. & Riek, R. 2011. In vivo demonstration that alpha-synuclein oligomers are toxic. *Proc Natl Acad Sci U S A,* 108**,** 4194-9.

Wiseman, F., Cancellotti, E. & Manson, J. 2005. Glycosylation and misfolding of PrP. *Biochemical Society Transactions,* 33**,** 1094-1095.

Wolman, M. & Bubis, J. J. 1965. The cause of the green polarization color of amyloid stained with Congo red. *Histochemie,* 4**,** 351-356.

Wong, E. & Cuervo, A. M. 2010. Autophagy gone awry in neurodegenerative diseases. *Nat Neurosci,* 13**,** 805-811.

Yang, T.-T., Hsu, C.-T. & Kuo, Y.-M. 2009. Cell-derived soluble oligomers of human amyloid-β peptides disturb cellular homeostasis and induce apoptosis in primary hippocampal neurons. *Journal of Neural Transmission,* 116**,** 1561-1569.

Yedidia, Y., Horonchik, L., Tzaban, S., Yanai, A. & Taraboulos, A. 2001. Proteasomes and ubiquitin are involved in the turnover of the wild-type prion protein. *Embo Journal,* 20**,** 5383-5391.

Yoshida, H. 2007. ER stress and diseases. *FEBS Journal,* 274**,** 630-658.

Young, K. F., Pasternak, S. H. & Rylett, R. J. 2009. Oligomeric aggregates of amyloid β peptide 1–42 activate ERK/MAPK in SH-SY5Y cells via the α7 nicotinic receptor. *Neurochemistry International,* 55**,** 796-801.

Youssef, I., Florent-Béchard, S., Malaplate-Armand, C., Koziel, V., Bihain, B., Olivier, J.-L., Leininger-Muller, B., Kriem, B., Oster, T. & Pillot, T. 2008. N-truncated amyloid-β oligomers induce learning impairment and neuronal apoptosis. *Neurobiology of Aging,* 29**,** 1319-1333.

Zanetti, O., Solerte, S. B. & Cantoni, F. 2009. Life expectancy in Alzheimer's disease (AD). *Arch Gerontol Geriatr,* 49 Suppl 1**,** 237-43.

Zhang, C., Jackson, A. P., Zhang, Z. R., Han, Y., Yu, S., He, R. Q. & Perrett, S. 2010. Amyloid-like aggregates of the yeast prion protein ure2 enter vertebrate cells by specific endocytotic pathways and induce apoptosis. *PLoS One,* 5.

Zhang, W., Hao, J., Liu, R., Zhang, Z., Lei, G., Su, C., Miao, J. & Li, Z. 2011. Soluble Abeta levels correlate with cognitive deficits in the 12-month-old APPswe/PS1dE9 mouse model of Alzheimer's disease. *Behav Brain Res,* 222**,** 342-50.

Appendix 1

Supplementary figure 1 RecPrP purification

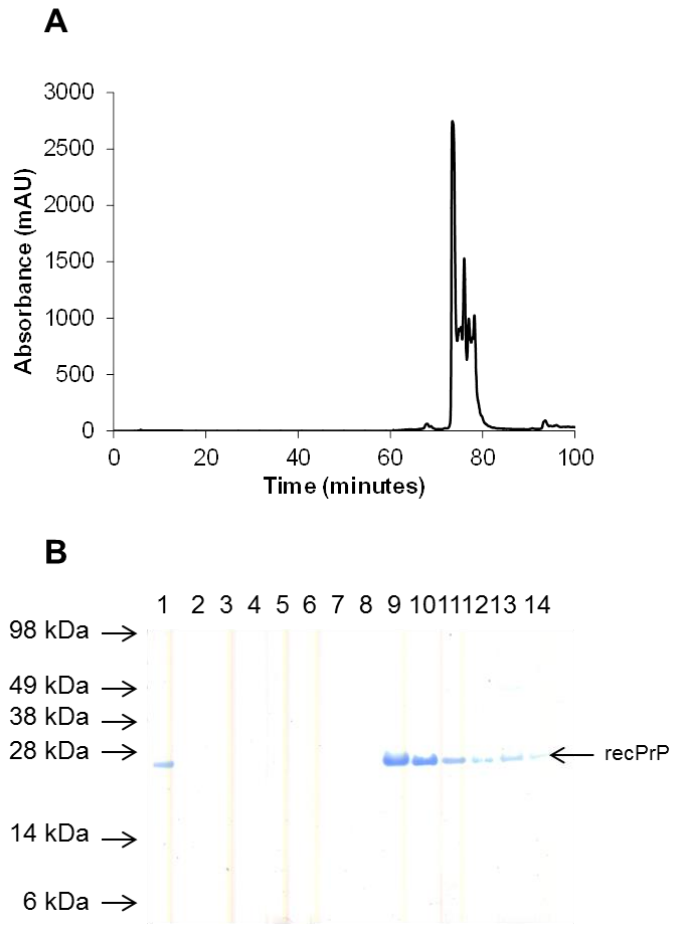

A+B) recPrP purification. A) Reverse phase chromatogram for recPrP purification, eluting peaks show separation of different oxidised forms of recPrP. B) SDS-PAGE with coomassie staining of the fractions collected from A. Lanes 9-14 correspond with the eluting peaks from A.